EARTH SCIENCES
SIMON FRASER UNIVERSITY

Groundwater Sensitivity to Climate Change: Abbotsford-Sumas Aquifer in British Columbia, Canada and Washington State, US

Final Report

Prepared by:

Jacek Scibek and Diana Allen
Department of Earth Sciences
Simon Fraser University
Burnaby, B.C. V3Y 2L4

Prepared for:

BC Ministry of Water, Land and Air Protection
and
Environment Canada

February 2006

EXECUTIVE SUMMARY

The sensitivity of a small, regional scale aquifer to predicted climate change is investigated. The trans-national Abbotsford-Sumas aquifer, located in the central Fraser Valley, is bisected by Canada-US boundary and is situated east of Vancouver BC and north of Bellingham, WA, centered around the City of Abbotsford, BC.

The system area is 160 km^2, and is comprised of heterogeneous glaciofluvial sediments, bounded by glaciomarine sediments that infill steep and variable bedrock topography of buried paleovalleys, bedrock outcrops and mountain ranges. The hydrostratigraphic units were modeled in three-dimensions from standardized, reclassified, and interpreted well borehole lithologs. A three dimensional groundwater flow model of variable spatial resolution (constrained by borehole spacing) was implemented in Visual MODFLOW, and calibrated to historic static water elevations in several thousand wells. The model accounts for large-scale heterogeneity of the sediment fill, in which the hydraulic conductivity and specific yield properties are spatially-distributed in the aquifer layers.

The climate change dataset used is that predicted by Canadian Global Climate Model 1 (CGCM1), for consecutive 30-year intervals from present to 2069. Downscaling of CGCM1 results was accomplished using 2 independently calculated methods: 1) SDSM, and 2) PCA k-nn method. A comparison of these methods showed SDSM to provide better representation of climate in the region.

Spatially-distributed and temporally-varying recharge zonation was mapped for the surficial aquifer. The method involved using GIS linked to the one-dimensional HELP (USEPA) hydrologic model that estimates aquifer recharge. The recharge model accounts for soil distribution, vadose zone depth and hydraulic conductivity, the extent of impermeable areas, surficial geology, as well as precipitation zonation across the aquifer. Recharge is driven by physically-based daily weather inputs generated by a stochastic weather generator that is calibrated to local observed climate.

Four year long climate scenarios were run, each representing one typical year in the present and future (2020s, 2050s, and 2080s), by perturbing the historical weather according to the downscaled CGCM1 global climate model results. The calibrated transient model was used for all climate scenarios. Results suggest observable, but small, changes in groundwater levels, forced by changes in recharge. Groundwater levels are predicted to decrease by between 0.05 m to more than 0.25 m due to climate change by the 2010-2039 period. Impacts on water levels are generally restricted to the upland areas, because the lower elevation portions of the model, where the major streams are located, are constrained by specified head boundary conditions; although, reductions in baseflow are anticipated due to the lowering of the groundwater gradient across the aquifer.

TABLE OF CONTENTS:

LIST OF FIGURES:

LIST OF MAPS:

LIST OF TABLES:

1. INTRODUCTION

1.1. BACKGROUND AND PURPOSE OF RESEARCH

Water resources are central to any study on climate change; however, most research to-date has been directed at forecasting the potential impacts to surface water hydrology (e.g., Whitfield and Taylor, 1998). Relatively little research has been undertaken to determine the sensitivity of groundwater systems to changes in critical input parameters, such as precipitation and runoff. In areas that rely heavily on groundwater, for example, for agricultural, domestic or industrial use, it is important that the potential impact of climate change be assessed so that adaptation measures can be taken if needed. One concern of water managers and government officials is the potential decrease of groundwater supplies under climate change conditions, another is the potential impact to streams that are fed by groundwater at periods of low flow.

It is expected that changes in temperature and precipitation will alter groundwater recharge to aquifers, causing shifts in water table levels in unconfined aquifers as a first response to climate trends (Changnon et al., 1988; Zektser and Loaiciga, 1993). These changes may decrease quantity and, perhaps, quality of water. In addition, because groundwater contributes to baseflow in stream, a change in the groundwater regime could have detrimental environmental effects on fisheries and other wildlife by changing baseflow dynamics in streams (Bredehoeft and Papadopulos, 1982; Gleick, 1986).

Aquifer recharge and groundwater levels interact, and depend on climate and groundwater use; each aquifer has different properties and requires detailed characterization and, eventually, quantification (e.g., numerical modeling) of these processes and linking of the recharge model to climate model predictions (York et al., 2002). In practice, any aquifer that has an existing and verified conceptual model, together with a calibrated numerical model, can be assessed for climate change impacts through simulations. The accuracy of predictions depends largely of scale of project and availability of hydrogeologic and climatic datasets.

The purpose of the current research study is to model the sensitivity to climate change, and identify the potential impacts of climate change on the Abbotsford-Sumas aquifer situated in southwestern British Columbia, Canada and northwestern Washington State, US (Map 1). This research project follows a comprehensive hydrogeological investigation and climate change impacts assessment of the Grand Forks aquifer in south-central British Columbia, Canada (Allen et al., 2004). The same methodology used in that study has been used here.

This report describes the methodology and results for the recharge component of this sensitivity analysis, and presents the results of the climate change impacts modeling. A detailed description of the model development, including the hydrostratigraphy, hydrology and model calibration, as well as a description of the current groundwater regime can be found elsewhere (Scibek and Allen, 2005). Specifically, this report provides a summary of the methodology and results of spatially distributed recharge applied to the transient groundwater model that is being used to assess climate change impacts on the aquifer.

Map 1 Location map of the model area in British Columbia and Washington State.

1.2. AQUIFER DESCRIPTION

The Abbotsford-Sumas aquifer (Map 2) is approximately 161 km^2 (62 sq miles) in aerial extent, and is roughly bisected by the Canadian-USA boundary. The aquifer consists of several interconnected unconfined and confined aquifers and spans uplands and three river valleys (lowlands or floodplains) on three sides. The uplands are centered on the City of Abbotsford, BC and extend westward through Langley, BC and south to Lynden, WA. The Sumas Valley is a large sediment-filled deep bedrock valley.

The aquifer is composed of uncompacted sands and gravels of the Sumas Drift, a glacial outwash deposit. There is significant heterogeneity of the hydrostratigraphic units, which results in complex groundwater paths. The thickness of Sumas Drift can be up to 65 m, and it is thickest in the northeast where glacial terminal moraine deposits are found. The deepest part of the aquifer system in this region is located along the US-Canada border beneath the City of Abbotsford and toward Lynden, WA, but the most productive areas are near Sumas, WA in south-west end of the Sumas Valley.

The coastal climate is humid and temperate, with significant rainfall over most of the year. Recharge to the aquifer is primarily from direct precipitation, mostly from October to May. Groundwater discharge occurs through springflow, and seepage to small streams and rivers. The largest rivers, hydraulically connected to the aquifer system, are the Nooksack River and the Sumas River. These are almost exclusively discharge zones. Small streams on the uplands, and small lakes, have more complex and temporally varying aquifer interactions. To the north is Fraser River floodplain, where a small component of groundwater discharge occurs.

The aquifer is highly productive, and provides water supply for nearly 10,000 people in the US (towns of Sumas, Lynden, Ferndale, Everson and scattered agricultural establishments) and 100,000 in Canada, mostly in City of Abbotsford, but also in township of Langley (Mitchell et al., 2000). Map 3 shows the locations of developed areas within the aquifer footprint. Almost half the groundwater is pumped to supply fish hatcheries in Abbotsford, BC. Industrial use is also becoming important (there is a power plant in construction near Sumas, WA).

Map 2 Location map of Fraser Valley and extent of model area.

1.3. RECHARGE TO THE ABBOTSFORD-SUMAS AQUIFER

Precipitation is the principle source of recharge to the Abbotsford-Sumas aquifer, and its range and patterns are significant factors to be considered when attempting to quantify the amount of recharge to the aquifer. There are over 30 climate stations in the Fraser Valley, some of which have been in operation for more than 50 years. There is a significant increase (over double) in total annual precipitation, as one moves from south to north and from west to east, which is attributed to orographic effects of the nearby Coast and Cascade Mountains.

About 75% of the annual precipitation occurs between October and March, when evaporation and evapotranspiration are minimal; hence it is only during this period that there is potential for rain water to percolate into the soils, and eventually to recharge or replenish the aquifers. The water levels in observation wells throughout this area attest to the fact that recharge is precipitation-driven, and specifically related to the amount of winter precipitation.

Variation in total annual precipitation is also significant, especially when there are many successive years of less than normal precipitation. During dry years, it is not uncommon for recharge to the ground water table to be insufficient to sustain yields in the shallower dug wells, and hence, deepening of wells is required to intercept the declining water table.

Map 3 Central Fraser Valley location map showing model area, cities and towns, topography, international border, and major rivers. White dotted outline shows model boundary, which encompasses the Abbotsford-Sumas aquifer.

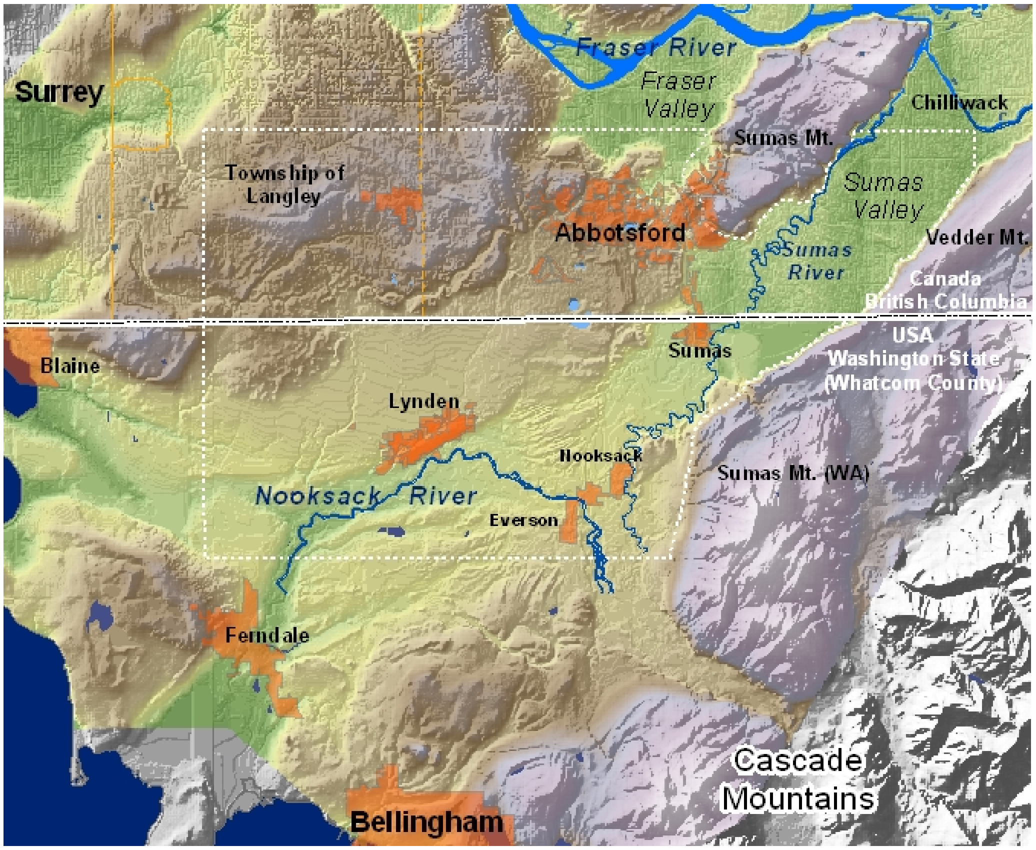

1.4. RECHARGE IN GROUNDWATER MODELS

Groundwater recharge rates depend on surface and subsurface properties (spatial variation) as well as precipitation amount. Recharge varies spatially with topography, land use and cover, and soil properties, and it varies temporally with climate. Recharge can be measured directly using soil permeameters and lysimeters, or using tracer methods, but the direct measurement methods are too expensive for large regional aquifers, and thus, are not practical. An indirect method of estimating recharge is from catchment-scale water balance analysis where stream gauges are available. Recharge may also be modeled using representative data for the aquifer and climate, which is the approach used in this study.

Groundwater recharge is also a very important boundary condition in numerical models, but site-specific recharge data are often not available or are difficult to estimate, thus, recharge is used as a fitting parameter during model calibration (Anderson and Woessner, 1994). For example, the Waterloo Moraine model (Martin and Frind, 1998) used such a calibration protocol. Where precipitation records are available and are representative of aquifer area, an assumed fraction of precipitation is often used as an estimate of recharge (Brodie, 1999). The validity of assumptions of recharge rates becomes very important in small-scale transient models, where detailed groundwater flowpaths and levels are required (Jyrkama et al, 2002). For the purposes of climate change impacts modeling, the recharge rates must be as accurate as possible to accurately represent the small shift from present to future climatic conditions.

The modeling of recharge used in this study will consider heterogeneity of soils, surficial geology, depth to water table, and any precipitation and temperature trends over the aquifer area. Full transient behaviour of recharge will be considered. In essence, the approach will follow that of Jyrkama et al. (2002) in which high-resolution spatially-distributed recharge estimates will be generated using the US EPA HELP (Hydrologic Evaluation of Landfill Performance) model (UnSat Suite software, Waterloo Hydrogeologic Inc., 2000), and adjusted for aquifer thickness, material type, soil type, and representative hydraulic properties. Spatially-distributed and temporally-varying recharge estimates will then be imported into Visual MODFLOW for groundwater flow modeling.

As a prerequisite to successful application of a recharge simulation of one-dimensional soil and sediment columns, the weather generator used with HELP must adequately reproduce the observed weather conditions, in particular, rainfall and temperature. Synthetic climate data will thus be calibrated to site-specific conditions using Environment Canada climate records, combined with parameters in the HELP model database.

Geographic Information Systems (GIS) is increasingly used in spatially-distributed hydrologic and hydrogeologic modeling, especially for data preparation for groundwater flow models (Brodie, 1999). In recharge modeling, the GIS data-handling capabilities allow raster or vector computations that use soil properties from digital soil maps, adjustment of permeabilities using land cover maps, and inputs of spatially-distributed precipitation and evapotranspiration maps into recharge models (Fayer et al., 1996). Coupled hydrologic-hydrogeologic regional models also rely heavily on GIS (Xiao et al., 1996; Zhang et al., 1999). Most recently, York et al. (2002) reviewed existing methods for recharge modeling as inputs for transient groundwater models, and used the HELP model together with GIS-based soil and landuse maps to calculate recharge over regional heterogeneous aquifer in New Jersey.

1.4.1. TIME STEPS FOR RECHARGE, CLIMATE AND WEATHER

In climate and recharge modeling, daily values are used as the basic time-averaged units. However, the groundwater model will receive monthly recharge inputs to limit the complexity of the simulations. The recharge is based on step-like climate scenarios, where in each scenario ("step"), the climate is the same and equivalent to that predicted by Global Climate Model (GCM) / downscaled / stochastic-generated, and then recharge is averaged for the scenario by month. The GCM ensures that physical processes are modeled spatially (on very coarse scale) and, more importantly, temporally. The downscaling procedure ensures that processes and resulting values of variables are as close to site-specific as possible, while preserving the GCM predictions. The stochastic weather ensures that daily values of variables are realistic, consistent, site specific, and preserve both values and variability predicted to change from current to future climate scenarios by the GCM.

The recharge model (HELP model in this project) uses daily inputs of weather to calculate daily recharge through soil columns. Thus, appropriate frequency, magnitude and duration of precipitation and other events are modeled. Typically 30 or more years are modeled within each climate scenario, and then monthly averages are computed to represent monthly variations of recharge that are representative of the climate regime being modeled. Because the stochastic weather generator requires more than 100 years of daily weather to be created to begin approaching the statistics specified for climate scenario (and local weather), the recharge model will also receive that long time period of simulated weather, ensuring that the averages are representative. The length of the weather time series is not meant to model actual changing climate year-to-year, but rather to model climate change in a step-wise fashion for each scenario and to generate a long enough weather time series to preserve and properly represent statistical properties for the site and the predicted climate for the scenario.

The groundwater model will be "transient", but only on monthly time steps due to computational limitations, although 10 day time steps could be modeled with some effort. Since most of the GCM summaries, downscaling tools, and stochastic weather generators are set-up for adjusting monthly statistics for daily weather, it makes sense to model transient groundwater flow also using monthly time steps. The actual groundwater flow model has more time steps, but inputs are modified and outputs generated on monthly time steps. Thus, monthly recharge is required as an input for each climate change scenario.

1.5. SCOPE OF WORK

This project encompasses two main topics: climate change predictions and recharge modeling, and groundwater flow modeling for quantifying the impact of climate change on groundwater levels. The following summarizes the steps taken.

GCM Climate Data

1. Scenarios from Canadian Global Coupled Model 1 (CGCM1) were downloaded from the CCIS website (CCIS, 2003a). These included 4 scenarios (current, 2020s, 2050s, and 2080s).

Recharge Modeling

1. Continuous time series daily precipitation (P) and temperature (T) data were analyzed.
2. A comparison of downscaling methodologies (SDSM and Environment Canada's k-nn ACS method) was undertaken.
3. Historic climate files were created for input to LARS-WG using results from SDSM; LARS-WG output was calibrated to observed climate data. Future climate data files were created for input to LARS-WG.
4. HELP projects were created: 64 different soil / Ksat / depth scenarios. A sensitivity analysis to investigate key parameters used in HELP was undertaken.
5. A distributed recharge map was developed for the aquifer. GIS layers included soils, geology, and depth to water.
6. Recharge was mapped by zone monthly and annually for all climate scenarios.

Groundwater Simulations

1. A three-dimensional groundwater flow model was developed for the Abbotsford-Sumas aquifer in a related study (Scibek and Allen, 2005).
2. The model was calibrated against mapped historic static water levels, where possible, against transient water levels in the observation wells, to establish the base case model for climate change simulations.

3. Various climate change scenarios were run (present and two future time periods).
4. The water budget components were documented and a comparison between these components for each scenario was undertaken.

1.6. OUTLINE OF REPORT

This report contains 4 main sections:

- Section 1.0 provides the background information for the project and provides context for the purpose, main objectives and scope of work for the project.
- Section 2.0 describes climate change scenario modeling, identifying the sources of climate data, General Circulation Models (GCMs) and downscaling.
- Section 3.0 provides downscaling results for precipitation, and temperature and solar radiation.
- Section 4.0 provides the weather input for the recharge model.
- Section 5.0 describes the methodology for recharge modeling using HELP
- Section 6.0 summarizes the recharge results for the Abbotsford-Sumas aquifer.
- Section 7.0 discusses the impacts of climate change on groundwater levels in the aquifer.
- Section 8.0 offers some conclusions.

1.7. ACKNOWLEDGEMENTS

The authors wish to acknowledge the financial support provided by Environment Canada, which led to the development of the three-dimensional groundwater flow model. Geologic, hydrologic and hydrogeologic data for this project were obtained from various maps and reports, and well lithology logs were available through the web-based WELLS database maintained by the BC Ministry of Water, Land and Air Protection. Climate database was available through Environment Canada.

Thanks to Matt Plotnikoff at SFU for helping with intermittent computer problems. Also special thanks to Aparna Desphande and Dr. Nadine Shuurman at SFU for their contribution towards the standardization of well lithology data and early geologic conceptual models.

2. CLIMATE CHANGE SCENARIO MODELING

2.1. SOURCES OF CLIMATOLOGICAL DATA

The historical weather data included average daily observations, monthly summaries, and annual summaries. Initially, station information was explored for sources of long term records at weather stations within the central Fraser Valley (both within Canada and the US), to determine the most useful and representative weather station(s) for the purpose of climate scenario modeling. A map showing the location of regional weather stations is shown in Map 4.

Map 4 Climate and weather stations in central Fraser Valley (BC and WA): selection of stations with long periods of record, availability of evapotranspiration or solar radiation data, or proximity to aquifer location. The Abbotsford International Airport station is identified with the yellow square.

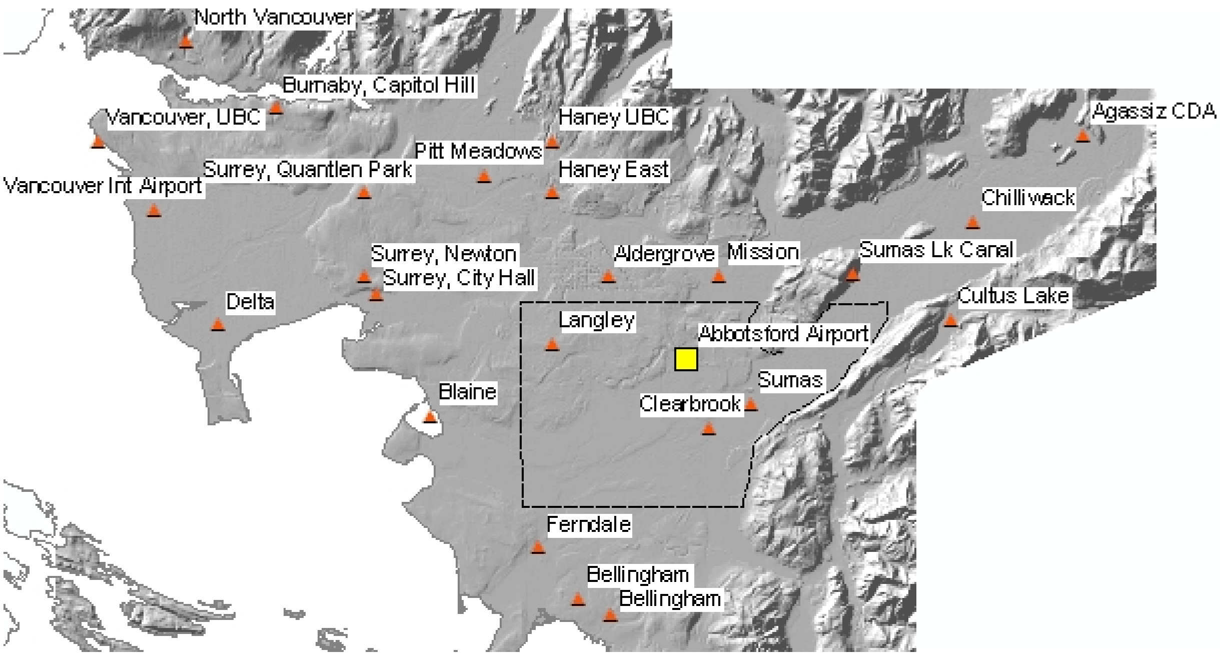

Data from Environment Canada were contained in a custom database system, which extracts daily listings for precipitation and temperature in CCC (Canadian Climate Centre), fixed width text format. The CCC files were converted using Visual Basic code to continuous time series readable by Access, Excel, and other programs. US data came in text format, which was easier to import and read than the CCC files. US data were downloaded from websites of the Western Climate Centre. Solar radiation was estimated from Carlson et al. (2002), NASA remotely sensed values, and from CRCM monthly predictions (CICS, 2003).

For climate change scenarios, the sources of data were primarily the Canadian Institute for Climate Studies (CICS, 2003) for all CRCM and CGCM1 scenarios (note: the acronyms and models are explained in next section). We also had access to daily CGCM1 data for precipitation from Zwiers (2001) and CICS (2003) for calibration of the SDSM downscaling tool.

Daily outputs of CRCM were not available to this project, although these exist. Also from CICS were links for the downscaling software, SDSM, and a stochastic weather generator, LARS-WG (discussed later).

2.2. GLOBAL CLIMATE MODELS

2.2.1. THE FIRST GENERATION COUPLED GLOBAL CLIMATE MODEL (CGCM1)

Climate simulation models and physically-based numerical models are used for climate prediction, the study of climate change and variability, and to better understand the various processes which govern our climate system. The global climate is modeled by various Global Climate Models (GCMs). One of these is the Coupled Global Climate Model (CGCM1).

In this report, the climate scenarios, and subsequent analyses and models of impacts on groundwater resources are derived from CGCM1 predictions. Therefore, a short introduction to CGCM1 workings and model results is necessary. The first version of the CGCM1 and its control climate are described by Flato et al. (2000). The Canadian Climate Centre for modeling and analysis (CCCma, 2003) describes the CGCM1 global climate model as follows. The details of the model and discussion of primary results may also be found in Climate Change Digest (as a .PDF) published by Environment Canada.

The atmospheric component of the model is essentially AGCM2 described by McFarlane et al. (1992). CGCM1 has a surface grid resolution of roughly 3.7° x 3.7°. An ensemble of four transient climate change simulations has been performed and is described in Boer et al. (2000a and 2000b). Three of these simulations use an effective greenhouse gas forcing change, corresponding to that observed from 1850 to 1990, and a forcing change corresponding to an increase of CO_2 at a rate of 1% per year (compounded) thereafter until year 2100 (the IPCC "IS92a" forcing scenario). The fourth simulation considers the effect of greenhouse gas forcing only. The change in climate predicted by a model clearly depends directly on this specification of greenhouse gas (and aerosol) forcing and, of course, these are not well known. The prescription described above is similar to the IPCC "business as usual" scenario, and using a standard scenario allows the results of this model to be compared to those of other modeling groups around the world. The ability of a climate model to reproduce the present-day mean climate and its historical variation adds confidence to projections of future climate change.

For the globe, between years 1980 and 2050, the prescribed CO_2 concentration doubles, and over this time, the greenhouse gas only run exhibits an increase in temperature of 2.7°C. The increase over the same period in the greenhouse gas plus aerosol run is 1.9°C; the difference of 0.8°C is the cooling effect of the aerosols. One can contrast these results with the equilibrium calculation of Boer et al. (1992), who used the same atmospheric model without the aerosol effect. They obtained a global average warming of 3.5°C upon doubling CO_2 concentration. These CGCM1 predictions correspond to observed temperature of the globe for historical and current periods (Jones, 1994).

2.2.2. SUMMARY OF CGCM1 PREDICTIONS FOR BC

In British Columbia, climate change has been detected from detailed examination of meteorological, hydrologic, sea level, and ecological records and investigations. Analysis of historical data indicates that many properties of climate have changed during the 20th century (Ministry of Water, Land and Air Protection of BC, 2002). Some of the changes were:

- Average annual temperature warmed by 0.6ºC on the coast, 1.1ºC in the interior, and 1.7ºC in northern BC.
- Night-time temperatures increased across most of BC in spring and summer.
- Precipitation increased in southern BC by 2 to 4 percent per decade.
- Lakes and rivers become free of ice earlier in the spring.
- Water temperature increased in rivers and streams.

Climate models and scenarios suggest that the climate in British Columbia will continue to change during the 21st century, according to summary report by Ministry of Water, Land and Air Protection of BC (2002). Future predictions include:

- Average annual temperature in BC may increase by 1ºC to 4ºC.
- Average annual precipitation may increase by 10 to 20 percent.
- Many small glaciers in southern BC may disappear.
- Some interior rivers may dry up during the summer and early fall.

In addition, climate change scenarios suggest that warmer winter temperatures will result in a greater proportion of precipitation falling as rain. GCM results showed that a CO_2 doubling in the atmosphere would result in an increase in the mean annual precipitation and the mean annual temperature for each of the stations examined throughout the province of BC. Annual winter and spring runoff are expected to increase, although the additional precipitation would be offset somewhat by greater evapotranspiration associated with rising temperatures and longer growing seasons (Coulson, 1997). Computed runoff, calculated under doubled CO_2 temperature and precipitation conditions, resulted in an 86% change for the climate station at Princeton, BC and a 71% change for Cranbrook, BC. For the South BC region, earlier snowmelt will be especially significant where the spring freshet may occur up to one full month earlier, and there will be a potential for increased peak flows in coastal and southern BC (Coulson, 1997). As well, the summer low flow period will be characterized by even lower streamflows.

2.2.3. SCALING APPROACH

GCM's do not accurately estimate local statistics of regional climate variables, but the internal consistency of these physically-based climate models provides the most likely estimates of ratios and differences (scaling factors) of climatic variables, such as precipitation and temperature from historical (base case) to predicted scenarios (Loaiciga et al., 1996). Thus, scaling factors are used to generate climate-change scenarios from historical time series. For example, Loaiciga et al. (2000) modeled recharge to extensive Edwards Aquifer in Texas using scaled historical precipitation and temperature records to GCM scenarios for doubling of CO_2 (denoted as $2xCO_2$) and present conditions ($1xCO_2$):

$$P\ 2xCO_2\ \text{scenario} = P\ 2xCO_2 / P\ 1xCO_2 * P\ \text{historical}$$
$$T\ 2xCO_2\ \text{scenario} = (T\ 2xCO_2 - T\ 1xCO_2) + T\ \text{historical}$$

The scaled time series of P and T can be used to model recharge, which is input to an aquifer numerical model for estimating the impacts on groundwater resources under various climate change scenarios. It is also possible to choose historical time series as a low, medium, and high P or T base case scenarios.

The question is then, what is the most reasonable base case? If the historical record is chosen only for drought years, then the base case represents the dry extreme of climatic range for that area, and climate change scenarios will show impacts to groundwater levels that would occur if climate change followed dry conditions, without any future wet years. This is unlikely. The most common approach is to take the entire historical period and average it to derive the base case, assuming that it is representative of pre-climate change conditions. Then, climate change scenario is generated by modifying the base case climatic time series. This approach tends to smooth out climatic variability and assumes average conditions before climate change occurs.

2.2.4. STATISTICAL APPROACHES

For many climate change studies, scenarios of climate change derived directly from GCM output are of insufficient spatial and temporal resolution. Spatial downscaling techniques are used to derive finer resolution climate information from coarser resolution GCM output, which have been designed to bridge the gap between the information that the climate modeling community can currently provide and that required by the impacts research community (Wilby and Wigley, 1997). The fundamental assumption behind all these methods is that the statistical relationships, which are calculated using observed data, will remain valid under future climate conditions.

A study by Cannon and Whitfield (2000) assessed whether the recent observed changes in streamflow conditions in British Columbia can be accurately predicted using an empirical downscaling approach. The results of that study suggested that neural network empirical downscaling models are capable of predicting changes in streamflow observed during recent decades using only large-scale atmospheric conditions as model inputs. Beersma (2000) showed climate scenarios useful for hydrologic impacts assessment studies. Climate downscaling techniques are treated in more detail by Hewitson and Crane (1996). A review of applications of downscaling from GCM to hydrologic modeling can be found in Xu (1999). Similar methods apply to temperature and precipitation predictions.

The National Center for Environmental Prediction (NCEP) maintains a Reanalysis Project database (Kalnay et al., 1996), which provides large-scale climate variables that can be used to define analogs with GCMs for climate modeling purposes. In the first step, the statistical characteristics of the observed time series at each station are computed. The time series for the relevant parameters are generated using the observed statistical properties. The long time oscillations are combined with shorter seasonal trends (standard deviations), while mean values are modified using an imposed linear trend (climate change). Short oscillations are superimposed randomly to make the time series more realistic. At least one climate change study involving aquifer modeling used this approach recently (Kruger et al., 2001).

In this project, the NCEP datasets will be used to calibrate the downscaling models, which model site-specific precipitation and temperature based on CGCM1 model outputs.

2.3. REGIONAL CLIMATE MODEL OF WESTERN CANADA

2.3.1. DESCRIPTION

An alternative to downscaling using statistical techniques is the use of a regional climate model (RCM). These numerical models are similar to global climate models, but are of higher resolution, and therefore, contain a better representation of, for example, the underlying topography within the model domain and, depending on the model resolution, may also be able to resolve some of the atmospheric processes that are parameterized in a global climate model (CCIS, 2003a).

A Canadian RCM (CRCM) has been developed through the collaboration of a modeling team at the Université du Québec à Montréal and the CCCma global climate modeling team in Victoria. CRCM has been used in the simulation of current and future climate for western Canada (Laprise et al., 1998; Caya and Laprise, 1999) at a spatial resolution of 45km. The data available are currently for western Canada only. The time periods for which data are available do not correspond to those recommended by the Intergovernmental Panel on Climate Change (IPCC) and are of shorter duration. This means that scenarios constructed from CRCM would not be consistent with those constructed from the global climate models. Very few simulations have been undertaken with CRCM, due mainly to computing costs, and this means that there is only a very small set of data available for use. Therefore, this limits the number of scenarios that can be constructed using CRCM data, and has implications for the exploration of scenario uncertainty (CCIS, 2003a).

2.3.2. THE APPLICATIONS OF THE CRCM

The CRCMs spatial resolution is fine enough to correctly represent climatic processes of small dimensions, such as the formation of clouds or thunderstorms, precipitation, evaporation and soil moisture. A regional climate model is a sub-model embedded within a world-wide model or a GCM. Once the studied area is determined, it must be isolated on the GCM so that the conditions at the boundaries of the region can be determined. These conditions are then introduced in the regional model, which will simulate the climate of the selected domain. Therefore, the regional simulation can take place over any region of the globe.

As an intelligent interpolator, the CRCM can be used to alleviate the lack of climatological observations in foreign regions, to generate chronological climatic series, or to simulate a future climate.

The CRCMs spatial resolution is adequate to evaluate the regional repercussions of climatic changes. As such, the CRCM is a performant previsional tool offered to the numerous ministries, public and private organisms concerned by climate change. With more and more sophisticated and realist simulations, these first line users can develop strategies to prevent (e.g., the Protocol of Kyoto, 1997, aiming to reduce greenhouse gas emission and signed by 84 countries) climate change or to better adapt themselves.

2.3.3. LIMITATIONS OF CRCM

The main limitation of the CRCM, as seen by the authors of this report, is the lack of daily data availability from model runs. Only monthly summaries and climatologies are given to registered members over the internet. To properly evaluate precipitation variability and its changes in the future, daily precipitation is required. Monthly summaries are useful for comparing absolute and relative changes in parameters, such as temperature and precipitation, but not their variability. This would be true only if the CRCM output was representative of local weather, or in other words, if the modeled time series was downscaled to the local conditions. That is not the case with CRCM because the CRCM is only a higher resolution version of CGCM, and as will be demonstrated in this report, CRCM output must still be downscaled to be useful.

In this report, the CRCM monthly summaries will be used to compare to downscaled results. Precipitation, temperature, and solar radiation will be compared for temporal changes in seasonal values between current and predicted climate scenarios. The lack of access to daily CRCM output prevented any downscaling of CRCM results, which would be the preferred choice over the CGCM1, because of higher resolution. These should be attempted to be used in future climate scenario modeling of groundwater if possible.

2.4. DOWNSCALING OF CGCM1 PREDICTIONS

2.4.1. STATISTICAL DOWNSCALING MODEL (SDSM)

Since GCMs have coarse spatial resolution, these atmospheric models are unable to resolve important small scale effects (smaller than GCM grids), such as clouds and topography, which strongly determine the local weather at a site. For example, precipitation data from GCM output has low variability in output values and is never zero, because the precipitation averages the whole 50000 km^2 grid cell. Whereas, at local ground sites, precipitation occurs in discrete events, separated by periods of dry weather. Furthermore, local topography and land cover also contribute to determining precipitation intensities and amounts. Even the higher resolution RCM models do not account for these effects adequately. Downscaling methods attempt to derive local weather from GCM and regional scale predictor variables.

The CICS Statistical DownScaling Model (SDSM), described in Wilby et al. (2002) and the SDSM manual, is a decision support tool for assessing local climate change impacts using a robust statistical downscaling technique for specific sites. The software performs predictor variable pre-screening, model calibration, basic testing, statistical analyses and graphic of climate data. SDSM version 2.3.3. (8 May, 2003) was used in this study.

SDSM requires large-scale predictor variable information in order to derive relationships between the large-scale and local climate. These relationships are developed using observed weather data. GCM-derived predictors are then used to drive these relationships, and thus, obtain downscaled information for the site in question for a number of future time periods. Predictor variable information is supplied here for use with SDSM. In order to operate SDSM all that a user is required to supply is the daily predictand, i.e., station data for the climate variable in question (CICS, 2003). The predicand variable is daily precipitation. The goal is to generate precipitation time series for future climates and compare to a base case climate, thus enabling the estimate of change in precipitation variability and amounts.

There are several limitations of SDSM. Daily precipitation amounts at individual stations continue to be the most problematic variable to downscale, and research is ongoing. This arises because of low predictability of daily precipitation amounts at local scales by regional forcing factors used in regression-based models such as SDSM for downscaling (SDSM manual). The unexplained behaviour is currently modeled stochastically within SDSM by artificially inflating the variance of the downscaled precipitation series to fit with daily observations. The model must be tested independently with a subset of daily precipitation data not used in model calibration. Also, to evaluate the uncertainties, multiple GCM model runs should be used.

2.4.2. METHODOLOGY FOR SDSM

Five data sets were downloaded from CICS website (listed and described in Table 1) for a grid location nearest to Abbotsford. The Calibration data set contains observed daily data for 1961-2000, derived from the NCEP Re-analysis data set (National Centre for Environmental Prediction) (Kalnay et al., 1996) for the period 1961-2000. Most climate modeling experiments in North America use the NCEP datasets for calibration of downscaling models. There were four CGCM1 scenarios, each with data for a number of potential predictor variables. The NCEP dataset includes relative humidity, whereas CGCM1 datasets do not, so specific humidity was used when calibrating the model. The "current climate" scenario was generated by CGCM1 for the period 1961-2000. This was the first greenhouse gas + sulphate aerosol (GHG+A1) experiment undertaken with the CGCM1 global climate model (Boer et al., 2000a). The subsequent "future climate" experiments using CGCM1 with GHG+A1 were for 2020s, 2050s, and 2070s.

Table 1 Data sets for SDSM downscaling scenarios (CICS, 2003)

Dataset	**Years**	**Description**
Calibration	1961-2000	Observed daily data derived from the NCEP Re-analysis data set (National Centre for Environmental Prediction (Kalnay et al., 1996) for the period 1961-2000.
CGCM1_Current	1961-2000	Daily output from the first greenhouse gas + sulphate aerosol experiment undertaken with the CGCM1 global climate model (Boer et al., 2000a) for the period 1961-2000.
CGCM1_2020s	2010-2039	Daily output from the CGCM1 GHG+A1 experiment for the period 2010-2039.
CGCM1_2050s	2040-2069	Daily output from the CGCM1 GHG+A1 experiment for the period 2040-2069.
CGCM1_2080s	2070-2099	Daily output from the CGCM1 GHG+A1 experiment for the period 2070-2099.

Once all input data files were prepared for SDSM, analysis began. The general steps in downscaling using SDSM are:

1) Quality control and data transformation
2) Selection of downscaling predictor variables
3) Model calibration using selected predictor variables
4) Generation of weather scenario (20 ensemble runs)
5) Analysis of observed and downscaled data
6) Generation of climate change scenarios
7) Analysis of scenario results and comparison to observed

Data quality and transformations

During quality control, all file formats are verified, missing data counted, and length of time series checked against start and end dates and number of days in a year. Quality analysis summaries and types of transformations performed in SDSM on daily data are shown in Table 2 (after trying several combinations). Incidentally, the same values were used in SDSM manual for sample model runs.

Table 2 Data quality and transformations in SDSM for precipitation and temperature.

	Precipitation	Temperature
Interval	daily	daily
Transformation	4th root	-
Variance inflation	15	11
Bias correction	0.80	.90
Event threshold	0	-
Number of days	14583	14581
Missing	28	30

Precipitation time series of daily values was transformed by 4^{th} root because such transformation "normalizes" the precipitation distribution (histogram) the best. This was verified by computing histograms of precipitation values for untransformed and transformed values using log, 4^{th} root, 1/x, and other options. The precipitation distribution is highly skewed toward low precipitation values (most frequent). After 4^{th} root transformation, the distribution was much less skewed. For temperature, no transformation was selected because of relatively normal distribution of daily temperatures.

During model calibration, through an iterative process of model fitting and plotting of analyzed results and comparing to observed, the precipitation variance was "inflated" using the inflation function at value of 15 with bias correction of 0.8. For precipitation, the event threshold was set at 0 (only consider days with precipitation in analysis). Variance inflation for temperature was less than precipitation; at 11. Bias correction was 0.9. Missing days were mostly for year 2000 because the original dataset only included 1961 to 1999, and the additional year was not downloaded due to problems with ECS website and time constraints, but should not make much difference in model calibration (the appropriate NCEP and CGCM1 datasets would be used for 1961-1999 only, omitting the last year in SDSM). Year length and standard start dates were adjusted depending on CGCM1 scenario (as described in CICS, 2002). Note that CGCM1 has 365 days in each year, i.e., leap years are not included, while calibration and observed data include leap years. The SDSM software accounts for this. All predictors, with the exception of wind direction, have been normalized with respect to the 1961-1990 mean and standard deviation (CICS, 2002).

Selection of predictor variables

Selecting the appropriate downscaling predictor variables is the most critical part of this whole process. There are 26 predictor variables for SDSM use provided by CICS; which are meteorological variables generated from CGCM1 model runs for the grid square (listed in Table 3). Multiple regression with the predicant variable (e.g., precipitation) are run, a correlation matrix produced, and several of the predictor variables that are the most correlated with the predicant (and are statistically significant, low p-value, $p < 0.05$) are selected – this is done on a monthly basis. The type of "process" (unconditional for temperature, and conditional for precipitation – where amounts depend on wet-day occurrence) is selected.

Different variables were selected for modeling precipitation and temperature, which is expected because of different atmospheric forcings on P and T, and different correlations with synoptic conditions, and thus, CGCM1 variables. The choice of variables is described in Table 3.

Model calibration (precipitation)

The results of predictor variable screening and selected best predictors for precipitation and temperature are listed in Table 3. The associated partial correlation coefficients and p-values monthly for predictor variables are shown in Table 4 for precipitation and Table 5 for temperature for Abbotsford, BC. These are the downscaling calibration results from CGCM1 using SDSM.

At Abbotsford, the daily precipitation was explained by mean sea level pressure (Mslp), specific humidity at 500 hPa height, zonal velocity component at 500 hPa height and near surface meridional velocity component. This would suggest that at CGCM1 grid scales for the central to eastern BC region, the precipitation events are associated with changes in mean sea level pressure, changes in humidity, and flow components, where as the meridional velocity component had the highest partial correlation with observed precipitation. Overall, these four predictor variables were the most useful for linking CGCM1 atmospheric variables to local precipitation at Grand Forks.

At Abbotsford, the local climate is similar to regional climate of the SW coast of British Columbia. The area experiences some increase in precipitation due to orographic effects, but the occurrence of precipitation and also air temperature are strongly controlled by weather systems arriving from the Pacific Ocean. The weather at this location is therefore similar to that modeled in the regional CGCM1 grid cell. As a result, the monthly r values are reasonably high and p-values are less than the 0.05 significance level for most months. When aggregated to seasonal precipitation, more days result in more degrees of freedom and r values are higher and significant at 0.05 level. Thus, seasonal precipitation trends are similar to regional CGCM1 predictions, but this breaks down somewhat on monthly time scales. Seasonal values mean more averaging-out of local weather effects and producing less meaningful regional trends.

The mean sea level pressure and specific humidity were useful as summer precipitation predictors, but the correlations were weaker than in other seasons (it's the season with lowest precipitation at this site). During the spring season, precipitation at Abbotsford was linked to CGCM1 through mostly mean sea level pressure and specific humidity values. In the winter the specific humidity and zonal velocity component, both at 500 hPa height, were the most useful, where as in autumn the mean seal level pressure became more important.

Table 3 Predictor variables for SDSM downscaling, generated from CGCM1 model runs.

Variable name	Description	Precipitation	Temperature
Temp	Mean temperature		✓
Mslp	Mean sea level pressure	✓	
p500	500 hPa geopotential height		✓
p850	850 hPa geopotential height		
Rhum	Near surface relative humidity		
Shum	Near surface specific humidity		✓
s500	Specific humidity at 500 hPa height	✓	
s850	Specific humidity at 850 hPa height		
**_f	Geostrophic airflow velocity		
p5_z	Vorticity at 500 hPa height		✓
**_z	Vorticity		
p_u	Zonal velocity component (near surface)		
p5_u	Zonal velocity component (at 500 hPa height)	✓	
p_v	Meridonal velocity component (near surface)	✓	
p5_v	Meridonal velocity component (at 500 hPa height)		
p8_u	Zonal velocity component (at 850 hPa height)		
p8_v	Meridonal velocity component (at 850 hPa height)		
**th	Wind direction		
p_zh	Divergence		
**zh	divergence		

** indicates p_ = near surface, p5_ = at 500 hPa height, p8_ = at 850 hPa height

Table 4 Correlations of predictor variables (monthly) for SDSM downscaling with daily precipitation for Abbotsford area. Variables are partial correlation coefficients (r) and probability (p) values are shown in rows; two highest r-values are highlighted in bold for each month, showing the most influential variables correlated to temperature. Seasonal r and p values are also shown because many of the monthly stats are below 0.05 significance level.

			Winter			Spring			Summer			Autumn		
			Dec	Jan	Feb	Mar	Apr	May	Jun	Jul	Aug	Sep	Oct	Nov
mslp	monthly	r	-0.20	-0.15	-0.17	**-0.15**	**-0.19**	**-0.14**	**-0.12**	**-0.10**	**-0.10**	**-0.13**	**-0.17**	**-0.22**
		p	0.00	0.00	0.00	0.00	0.00	0.00	0.00	0.00	0.00	0.00	0.00	0.00
	seasonal	r	-0.17			-0.15			-0.10			-0.16		
		p	0.00			0.00			0.00			0.00		
p_v	monthly	r	0.15	0.12	0.02	0.15	**0.15**	**0.13**	**0.13**	0.07	0.05	**0.11**	0.12	0.14
		p	0.00	0.00	0.43	0.00	0.00	0.00	0.00	0.04	0.13	0.00	0.00	0.00
	seasonal	r	0.10			0.14			0.08			0.13		
		p	0.00			0.00			0.00			0.00		
p5_u	monthly	r	**0.22**	**0.23**	**0.19**	0.15	0.14	0.05	0.02	0.02	0.03	0.05	**0.13**	0.21
		p	0.00	0.00	0.00	0.00	0.00	0.11	0.49	0.41	0.31	0.15	0.00	0.00
	seasonal	r	0.21			0.11			0.02			0.14		
		p	0.00			0.00			0.20			0.00		
s500	monthly	r	**0.25**	**0.22**	**0.22**	**0.21**	0.11	0.10	0.06	**0.11**	**0.07**	0.05	0.08	**0.21**
		p	0.00	0.00	0.00	0.00	0.00	0.00	0.05	0.00	0.04	0.10	0.01	0.00
	seasonal	r	0.23			0.15			0.08			0.11		
		p	0.00			0.00			0.00			0.00		

Table 5 Correlations of predictor variables (monthly) for SDSM downscaling with daily mean temperature for Abbotsford, BC. The variables are partial correlation coefficients (r) and probability (p) values are shown in rows; two highest r-values are highlighted for each month, showing the most influential variables correlated to temperature.

		Winter			Spring			Summer			Autumn		
		Dec	Jan	Feb	Mar	Apr	May	Jun	Jul	Aug	Sep	Oct	Nov
p5_z	r	0.08	0.03	0.01	0.07	0.08	0.09	0.14	0.08	0.16	0.26	0.11	0.08
	p	0.01	0.27	0.00	0.03	0.02	0.00	0.00	0.02	0.00	0.00	0.00	0.01
p500	r	0.10	0.13	0.30	0.39	0.48	0.60	0.64	0.57	0.64	0.56	0.24	0.15
	p	0.00	0.00	0.00	0.00	0.00	0.00	0.00	0.00	0.00	0.00	0.00	0.00
sphu	r	0.02	0.17	0.14	0.11	0.30	0.31	0.27	0.09	0.22	0.23	0.10	0.13
	p	0.40	0.00	0.00	0.00	0.00	0.00	0.00	0.00	0.00	0.00	0.00	0.00
Temp	r	0.81	0.15	0.19	0.12	-0.13	-0.24	-0.21	0.01	-0.15	-0.09	0.17	0.24
	p	0.00	0.00	0.00	0.00	0.00	0.00	0.00	0.56	0.00	0.01	0.00	0.00

Model calibration (temperature)

Temperature was downscaled from CGCM1 using mean temperature predictor variable and few other supporting variables that increased the prediction through their partial correlation with observed temperature. Note that the mean temperature variable in CGCM1 is regional and is an average of the large model grid cell. Nevertheless, this is much an improvement over precipitation because CGCM1 does not model precipitation directly (at least not in the dataset provided by CICS for downscaling). Other supporting predictors were 500 hPa geopotential height, near surface specific humidity, and vorticity at 500 hPa height.

At monthly time scale, the 500 hPa geopotential height (and not the mean temperature in CGCM1 grid cell) was usually the best predictor of observed near surface temperature, but not in all months, when other predictors were important. At Abbotsford, temperature had high r-values to observed temperature (from November to December, best in December) and most were significant at 0.05 level (and even at 0.001 level), except in June, which is typically rainy month in summer at Abbotsford. Negative correlation coefficients for spring and summer season temperature in the grid cell indicate that regional temperature in that grid cell in CGCM1 model, mostly over the ocean, is not useful in predicting surface temperatures at Abbotsford.

Generation of weather scenario

Four scenarios were generated: current climate, 2020's climate, 2050's climate, and 2080's climate (as discussed previously). Predictor daily data sets were automatically selected from the corresponding CGCM1 outputs in SDSM, as defined during variable screening process. Daily data sets were generated for each scenario. All results were analyzed in SDSM, and appropriate monthly statistics were generated. For precipitation these were: mean, median, max, variance, dry and wet spell length, and % wet days. Note that minimum precipitation is always zero, so it was not analyzed. For temperature the statistics were: mean, median, min, max, variance, and inter-quartile range. After each scenario run, the statistics were compared in SDSM using graphs to observed datasets.

Analysis of observed and downscaled data

The daily precipitation time series were analyzed using conditional option, thus only WET days were taken into account. For the purpose of graphical displays, and later for inputs to the stochastic weather generator, the mean daily precipitation was converted to mean monthly precipitation, and then converted to mean monthly precipitation for all days in the month by multiplying by % of wet days in a month. Thus, the shown precipitation monthly means are comparable to observed normals, which are generally calculated based on the entire month (i.e. not only on wet days). For each month:

[Mean Monthly Ppt WET] **=** [Mean Daily Ppt WET] **x** [Number of Days in Month]
[Mean Monthly Ppt ALL] **=** [Mean Monthly Ppt WET] **x** [% Wet Days in Month]

where ALL refers to all days in month, WET refers to only days with Ppt > 0 in a month.

The resulting statistics and daily output were imported to a pre-programmed spreadsheet, which computes monthly total precipitation values (from mean daily values for each month), coverts to WET and DRY precipitation averages for comparing to observed, graphs all results by variable and month (grouped by SDSM outputs and compares to “PCA k-nn outputs” – see next section), computes % error for calibration bias, and model bias to observed. It also includes custom codes for exporting and file formatting of SDSM results to LARS-WG format for subsequent stochastic weather generation.

2.4.3. DOWNSCALING RESULTS FROM ENVIRONMENT CANADA

Downscaling was also undertaken using a different method, and the results compared to SDSM. The Environment Canada downscaled data set was provided by Whitfield (personal communication, 2002), based on precipitation and temperature downscaling methodology used for the Georgia Basin Study by Whitfield et al. (2002). The downscaled daily precipitation time series was computed for Abbotsford for the time period 1961 to 2099, from which “scenario” data sets were extracted to compare with other results.

The details and most references for the methodology are provided in Whitfield et al. (2002). In essence, future temperature and precipitation conditions at the stations were estimated using analog downscaling models (Barnett and Preisendorfer, 1978), forced by atmospheric circulation fields from CGCM. Large-scale climate variables used to define analogs with CGCM variables were taken from the NCAR/NCEP reanalysis model database (Kalnay et al., 1996). To help speed the downscaling process and to remove redundant variables, the dimension of the large-scale climate dataset was further reduced using principal component analysis (PCA). Time-series of variables at each grid-point were first standardized to have zero mean and unit standard deviation over the 1971-1995 period (note that in SDSM, the calibration and scenario data were also standardized). A *k*-nearest neighbour (*k*-nn) model was used to link principal component scores of the climate fields with the maximum temperature, minimum temperature, and precipitation series from Danard and Galbraith’s (1997) dataset. In the *k*-nn model, predictions are made by selecting the *k* days from the historical dataset that most closely resembles the current day’s climate conditions. Prior to comparison, modeled temperature series were rescaled so that the modeled and observed means and standard deviations were equal (Huth et al., 2001). For precipitation, model outputs were inflated by multiplying by the ratio of the observed and predicted means. This preserves total precipitation amounts, but leads to a slight underestimation of precipitation variance. Hereafter, the Whitfield et al. (2002) method for downscaled precipitation time series is referred to as principal-component k-nearest neighbour method (PCA k-nn).

3. DOWNSCALING RESULTS AND CGCM1 PREDICTED CLIMATE SCENARIOS

3.1. CLIMATE NORMALS

The observed climate dataset comprises monthly normals as shown in Table 6 and Figure 1 measured at the Abbotsford International Airport.

Table 6 Climate Normals for Abbotsford International Airport (Environment Canada). Precipitation statistics rounded to the nearest mm.

	Jan	Feb	Mar	Apr	May	Jun	Jul	Aug	Sep	Oct	Nov	Dec	Year
Temperature:													
Mean Temperature	2.6	4.7	6.8	9.5	12.5	15.1	17.5	17.7	15	10.2	5.7	2.8	10
Standard Deviation	2.2	1.8	1.4	1.2	1.3	1.2	1.1	1.2	1.3	0.9	1.9	1.9	A
Max. Temperature (°C)	5.8	8.5	11.3	14.5	17.8	20.3	23.4	23.8	21	15	9.1	5.9	14.7
Min. Temperature (°C)	-0.6	0.8	2.3	4.4	7.2	9.9	11.5	11.5	8.8	5.4	2.3	-0.3	5.3
Extreme Max. (°C)	17.7	20.6	24.9	29.8	36	34.7	37.8	36.3	37.5	29.3	20.6	18.2	37.8
Date (yyy/dd)	986/ 10	968/ 27	994/ 28	998/ 30	983/ 29	982/ 18	958/ 27	977/ 17	988/ 03	987/ 01	949/ 02	980/ 26	958/ 27
Extreme Min. (°C)	-21.1	- 18.9	- 12.8	-4.4	-2.2	1.1	2.2	3.3	-1.7	-7.5	-16.7	-20	-21.1
Date (yyy/dd)	950/ 18	950/ 01	955/ 04	975/ 01	954/ 01	976/ 03	945/ 04	947/ 19+	972/ 27	984/ 31	985/ 27	968/ 29	950/ 18
Precipitation:													
Rainfall (mm)	174	148	142	120	99	79	50	49	76	145	234	191	1508
Snowfall (mm w.eq.)	23	13	4	0	0	0	0	0	0	0	6	17	64
Precipitation (mm)	197	161	146	120	99	79	50	49	76	145	240	208	1572
Mean Snow Depth (cm)	2	1	0	0	0	0	0	0	0	0	0	1	0
Median Snow Depth	0	0	0	0	0	0	0	0	0	0	0	0	0
Snow Depth at Month-end	1	0	0	0	0	0	0	0	0	0	0	4	1

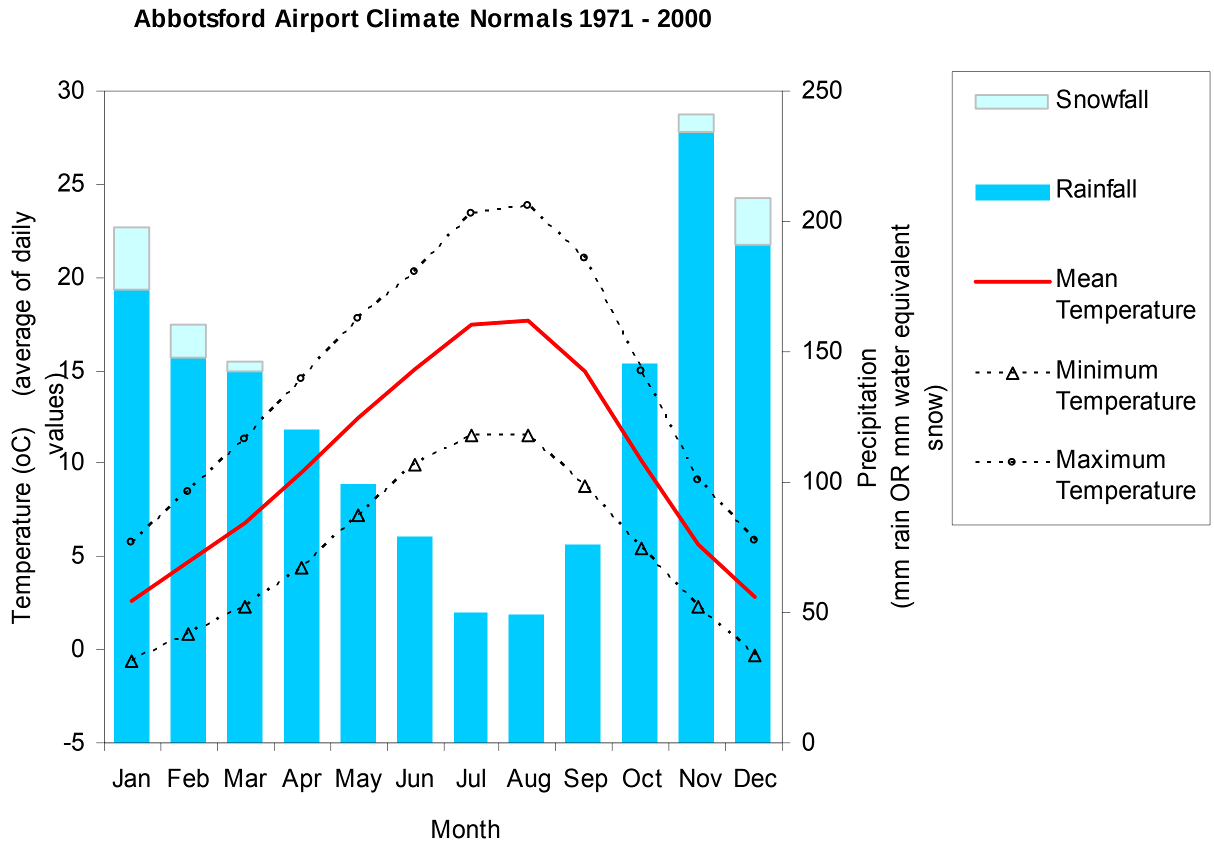

Figure 1 Climate normals for Abbotsford International Airport.

3.2. PRECIPITATION VARIABLES

Precipitation time series were analyzed for the following variables:

1) mean monthly precipitation
2) standard deviation in daily precipitation
3) wet days %
4) dry series length
5) wet series length

3.2.1. ABSOLUTE CHANGE GRAPHS AND MODEL CALIBRATION GRAPHS

Results are arranged by variable (e.g., mean monthly precipitation, standard deviation of precipitation, % wet days, dry spell length, wet spell length), thus giving 5 sets of "grouped" graphs. For each variable, there are two figures. One figure has two graphs comparing results for the two downscaling methods (SDSM and PCA k-nn). The second figure, placed lower, compares the observed variable values to those modeled, and presents two smaller graphs of model performance: 1) calibration bias of NCEP dataset to observed, and 2) base case scenario bias of current climate CGCM1 downscaled results to observed, all for the same time period 1961-2000.

The graph sets are colour-coded and are arranged identically for easy inter-comparison between different variables. All graphs show monthly statistics (on x-axes). The mean precipitation and other variables are graphed as monthly time series on the y-axes. The observed data are always graphed as background fill (area graph), while the downscaled results are line graphs, superimposed on observed data graph. The styles and colours of line graphs are always the same for each climate scenario (e.g. 2010-2039) on all graphs. The model bias graphs are also colour-coded and scaled similarly for easy inter-comparison.

Before looking at predicted changes in precipitation and temperature, it is important to examine the calibration results, and keep in mind the limitations and any model bias. Therefore, these are discussed first.

3.2.2. RELATIVE CHANGE GRAPHS

Another way of looking at temporal change in precipitation from current to future climate scenarios is to look at relative change, as shown in Figure 12 for downscaled precipitation and Figure 13 for raw CRCM data (not downscaled but better than raw CGCM1 data). Note that relative values for future climates are shown in temporal order, but values are not cumulative, or in other words, the precipitation for the future climate scenario is compared to present climate (this is not a cumulative precipitation change graph).

relative change in Ppt = current Ppt / future Ppt

Similarly, other variables are calculated for relative change graphs, such as standard deviation in precipitation, % WET days, and others. All relative precipitation changes are relative to current climate from CGCM1 model run; values less than 1.0 mean a decrease in precipitation, and above 1.0 mean an increase in precipitation relative to current (1961-2000).

3.2.3. PRECIPITATION VARIABILITY

The SDSM model calculated the variance of daily precipitation, which was converted to standard deviation (stdev = sqrt (variance)) because the LARS-WG requires standard deviation of precipitation as input for climate scenario modeling. Precipitation variability refers to distribution of precipitation daily values. The distribution is typically logarithmic and definitely not "normal" in shape. The variance and standard deviation statistics are for such highly skewed distribution. When variance in precipitation changes, the relative frequencies of small precipitation events as compared to larger ones also change. This is the meaning of precipitation variance in this case.

3.2.4. WET AND DRY SPELLS AND % WET DAYS

Wet and dry spells are required in the serial stochastic weather generator to construct the precipitation time series. Thus, the downscaling results are rather important here. Wet spells model the duration of rain events (where wet spell length refers to number of consecutive days with non-zero precipitation or at least higher than 0, and trace amount is considered as positive rainfall here).

3.3. CLIMATE SCENARIOS: PRECIPITATION

3.3.1. MEAN MONTHLY PRECIPITATION

Monthly graphs of mean precipitation (Figure 2) show relatively good fit between the CGCM1-predicted and downscaled with SDSM precipitation and observed normals. SDSM overestimates rainfall in November, but is relatively close to observed in other months. The SDSM model has low calibration bias (about -8%) to standard NCEP dataset (Figure 3). Thus, for Abbotsford, the CGCM1 model was able to adequately predict current climate in terms of monthly precipitation means. There is some "model bias" between the CGCM1 output and current observed. Summer precipitation is about 30% underestimated, and some autumn rainfall is overestimated by 20%, but in 5 other months the model bias was close to zero, which is very good in light of fundamental limitations of CGCM1.

The PCA k-nn downscaling (Environment Canada, 2003) of the same dataset for the same location gave very similar results than SDSM downscaling. PCA k-nn performed better for late autumn than SDSM, but was not as good in other months. The temporal changes of precipitation are similar in magnitude, but often opposite in direction (sign). Overall, both downscaling methods agree rather well on mean monthly precipitation for Abbotsford for current and future climate scenarios for most months (that there is little temporal change predicted).

The relative change summaries were grouped seasonally (Figure 12) at first. At Abbotsford, precipitation is predicted to increase in the summer at an increasing rate of change into the future according to SDSM results, and will end up 1.2 times larger than present monthly values. However, PCA k-nn analysis showed a different trend (as was noted on monthly graphs previously), where precipitation will decrease in the future in the summer. The two downscaling models also disagree on winter precipitation (decrease into future according to SDSM but increase as per PCA k-nn method). Spring and autumn precipitation will remain relatively close to present although PCA k-nn predicted short term increase in autumn precipitation (into 2020s). Which downscaling method is to be trusted?

One way of analyzing the results is to look at raw CRCM outputs (Figure 13 - not downscaled). CRCM predicts that precipitation will decrease in the summer (as PCA k-nn method downscaled from CGCM1 suggested, but only for 2020s and then increase into 2080s as predicted by SDSM downscaling), remain constant in spring and winter to 2020s then increase, and initially increase in autumn, but then decrease (similar to PCA k-nn downscaling results). Thus, CRCM output tends to agree more with PCA k-nn results that at least until 2050s precipitation will decrease in the summer. However, CRCM precipitation has a very large grid cell and does not represent local conditions at Abbotsford, so such comparisons are questionable.

The full story lies with monthly trends in precipitation as shown in Figure 14. Precipitation relative changes were graphed monthly for SDSM results – seasonal average is also plotted. In the spring months three months (March to May) have very similar trends. In the summer, precipitation will increase in all months, but more in July and August than in June (which is transition from spring to summer regime). In autumn, precipitation will remain similar to present although with slight initial increase in Sep – Oct period in 2020s, but then decline in later part of century. In winter, precipitation will decrease in all months to about 80% of current levels. The monthly trends for PCA k-nn method (Figure 15) show a slightly wider range in monthly variation in precipitation predictions, but the seasonal trends are representative of the three months in each season group. The monthly variability in precipitation predictions follows the seasonal trends, but there are important inter-monthly differences that should not be averaged out or ignored in seasonal trends.

Finally, what is the precipitation change as modeled by CGCM1 for Abbotsford? At this time, both the SDSM and the PCA k-nn methods disagree on the trends in precipitation, but agree that the changes will be relatively small (within 10% of present values for most months). Still, large uncertainties exist in actual precipitation forecasting ability of GCMs and the ability to downscale to local conditions, and thus, quantify relative and absolute changes in precipitation. Both SDSM and PCA k-nn results will be used in stochastic weather generator to create daily precipitation series for Abbotsford as two separate sets of climate scenarios. Note that the ranges of precipitation increase are quantified by the downscaled results to within 20% of current climate, the differences are in seasonal and monthly details, which cannot be resolved in favour of either method at this time.

3.3.2. PRECIPITATION VARIABILITY

The figures and results are arranged similarly to monthly precipitation amounts. The monthly precipitation variability, as estimated by standard deviation of daily values in the time series, is plotted in Figure 4. The SDSM results again fit better the observed precipitation variability than PCA k-nn results, which underestimates observed variability more severely. The predictions are similar in magnitude, but not direction among the two methods of downscaling. The SDSM model was relatively well calibrated to NCEP data, with slight overestimation of variability in spring, and up to 20% underestimation in mid-summer, but overall less than 10% calibration error to NCEP dataset. The downscaled variability if precipitation is very similar to observed, supporting the results of SDSM. The relative change in precipitation variability was graphed in Figure 16. As formerly stated, the SDSM predictions show almost no change from present, while PCA k-nn shows large decrease in variability of precipitation in the summer, and a small increase in spring after 2020's, but little change in winter and autumn.

3.3.3. WET DAYS, DRY SPELLS AND WET SPELLS

Monthly % of wet days indicates how often it rains in that month. It is an indirect measure of both frequency and duration of precipitation events, but does not indicate precipitation amount. As such indicator, it was downscaled and graphed as monthly averages in Figure 6. Both downscaling methods performed similarly well, although SDSM was closer to observed in winter and summer months than PCA k-nn. The SDSM model was very well calibrated to NCEP data set (Figure 7). Summer months were underestimated in % wet days by about 20% compared to observed, and other months were usually well matched to observed. Figure 17 shows relative changes in % wet days. To be consisted with predicted increase in mean monthly precipitation in the summer months, the SDSM also indicated an increase in % wet days in summer months into the future. In other seasons the changes were small and similar to present values. PCA k-nn model showed a large decrease in summer months of % wet days, in contrast to SDSM, but both downscaled results show a small decrease in % wet days in spring, and disagree on winter and autumn (opposite but small changes – close to present climate).

The dry spell lengths (Figure 8) were well represented by downscaled CGCM1 outputs. The available CGCM1 predicant variables were able to predict the shape of annual distribution of dry spell lengths, but the downscaled model in SDSM had on average -30% difference to NCEP dataset (Figure 9). The monthly trends of DRY spell length were similar to observed, but usually 40% lower in most months (except May to July). The PCA k-nn downscaling gave similar results to SDSM. Magnitudes of temporal changes in DRY spell lengths for future climates were relatively small in SDSM results, but larger for summer and autumn months in PCA k-nn results.

Both downscaled sets of results agree that in spring and winter the DRY spell length will not change in the future significantly (Figure 18). SDSM predicted a decrease in summer and autumn (again consistent with its prediction of precipitation increase), and PCA k-nn predicted an increase in summer, spring, and autumn, but a variable trend with no long-term change in winter. The downscaling methods totally disagree on DRY spell length predictions for Abbotsford, thus there is large uncertainty about what DRY spell length will do in the future as described here.

WET spell lengths were downscaled with similar results in SDSM and PCA k-nn algorithms. Both underestimate seriously the length of WET spells of actual (Figure 10). The PCA k-nn method of downscaling produced much better results (closer to observed) than did SDSM, which had over -40% calibration error to NCEP dataset and even larger model bias to observed (Figure 11). Both sets of results underestimated summer WET spell lengths by about 50%, but fitted autumn ones much better. SDSM was not good at modeling winter and spring WET spell lengths but PCA k-nn was very good for that time period.

In relative change graphs (Figure 19), both sets of downscaling results show that WET spell length will be lower than present during spring (by about 10%), but show opposite trends for winter (SDSM suggests about 20% decrease while PCA k-nn suggests 15% increase). Summer and autumn WET spells did not change much in 2020's from present but then were variable depending on downscaling method.

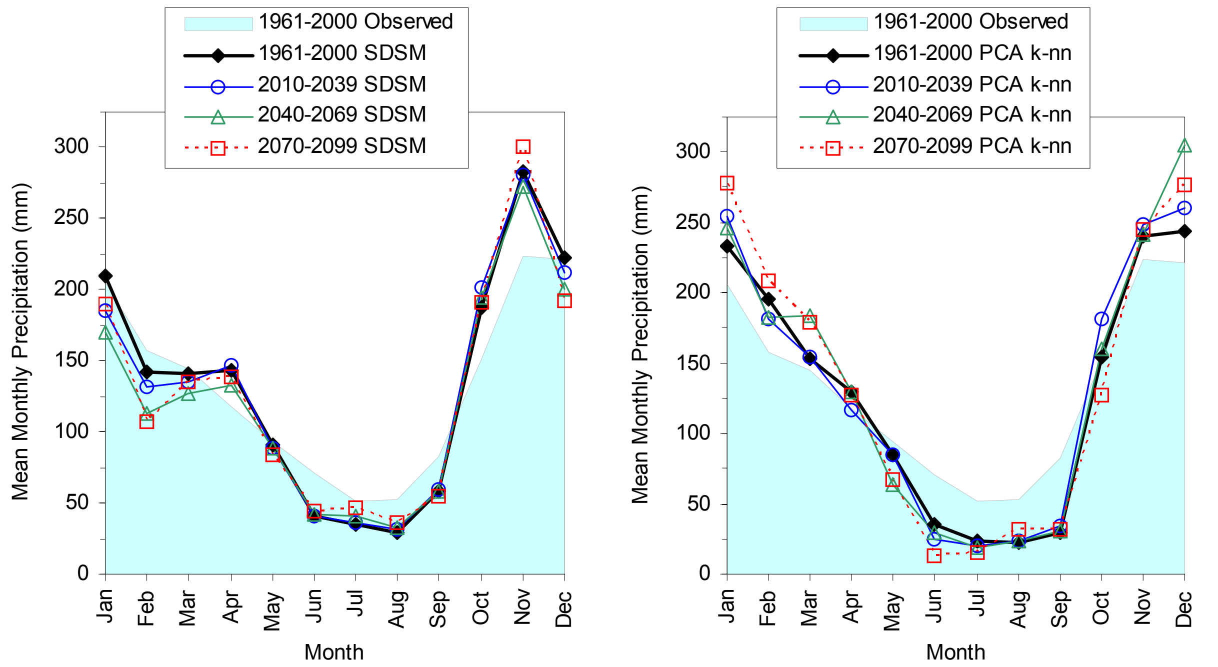

Figure 2 Mean monthly **precipitation** at Abbotsford, BC: observed and downscaled from CGCM1 model runs for current and future climate scenarios using two downscaling methods: (a) SDSM, (b) PCA k-nn.

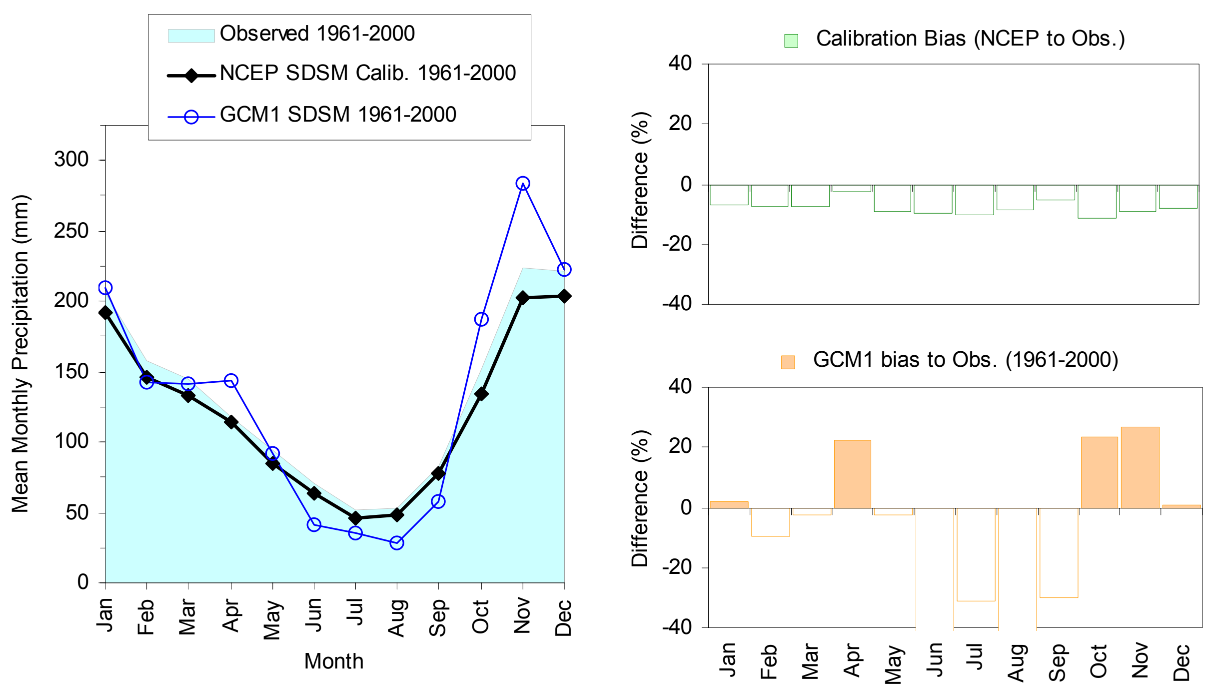

Figure 3 Comparing observed and downscaled **precipitation** at Abbotsford, BC. SDSM downscaling model performance: (a) monthly precipitation, (b) calibration bias, (c) bias between SDSM downscaled CGCM1 Current precipitation and observed.

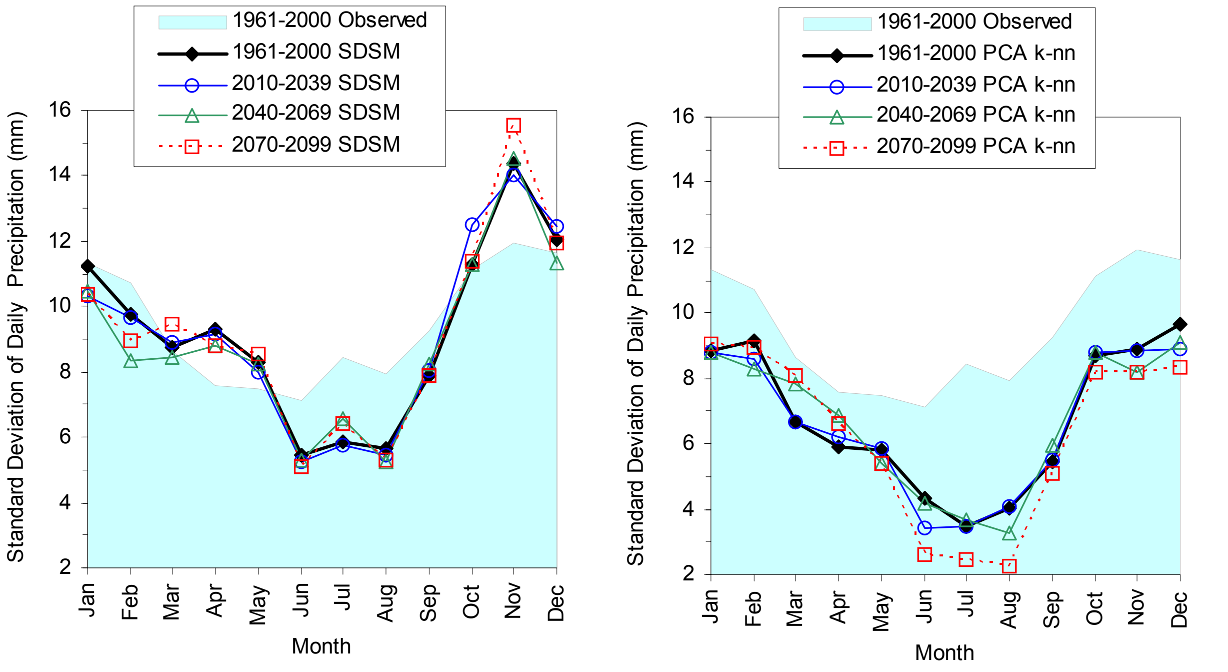

Figure 4 Mean monthly **standard deviation of precipitation** at Abbotsford, BC: observed and downscaled from CGCM1 model runs for current and future climate scenarios using two downscaling methods: (a) SDSM, (b) PCA k-nn.

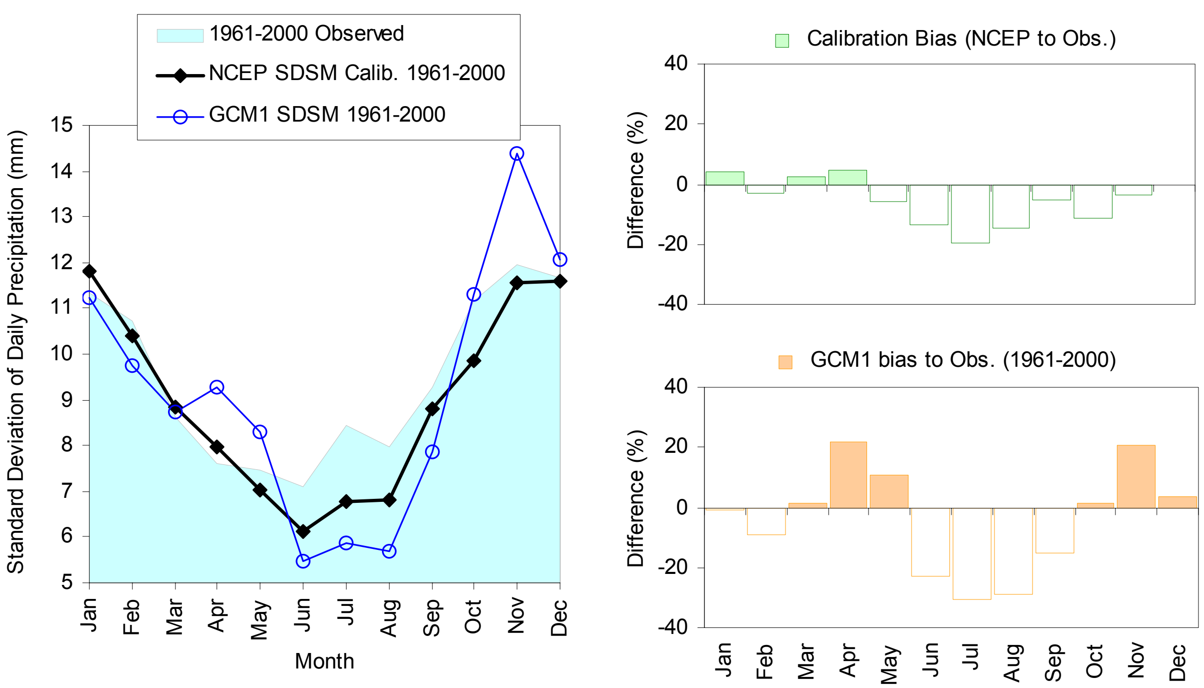

Figure 5 Comparing observed and downscaled **standard deviation of precipitation** at Abbotsford, BC. SDSM downscaling model performance: (a) monthly variance in precipitation, (b) calibration bias, (c) bias between SDSM downscaled CGCM1 Current variance in precipitation and observed.

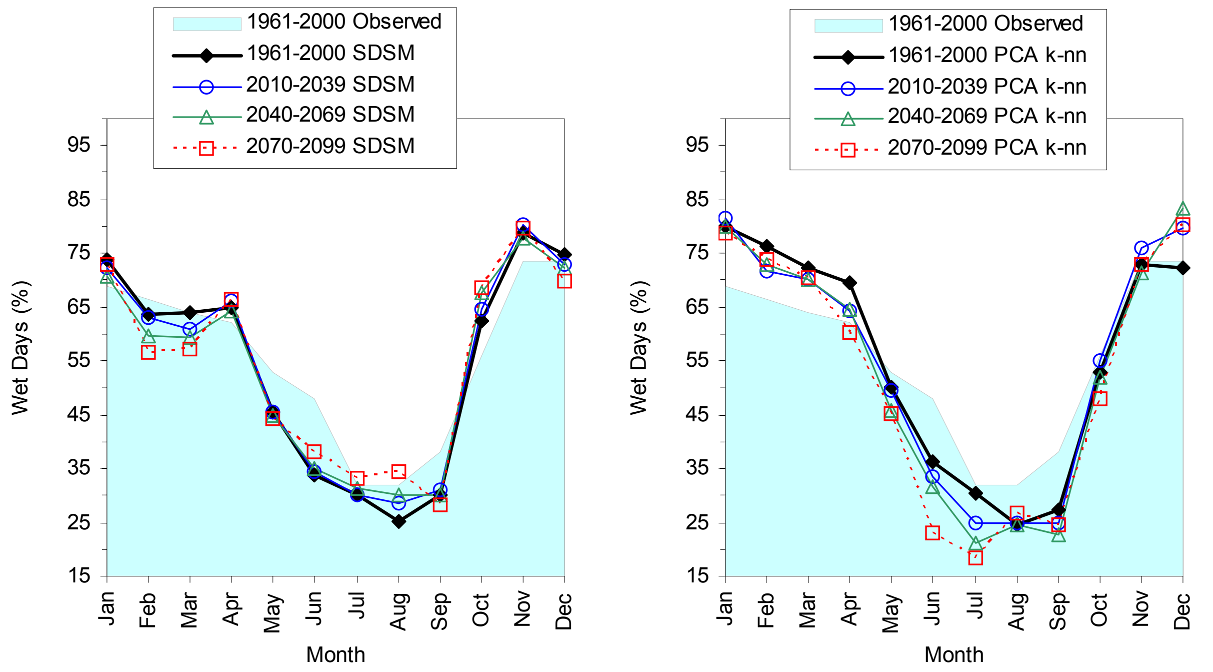

Figure 6 Mean monthly **% WET days** at Abbotsford, BC: observed and downscaled from CGCM1 model runs for current and future climate scenarios using two downscaling methods: (a) SDSM, (b) PCA k-nn.

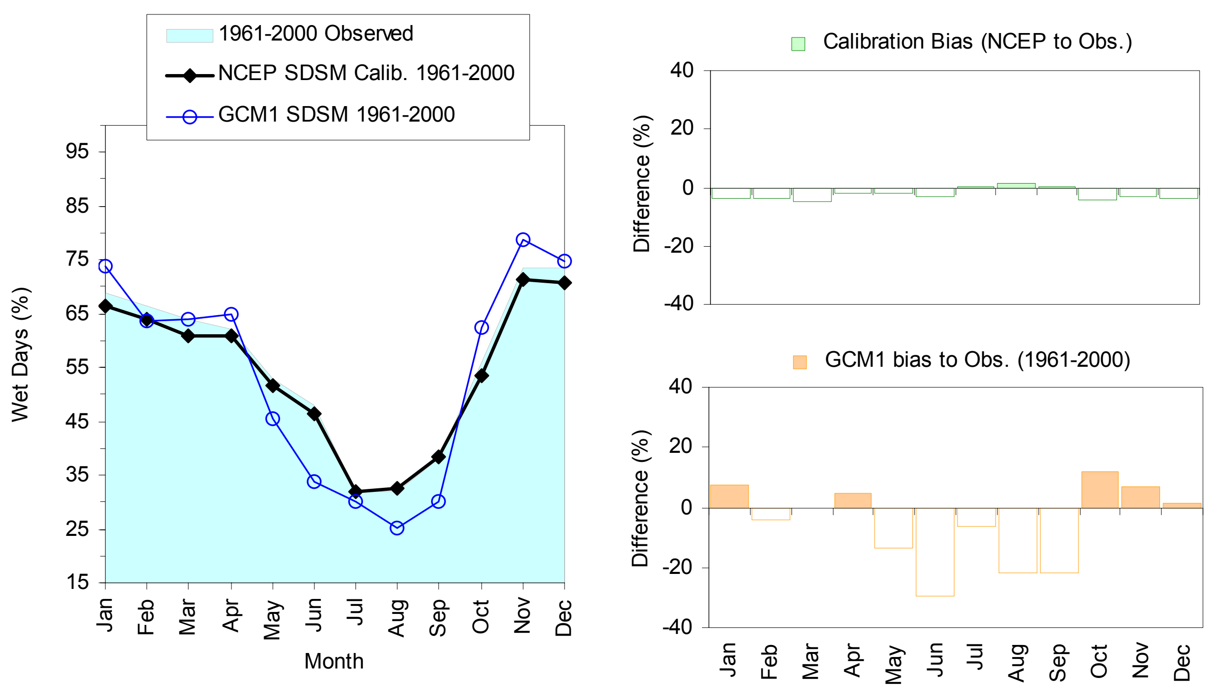

Figure 7 Comparing observed and downscaled **% WET days** at Abbotsford, BC. SDSM downscaling model performance: (a) monthly % WET days, (b) calibration bias, (c) bias between SDSM downscaled CGCM1 Current % WET days and observed.

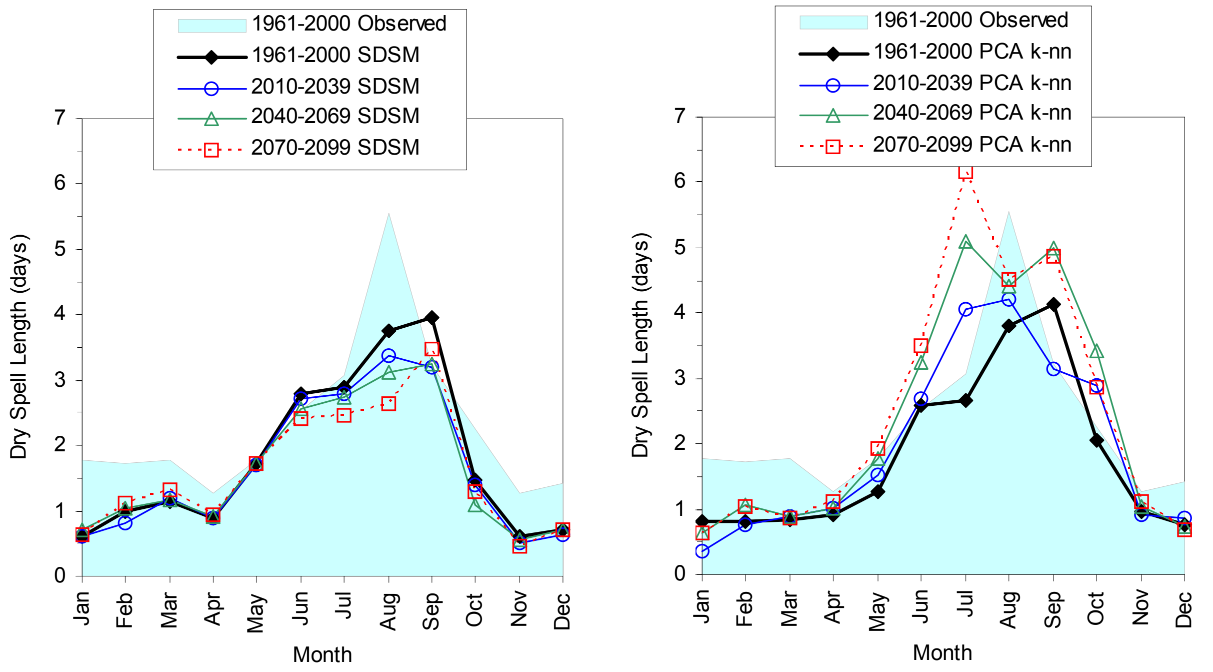

Figure 8 Mean monthly **DRY spell length** at Abbotsford, BC: observed and downscaled from CGCM1 model runs for current and future climate scenarios using two downscaling methods: (a) SDSM, (b) PCA k-nn.

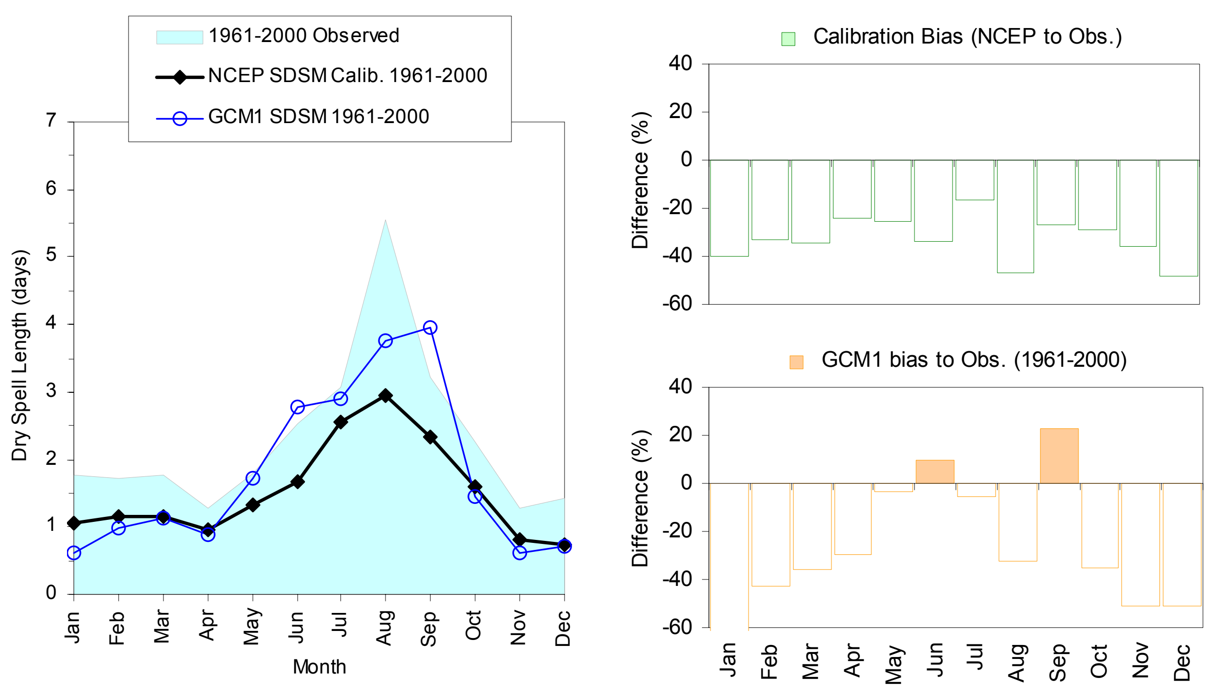

Figure 9 Comparing observed and downscaled **DRY spell length** at Abbotsford, BC. SDSM downscaling model performance: (a) monthly DRY spell length, (b) calibration bias, (c) bias between SDSM downscaled CGCM1 Current DRY spell length and observed.

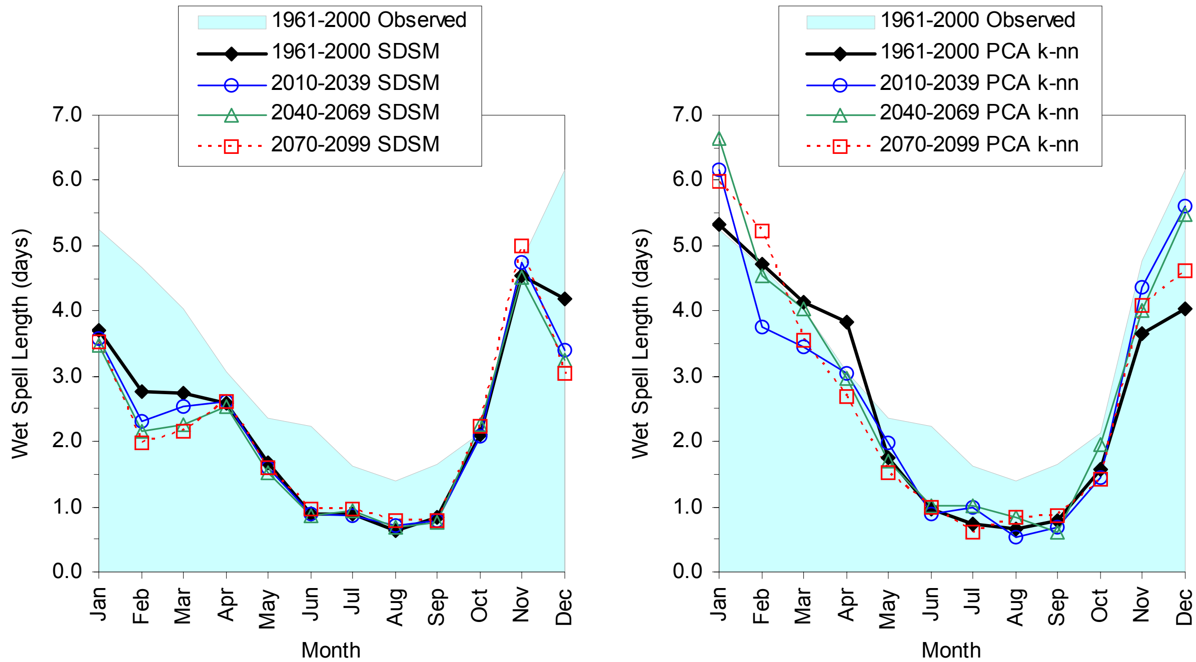

Figure 10 Mean monthly **WET spell length** at Abbotsford, BC: observed and downscaled from CGCM1 model runs for current and future climate scenarios using two downscaling methods: (a) SDSM, (b) PCA k-nn.

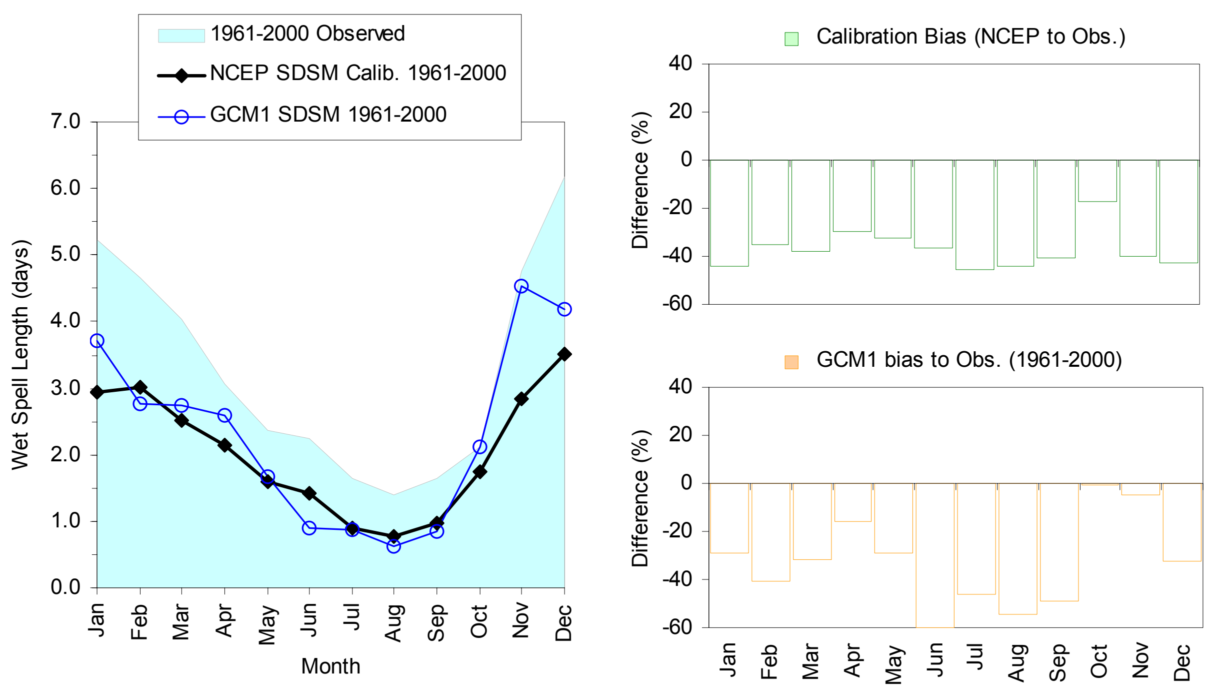

Figure 11 Comparing observed and downscaled **WET spell length** at Abbotsford, BC. SDSM downscaling model performance: (a) monthly WET spell length, (b) calibration bias, (c) bias between SDSM downscaled CGCM1 Current WET spell length and observed.

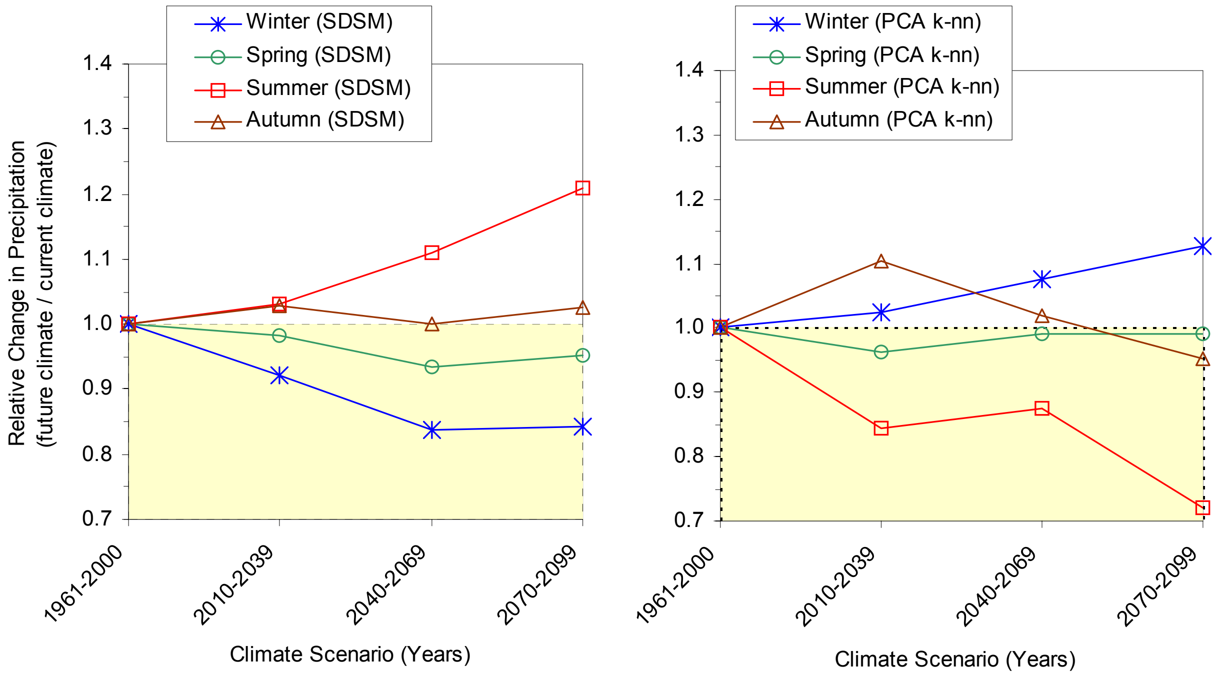

Figure 12 Relative change in **precipitation** predicted by CGCM1 model runs, after downscaling for Abbotsford, BC. Compared are two different downscaling results: (**a**) SDSM method, (**b**) PCA k-nn method.

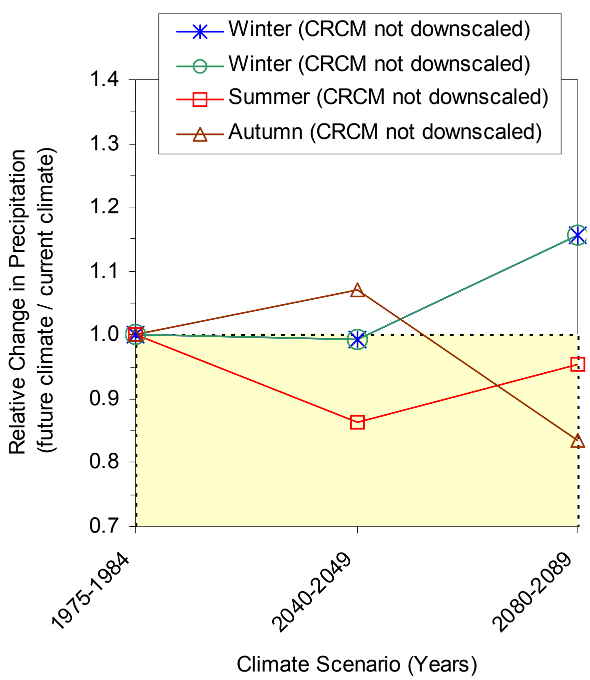

Figure 13 Relative change in **precipitation** predicted by CRCM model runs, **not downscaled**, for Abbotsford, BC.

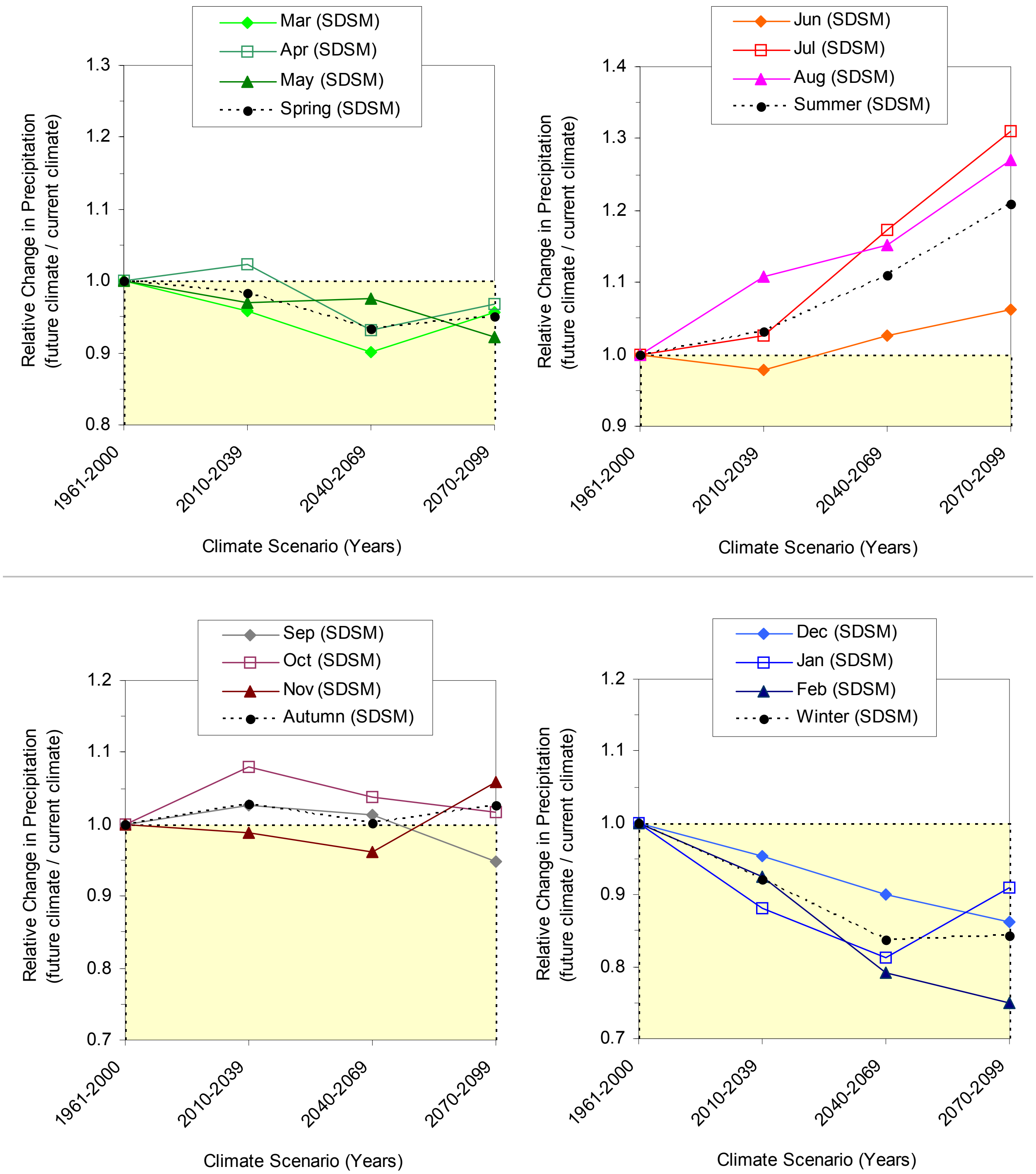

Figure 14 Relative change in monthly and seasonal **precipitation** predicted by CGCM1 model runs, after downscaling with SDSM for Abbotsford, BC. Comparing four seasons, and months within each season: (**a**) Spring, (**b**) Summer, (**c**) Autumn, (**d**) Winter.

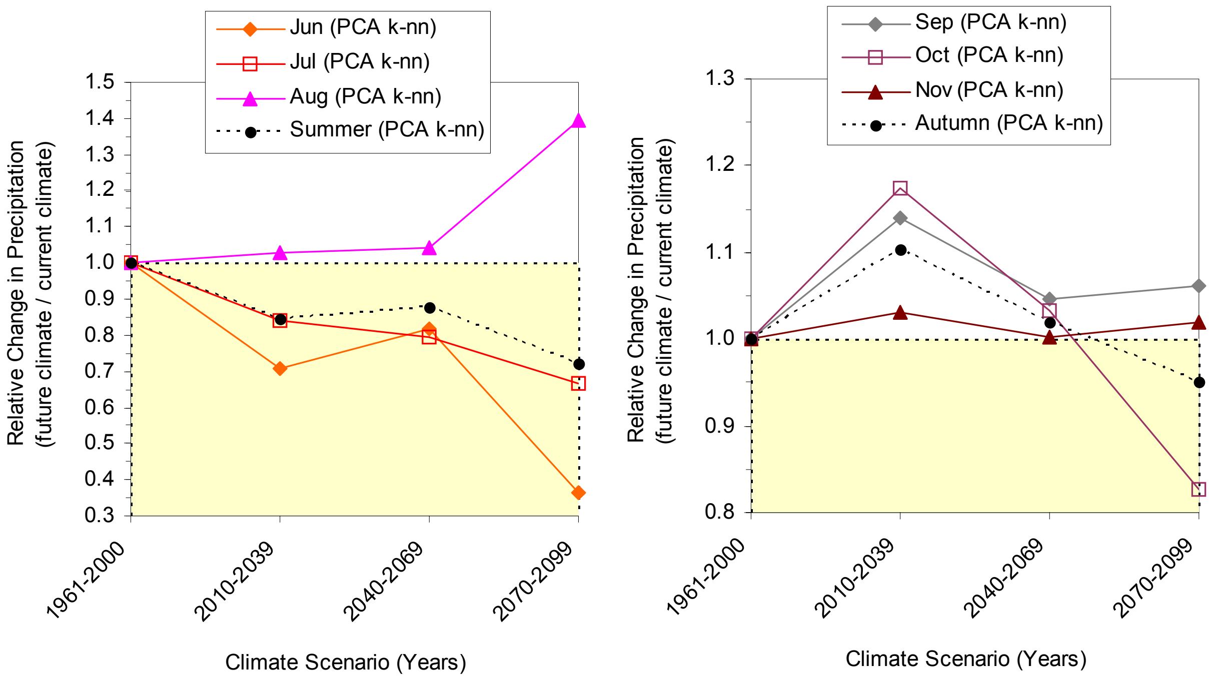

Figure 15 Relative change in monthly and seasonal **precipitation** predicted by CGCM1 model runs, after downscaling with **PCA k-nn method**, for Abbotsford, BC. Comparing (a) Summer, and (b) Autumn.

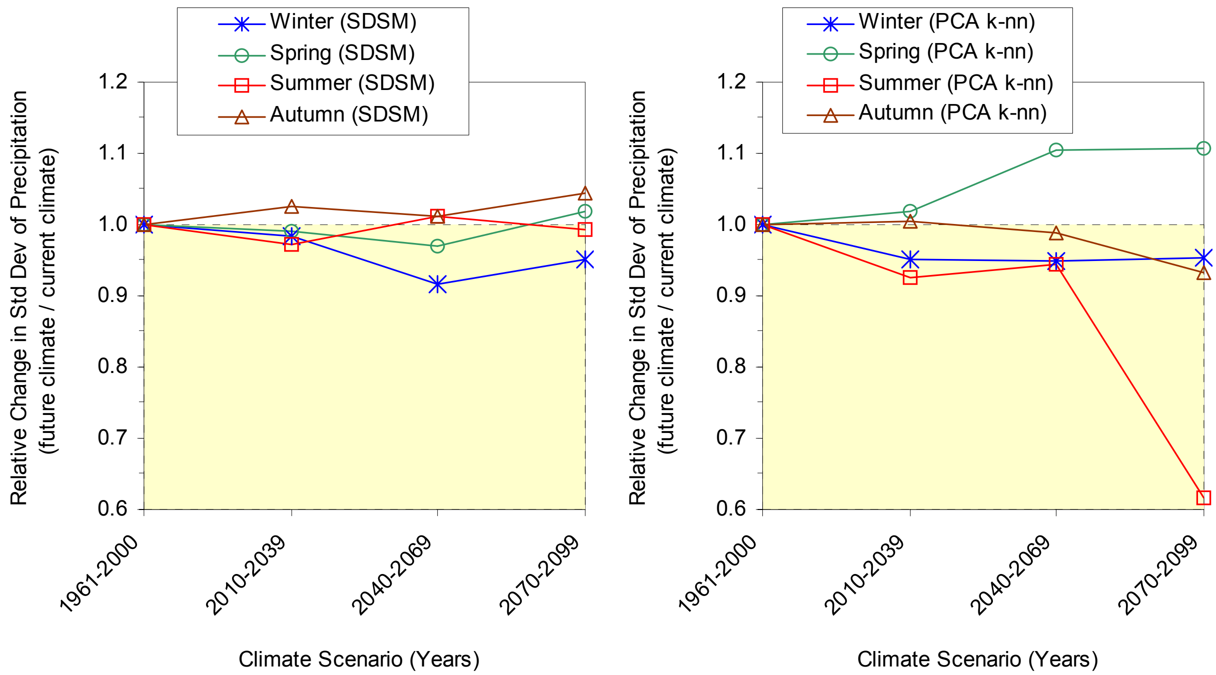

Figure 16 Relative change in **standard deviation of precipitation**, by season, predicted by CGCM1 model runs, for Abbotsford, BC, after downscaling with (a) SDSM and compared to downscaled with (b) PCA k-nn method.

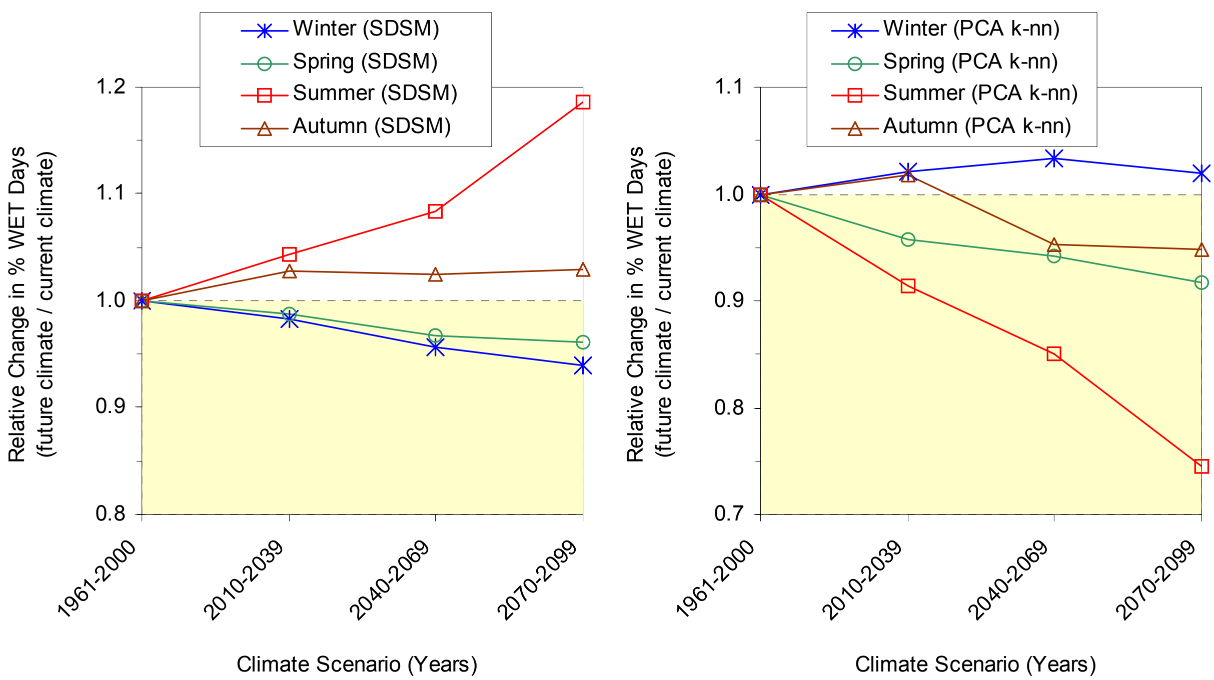

Figure 17 Relative change in **% WET days**, by season, predicted by CGCM1 model runs, for Abbotsford, BC, after downscaling with (a) SDSM and compared to downscaled with (b) PCA k-nn method.

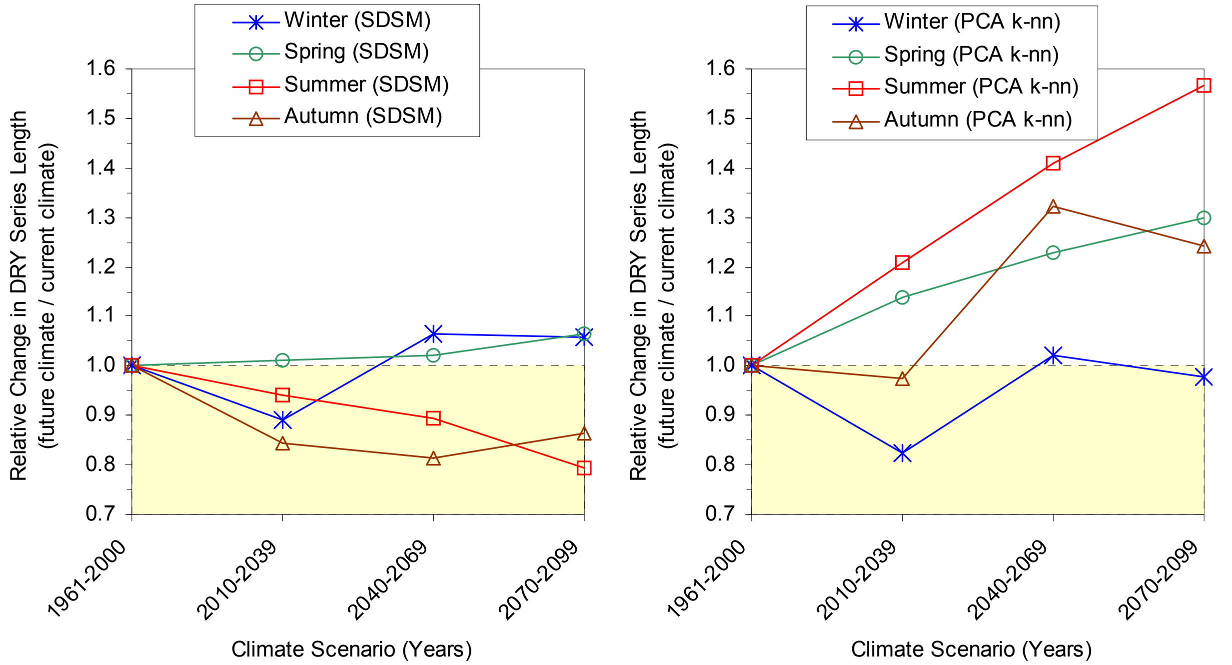

Figure 18 Relative change in **DRY spell length**, by season, predicted by CGCM1 model runs, for Abbotsford, BC, after downscaling with (a) SDSM and compared to downscaled with (b) PCA k-nn method.

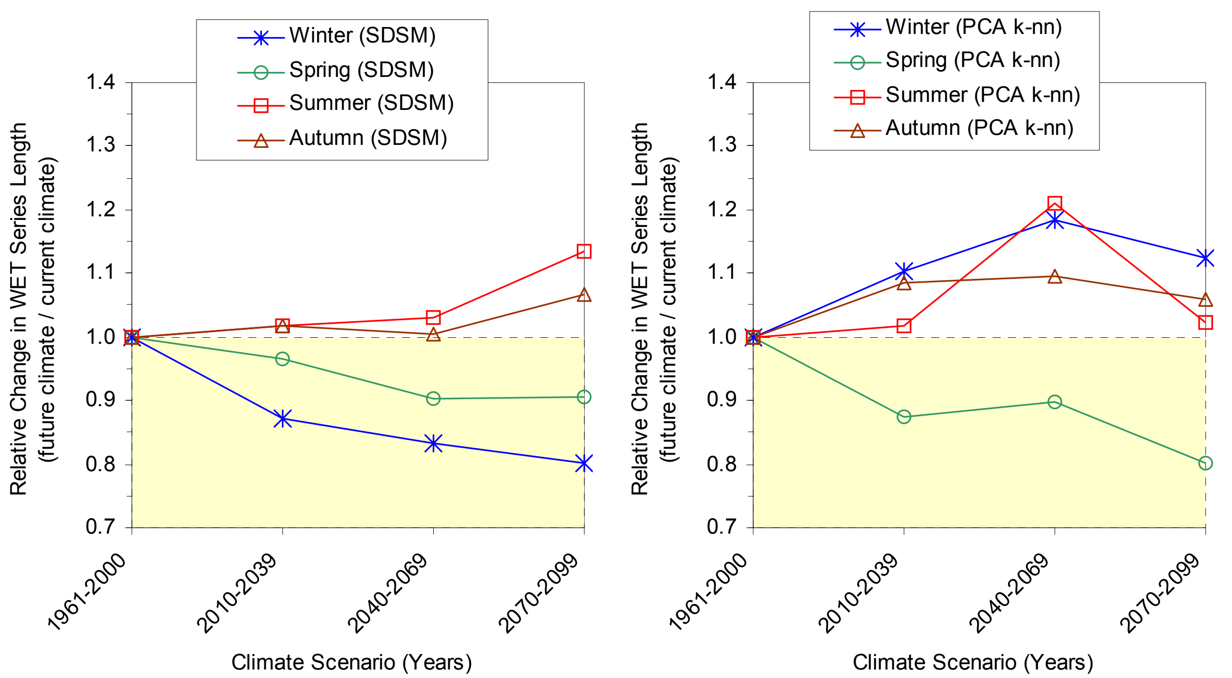

Figure 19 Relative change in **WET spell length**, by season, predicted by CGCM1 model runs, for Abbotsford, BC, after downscaling with (a) SDSM and compared to downscaled with (b) PCA k-nn method.

3.4. TEMPERATURE VARIABLES

Temperature time series were analyzed for the following variables:

1) mean daily temperature
2) standard deviation in daily temperature

Mean monthly temperature was calculated from mean daily values, which were downscaled from daily CGCM1 model runs for current and future climate scenarios.

3.4.1. ABSOLUTE CHANGE GRAPHS AND MODEL CALIBRATION GRAPHS

Similar to the precipitation results, the results were arranged by variable, thus giving 2 sets of "grouped" graphs (one variable per page). For each variable, there are two figures. One figure has two graphs comparing results for the two downscaling methods (SDSM and PCA k-nn). The second figure, placed lower, compares observed variable values to those modeled, and presents two smaller graphs of model performance: 1) calibration bias of NCEP dataset to observed; and 2) base case scenario bias of current climate CGCM1 downscaled results to observed, all for the same time period 1961-2000.

The graph sets are colour-coded and arranged identically for easy inter comparison between different variables. All graphs show monthly statistics (on x-axes). The mean temperature and standard deviation in temperature are graphed as monthly time series on the y-axes. The observed data are always graphed as background fill (area graph), while the downscaled results are line graphs, superimposed on observed data graph. The styles and colours of line graphs are always the same for each climate scenario (e.g. 2010-2039) on all graphs. The model bias graphs are also colour-coded and scaled similarly for easy inter comparison.

As was done for precipitation, daily temperature variability was represented by variance in temperature during downscaling, then converted to standard deviation of daily temperatures, because LARS-WG requires input in that form for stochastic weather generation.

In the temperature graphs, only absolute changes in temperature are shown (in degrees C) because that is more meaningful, and also to be consistent with inputs to LARS-WG and to published GCM scenarios. These are mean monthly temperatures derived from mean daily temperatures. It can be assumed that minimum and maximum temperatures increase accordingly. However, relative changes in standard deviation of temperature are given in relative amounts (ratios) as were calculated for precipitation.

3.5. CLIMATE SCENARIOS: TEMPERATURE

3.5.1. MEAN MONTHLY TEMPERATURE

The downscaled temperatures using SDSM were very close to observed (30 years) at Abbotsford in all months (Figure 20). The calibration bias for temperature to NCEP dataset (as graphed in Figure 21) was very small (less than 1%), and the model bias of downscaled CGCM1 to observed was less than 10% for most months and differed by only 1°C in months where % model bias was greater than 15% (due to temperatures close to 0°C – the % difference is a poor indicator for temperatures close to 0°C). The alternative downscaling method PCA k-nn produced similar, but less, calibrated results to observed, thus SDSM performed much better relative to observed temperatures at Abbotsford. This is evident from the monthly graphs in Figure 20.

The temporal trends for future climates in terms of temperature are very similar to both downscaled results. It is simple and consistent: temperatures are predicted to increase in all months from present to future. The differences are in rates of increase which are explored in temporal change graphs (absolute change in temperature graphs) by season and monthly in Figure 24. Both SDSM and PCA k-nn agree that summer temperatures will increase at relatively constant rate of less than 1°C per 30 years, going up 2.5°C by the end of the century compared to present. Rates of change in other seasons will be higher than in summer, also at relatively constant rates of increase, and ending up between 2.5 and 3°C higher than present by the 2080s. The CRCM results (Figure 25, not downscaled) also show consistent temperature increase trends for all seasons similar to those predicted by SDSM downscaled results from CGCM1.

Monthly temperature changes are very consistent within seasons, showing changes similar to mean seasonal (Figure 26). In other words, there is very little inter-monthly variation in predicted changes in temperature, or at least much less than was the case for precipitation. The PCA k-nn downscaled temperatures (Figure 27) show larger monthly differences for summer months than do SDSM results, but PCA k-nn output was is representative of observed temperatures, so the downscaling algorithm is deemed to have not worked as well as SDSM.

3.5.2. TEMPERATURE VARIABILITY

Standard deviations of downscaled daily temperatures are graphed in Figure 22. SDSM was able to downscale the temperature variability much better than PCA k-nn method in all months except in Autumn. SDSM performed remarkably well from spring to summer months. Both downscaling methods underestimated temperature variability in winter season. The NCEP calibration bias was low; about -10% or less (Figure 23), whereas the % differences between downscaled current temperature from CGCM1 and observed varied over the year Most were about 20%, except in winter.

Relative changes in temperature standard deviation (Figure 28) differ between SDSM and PCA k-nn results. SDSM output shows that in winter T stdev will increase by 20%, have small increase in spring and autumn, and no change in summer. Overall, except winter, not much change in temperature variability was predicted until the 2080s, when autumn and spring values also go up. PCA k-nn indicates a decrease in T stdev in summer and autumn, but an increase in other seasons. In light of better performance of SDSM, the standard deviation of temperature will be used from SDSM downscaled predictions.

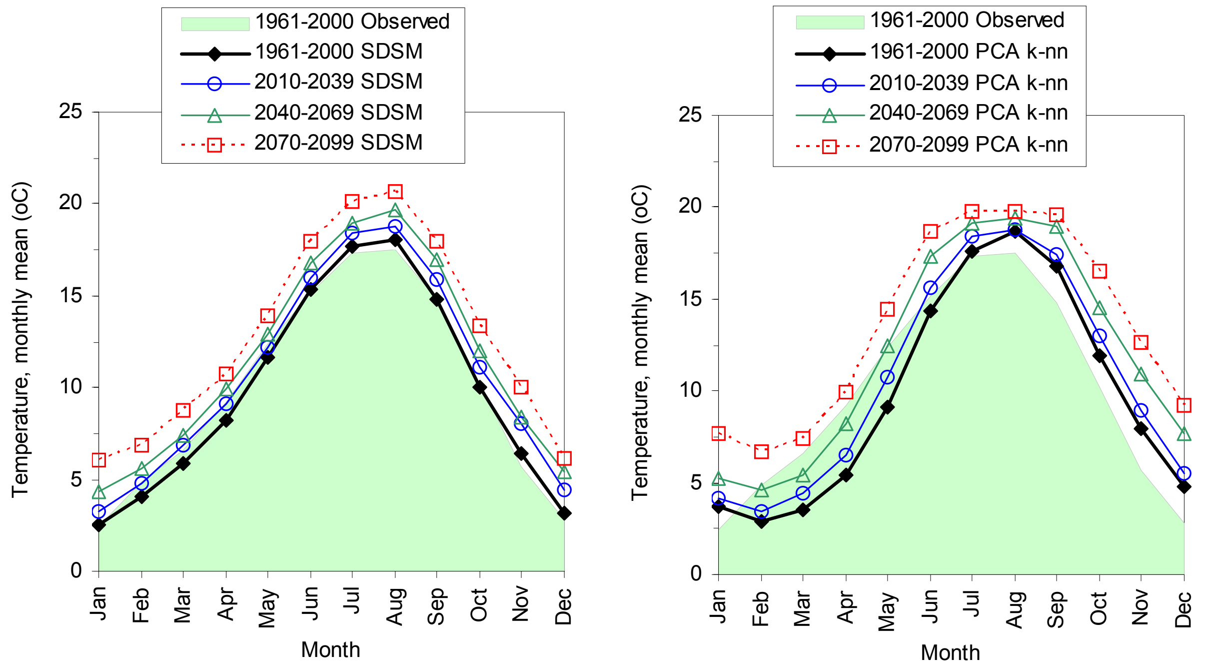

Figure 20 Mean monthly **temperature** at Abbotsford, BC: observed and downscaled from CGCM1 model runs for current and future climate scenarios using two downscaling methods: (a) SDSM, (b) PCA k-nn.

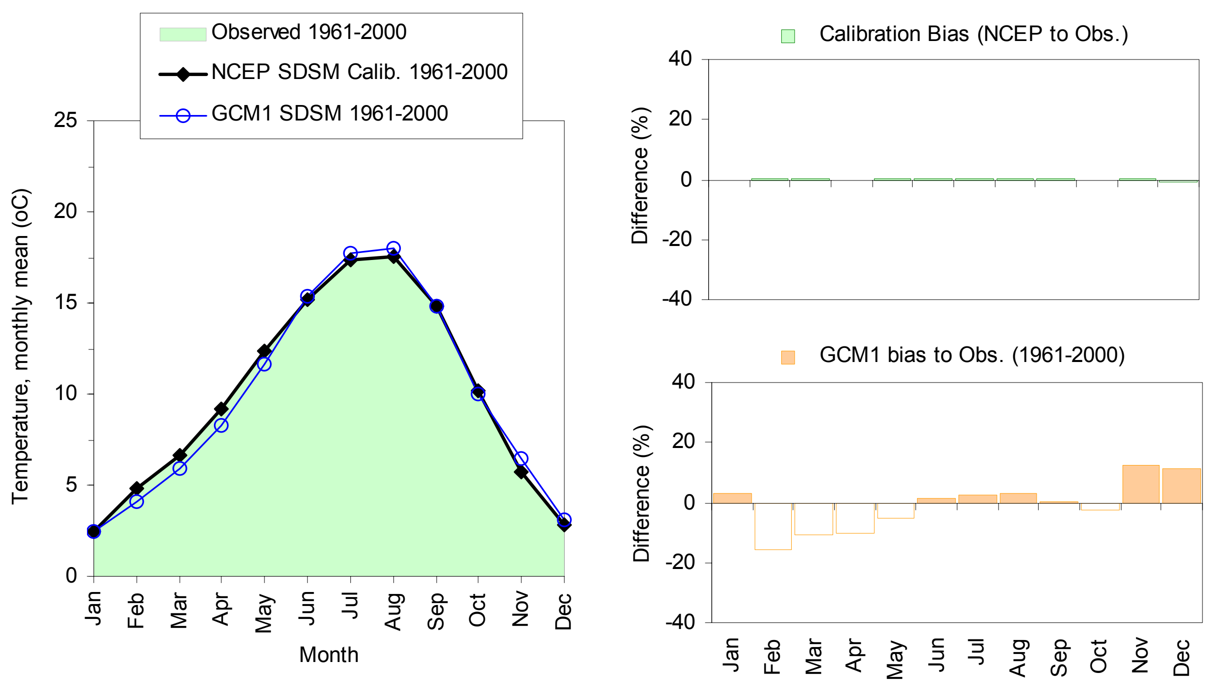

Figure 21 Comparing observed and downscaled **temperature** at Abbotsford, BC. SDSM downscaling model performance: (a) monthly precipitation, (b) calibration bias, (c) bias between SDSM downscaled CGCM1 Current precipitation and observed.

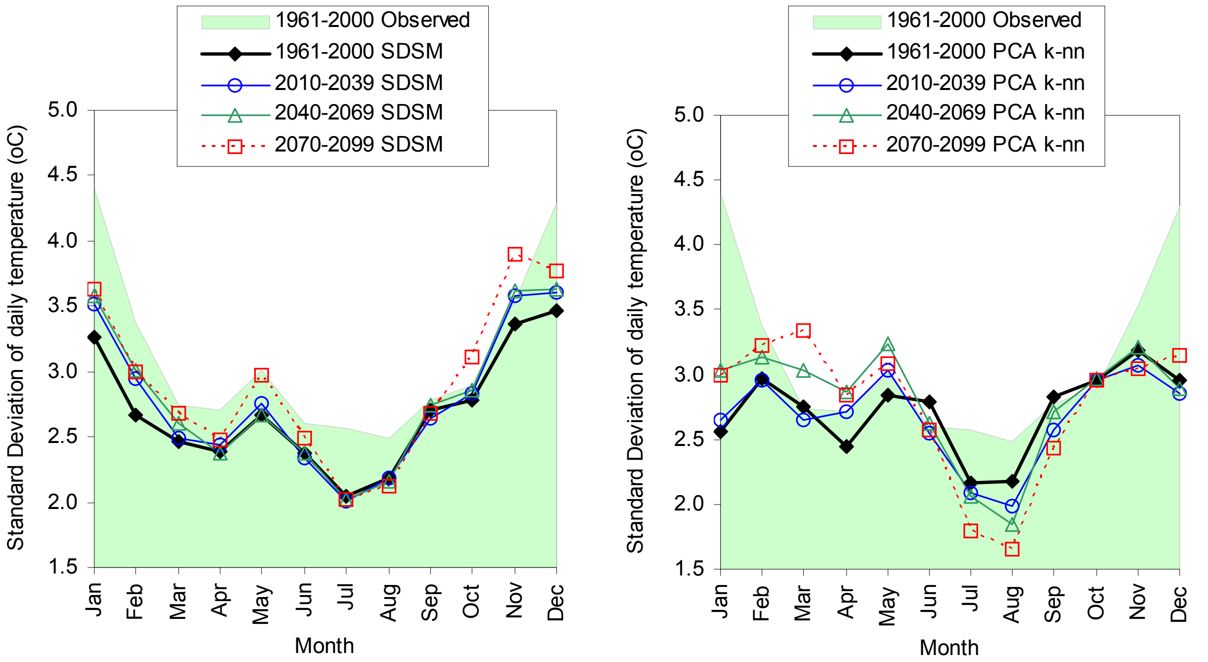

Figure 22 Mean monthly **standard deviation of temperature** at Abbotsford, BC: observed and downscaled from CGCM1 model runs for current and future climate scenarios using two downscaling methods: (a) SDSM, (b) PCA k-nn.

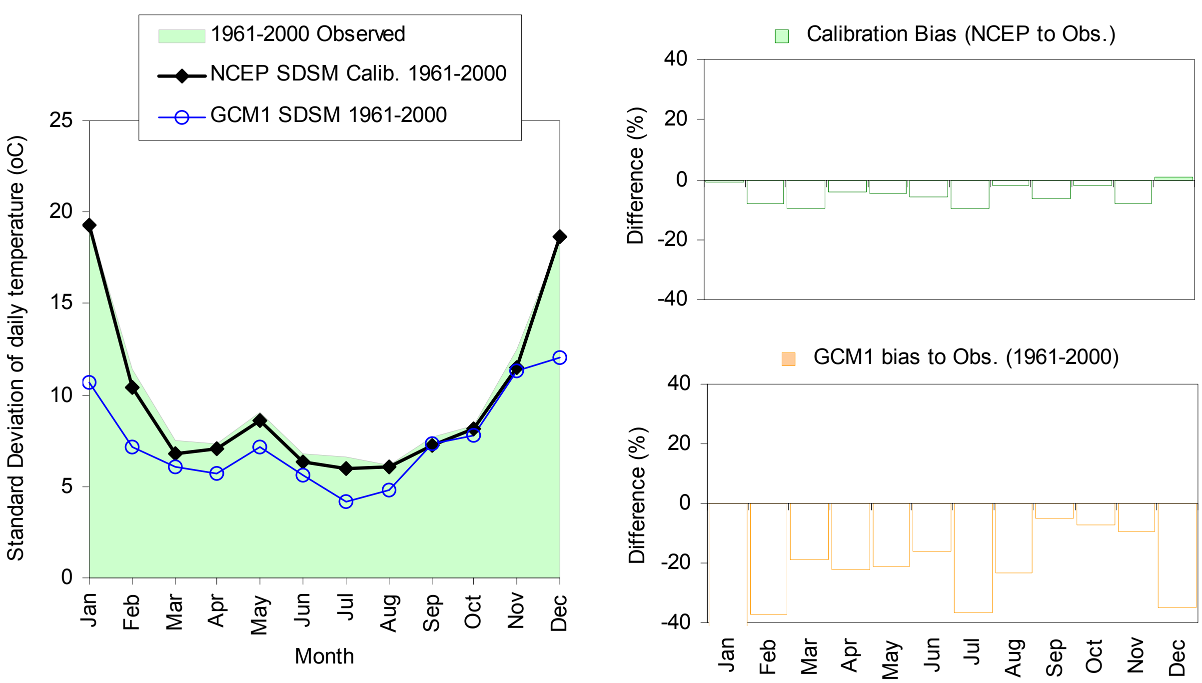

Figure 23 Comparing observed and downscaled **standard deviation of temperature** at Abbotsford, BC. SDSM downscaling model performance: (a) monthly precipitation, (b) calibration bias, (c) bias between SDSM downscaled CGCM1 Current precipitation and observed.

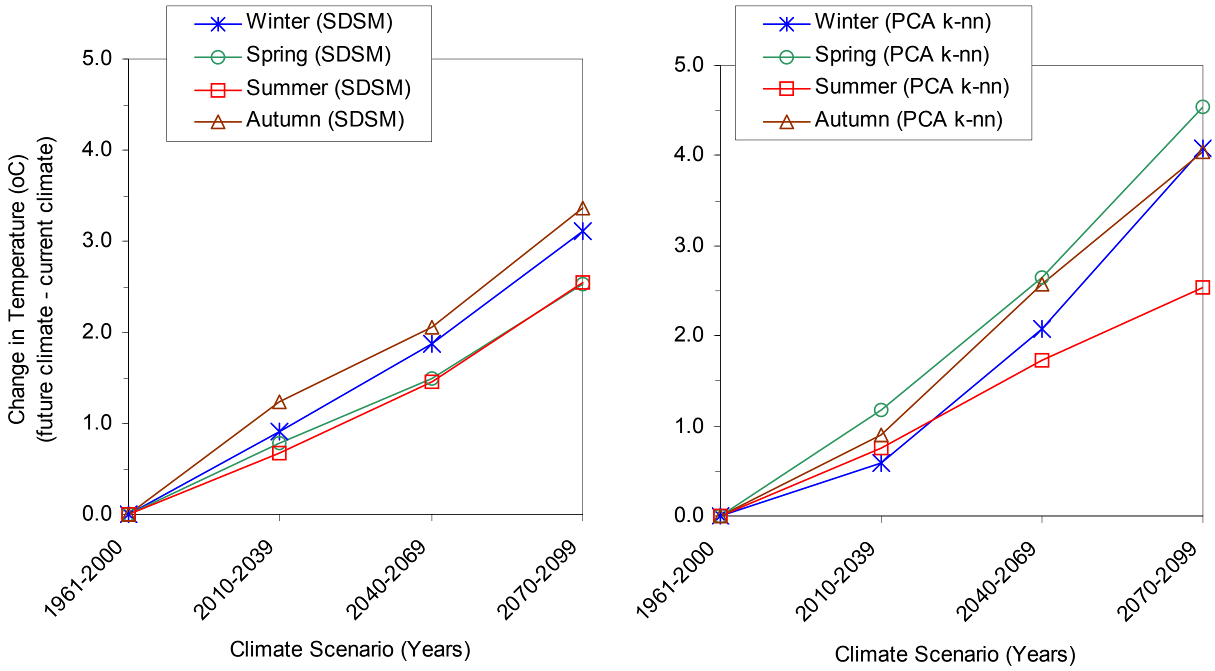

Figure 24 Absolute change in **temperature** predicted by CGCM1 model runs, after downscaling for Abbotsford, BC. Compared are two different downscaling results: (**a**) SDSM method, (**b**) PCA k-nn method.

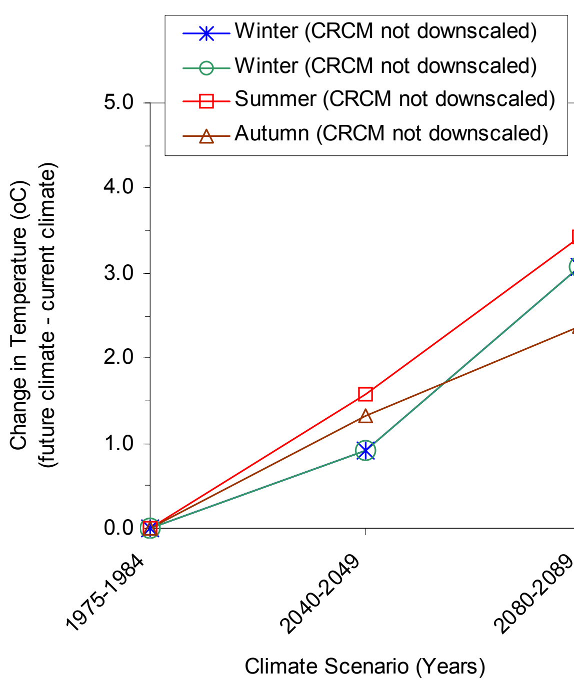

Figure 25 Absolute change in **temperature** predicted by CRCM model runs, **not downscaled**, for Abbotsford, BC.

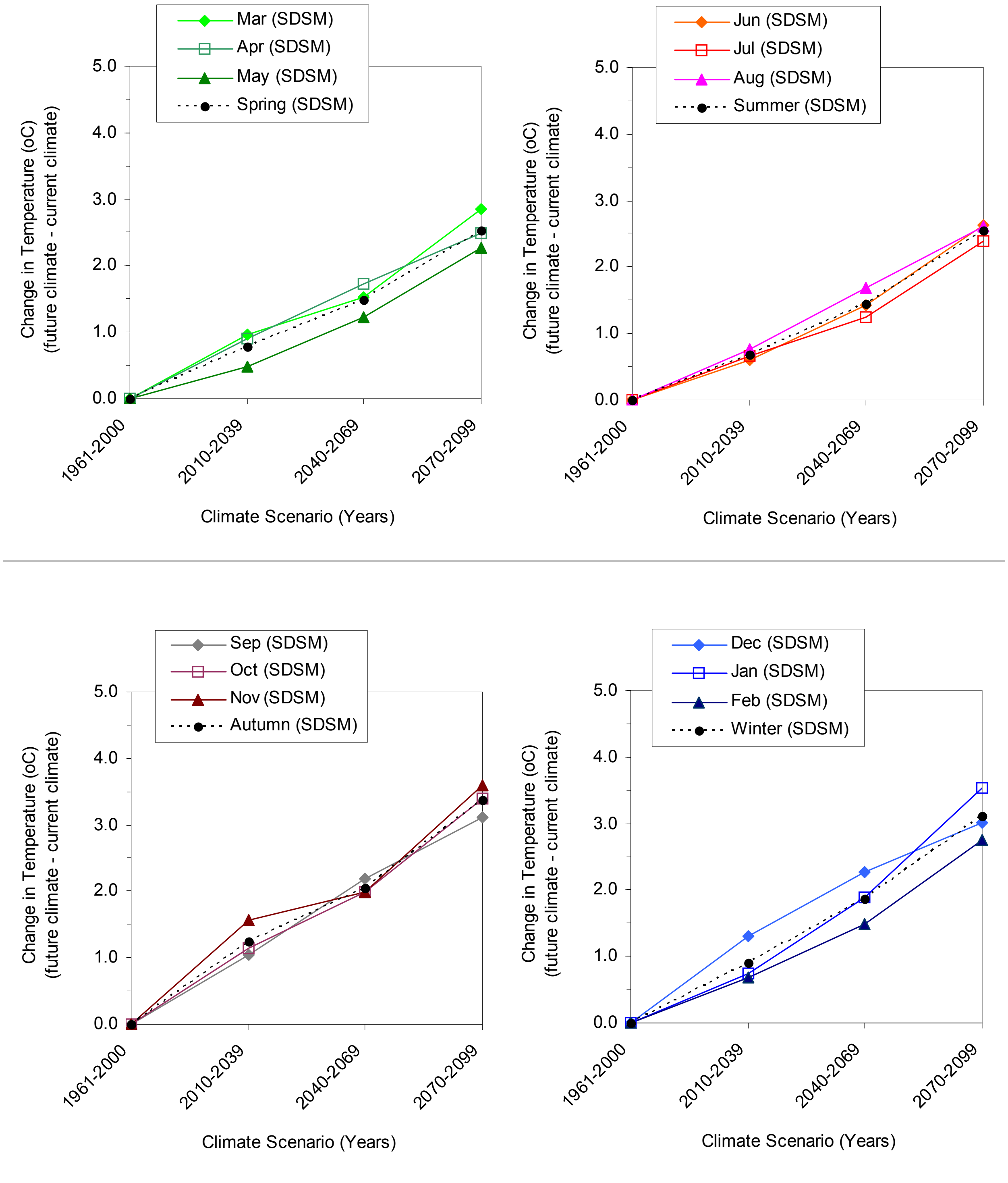

Figure 26 Absolute change in monthly and seasonal temperature predicted by CGCM1 model runs, after downscaling with SDSM for Abbotsford, BC. Comparing four seasons, and months within each season: (**a**) Spring, (**b**) Summer, (**c**) Autumn, (**d**) Winter.

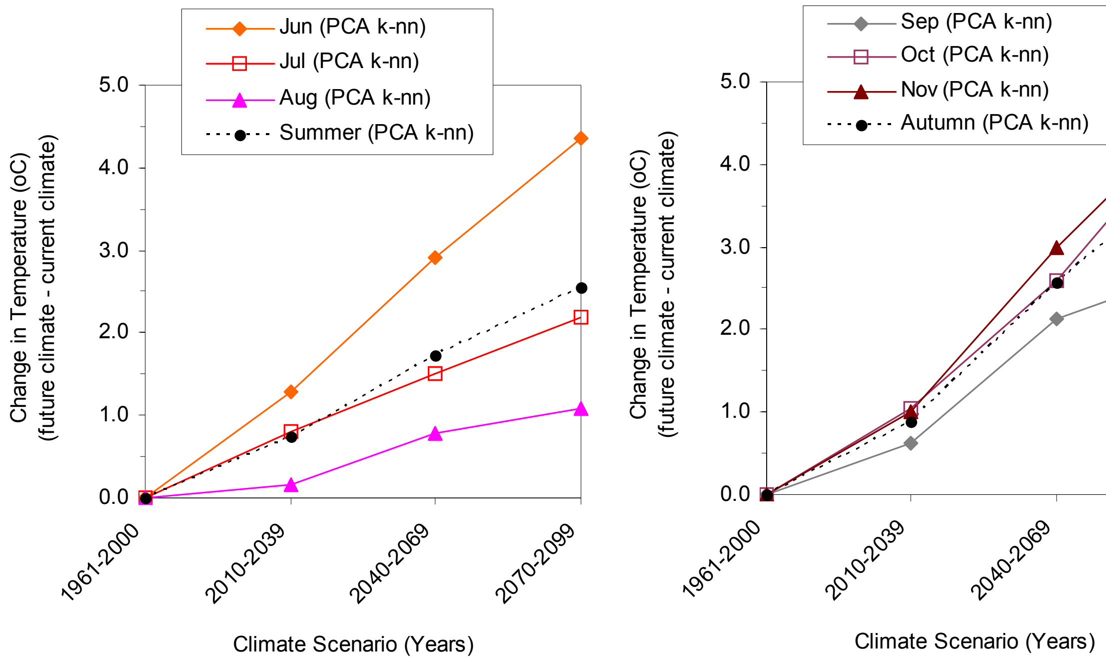

Figure 27 Absolute change in monthly and seasonal **temperature** predicted by CGCM1 model runs, after downscaling with **PCA k-nn method**, for Abbotsford, BC. Comparing (a) Summer, and (b) Autumn.

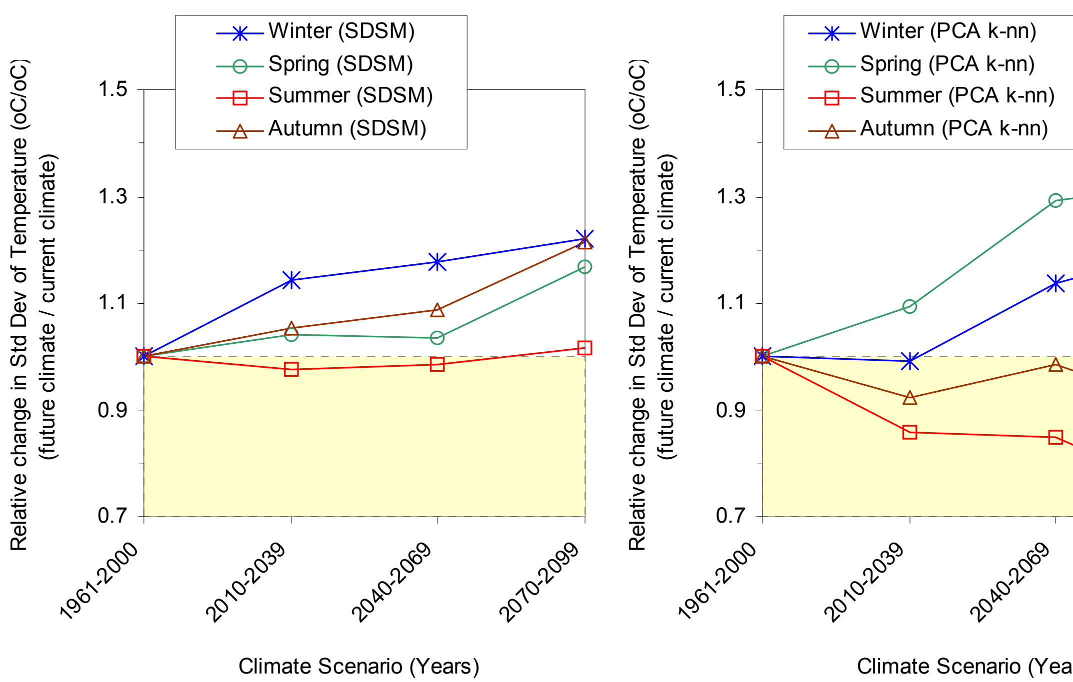

Figure 28 Relative change in **standard deviation of temperature**, by season, predicted by CGCM1 model runs, for Abbotsford, BC, after downscaling with (a) SDSM and compared to downscaled with (b) PCA k-nn method.

3.6. SOLAR RADIATION FROM CRCM (NOT DOWNSCALED)

It was not possible to downscale solar radiation for Abbotsford due to the lack of observed mean daily incident solar radiation at this location. The LARS-WG weather generator requires an input of absolute changes in solar radiation relative to base case climate in order to generate weather for future climate change scenarios. As a substitute, the CRCM monthly normals of daily solar radiation were used for the climate scenarios.

To calculate relative changes in solar radiation for future climates relative to current, CRCM solar radiation monthly values were used and assumed representative. The CRCM solar radiation values were not downscaled. Data were extracted from monthly CRCM outputs for grid cells representing the central Fraser Valley and imported from the CICS website (CICS, 2003). The changes were relatively small (Figure 29), so the downscaled model is assumed to be not sensitive to errors or scale effects in solar radiation values taken from CRCM.

Absolute changes of solar radiation from CRCM, by month, are graphed in Figure 30 for current climate and future climates. Changes are relatively small and there are no clear seasonal patterns.

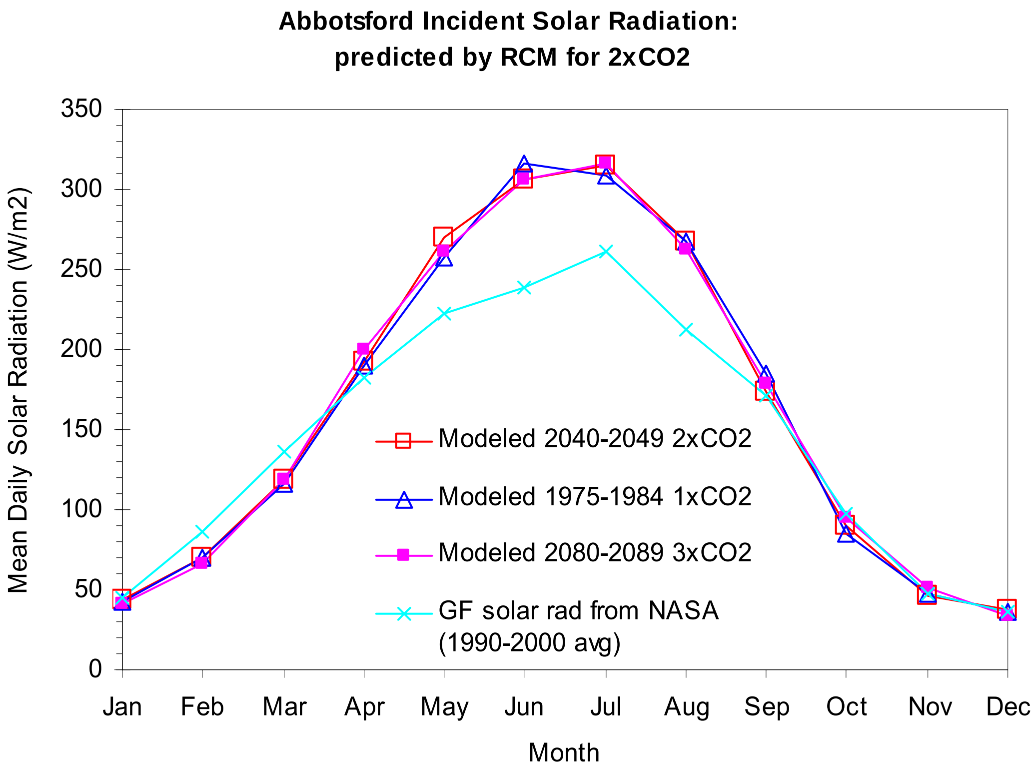

Figure 29 Mean daily **solar radiation** (averaged per month), modelled by CRCM without downscaling at Abbotsford. Scenarios correspond to CGCM1 climate scenarios.

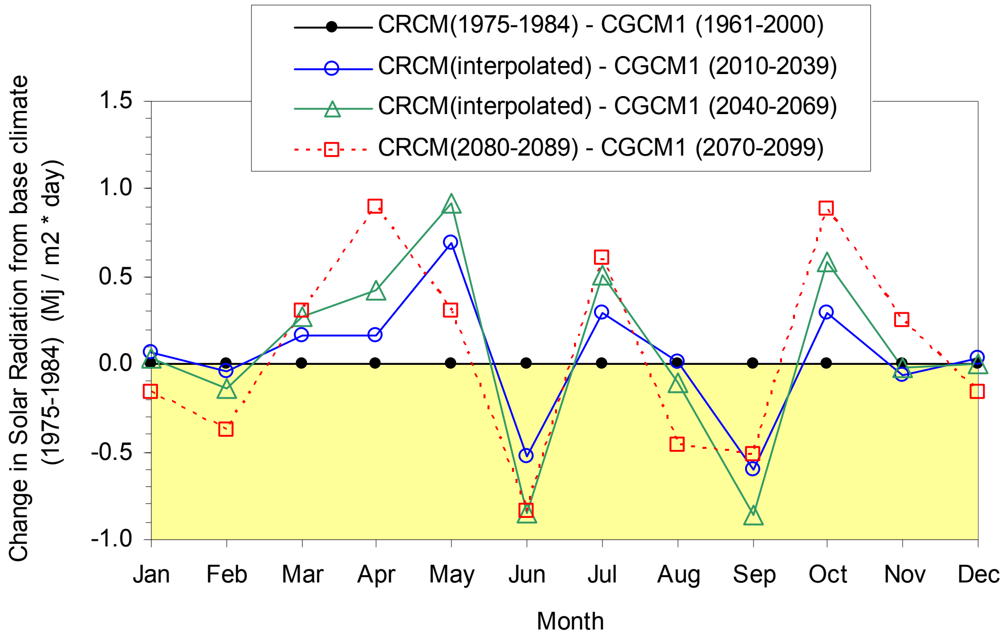

Figure 30 Change in **solar radiation** (mean daily averaged per month) from current climate, modeled by CRCM without downscaling at Abbotsford, BC. Scenarios correspond to CGCM1 climate scenarios.

4. WEATHER INPUTS FOR RECHARGE MODEL

4.1. GENERATING DAILY WEATHER

4.1.1. WEATHER GENERATORS: INTRODUCTION

Stochastic weather generators were originally developed for two main purposes:

1. To provide a means of simulating synthetic weather time-series with statistical characteristics corresponding to the observed statistics at a site, but which were long enough to be used in an assessment of risk in hydrological or agricultural applications.

2. To provide a means of extending the simulation of weather time-series to unobserved locations, through the interpolation of the weather generator parameters obtained from running the models at neighbouring sites.

A stochastic weather generator produces artificial time series of weather data for a location based on the statistical characteristics of observed weather at that location. For each month, different model parameters are used in order to reflect seasonal variation in both the values of climatic variables and their cross-correlations (CEAA, 2003). It also allows changes in climate variability to be incorporated, and not just changes in mean values. This is very important if actual predicted weather (best scientific guess) is to be simulated, and not just "what-if" scenarios of weather change (e.g., by certain percentage of mean value).

Semenov and Barrow (2002) noted that a stochastic weather generator is not a predictive tool that can be used in weather forecasting, but is simply a means of generating time-series of synthetic weather statistically 'identical' to the observations. New interest in local stochastic weather simulation has arisen as a result of climate change studies. At present, output from global climate models (GCMs) is of insufficient spatial and temporal resolution and reliability to be used directly in impact models. A stochastic weather generator, however, can serve as a computationally inexpensive tool to produce multiple-year climate change scenarios at the daily time scale, which incorporates changes in both mean climate and in climate variability (Semenov and Barrow, 2002).

There are two basic types of stochastic weather generator:

1) "Richardson" weather generator (WGEN) (Richardson, 1981; Richardson and Wright, 1984)
2) "serial" (Racsko et al., 1991; Semenov et al., 1998)

Both types of weather generator require initial calibration, based on observed station data (Richardson, 2000). WGEN is the weather generator incorporated into the UnSat Suite software, which drives HELP simulations for infiltration. WGEN has been known for inadequate modeling of persistent wet or dry periods (Wilks and Wilby, 1999). In contrast, the serial weather generators (e.g., LARS-WG) avoid this shortcoming. These models determine sequences of dry and wet series of days, then generate other climatic variables. Another potential problem with WGEN is solar radiation. It is generated using a simplistic approach where incident solar radiation is calculated from a function that estimates solar irradiance on cloudless sky conditions based on the location of station. For wet days, this value is simply decreased by a constant value to represent expected increase of cloudiness associated with occurrence of precipitation. However, precipitation is a daily average (including night and day), whereas incident solar radiation occurs only in daytime. Cloud cover often occurs without precipitation, and depending on local climate, intense precipitation can occur on a day with relatively large incident solar radiation averaged for a day.

Ultimately, WGEN was not used in this study as it was shown to poorly reproduce historic climate in a parallel study in Grand Forks (Allen et al., 2004). A newer stochastic weather generator, LARS-WG, was used to model artificial weather series for this study. Nonetheless, a comparison of the precipitation output of these two weather generators is illustrated in a later section.

4.2. LARS-WG: STOCHASTIC WEATHER GENERATOR WITH SERIAL APPROACH TO PRECIPITATION

4.2.1. LARS-WG

LARS-WG is a stochastic weather generator that can be used for the simulation of weather data at a single site (Racsko et al., 1991; Semenov et al., 1998), under both current and future climate conditions. These data are in the form of daily time-series for a suite of climate variables, namely, precipitation (mm), maximum and minimum temperature (°C) and solar radiation (MJm^{-2} day^{-1}).

LARS-WG is based on the series weather generator described in Racsko et al. (1991). It utilizes semi-empirical distributions for the lengths of wet and dry day series, daily precipitation and daily solar radiation. The simulation of precipitation occurrence is modeled as alternate wet and dry series, where a wet day is defined to be a day with precipitation > 0.0 mm. The length of each series is chosen randomly from the wet or dry semi-empirical distribution for the month in which the series starts. In determining the distributions, observed series are also allocated to the month in which they start. For a wet day, the precipitation value is generated from the semi-empirical precipitation distribution for the particular month independent of the length of the wet series or the amount of precipitation on previous days. Daily minimum and maximum temperatures are considered as stochastic processes, with daily means and daily standard deviations conditioned on the wet or dry status of the day (Semenov and Barrow, 2002).

Such daily output fits perfectly in the recharge modeling scheme because the recharge is based on step-like climate scenarios, whereas in each scenario (“step”), the climate is the same and equivalent to predicted by GCMs / downscaled / stochastic-generated, and then recharge is averaged for the scenario by month. The GCMs ensure that physical processes are modeled spatially (on very coarse scale) and, more importantly, temporally. The downscaling ensures that processes and resulting values of variables are as close to site-specific as possible, while preserving the GCM predictions. The stochastic weather ensures that daily values of variables are realistic, consistent, site specific, and preserve both values and variability predicted to change from current to future climate scenarios by GCMs.

The recharge model (HELP model in this project) uses daily inputs of weather to calculate daily recharge through soil columns. Thus, appropriate frequency, magnitude and duration of precipitation and other events are modeled. Typically 30 or more years are modeled within each climate scenario, and then monthly averages are computed to represent monthly variation of recharge, which is representative of the climate regime being modeled. Because the stochastic weather generator requires more than 100 years of daily weather to be created to begin approaching the statistics specified for a climate scenario (and local weather), the recharge model will receive also that long time period of simulated weather, and the averages will be representative. See graphs comparing climate scenario inputs to LARS-WG model and outputs from 100 y weather run in Figure 35. The length of weather time series is not meant to model actual changing climate year-to-year, but to model climate change step-wise for each scenario and to generate long enough weather time series to preserve and properly represent statistical properties for the site and predicted climate for the scenario.

The groundwater flow model will be "transient", but only on monthly time steps due to computational limitations, although 10 day time steps could be modeled with some effort. Since most of the GCM summaries, downscaling tools, and stochastic weather generators are set-up for adjusting monthly statistics for daily weather, it makes sense to model transient groundwater flow also on monthly time steps. The actual groundwater flow model has more time steps, but inputs are modified and outputs generated on monthly time steps. Thus, monthly recharge is required as an input for each climate change scenario.

4.2.2. METHODOLOGY: GCM OUTPUT

Data were extracted from CGCM1 daily output, because that was available at the time for downloading. Data were obtained from Zwiers (2001). Available were three 21-year time series of daily precipitation amounts simulated by the CGCM1 climate model in each of three 21-year "windows" representing the climates of 1975-95, 2040-60 and 2080-2100. That is, a total of 3x (3x21)=189 years of simulated daily precipitation data are available. This climate modeling case was run to explore the changes in extremes in precipitation over Canada (Kharin and Zwiers, 2000).

4.2.3. METHODOLOGY: CLIMATE SCENARIOS IN LARS-WG FROM SDSM DOWNSCALING

Table 7 shows an example of the output file from SDSM, which is input to LARS-WG.

Table 7 Climate scenario input (scenario file example) from SDSM to LARS-WG stochastic weather generator. Shown is the base case current climate scenario and three future climate scenarios for Abbotsford, BC.

m.rain = precipitation relative change (future / base) or (base / base)
wet = WET spell length relative change
dry = DRY spell length relative change
tem = temperature absolute change
sd = standard deviation of temperature relative change
rad = solar radiation absolute change

base (present)

	m.rain	wet	dry	tem	sd	rad
Jan	1.00	1.00	1.00	0.00	1.00	0.00
Feb	1.00	1.00	1.00	0.00	1.00	0.00
Mar	1.00	1.00	1.00	0.00	1.00	0.00
Apr	1.00	1.00	1.00	0.00	1.00	0.00
May	1.00	1.00	1.00	0.00	1.00	0.00
Jun	1.00	1.00	1.00	0.00	1.00	0.00
Jul	1.00	1.00	1.00	0.00	1.00	0.00
Aug	1.00	1.00	1.00	0.00	1.00	0.00
Sep	1.00	1.00	1.00	0.00	1.00	0.00
Oct	1.00	1.00	1.00	0.00	1.00	0.00
Nov	1.00	1.00	1.00	0.00	1.00	0.00
Dec	1.00	1.00	1.00	0.00	1.00	0.00

2010-2039

	m.rain	wet	dry	tem	sd	rad
Jan	0.88	0.97	0.98	0.74	1.16	0.06
Feb	0.92	0.84	0.82	0.67	1.21	-0.04
Mar	0.96	0.92	1.06	0.96	1.02	0.16
Apr	1.02	1.02	0.98	0.90	1.04	0.16
May	0.97	0.96	0.99	0.49	1.06	0.69
Jun	0.98	0.99	0.97	0.60	0.97	-0.52
Jul	1.03	0.97	0.97	0.67	0.96	0.30
Aug	1.11	1.12	0.90	0.77	1.00	0.01
Sep	1.03	0.94	0.81	1.04	0.96	-0.60
Oct	1.08	0.99	0.95	1.14	1.03	0.29
Nov	0.99	1.05	0.80	1.56	1.13	-0.07
Dec	0.95	0.81	0.91	1.30	1.08	0.04

2040-2069

	m.rain	wet	dry	tem	sd	rad
Jan	0.81	0.94	1.14	1.89	1.21	0.04
Feb	0.79	0.78	1.05	1.48	1.27	-0.14
Mar	0.90	0.82	1.03	1.52	1.12	0.27
Apr	0.93	0.98	1.04	1.72	0.99	0.42
May	0.98	0.92	1.00	1.22	1.00	0.92
Jun	1.03	0.97	0.92	1.43	1.00	-0.85
Jul	1.17	1.06	0.95	1.25	0.97	0.51
Aug	1.15	1.08	0.83	1.68	0.98	-0.10
Sep	1.01	0.89	0.82	2.19	1.02	-0.86
Oct	1.04	1.07	0.75	1.99	1.05	0.58
Nov	0.96	0.99	0.92	1.99	1.16	-0.02
Dec	0.90	0.78	1.02	2.26	1.10	0.01

2070-2099

	m.rain	wet	dry	tem	sd	rad
Jan	0.91	0.95	1.03	3.54	1.23	-0.16
Feb	0.75	0.71	1.12	2.76	1.26	-0.37
Mar	0.96	0.78	1.17	2.84	1.18	0.30
Apr	0.97	1.01	1.04	2.49	1.07	0.90
May	0.92	0.96	1.01	2.27	1.24	0.31
Jun	1.06	1.08	0.86	2.62	1.09	-0.84
Jul	1.31	1.11	0.85	2.39	0.98	0.61
Aug	1.27	1.26	0.70	2.62	0.95	-0.46
Sep	0.95	0.91	0.88	3.12	0.98	-0.51
Oct	1.02	1.05	0.88	3.40	1.25	0.89
Nov	1.06	1.10	0.73	3.59	1.34	0.25
Dec	0.86	0.73	1.00	3.01	1.18	-0.16

4.3. CALIBRATION OF LARS-WG

Model calibration notes and procedures are taken from LARS-WG manual, and excerpts are used here to give an overview of the calibration process.

Model calibration in LARS-WG involves "site analysis" procedure when the observed weather data are analyzed to determine their statistical characteristics. LARS-WG will be able to simulate artificial weather data based on as little as a single year of observed weather data. However, since the simulated weather data will be based on these observed data, then the more data used, the closer is LARS-WG likely to be able to match the true climate for the site in question. The use of at least 20-30 years of daily weather data is recommended. In order to be able to capture some of the less frequent climate events (e.g., droughts) as long an observed record as possible should be used.

Note that unlike the DRY/WET series for precipitation, the air temperature is modeled in LARS-WG by using Fourier series, i.e., the annual cycle of temperature is described using sine and cosine curves. These curves can be constructed with information pertaining to only a small number of parameters, i.e., the mean value, amplitude of the sine/cosine curves and phase angle. Both maximum and minimum temperature are modeled more accurately by considering wet and dry days separately.

"QTest" carries out a statistical comparison of synthetic weather data generated using LARS-WG with the parameters derived from observed weather data. In order to ensure that the simulated data probability distributions are close to the true long-term observed distributions for the site in question, a large number of years of simulated weather data should be generated. The synthetic data are then analyzed, and parameter files are produced containing probability distribution, mean and standard deviation information.

The χ^2, t- and F- tests assume that the observed weather is a random sample from some existing distribution, which represents the 'true' climate at the site. In the absence of any changes in climate, this true distribution could be estimated accurately from observed data over a very long time period. The simulated climate distribution is estimated from a long run of synthetic weather data generated by LARS-WG using the parameter files output during the model calibration process. The statistical tests carried out in QTest look for differences between the simulated climate and the 'true' climate. Each of the tests considers a particular weather statistic and compares the values from the observed and simulated data. All of the tests calculate a p-value, which is used to accept or reject the hypotheses that the two sets of data could have come from the same distribution (i.e., there is no difference between the 'true' and simulated climate for that variable). Therefore, a very low p-value means that the simulated climate is unlikely to be the same as the 'true' climate (see Table 7). If the p-value is not very low, it is plausible that the climates are the same, although statistical tests cannot prove this.

4.3.1. REASONS FOR DISCREPANCIES IN MODELED WEATHER TO OBSERVED

Significant differences between simulated and observed data are likely to be due to LARS-WG smoothing the observed data. For example, LARS-WG fits smooth curves to the average daily mean values for minimum temperature and for maximum temperature. It does this in order to eliminate, as much as possible, the random noise in the observed data in order to get closer to the actual climate for the site. Differences are likely to be due to departures of the observed values from the smooth pattern for the data.

Random variation in the observed data: Random variations from month to month are likely to be greater when there is less observed data. If the differences are due to such random variations, the smoothing employed by LARS-WG will mean that the simulated weather is likely to be closer to the actual climate for the site than the observed data and so the simulated data can be accepted. [LARS-WG assumes that the observed climate is stationary; if there are any trends in the observed data then these need to be removed before LARS-WG is used.]

Climate anomalies: The variations in the data may be due to some unusual climatic phenomenon and so the data may actually be typical of the climate for the site. It is likely that in this case LARS-WG will not match the climate for that part of the year. In this case, careful consideration is needed of the effect on your application of the differences between LARS-WG and the typical climate.

4.3.2. CALIBRATION TO RAINFALL PARAMETERS

In Figure 31 the mean monthly rainfall values for LARS-WG generated weather at Abbotsford are within 2 mm/month (within 5%) or closer for all months (compared to 40-50 mm/month precipitation values). The seasonal variation in rainfall shows very good fit to observed rainfall normals. Variability of rainfall (standard deviation of monthly precipitation) is also preserved in synthetic weather, but there are relatively small discrepancies between modeled and observed precipitation in May-Jul and Nov. This “error” is related to ability of LARS-WG to model rainfall intensities and wet/dry weather time series. The model’s ability to simulate WET and DRY series of weather, and extreme weather spells, was evaluated as suggested in LARS-WG manual, and results are in Table 8. The chi-test gave very good results for WET/DRY precipitation series (small 1-p values for all seasons), indicating very good fit of modeled to observed data. The model performance for extreme weather spells was much worse. The science of weather generation is still evolving and even such models as LARS-WG cannot properly replicate the occurrence of rare and extreme weather spells (of cold and hot temperatures) because these are site-specific and occur due to unique weather conditions. However, the amounts of precipitation are not likely to be affected by the extreme weather events, even if poorly modeled. Precipitation distribution (histograms by month) were very well reproduced in the LARS-WG synthetic weather according to chi-test.

Figure 31 Monthly Rainfall at Abbotsford, BC, observed for period of record 1975-1995 (base climate scenario) and modeled with stochastic LARS-WG weather generator (20 year run): (a) Precipitation Amounts as mean monthly precipitation (b) Precipitation Variability as standard deviation of mean monthly precipitation.

(a) Precipitation Amounts

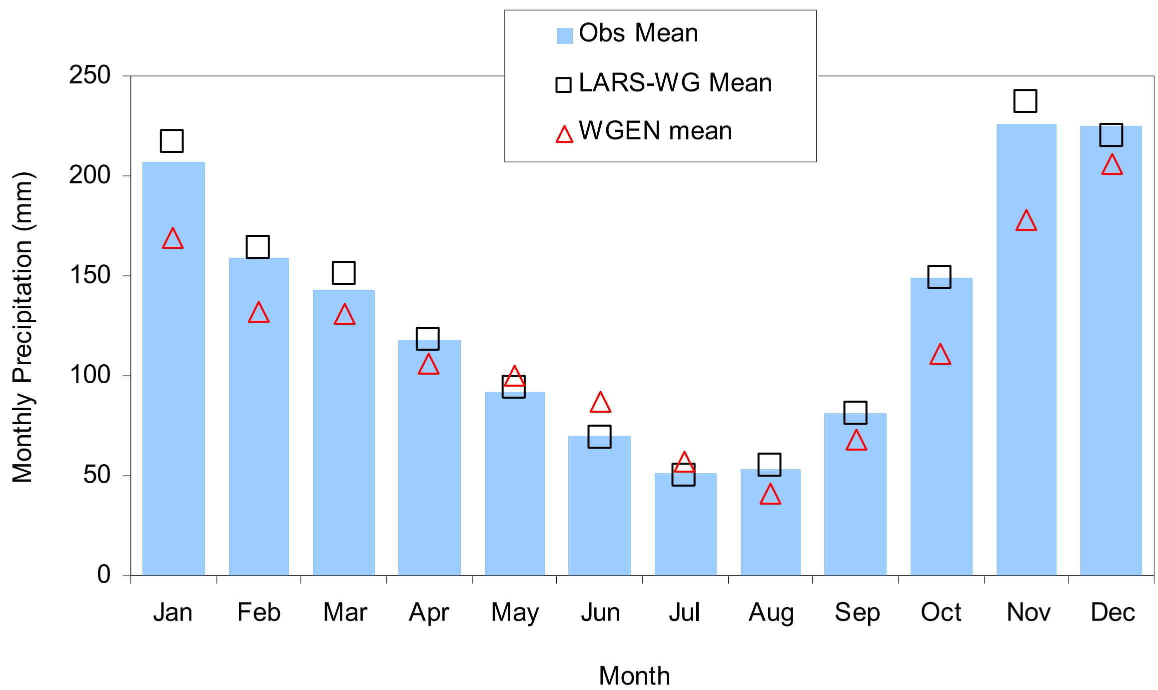

(b) Precipitation Variability

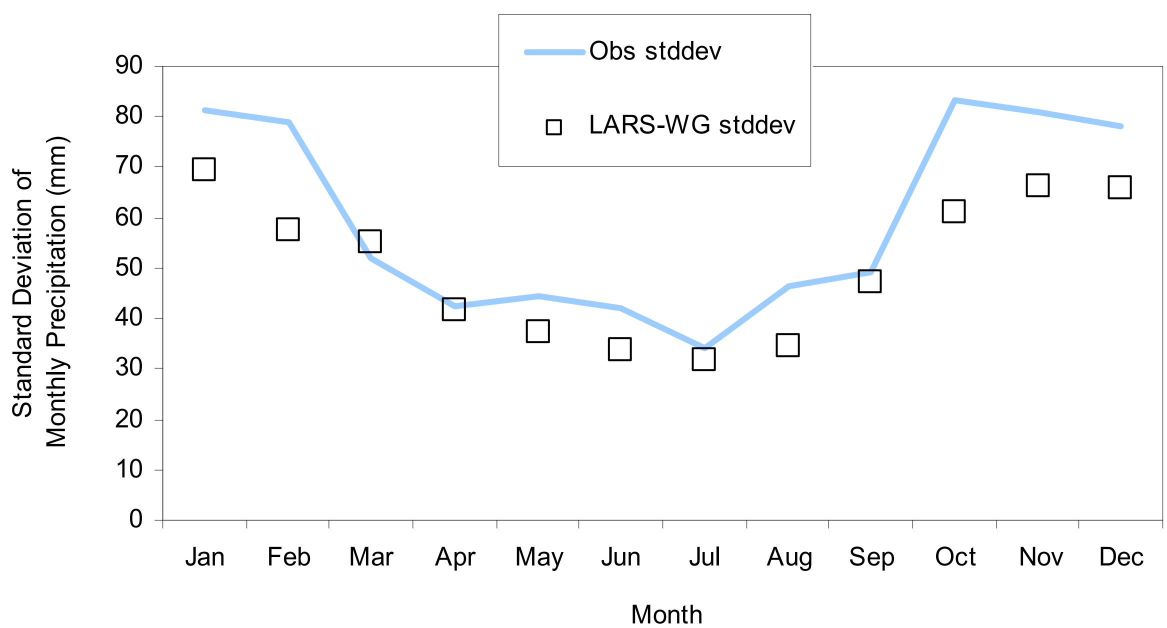

Table 8 Results of calibration of LARS-WG synthetic weather generator for Abbotsford precipitation. Q-test for WET / DRY series, extreme weather spells, and precipitation distributions by month (comparing synthetic weather and ability of LARS-WG to generate weather to observed weather).

WET / DRY precipitation series

Months	Weather Series	df	chi^2	p-value	Comments
Dec - Feb	WET	12	16.750	0.159	poor fit
	DRY	9	1.180	0.999	very good fit
Mar - May	WET	9	3.220	0.955	very good fit
	DRY	9	0.870	1.000	very good fit
Jun - Aug	WET	8	2.520	0.961	very good fit
	DRY	9	2.660	0.976	very good fit
Sep - Nov	WET	7	0.730	0.998	very good fit
	DRY	9	0.860	1.000	very good fit

Extreme Weather Spells

Months	Weather Series	df	chi^2	p-value	Comments
Dec - Feb	FROST	8	28.870	0.000	poor fit
	HOT	0	0.000	1.000	no hot spells in winter
Mar - May	FROST	6	5.120	0.529	good fit
	HOT	2	0.340	0.842	good fit
Jun - Aug	FROST	1	0.000	1.000	no frost in summer
	HOT	4	33.730	0.000	poor fit
Sep - Nov	FROST	6	6.970	0.323	moderate fit
	HOT	2	0.010	0.993	very good fit

Precipitation distribution

Months	df	chi^2	p-value	Comments
Jan	8	0.450	1.000	very good fit
Feb	8	0.280	1.000	very good fit
Mar	8	0.980	0.998	very good fit
Apr	9	1.320	0.998	very good fit
May	8	1.580	0.991	very good fit
Jun	8	1.900	0.984	very good fit
Jul	7	1.110	0.993	very good fit
Aug	9	2.350	0.985	very good fit
Sep	9	1.010	0.999	very good fit
Oct	9	0.490	1.000	very good fit
Nov	8	0.170	1.000	very good fit
Dec	9	1.830	0.994	very good fit

* high low chi2 and p near 1.00 indicate good fit

4.3.3. CALIBRATION TO TEMPERATURE PARAMETERS

The stochastic weather generator reproduced air temperatures very precisely as calibrated from the observed records. Monthly minimum and maximum temperatures (averages) of modeled and observed are almost identical on a graph in Figure 32 (a). Daily minimum and maximum temperature variability (standard deviation) were calculated both for daily values and for monthly (mean) values. In both cases, the modeled temperature variability was very close to observed. In winter months, LARS-WG produced 0.5 to 1.0°C cooler minimum temperatures than observed, when comparing variability in monthly values.

Figure 32 Monthly mean air temperature at Abbotsford, BC, observed for period of record 1975-1995 (base climate scenario) and modeled with stochastic LARS-WG weather generator (20 year run): (a) Minimum and maximum Temperature, averaged monthly from daily temperature data (b) Temperature Variability as standard deviation of mean daily temperature, averaged monthly.

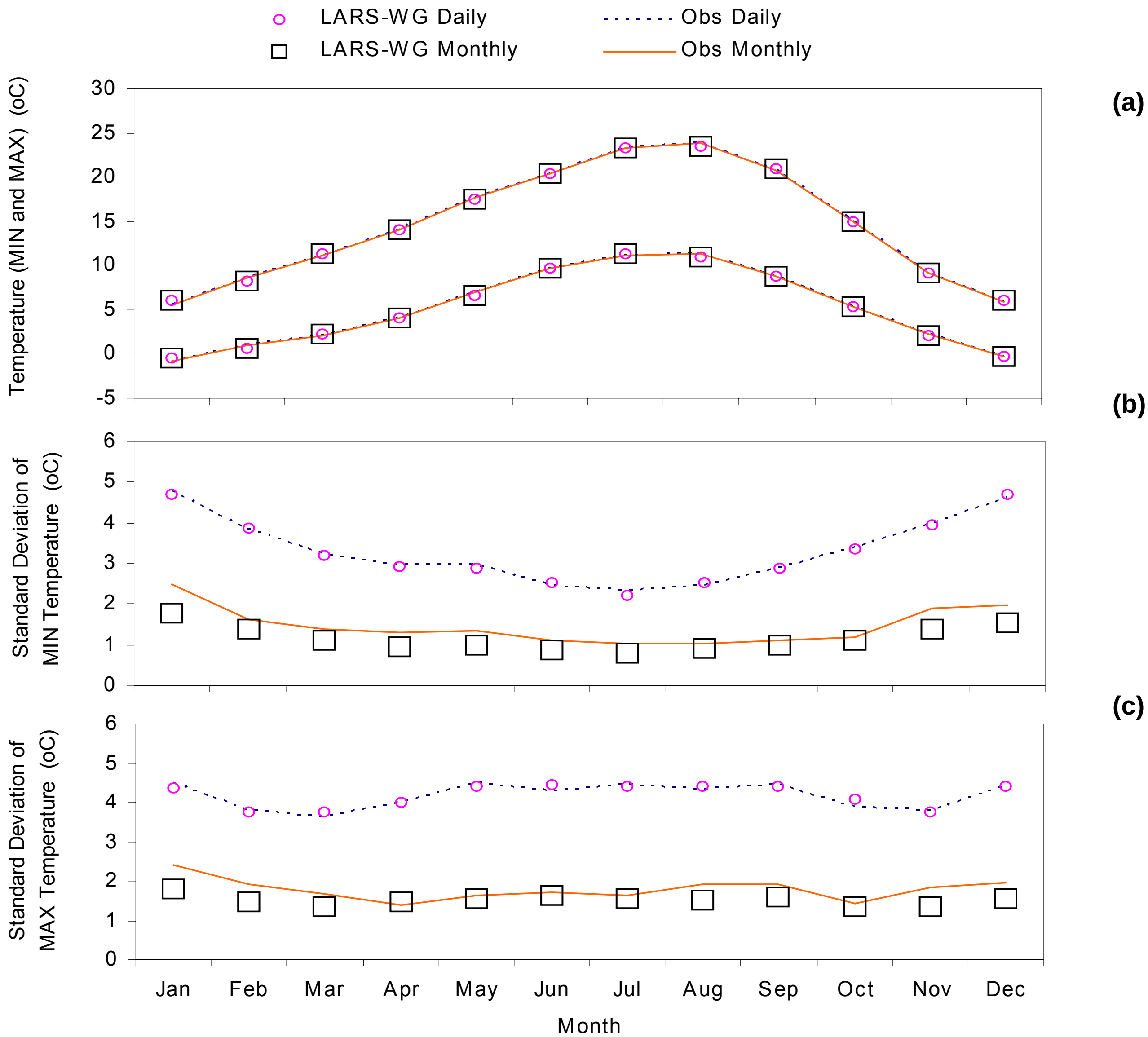

4.3.4. CALIBRATION TO SOLAR RADIATION PARAMETERS

Solar radiation was reproduced very well in stochastic weather of LARS-WG output. Mean solar radiation values in Figure 33 (a) in weather generator output were within 1% of observed values. Monthly variability in daytime solar radiation was also reasonably well preserved in stochastic weather model, although daily values were greatly under-predicted, compared to observed. This under-prediction in variability might cause small error in evapotranspiration estimates in HELP recharge model, once the LARS-WG weather is input into HELP, but the modeled daily and monthly solar radiation values were matching closely those observed.

Figure 33 Monthly and daily solar radiation (based on daily values) at Abbotsford, BC, modeled using cloud opacity and clear sky radiation for period of record 1975-1995 (base climate scenario) and modeled with stochastic LARS-WG weather generator (300 year run): (a) Monthly mean of daily values of Solar Radiation (b) Solar Radiation Variability as standard deviation of daily values and monthly means (of daily values).

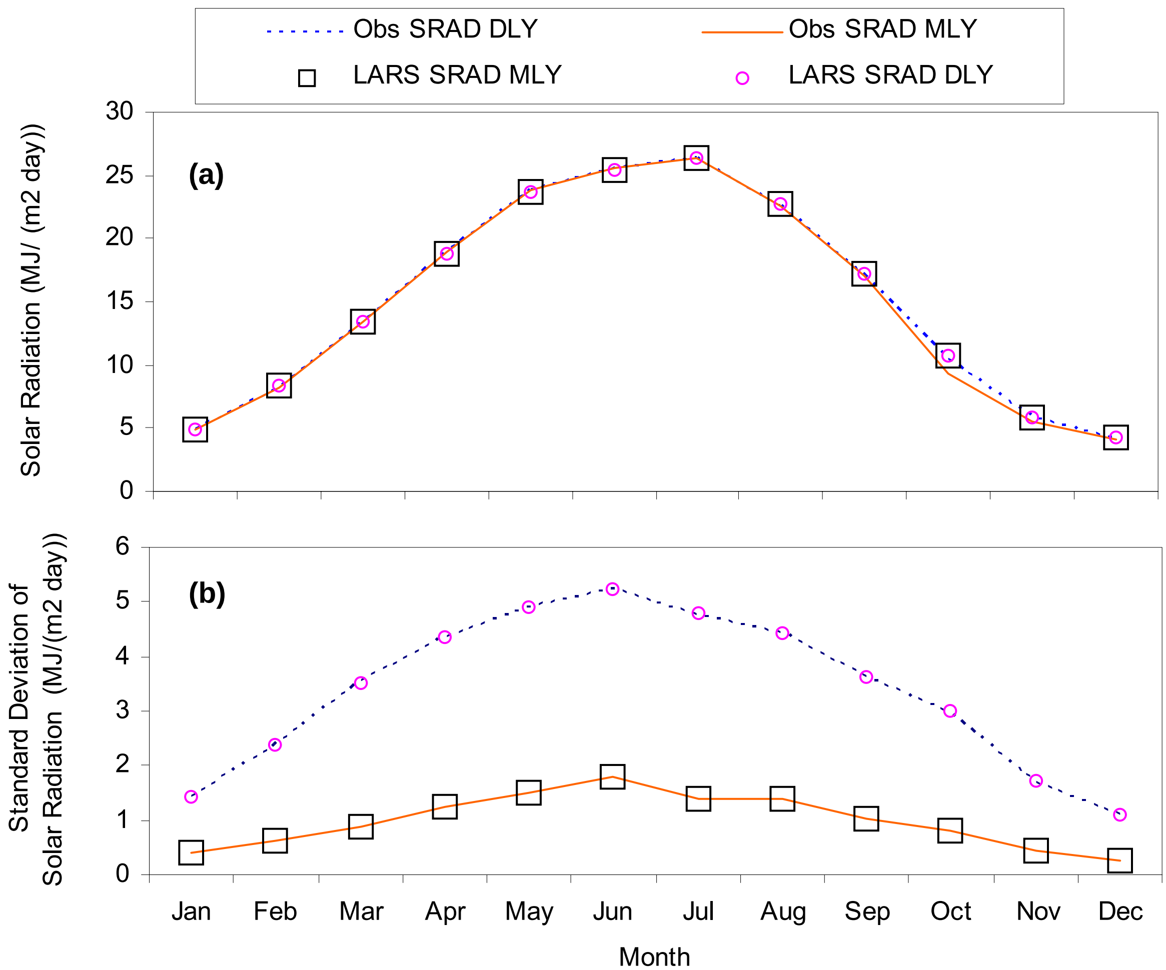

Figure 34 Comparing scenario input and LARS-WG output of 100 years of synthetic weather for 2010-2039 climate scenario: relative change in monthly precipitation, temperature, and solar radiation parameters compared to observed as test of LARS-WG model performance for Abbotsford weather generation.

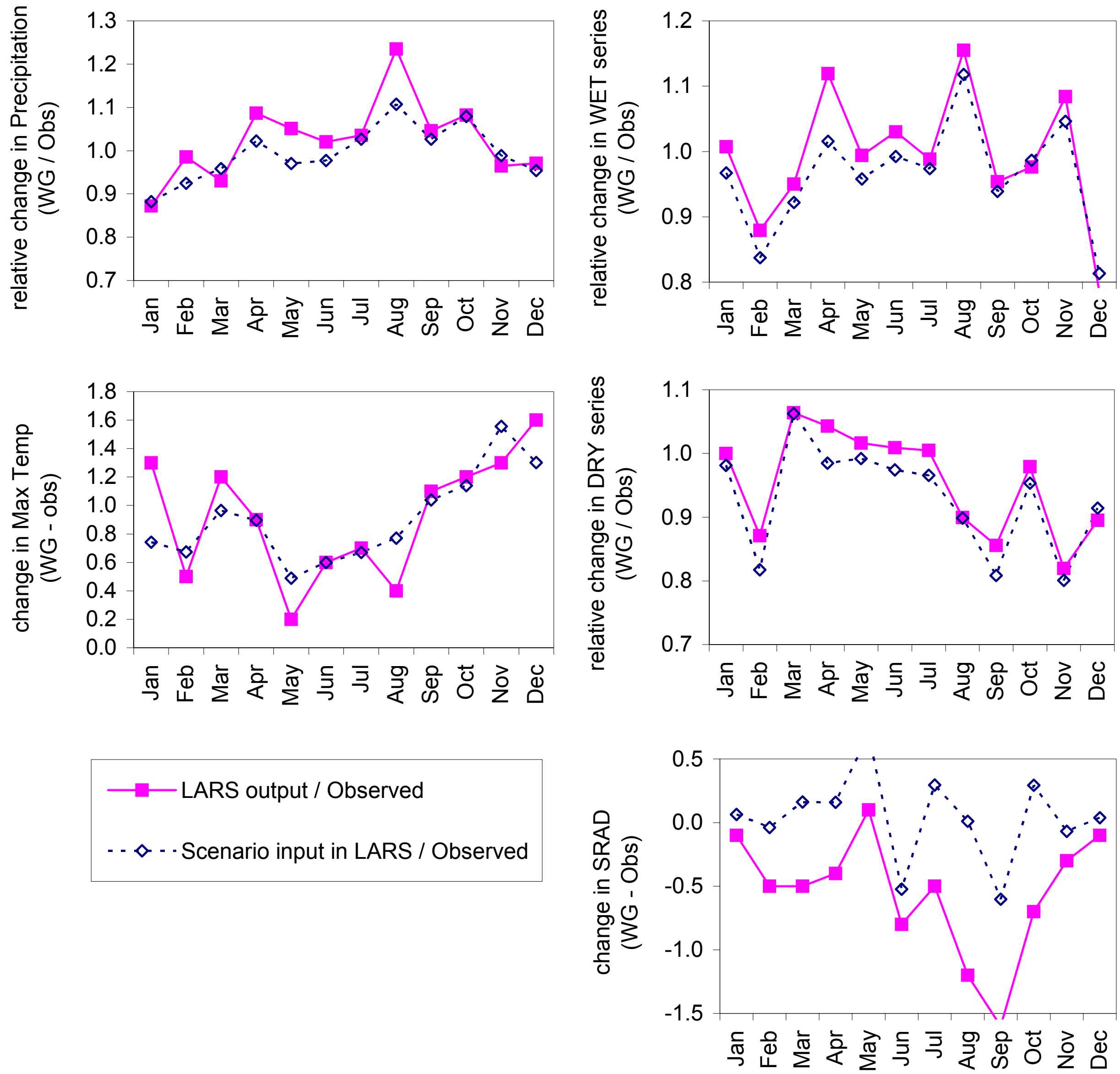

5. METHODOLOGY FOR RECHARGE MODELING USING HELP

5.1. INTRODUCTION

There are many physical properties of the subsurface that affect recharge to an unconfined aquifer and, as for other properties, they have three-dimensional distribution, and some change with time, such as soil moisture and depth to water table. The available data constrain the choice of parameters with relatively good ground truthing, and other parameter values must be inferred from other information and essentially estimated.

The ground truth data currently available are listed below. The parameters are listed in order of presumed importance in each group, but that will be explored further in HELP model sensitivity analysis to each. Usually, the type of local climate and, more specifically, seasonal distribution of precipitation will have dominant control on aerial recharge (at least the maximum possible recharge). The aquifer properties will control the actual amount of recharge into the aquifer, where the aquifer properties are assumed not to change with time, except unsaturated zone thickness, which will fluctuate seasonally. Ground surface properties, such as vegetation cover, have strong seasonality, and irrigation practices might have strong effect on local recharge rates.

Climatic variables:

1) precipitation (both depth and rate are important)
2) evapotranspiration
3) surface runoff

Aquifer media properties:

1) unsaturated zone hydraulic properties from lithology at point locations (estimated equivalent saturated hydraulic conductivity)
2) unsaturated zone thickness (depth to water table)
3) soil types
4) soil thickness
5) elevation and slope of ground surface (which affect runoff)

Ground surface properties (human modified):

1) vegetation cover (that affect evapotranspiration)
2) irrigation rates and areas affected (return flow to recharge)

There is a degree of uncertainty in each of these properties because data come from various sources and formats, which are discussed below. The authors of this report believe that the recharge model presented here is a best scientific guess at the actual values, and the only way to overcome the limitations of the assumptions, and to decrease uncertainty, is to collect more field data.

5.2. APPROACH TO RECHARGE MODELING

The overall approach to recharge modeling is identical to that used in a parallel study in Grand Forks, BC to similarly investigate the impact of climate change on groundwater (Allen et al., 2004). Spatially-distributed and temporally-varying recharge was modeled using GIS linked to the one-dimensional HELP.

First, several of the major factors that affect recharge are accounted for:

1) soil properties
2) hydraulic conductivity
3) depth of unsaturated zone (depth to water table)

Hydraulic conductivity of the aquifer media above the water table (calculated on well by well basis) was determined from a standardized well lithologs. The average value at each well represents the ensemble of materials present, and their vertical distribution. Hydraulic conductivity was then interpolated over the unsaturated zone depth to give spatial distribution (as best as could be derived from available data). Soils were also spatially distributed, and so was the depth of unsaturated zone (depth to water table).

The temporal variation of precipitation was accounted for by calculating monthly recharge values (as opposed to annual only), which give relatively good temporal distribution of recharge and capture the main inter-annual variation.

The use of spatial analysis tools in GIS environment allowed for spatial and temporal data integration. Therefore, the following results have both temporal and spatial components.

5.3. HELP MODEL SPECIFICS

5.3.1. SOFTWARE DESCRIPTION

The program WHI UnSat Suite (Waterloo Hydrogeologic Inc., 2000), which includes the sub-code Visual HELP (US EPA Hydrologic Evaluation of Landfill Performance model), is used to estimate recharge to the Abbotsford-Sumas aquifer. HELP is a versatile quasi-two-dimensional model for predicting hydrologic processes at landfills and testing the effectiveness of landfill designs, and enabling the prediction of landfill design feasibility. HELP is also effective in estimating groundwater recharge rates. Inputs consist of a representative sediment column with defined soil and sediment properties, engineering design features, surface slope, meteorological conditions, and evaporation rates. HELP uses numerical solution techniques that account for the effects of surface storage, snowmelt, runoff, infiltration, evapotranspiration, vegetative growth, soil moisture storage, and various engineering parameters (e.g., lateral subsurface drainage). The natural water balance components that the program simulates include precipitation, interception of rainwater by leaves, evaporation by leaves, surface runoff, evaporation from soil, plant transpiration, snow accumulation and melting, and percolation of water through the profile.

5.3.2. SEDIMENT COLUMNS

For the soil and sediment columns, the materials must be defined and the user must specify:

- Soil (porosity, field capacity, wilting point, and hydraulic conductivity)
- Engineering design data (liners, leachate and runoff collection systems, surface slope)

The profile structure can be multi-layered, consisting of a combination of natural (soil) and artificial materials (e.g., waste, geomembranes). In the current application, HELP will use only natural geological materials consistent with those found in the aquifer.

Soil media is the upper weathered zone of the earth, which averages a depth of 6 feet or less from the ground surface (Osborn et al., 1998). Soil has a significant impact on the amount of recharge that can infiltrate into the ground. In general, the less the clay shrinks and swells, and the smaller the grain size of the soil, the less likely water (and contaminants) will reach the water table.

The overall percolation column design in this study includes only two layers:

1) Soil (vertical percolation layer)
2) Aquifer media (horizontal drainage layer or vertical percolation layer)

UnSat Suite includes a user interface to facilitate soil column design and project management (see Figure 45 Appendix B). HELP includes a database of soils and aquifer media with appropriate hydraulic properties, but new materials can be defined using the material editor (Figure 46). There is no difference in model performance whether the vertical percolation layer or the lateral drainage layer is used for the bottom layer if there is no specified lateral inflow into the percolation column (as in this case).

5.3.3. INITIAL MOISTURE CONTENT

Before running the simulations, the initial water content of different layers should be specified. UnSat Suite gives the user the option to have the initial water content values specified by the user or computed by the model (as nearly steady-state values). With the latter, which is the default, UnSat Suite assigns realistic values for the initial water moisture storage of layers and simulates one year of hydrology. The values of moisture storage obtained from this simulation are then used as initial values, and the simulation starts again at year one.

5.3.4. WEATHER INPUTS

HELP requires three different types of meteorological data that must be provided as daily values:

- Precipitation
- Solar radiation
- Mean air temperature

Data, representing meteorological conditions, can be imported from a particular meteorological station file or synthetically simulated with the Weather Generator.

Air temperature

Mean air temperature can be input as daily time series or as monthly normals, and then modeled with the weather generator (as in this case).

Solar radiation

Solar radiation is specified as daily time series. In this study, the solar radiation was modeled separately then combined with precipitation and temperature time series, for input to stochastic weather generator calibration.

Precipitation

Precipitation is applied from specified daily time series, or created by weather generator from monthly normals (as in this case). It is the most important climatic variable controlling recharge.

Evapotranspiration

Evapotranspiration is computed by HELP at the soil-air interface of the upper layer in the soil column. The HELP model requires a set of parameters to simulate evapotranspiration, which are constants for the duration of the simulation. The model uses a complicated multi-level procedure for calculating different types of evaporation and evapotranspiration. The subroutines of this model allow calculation of evaporation from snow, soil and leaves. In addition, the model calculates vegetation growth and transpiration. In total, around 70 equations describe these processes. Fortunately, the number of parameters which require the user's input are limited. These include:

- Evaporative zone depth
- Maximum leaf area index
- Growing Season start and end day
- Average wind speed
- Quarterly relative humidity

The evaporative zone depth is the maximum depth from which water can be removed by evapotranspiration. A value of 20 cm was used for these simulations. This value is at the lower end of the range of values possible and is characteristic of sandy soils.

Runoff

For runoff calculations, it is necessary to specify the area over which runoff can occur and the type of surface vegetation. These two parameters remained fixed at 100% runoff area and a fair stand of grass, respectively, for all simulations. The rainfall-runoff processes in UnSat Suite are modeled using the USDA (US Department of Agriculture) Soil Conservation Service (1985) curve-number method, which is widely accepted and allows the user to adjust the runoff calculation to a variety of soil types and land management practices. The curve number (CN) is defined with respect to the runoff retention parameter (S), which is a measure of the maximum retention of rainwater after runoff starts (in inches):

$$CN = 1000 / (S + 10)$$

The maximum value of CN, which is 100, occurs when there is no infiltration. The smaller the CN, the more rainwater will infiltrate the soil. The minimum realistic value for CN can be assumed to be appropriately equal to 50. UnSat Suite uses different procedures to adjust the value of CN to surface slope, soil texture, and vegetation class. By default, the model automatically calculates the CN. The default condition was used for all simulations. For purposes of simplicity, zero slope was assigned to each model layer. The topography of the two aquifer surfaces is slightly undulating or sloping, but over small areas the surface is approximately horizontal. Steep escarpments are exceptions, but the relative area of these features is very small compared to the aerial aquifer extent.

5.4. SPECIFIC STEPS OF RECHARGE MODELING

The overall methodology was to select soil type representative of very high, high, medium, and low permeability. Similarly, four representative values of saturated hydraulic conductivity (K_{sat}) of the unsaturated aquifer media above water table are selected, through which recharge water percolates. The same or equivalent soil layers in HELP soil profiles are used as the capping soil units for recharge calculation. If recharge is sensitive to depth of percolation column, then representative depths are selected from depth statistics. A total of 4 x 4 x 4 = 64 scenarios of soil columns will be represented by the various combinations of depth, K_{sat}, and soil. Recharge is computed for all columns using the same weather data set for 10 years of weather, thus allowing for calculation of monthly and long term mean recharge for each column. Raster calculations are done to compute spatially distributed recharge for the base case (no climate change). The aquifer area is then classified using the scenarios and recharge values are linked to the classified aquifer map, obtaining spatially-distributed recharge, which could be interpolated or smoothed as necessary.

The final step involves transferring recharge values into the transient groundwater flow model. For the transient model, recharge varies with time, monthly time steps at a minimum, so the number of HELP analyses rises significantly. However, HELP already produces monthly recharge estimates (based on the average over the selected time scale, e.g., 10 years of weather from the weather generator). The same weather data set is used for all soil columns for a given climate scenario.

5.4.1. STANDARDIZATION OF THE WATER WELL DATABASE LITHOLOGY LOGS

Lithology data, obtained directly from the BC Ministry of Water, Land and Air Protection Water WELLS Database, were standardized using custom software developed at SFU[1]. Standardization involves geologic term recognition and association of terms with some standard terminology that is common to most hydrogeologic environments. Well logs typically record either a single material type at each depth interval, or a combination of material types. Where a single term is used, a standardized form of the term is retained in the standardization. For example, the term “fine sand” retains a material description of “sand”. Where more than one material type is recorded, each is recorded as a separate material type (e.g., material 1 and material 2). Using this protocol, the well logs for Abbotsford-Sumas were standardized and up to three material types were identified and retained. The top and bottom depths of each unit were similarly recorded. The resulting spreadsheet is available as part of this study.

5.4.2. CALCULATING VERTICAL SATURATED HYDRAULIC CONDUCTIVITY

[1] This code has been recently used to provide a set of standardized lithologic terms for the entire WELLS database.

The HELP model, which was used for recharge estimation, requires estimates of K_{sat} (or K_z) in the vadose zone. For all hydrostratigraphic units in all layers, representative values of K were assigned, and representative vertical hydraulic conductivity was computed for each raster cell 50x50 m over the aquifer area. According to Leonards (1962), an equivalent vertical hydraulic conductivity (Kz), which is at right angles to stratification of assumed homogeneous and isotropic units, is given by formula:

$$Kz = \frac{\sum m_i}{\sum \left(\frac{m_i}{K_i} \right)}$$

where m_i is the thickness of layer i having equivalent hydraulic conductivity K_i. Although other methods of averaging are available (Domenico and Schwartz, 1998), the K_i values for the layered media in standardized lithologs are not as reliable and numerous as to be able to perform more complex statistical analyses, thus the simple averaging method presented here was used. The averaged units m_i are, by default, homogeneous and isotropic as represented by equivalent K_i. There are no data for the aquifer on microscale isotropy.

The thickness of the saturated zone depends on the position of the water table elevation (estimated from all data sources). The MODFLOW model layering intercepted the water table in different model layers (Map 5). This map is similar to map of depth-to-water-table. MODFLOW layers that intercept the water table are from 1 to 5 (top of model downward, decreasing in elevation).

Map 5 Map of MODFLOW layer (numbers) that contain the water table surface.

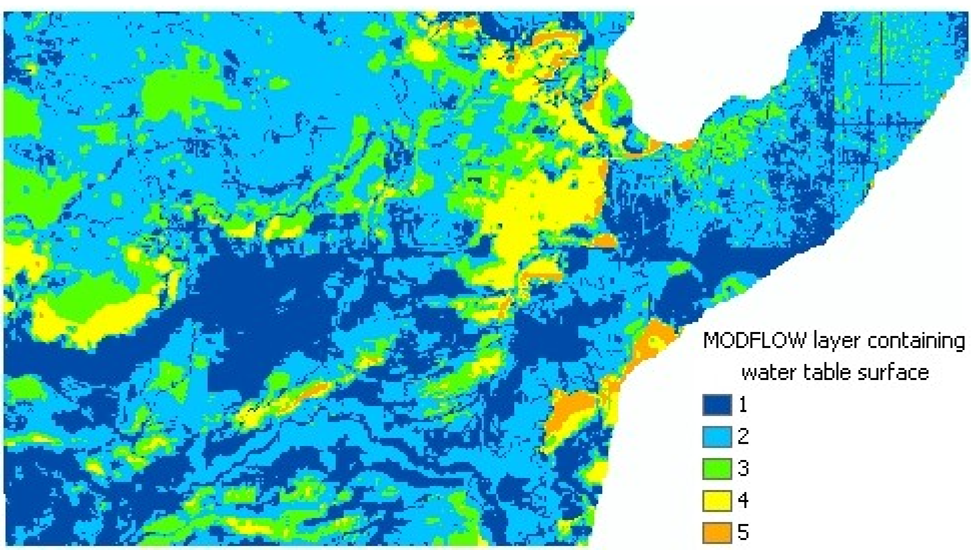

Figure 35 shows a histogram of K_z values for all 50x50m grid locations over the aquifer area. K_z values over a million pixels ranged from 0.1 to 105 m/d, median of 50.91 m/d, mean 46.3 m/d, and quartile values of 0.51 and 89.84 m/d. The K_{sat} in the vadose zone were interpolated using Inverse Distance Weighed interpolator (power 2, number of points = 5, output cell size 100 m), and computed on representative vertically averaged Log K_{sat} values at all available point locations where lithologs exist.

After interpolation, 10^(Log K_{sat}) of the interpolated raster was computed. K_{sat} values were then converted to units of m/d. Five K_z classes were chosen as $1x10^{-6}$ to 20 m/d, 21 to 40 m/d, 41 to 60 m/d, 61 to 80 m/d, and 81 to 120 m/d (Map 6). The higher values mean that water will percolate more easily through the vadose zone during recharge events. Representative material K_{sat} in HELP soil columns will be 315, 40, 1.4, and 0.015 m/d (mid value in each class).

Figure 35 Histogram of averaged vertical Kz (above water table) for all 50x50m pixels over Abbotsford-Sumas aquifer**.**

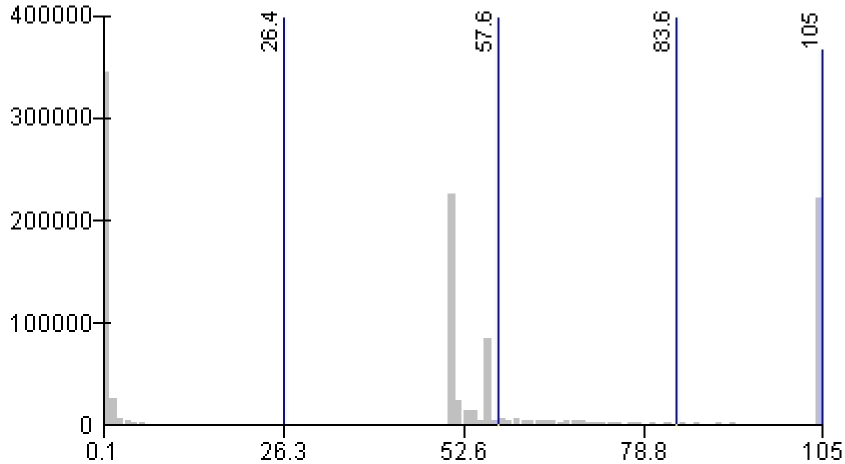

Overall, the K_z distribution is very heterogeneous (Map 7). Low K_z values occur over Fort Langley Formation (stony clays) sediments in the western part of model area, and in Sumas Valley in the former location of a lake (lacustrine silts). There are also low K_z values along river channels where there are mapped silts and other low-K deposits (slack water deposits). Moderate K_z values occur in Sumas Valley, due to floodplain silty sands cover, and over southern parts of the aquifer system. High K_z values are found in Abbotsford City area, in the uplands associated with highly permeable Sumas Drift consisting of gravels and sands, interspersed with till deposits.

Table 9 provides the descriptive statistics of averaged vertical Kz (above water table) for all well locations in Abbotsford-Sumas aquifer, and the assignment of Kz categories for recharge modeling in HELP module in UnSat Suite.

Map 6 Average computed vertical hydraulic conductivity in the unsaturated zone, based on material types in 20 m grid cells, mapped hydrostratigraphic units, assignment of average K values (assuming) Kz = Kxy within each unit, and vertical averaging to approximate Kz.

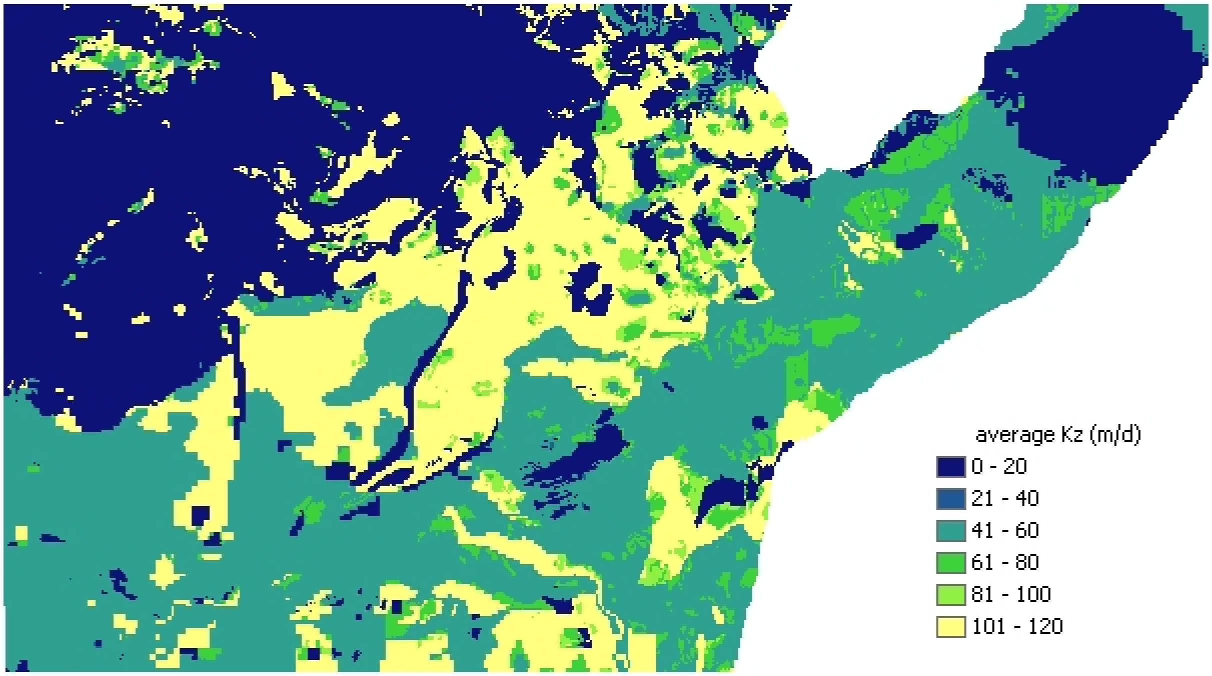

Table 9 Descriptive statistics of averaged vertical Kz (above water table) for all well locations in Abbotsford-Sumas aquifer, and assignment of Kz categories for recharge modeling in HELP module in UnSat Suite.

	Kz (m/d)
Mean	46.20
Median	50.91
Standard Deviation	39.4
Minimum	0.100000
Maximum	105.00

Kz (m/d)	Kz (cm/s)	K categories in HELP model
5.00E-01	5.787E-04	low
5.10E+01	5.903E-02	mod
7.50E+01	8.681E-02	high
1.05E+02	1.215E-01	v high

Map 7 Distribution of K_Z in unsaturated zone above water table in Abbotsford-Sumas aquifer.

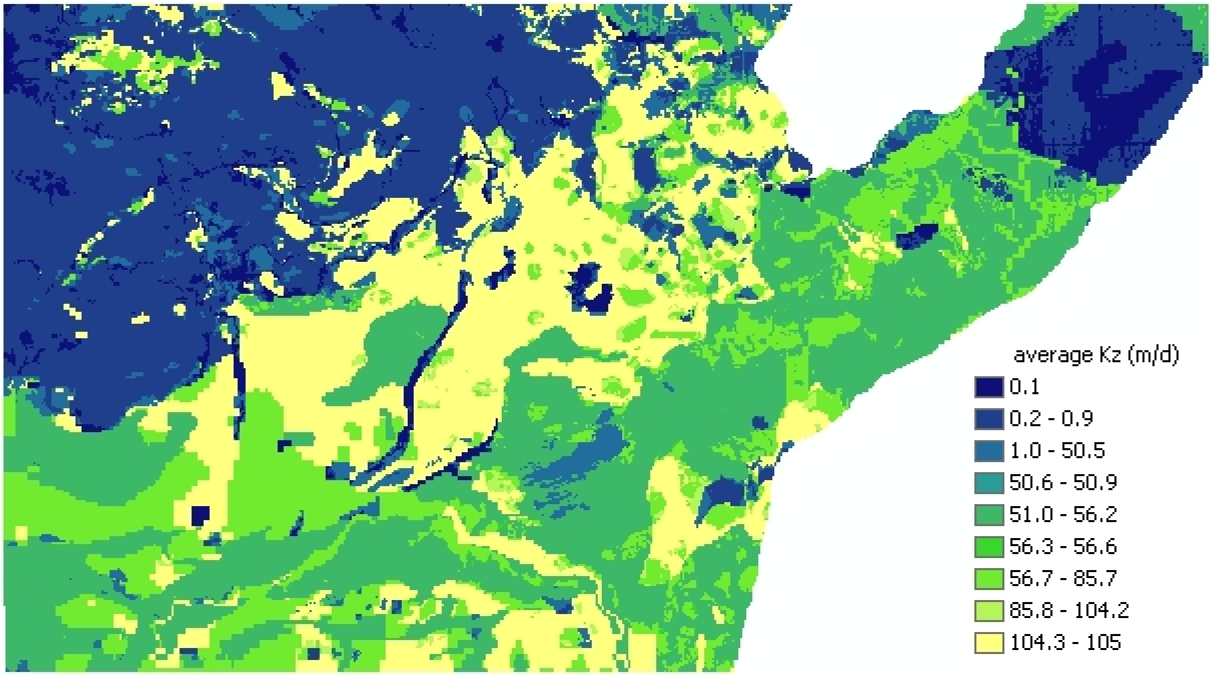

5.4.3. SOIL TYPE (PERMEABILITY)

Soil maps for the Abbotsford-Sumas aquifer were obtained published soils maps for the Fraser Valley (BC). Whatcom County soil data were obtained from National SSURGO Data, US Dept of Agriculture, Natural Resources Conservation Service http://www.ncgc.nrcs.usda.gov/branch/ssb/products/ssurgo/data/wa.html.

Soil permeability was represented as a drainage property represented by code from 1 to 6 (low to very high) on the British Columbia soil map of Fraser Valley, and 1 to 3 (low to high) on the Washington State soil map for Whatcom County (Table 9). Map 8 shows the soil permeability over the aquifer. Rock outcrops surround the aquifer outline, and very small outcrops occur within the aquifer area. Rock outcrops were assigned special code for low permeability, relative to unconsolidated sediments in the valley that form the aquifer.

Since most of these soils are rapidly drained, the unconfined surficial aquifer is directly connected to the ground surface such that rainfall and meltwater is expected to rapidly infiltrate and recharge the aquifer. Sumas Valley floodplain has an expected reduced infiltration due to higher content of fine grained sediments. Surface runoff may occur on steeper slopes and on low permeability soils, where small ponds are present, which fill up seasonally and evaporate in drier periods.

A small portion of the aquifer is occupied by the City of Abbotsford and other smaller communities (Sumas, Lynden, Aldergrove), with associated transportation network and built-up areas (Map 9). In these areas, a large proportion of the ground surface is paved, compacted, or covered by structures, such that most of the rainfall and meltwater is redirected to stormflow network and removed. Infiltration to unconfined aquifer is limited in those areas. Thus, paved areas were assigned lower permeability regardless of underlying soil types.

For the purpose of recharge modeling, the GIS soil map was converted to raster format with 20 m resolution, then reclassified into 5 soil rating categories based on S-ratings[2] of soil in DRASTIC aquifer vulnerability mapping method. There were no soils with S-rating of 7, and only a few small patches with ratings below 6, which were then combined with those having rating of 6 as representing low permeability class. Paved areas and rock outcrops were given rating of 1 (lowest). This raster map was used as one of the variables that generated spatially-distributed recharge estimates for the aquifer. For the purpose of recharge analysis using the HELP vertical percolation columns, the soil types in the HELP model were matched by permeability class and assigned representative S-rating (see Table 10). Vertical saturated K values were used as given in HELP database for various soil types that were selected. The final relative permeability map, indicating very high, high, moderate, low and paved is shown in Map 10. Table 11 lists low permeability soil types, Table 12 the area covered by moderate and variable permeability soil types, and Table 13 the high to very high permeability soil types, all sorted by area.

Map 8 Soil permeability over Abbotsford-Sumas aquifer (from soil maps).

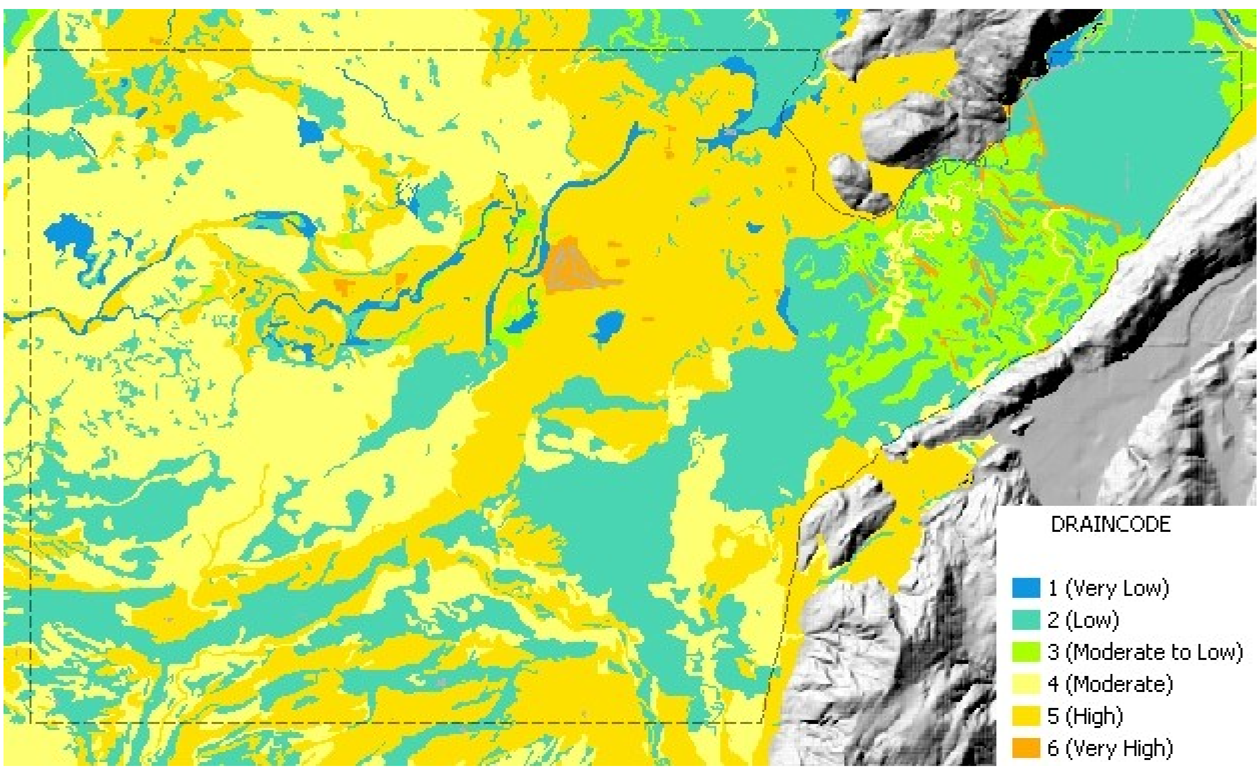

[2] S rating is used in the DRASTIC method of assessing intrinsic vulnerability of the aquifer. The S rating is a relative rating, with high values indicating higher relative ease of drainage. Scale of 1 to 10.

Map 9 Urbanized areas that are paved to large extent.

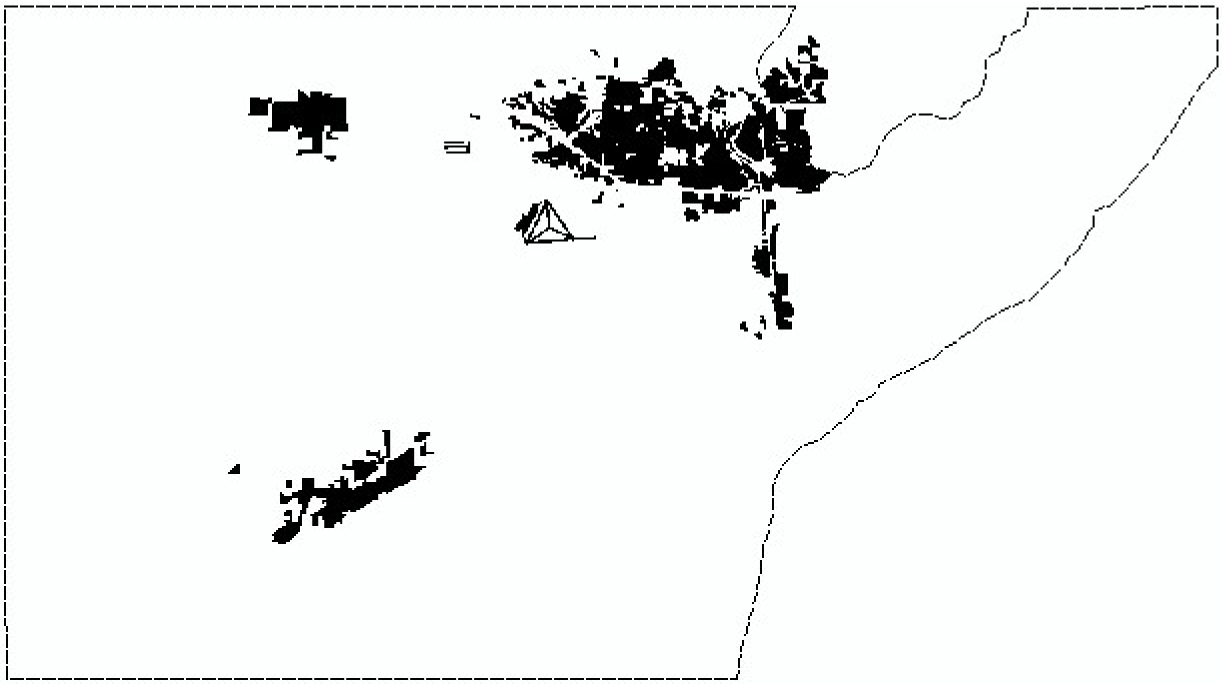

Map 10 Relative Soil permeability map derived from soil drainage map.

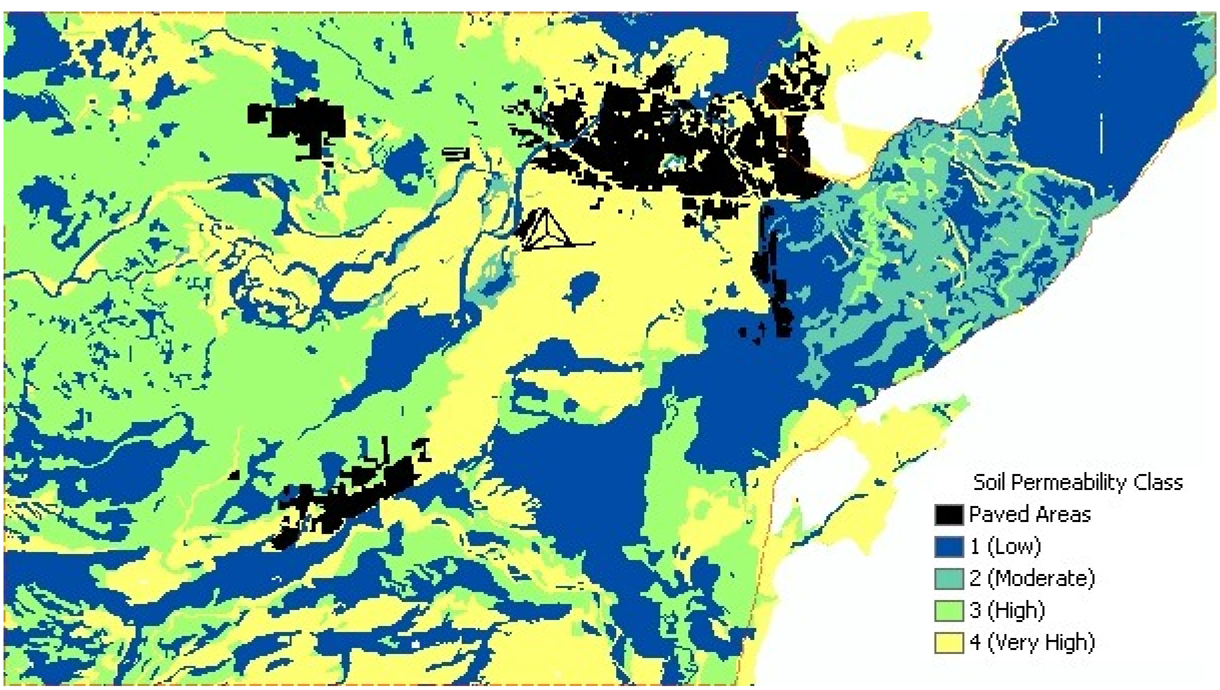

Table 9 Soil types in Abbotsford-Sumas aquifer area, soil properties, drainage and soil rating codes, and area covered in central Fraser Valley.

SOILCLASS 1	SOILCLASS 2	Soil Name	Drainage / Permeability	Parent Material (primary)	Grain size	Drain Code	Classed (1 to 4)	Area (ha)
LM-JN	a	Lumbum Soils	Low	Lacustrine or Floodplain	Organic	1	1	1490
AD-MH	B; S 0-1	Abbotsford Soils	High	Glacial Outwash	Gravel, Sand lenses	5	4	2994
RD	ef	Ryder Soils	Moderate	Glacial Outwash	Stony Till, Gravel lenses	5	4	2649
RD-LZ-LX	de	Ryder Lonzo Laxton S	Moderate	Glacial Outwash	Till, gravel, sand	variable		
CL-AD	cb; S 2-3	Columbia Soils	High	Glaciofluvial	Gravel, Gravelly Sand	5	4	5188
RS	A	Ross Soils	Low	Floodplain	Silty Clay, Till and Gravel	1	1	555
DR-LH		Defehr Soils	Moderate		Sand or Gravel and Till	3	2	199
MH		Marble Hill Soils	High	Glaciofluvial	Gravel, Gravelly sand	5	4	2796
AN-GN-BK	VD-VD-BD	Floodplain Soils	Low	Fluvial	Silt, Clay			
KD		Kennedy Soils	High	Fluvial	Sand	6	4	253

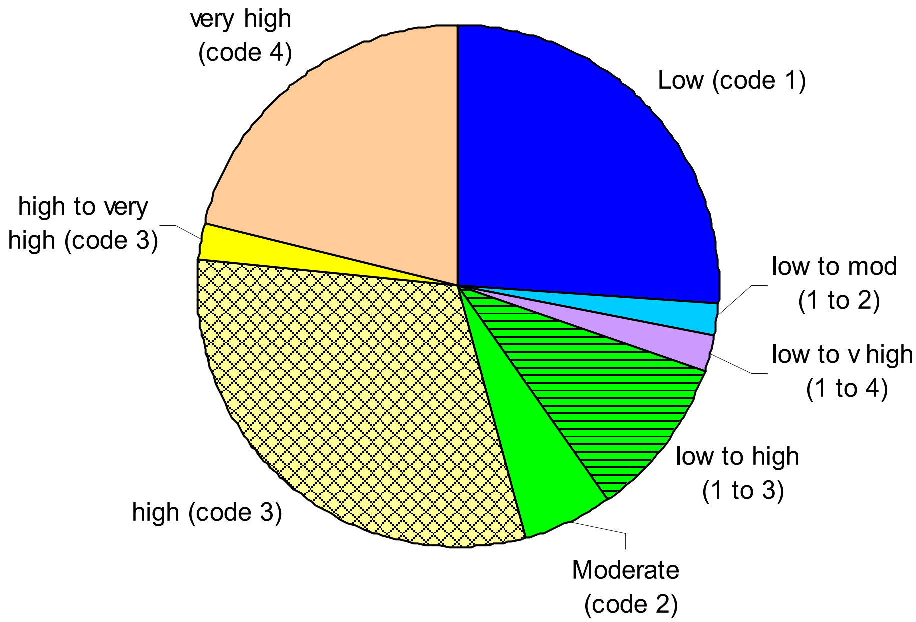

Figure 36 Proportion of soil types by soil permeability categories in Abbotsford-Sumas aquifer region.

Table 10 Soil types in HELP model, soil hydraulic conductivities, and assigned S-rating and permeability class for recharge modeling.

Vertical percolation layer in HELP	Vertical Kz (sat)		SRating	Permeability
	(cm/s)	(m/d)		
Silty Loam	1.90E-04	0.164	5 to 6	low
Loam	3.70E-04	0.320		
Fine Sandy Loam	5.20E-04	0.449		
Sandy Loam	7.20E-04	0.622	8	moderate
Loamy Fine Sand	1.00E-03	0.864		
Loamy Sand	1.70E-03	1.469	9	high
Sandy Gravelly Soils (new type)	5.80E-03	5.011	10	v high

Table 11 Low permeability soil types in Abbotsford-Sumas aquifer, sorted by total area.

Soil Name	Total Area (ha)	Soil Name	Total Area (ha)
SUMAS	3661	PREST	349
PANGBORN	2687	LANGLEY	309
CLOVERDALE	2608	WESTLANG	296
ORIDIA	1741	YELM	271
LUMBUM	1490	NIVEN	248
SCAT	1392	SIM	187
HERON	1196	VEDDER SHALLOW VAR	177
SKIPOPA	1096	HOPEDALE	175
ALBION	1006	RICHMOND	164
BUCKERFIELD	937	HJORTH	160
FISHTRAP	777	ELK	150
JUDSON	734	BOOSEY	143
LEHMAN	727	KATZIE	124
HAZELWOOD	692	MCELVEE	108
GIBSON	675	EVERSON	104
ANNIS	617	HISTOLSOLS	98
TRIGGS	607	EMBREE	95
PUGET	599	HALLENTON	89
HALLERT	598	MCLELLAN	82
SHALCAR	575	URBAN	77
BELLINGHAM	557	PREST SHALLOW VAR	45
ROSS	555	NICOMEKL	44
GLEN VALLEY	546	LULU	38
VEDDER	542	TACOMA	37
DIXON SHALLOW VAR	493	ELIZA	34
BANFORD	485	SANDEL	23
BEHARREL	471	PAGE SHALLOW VAR	22
DIXON	461	PREST ANTH VAR	17
VINOD	434	ROSS SHALLOW VAR	7
PAGE	425	CHUCKANUT	5
CARVOLTH	412	COMAR	3
CALKINS	375	HOVDE	3
SNOHOMISH	369	SPETIFORE	2

Table 12 Moderate and variable permeability soil types in Abbotsford-Sumas aquifer, sorted by total area.

Moderate permeability (code = 2)

Soil Name	Total Area (ha)
BATES	1927
FAIRFIELD	1289
VYE	1241
BERRY	983
LIVINGSTONE	615
COGHLAN	346
SUMMER	345
DEFEHR	199
FADDEN	153
VYE SHALLOW VAR	125
MURRAYVILLE	115
BATES SHALLOW VAR	90
DEWDNEY	65

variable permeability in soil class

Soil Name	Total Area (ha)
low to mod perm (1 to 2)	
BRISCOT	2579
low to high perm (1 to 3)	
HALE	3932
MT. VERNON	3372
EDMONDS	3191
CLIPPER	1322
LABOUNTY	759
RIVERWASH	314
PILCHUCK	278
ANDIC	50
low to v high perm (1 to 4)	
LAXTON	2237
(other)	530

Table 13 High to very high permeability soil types in Abbotsford-Sumas aquifer, sorted by total area.

very high permeability (code = 4)

Soil Name	Total Area (ha)
COLUMBIA	5188
KICKERVILLE	3337
ABBOTSFORD	2994
MARBLE HILL	2796
RYDER	2649
SUNSHINE	2002
PUYALLUP	1825
BARNHARDT	1010
LONZO CREEK	926
SQUALICUM	754
PEARDONVILLE	684
LYNWOOD	678
EVERETT	583
BLETHEN	505
GRAVEL PIT	422
KENNEDY	253
BARNESTON	210
GREVELL	205
ABBOTSFORD ANTH VAR	192
MATSQUI	134
PITS	123
CAPILANO	97
LICKMAN SHALLOW VAR	70
RECENT ALLUVIUM	56
PEARDONVILLE SHA VAR	42
POIGNANT	29
OAKES	26
ISAR	17
WINSTON	10
CANNELL	6

high permeability (code = 3)

Soil Name	Total Area (ha)
LYNDEN	6243
WHATCOM	23763
BOSE	3622
NICHOLSON	2869
MILNER	1792
SARDIS	695
MONROE	428
LICKMAN	275
KLINE	192
WHITEHORN	166
NATI	138
SEHOME	32
SQUIRES	7
RINKER	4

high to very high perm (3)

TROMP	2619
BIRCHBAY	220

5.4.4. SOIL THICKNESS

The vertical soil profiles and thicknesses are also important in determining soil permeability and recharge to deeper layers. There are two sources of information regarding soil thickness: well lithologs soils maps. For the BC side of the study area, the soil depths were taken to represent the mid points of soil polygons from Lower Mainland digital soil maps. The mean value for total soil depth was tabulated by soil drain code (soil permeability for that soil type for that polygon) (Figure 36). Most of the soil polygons were between drain code 2 and 5. Mean soil depth is poorly correlated with soil drain code except the much thicker very rapidly drained soils of drain code 6. Soil depth is not provided on the US soils maps.

In 2164 lithologs, the drillers recorded the thickness of overburden and soil, but did not specify distinguish between the two. The median thickness of soil (or overburden) was 0.92, and the median was 0.60 m if few large overburden depths were excluded (>12 m). A histogram shows that soil thickness is generally 0.4 to 1.6 m thick (Figure 37). Soils are expected to vary in thickness over micro-topography, thus any aquifer-wide interpolation of thickness would have very large error (locally).

Spatially, (Map 11), there is quite large heterogeneity of soil thickness (as simply interpolated by inverse square method from soil polygon mid points). Some exceptions are: in the Sumas Valley, towards Chilliwack, where the soils are very thin – there used to be a lake in that area, but it has been drained for irrigation control purposes. Lacustrine silts underlie those thin soils.

Where soils are absent, less moisture is stored in shallow subsurface and less evapotranspiration is expected to occur than in thick soil areas. For the modeling purposes, soil thickness will be assumed to be 1.0 m in all percolation columns, since there are not enough data to properly assign soil thickness at all points.

Map 11 Soil thickness distribution from soil and lithology data over Abbotsford-Sumas aquifers: (a) interpolated from soil database, center points of soil map polygons, (b) interpolated from litholog database (soil or overburden < 2 m thick as indicated in lithologs).

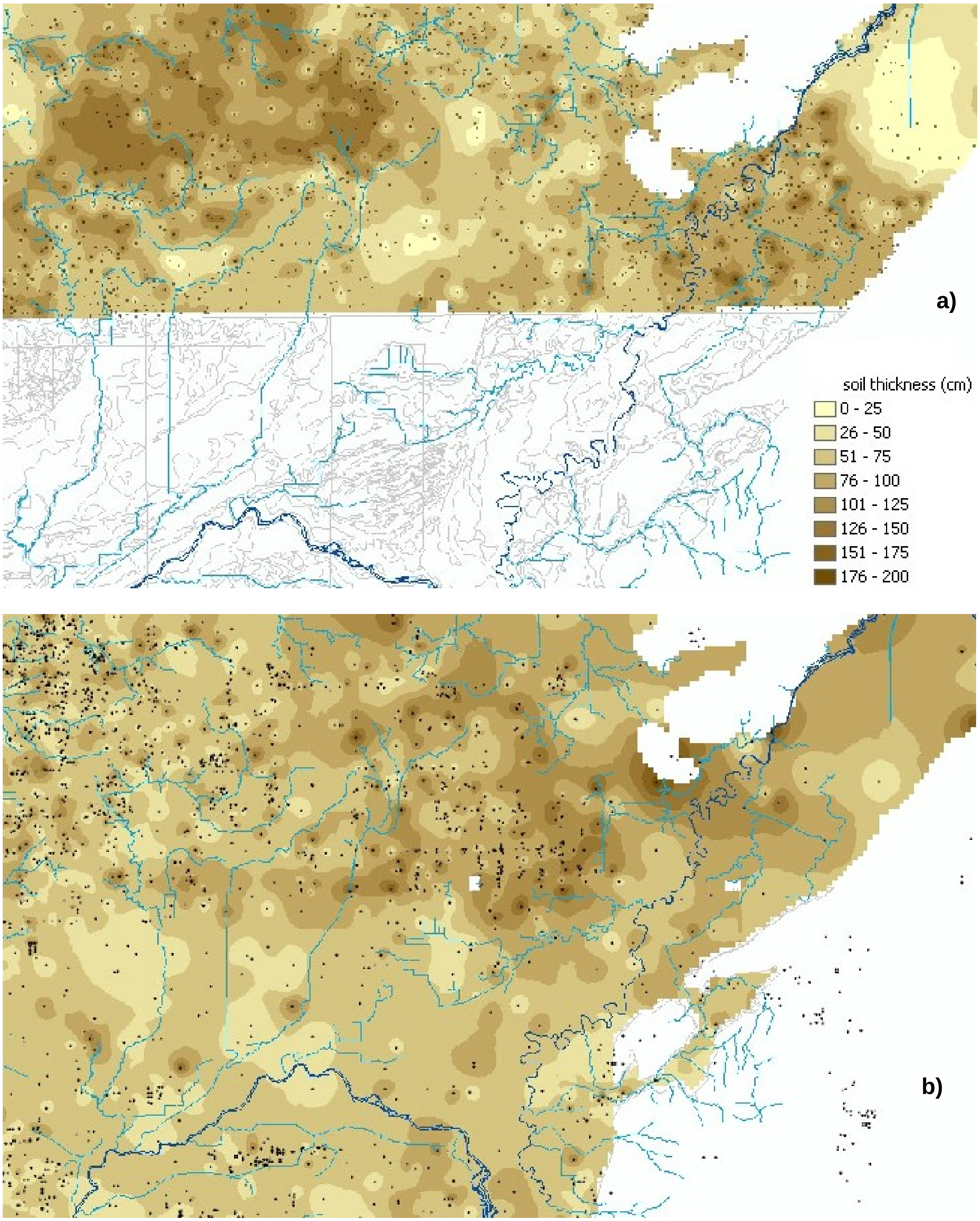

Figure 37 Mean soil depths grouped by soil permeability (drain code). (a) data from digital soil maps and polygons – centers of polygons, (b) data from borehole lithologs where soil was indicated as top unit. Soil polygons are from BC side of central Fraser Valley, and litholog data are from both BC and WA sides of central Fraser Valley.

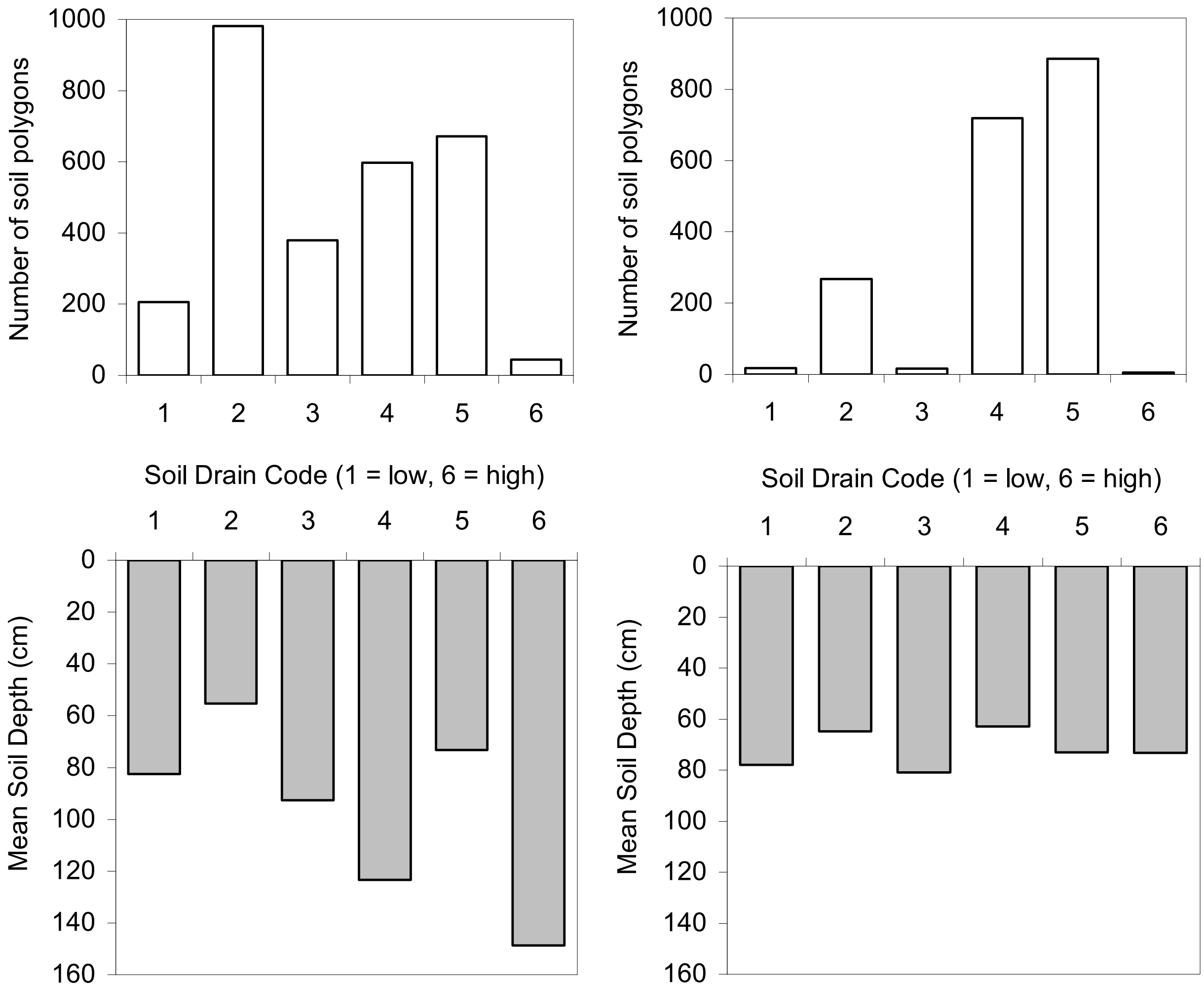

Figure 38 Thickness of soil and other overburden in standardized well lithologs in central Fraser Valley. Histograms of thickness of all litholog units in all wells and occurrence order in lithologs.

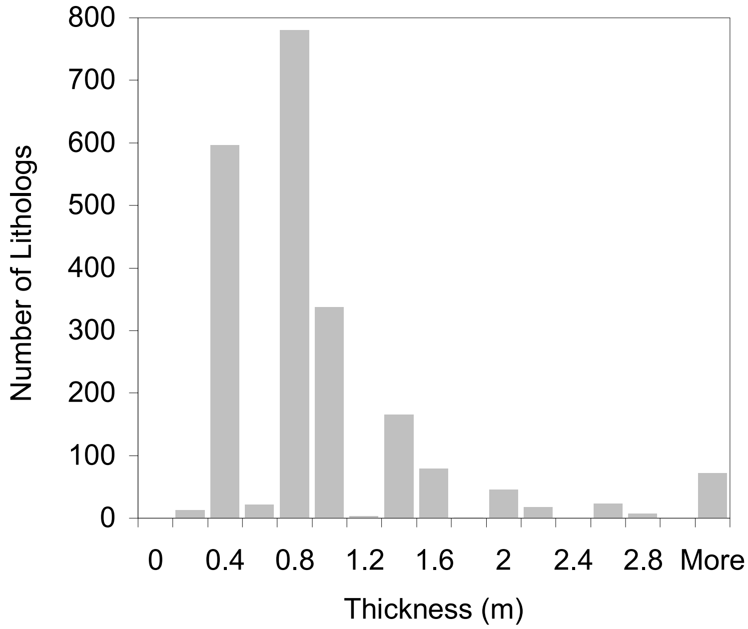

5.4.5. DEPTH TO WATER TABLE

The depth to water is the distance (here in feet) from the ground surface to the water table. It determines the depth of material through which water must travel before reaching the water table. Depth to water was estimated for wells in the Abbotsford-Sumas aquifer directly from the historic static water levels recorded in drillers' logs. Static water levels provide a one-time measure of the depth of water in the well. Normally, these measurements are made immediately following drilling, and therefore, can result in lower values that would be measured some time following drilling when the well has re-equilibrated with the surrounding aquifer water levels. The Abbotsford-Sumas aquifer is a highly permeable aquifer, consequently, the hydraulic disturbance during drilling activities can be expected to dissipate fairly quickly. In this respect, it is reasonable to assume that post-drilling measurements of water level may be similar to those of the surrounding undisturbed aquifer. In addition to drilling disturbance, water levels vary throughout the year in an aquifer according to seasonal factors (e.g., changes in recharge and changes in storage). Because wells are drilled at different times of the year, the static water elevations recorded following drilling might be expected to vary depending on season. Notwithstanding, static water level measurements are assumed to be representative of groundwater levels in the aquifer, and act as a surrogate for ambient groundwater conditions in the aquifer.

Values of static water level (recorded as depth to water in a well), were imported into ARCGIS as point values that are representative of the water level at each well. The median depth was 5 m, mean was 8.0 m, standard deviation 9.3 m (the histogram is skewed by many small depths to water table and a few large ones near scarps), but range was from 0 to 78 m (Figure 39).

A composite water surface was calculated using a geostatistical analysis involving interpolation between points, and extrapolation to the boundary of the aquifer. By subtracting the water table surface from the ground surface (using digital elevation model), a map of depth to water table was produced in 20 m raster format (shown in Map 12).

Depth to water table determines the total thickness of HELP soil column for recharge computation. Five depths were selected using quartiles of the distribution of the depths (min and max bounding values) (Map 13). The depth classes were chosen as 0 to 2 m, 2.1 to 5 m, 5.1 to 13.0 m, 13.1 to 78 m, with roughly 25% of aquifer area in each category (four categories).

Figure 39 Depth to water table from ground surface at well locations in Abbotsford-Sumas aquifer - histogram of raster map of depth to water table (50 m grid) with quartiles (solid lines) and mean (dashed line).

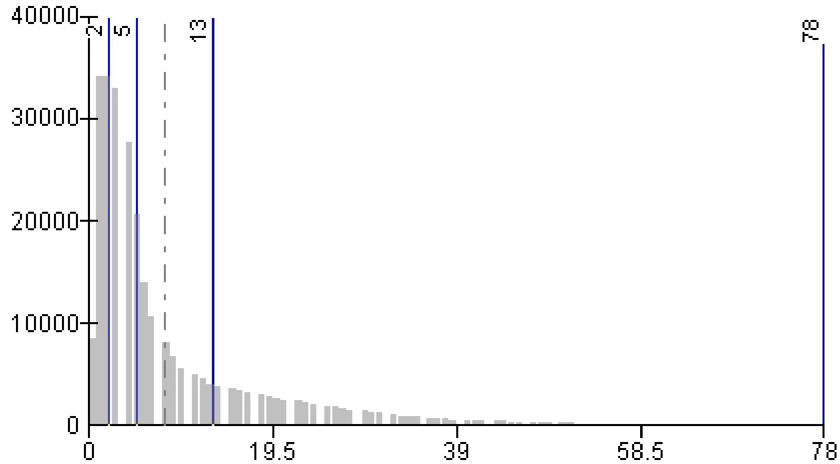

Map 12 Depth to water table from ground surface in Abbotsford-Sumas aquifer.

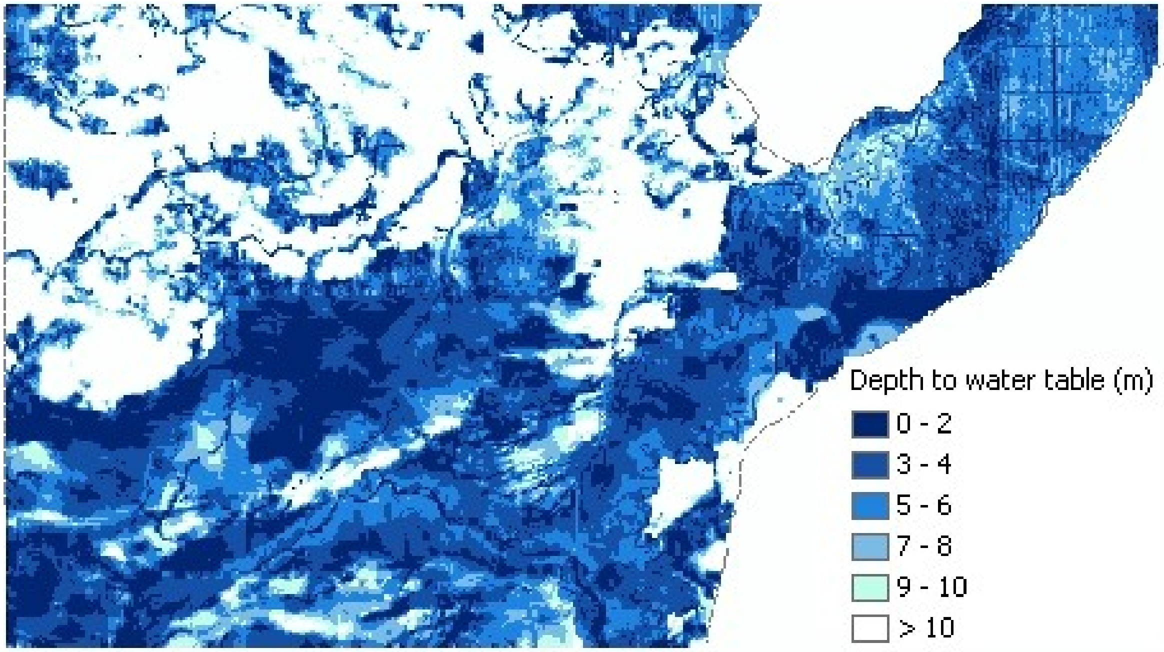

Map 13 Depth to water table classed map for Abbotsford-Sumas aquifer.

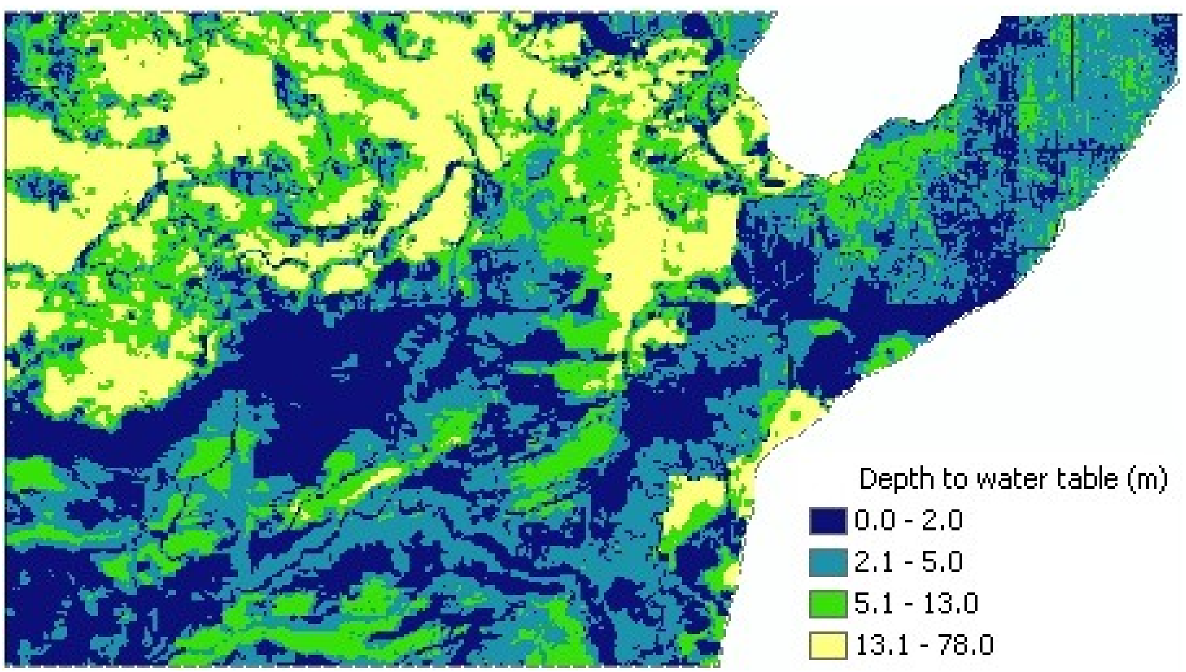

5.4.6. RECHARGE SCENARIOS

Recharge scenarios were generated for all combinations of defined classes (4 categories each) of Kz, depth to water, soil type. The four Kz classes were “very high”, “high”, “moderate”, and “low” hydraulic conductivity of unsaturated zone aquifer media. Depth to water classes were used: 3, 8, 11, and 25 metres (coded as d3, d8, …). Soil classes were coded in terms of permeability as “low”, “moderate”, “high”, and “very high”. Soil thickness was held at 1.0 m.

Using ArcGIS, the aquifer was reclassified into percolation column scenario polygons, based on cross-referencing of 3 raster images for the 3 variables (classed maps). The conditional statement for raster calculation had 64 conditions specified, was rather long, and was constructed on a spreadsheet before using in ArcGIS. The resulting map of percolation column scenarios (Map 14 below) shows that there is relatively high spatial resolution of the differences between the 3 variables of aquifer media over most parts of the aquifer.

More categories of K_z and depth could be added, but that would result in many more percolation columns in HELP model, thus more data analysis requirements. K_z is interpolated and larger number of K_z classes would represent that interpolated K_z distribution more smoothly, but it would not improve the accuracy of the model because K_z distribution is not that well known; in itself it is heavily averaged and has many assumptions. Depth to water table is relatively well known, probably the best of these 3 parameters, but in areas where depth has low variation, the addition of more depth classes would not improve the resolution (the scenario map would look almost identical to present one).

Over paved areas, the recharge was reduced by 50%, to simulate storm runoff into drains.

Map 14 Spatial distribution of aquifer media categories (recharge scenarios) for the model area.

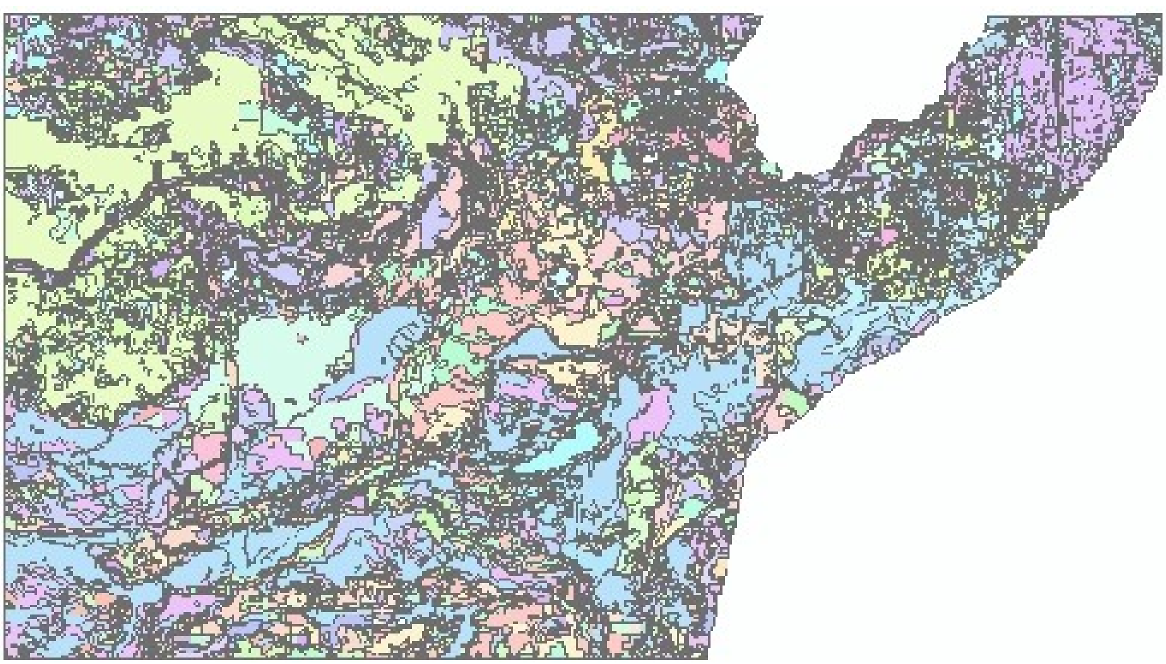

5.4.7. PRECIPITATION GRADIENT

Recharge estimates based only on soil type, vadose zone properties, and mean annual rainfall, had to be adjusted for the precipitation gradient. Over the model area, the mean annual precipitation ranges from 1050 mm in the southern edge near Bellingham, WA, to 1500 mm near Abbotsford Airport in the 80 m uplands, and is estimated to be above 1600 mm in the northern edge of the model. There is 300 mm difference between the valleys of Nooksack and Sumas Rivers and the uplands to the north-west (Abbotsford City and Langley township). There is also strong gradient in NE direction along the Sumas Valley from Sumas WA to Chilliwack BC. Numerous weather stations were selected for interpolation using Kriging technique (Table 14 and Map 15).

Table 14 Weather stations with precipitation in Fraser Valley (BC and WA state) used to model precipitation gradient across Abbotsford-Sumas aquifer model extent.

StID	Station	Elevation (m asl)	Annual P (mm)	Years	Lat	Long
1100030	Abbotsford Airport	58	1573.2	1971-2000	49.03	-122.37
1100120	Agassiz CDA	15	1727.4	1889-2000	49.25	-121.77
1100240	Aldergrove	76	1713.0	1953-1980	49.12	-122.48
450574	Bellingham FCWOS AP, WA	5	898.1	1947-2000	48.80	-122.53
450564	Bellingham, WA	36	982.0	1971-2000	48.78	-122.48
450729	Blaine, WA	2	1035.1		48.98	-122.75
1101146	Burnaby, Capitol Hill	183	1939.6		49.28	-122.98
1101530	Chilliwack	11	1787.8	1950-2000	49.17	-121.93
451484	Clearbrook, WA	18	1162.6	1971-2000	48.97	-122.33
1102220	Cultus Lake	46	1566.9	1971-2000	49.07	-121.97
1102417	Delta Ladner South	2	1008.1	1971-2000	49.07	-123.07
CW0213	Ferndale, WA	18	972.8		48.85	-122.59
1103326	Haney East	31	1788.5	1971-2000	49.20	-122.57
1103332	Haney UBC RF	147	2193.8		49.25	-122.57
1104555	Langley, Lochiel	101	1486.9		49.05	-122.57
454679	Lynden, WA	19	1082.0	1931-2000	48.97	-122.33
1105190	Mission	60	1764.5	1971-1992	49.12	-122.32
1105655	North Vancouver, Capilano	93	2043.7	1971-2000	49.35	-123.12
110FAG9	Pitt Meadows	5	1707.9	1974-1993	49.22	-122.67
1107785	Sumas Lk Canal	6	1798.4	1957-2000	49.12	-122.12
	Sumas WA	11	1150.6		48.99	-122.27
1107876	Surrey, Municipal Hall	83	1370.1	1962-2000	49.10	-122.83
1107878	Surrey, Newton	73	1409.2	1971-2000	49.12	-122.85
1107873	Surrey, Quantlen Park	78	1585.9	1971-2000	49.20	-122.85
1108447	Vancouver Airport	3	1167.1	1936-2000	49.18	-123.17
1108487	Vancouver UBC	87	1287.5	1957-2000	49.25	-123.25

(data: Environment Canada, 2004; Wester Climate Center, WA, 2004)

Map 15 Weather stations used in interpolating precipitation trends over central Fraser Valley.

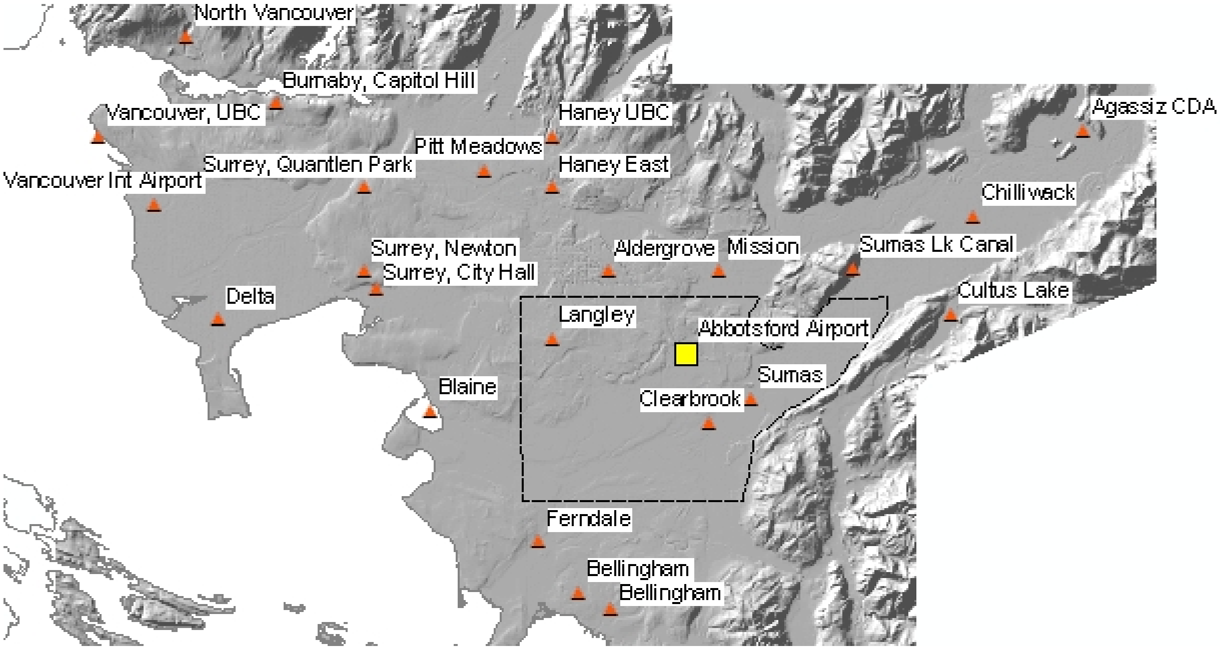

The trend in precipitation is a function of location and elevation (Map 16). Most of the stations were between 0 and 100 m asl, so elevation effect should be minor. There is increase in precipitation in NNE direction over the valley, and mostly in a northerly direction over the model area near Abbotsford, BC. At these elevations the amount of snow water equivalent is minor compared to rainfall amount – on average.

The precipitation map was computed as percent difference in mean annual precipitation to that recorded at Abbotsford Airport, which was used as the index station for weather generation in HELP (Map 18). Thus, all recharge estimates were adjusted proportionally by the same percent difference, assuming that recharge is directly proportional to precipitation for any given recharge zone (Map 19). This is the simplest method of such calculation, otherwise the inputs to HELP model would have to be estimated for all locations of the model prior to determination of recharge zones by the HELP model output. A major assumption is that the precipitation gradient is similar throughout the "typical" year. The gradient magnitudes are different in the 12 months, but gradient direction should be similar to mean annual precipitation gradient (Map 17). The final recharge map for the Abbotsford-Sumas aquifer region is shown in Map 20 (precipitation bands are visible superimposed on variation in recharge due to subsurface/surface properties). A detailed recharge map is shown in Map 21. The entire model area has over 800 recharge zones.

5.4.8. COMPARISON OF RECHARGE RESULTS TO PREVIOUS STUDIES

Kohut (1987) estimated that the average annual ground water recharge to the aquifer was equivalent to at least 37% of the average annual precipitation and that the annual recharge was about 26.8M m^3 (or 850 L/s).

The LENS study area, which covers most of the central Sumas–Blaine aquifer (note this is terminology used by Cox and Kahle, 1999), has recharge values in six classified ranges within the study area ranging from 11 to 50 in/year (280 to 1270 mm/year), increasing roughly from south / south-west to east / north-east (Cox and Kahle, 1999). Our HELP recharge estimates show 650 to 1000 mm/year recharge in the vicinity of this area. The aquifers near the City of Sumas have annual ground water recharge ranging from 30 in/year (760 mm/year) in the Upland area and 6 in/year (152 mm/year) in the Sumas Valley (City of Sumas Wellhead Protection program/Plan Report). The recharge to lowland areas might be smaller than estimated by HELP model, but the flow model is not as sensitive to recharge in those lowland areas as it is in upland areas. According to Cox and Kahle (1999), (estimates are based on Vaccaro et al., 1996, and Kohut, 1989), most of the Fishtrap watershed has a recharge of 660 – 762 mm/year. A point estimate at Abbotsford Airport, just outside of Fishtrap water shed has 965 mm/year (Washington State Department of Ecology, 2001). Assuming the recharge to be the unknown in the mass balance equation, an inverse estimation for recharge can be performed using the other components of the water balance, resulting in 416 mm/year or about 1/3 of mean annual precipitation. Overall, our new recharge estimates seem acceptable in light of previous estimates.

Map 16 Mean annual total precipitation in Fraser Valley interpolated from a selection of weather stations with long records, showing trend over Abbotsford-Sumas aquifer model extent.

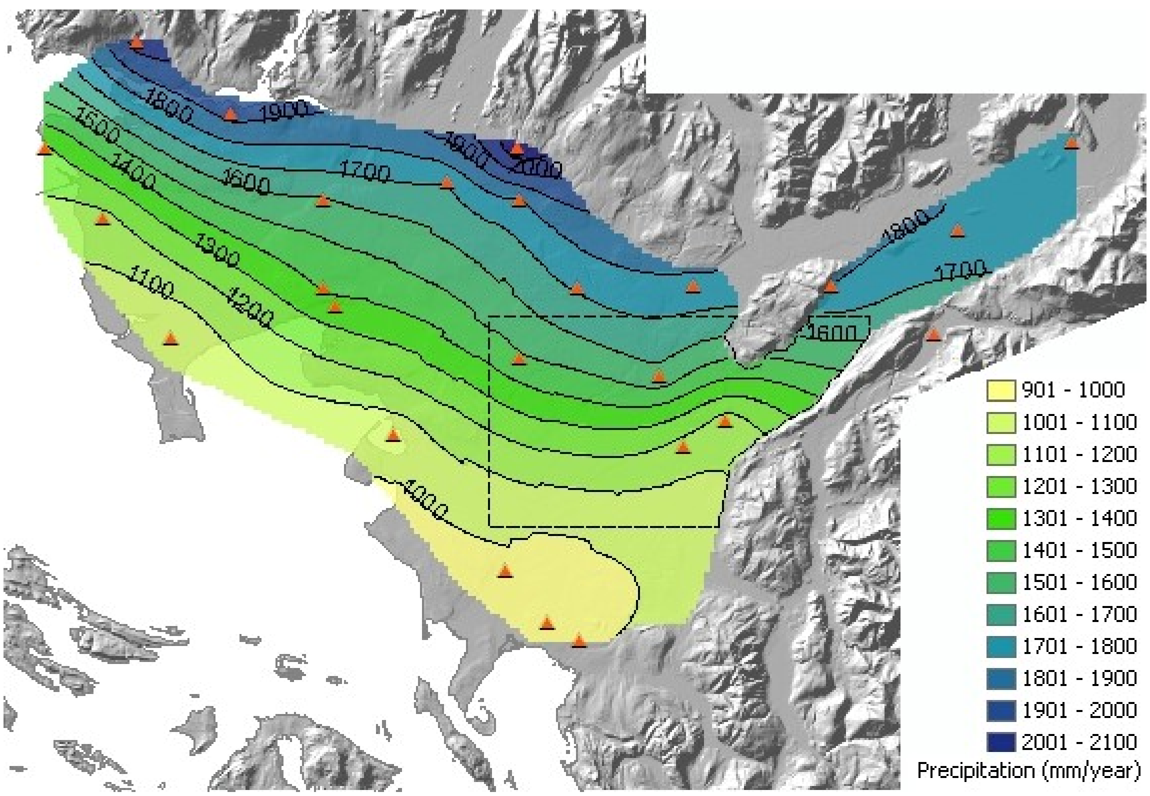

Map 17 Mean monthly precipitation (period of record or last 30 years) interpolated from selected weather stations in Fraser Valley (a) March, (b) June, (c) November.

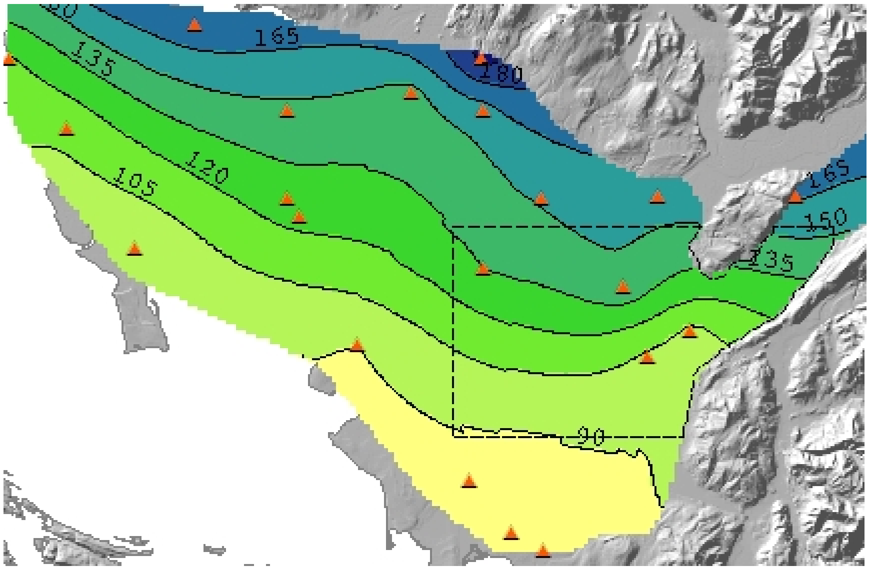

(a) March

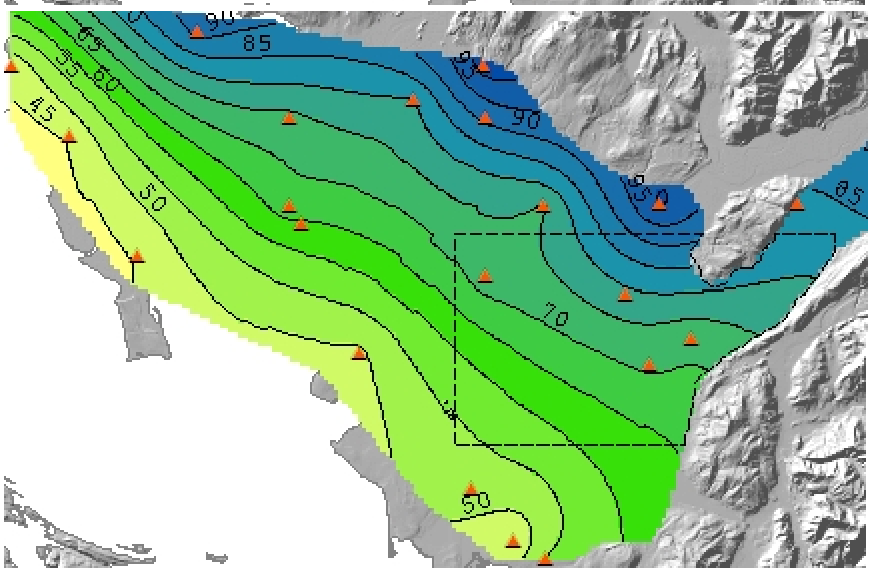

(b) June

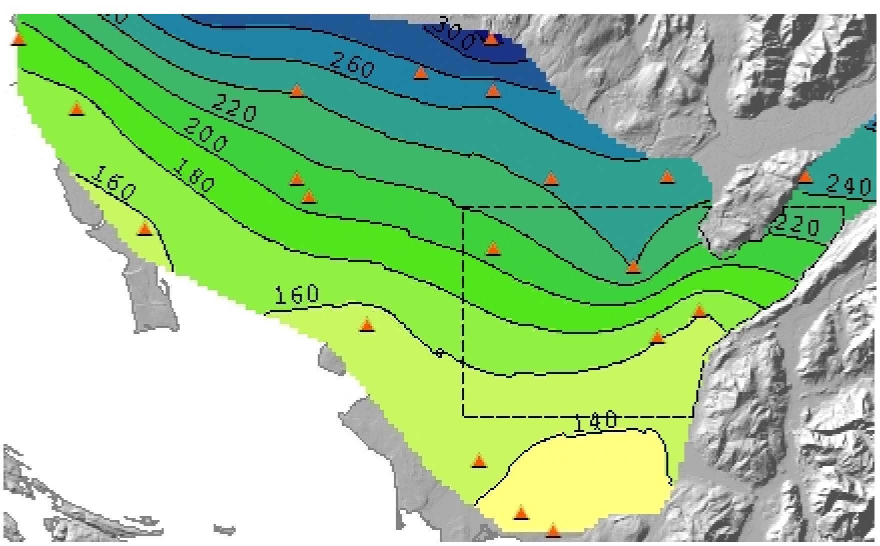

(c) November

Map 18 Percent difference in mean annual precipitation relative to mean annual precipitation at Abbotsford Airport calculated from interpolated mean annual precipitation in central Fraser Valley.

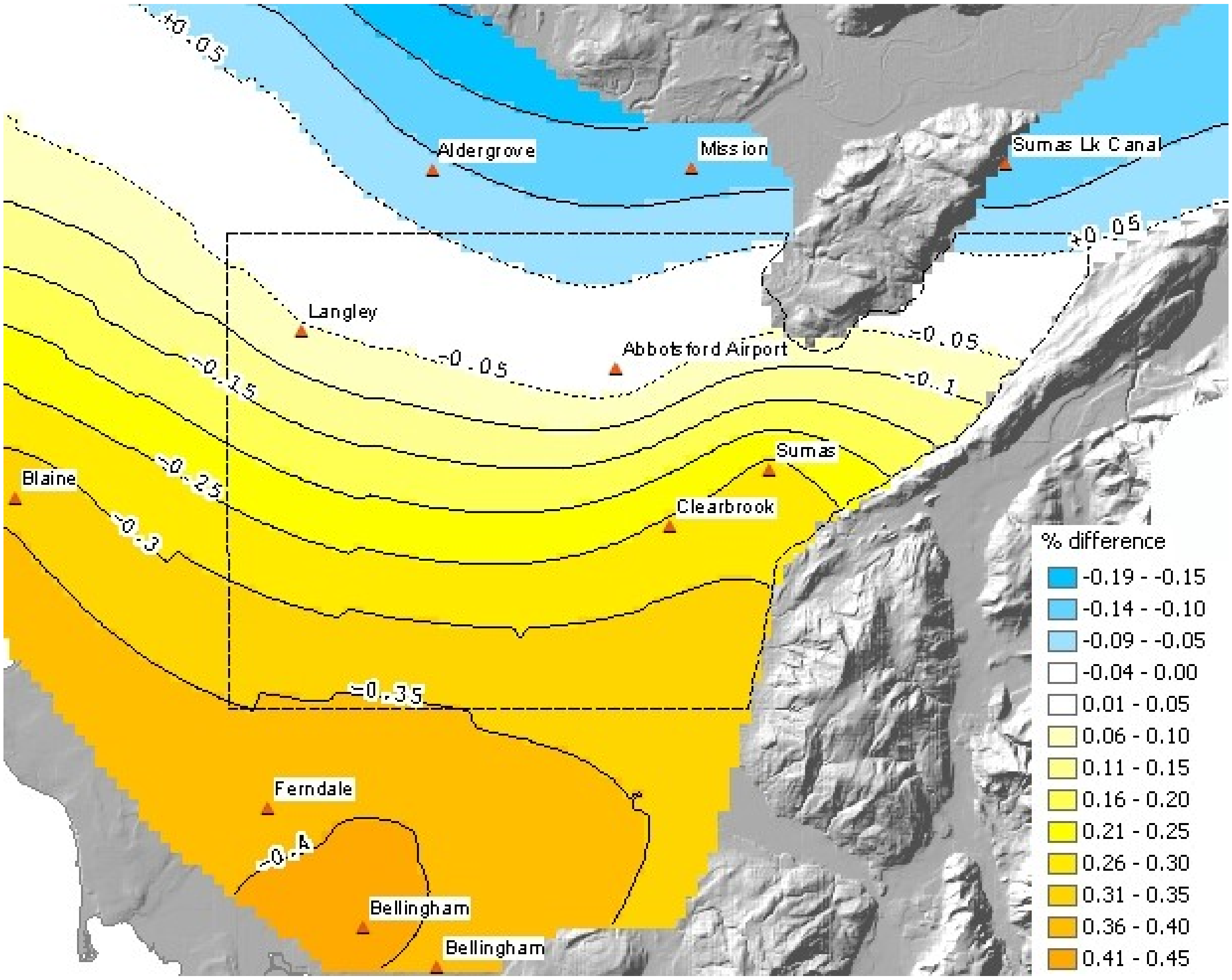

Map 19 Percent difference in mean annual precipitation relative to mean annual precipitation at Abbotsford Airport: (a) zonation of percent differences for model area – used to adjust recharge values, (b) adjusted recharge shown in zone nearest to Abbotsford Airport.

(a)

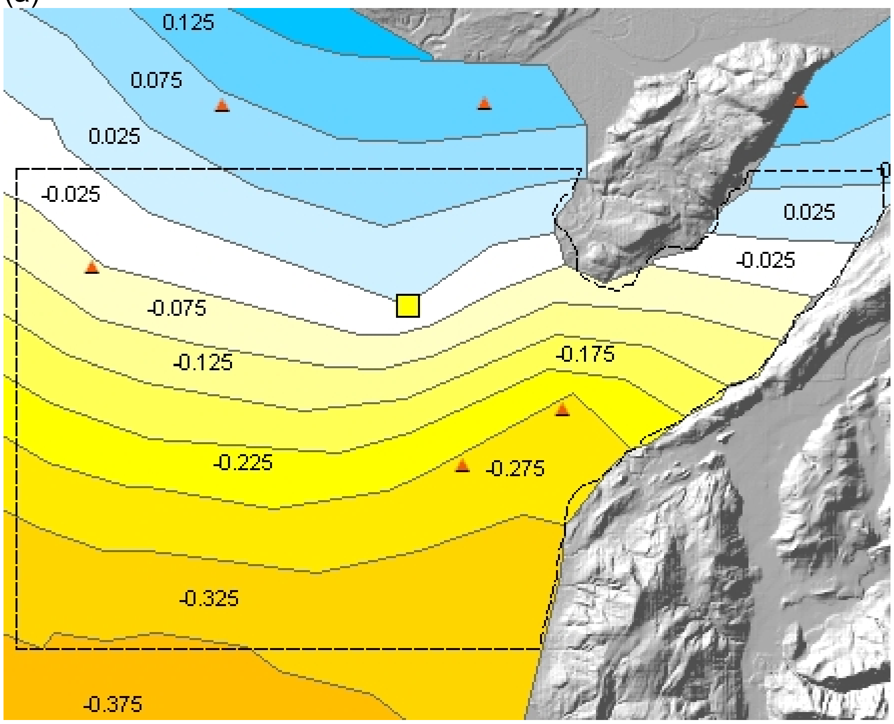

(b)

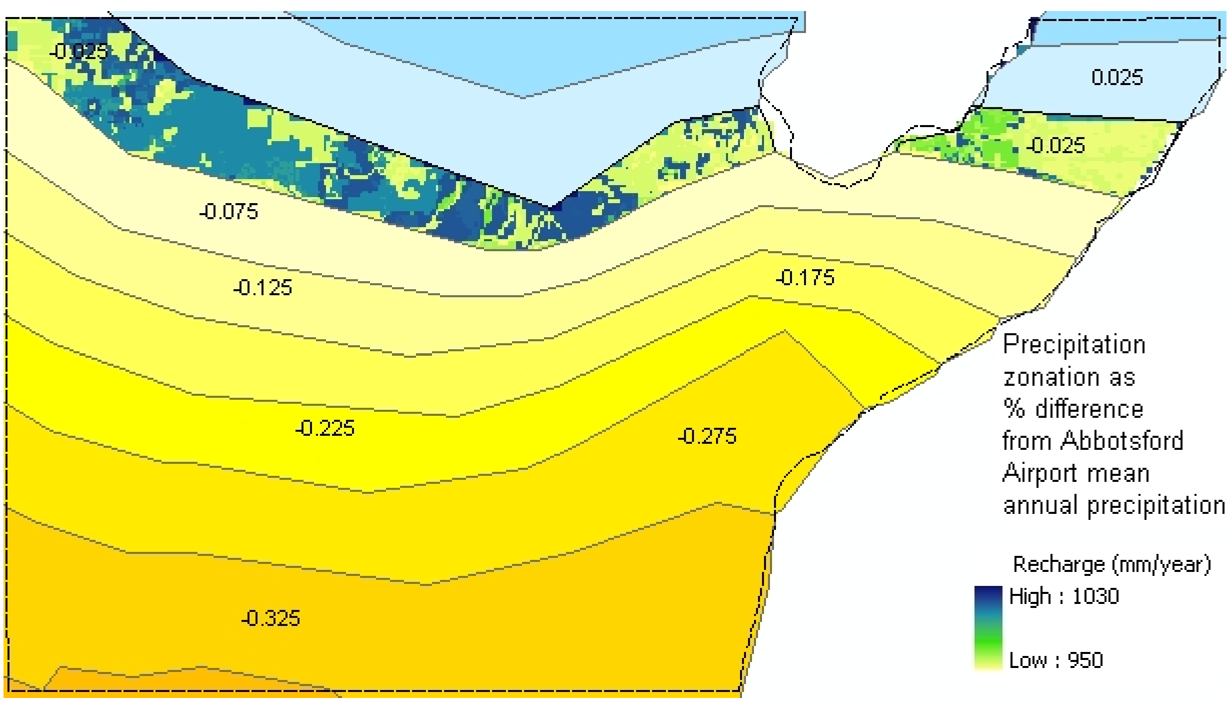

Map 20 Recharge zones imported to Visual Modflow showing detail near Abbotsford Airport area where paved runway has 50% less recharge compared to surrounding cells.

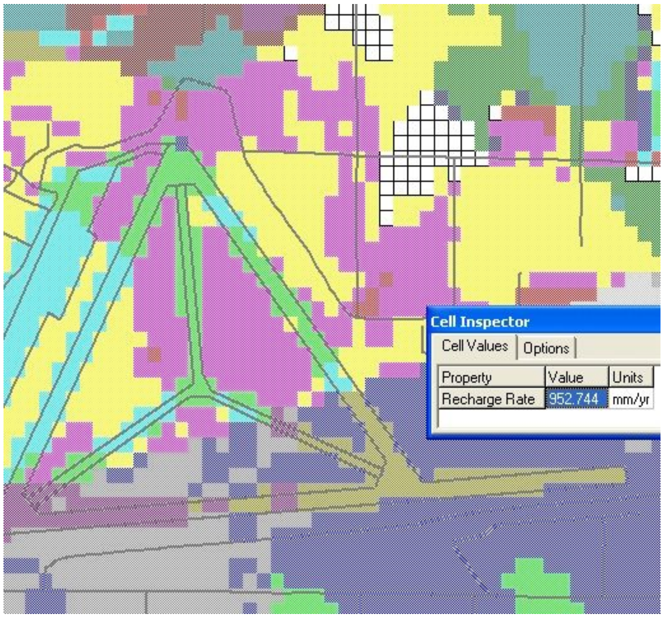

5.5. SENSITIVITY ANALYSIS OF RECHARGE TO HELP PARAMETERS (SOIL COLUMNS)

It is important to evaluate the sensitivity of HELP modeled recharge to soil column depth of aquifer media (i.e., water table depth). If the effect is strong, for each month in the year, the aquifer will have to be reclassified into new assignments of the 27 categories of infiltration columns, using depths to water table at the end of previous month. The problem is that these are not known until the groundwater model is run in transient mode up to that month, but the groundwater flow model requires prior recharge inputs for it to predict the groundwater levels. This results in a circular problem.

Figures 40 and 41 (and Figure 42 for recharge as % of precipitation) and the following summarize the sensitivity of recharge to several parameters:

1. No noticeable or very small (< 5% change) effect on recharge (of percolation layer parameters):
    - stand of grass type
    - wilting point
    - field capacity
    - initial moisture content

2. Moderate effect on recharge:
    - soil thickness
    - porosity of percolation layer

3. Strong effect on recharge:
   - depth of vadose zone (percolation layer)
   - soil type
   - K sat of vadose zone

Figure 40 Sensitivity of HELP modeled recharge estimates, to least controlling factors in HELP model (a) type of stand of grass on ground surface, (b) initial moisture content, (c) wilting point of soil, (d) field capacity of soil.

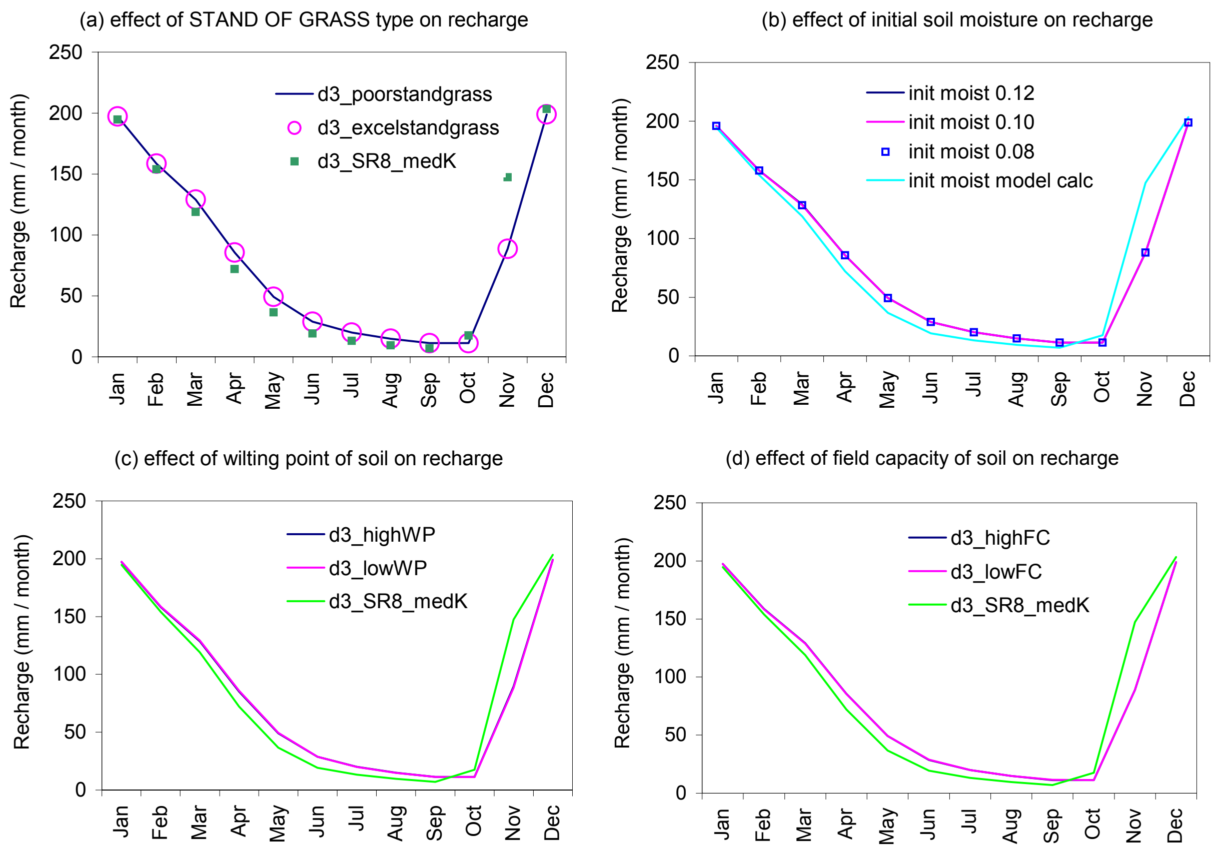

Figure 41 Sensitivity of HELP modeled recharge estimates to (a) saturated vertical hydraulic conductivity of vadose zone, (b) soil permeability, (c – d) depth of vadose zone and soil permeability, (e) soil thickness, (f) porosity of vadose zone material.

(a) effect of K sat on recharge (d = 3m, high soil perm.)

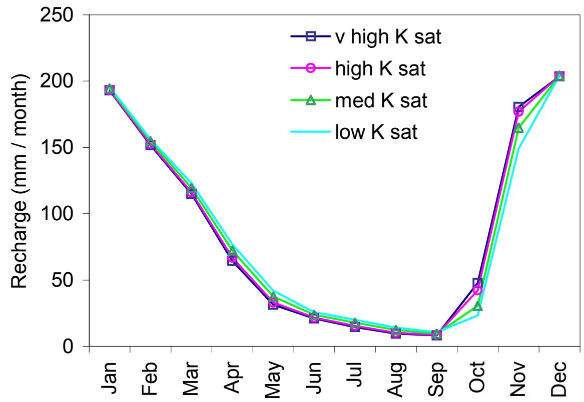

(b) effect of SOIL PERM. on recharge (d = 3 m, med K sat)

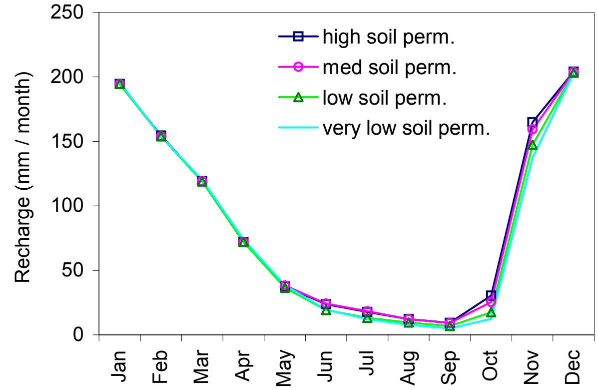

(c) effect of DEPTH on recharge (high Ksat, high soil perm.)

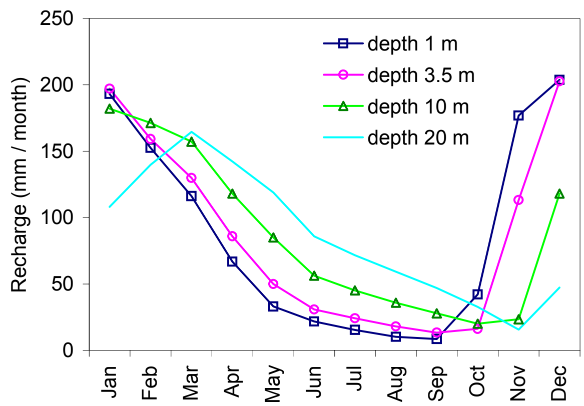

(d) effect of DEPTH on recharge (high Ksat, low soil perm.)

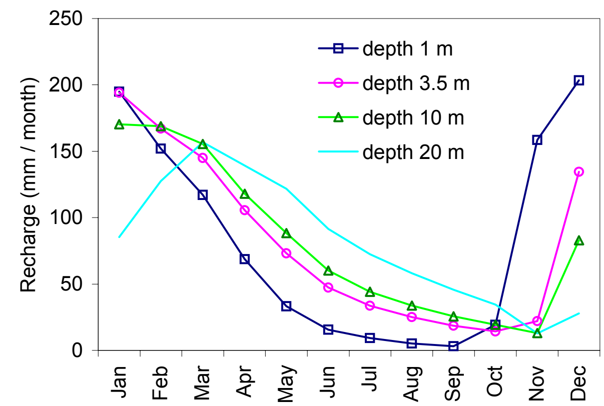

(e) effect of SOIL THICKNESS on recharge (d = 3 m, med Ksat)

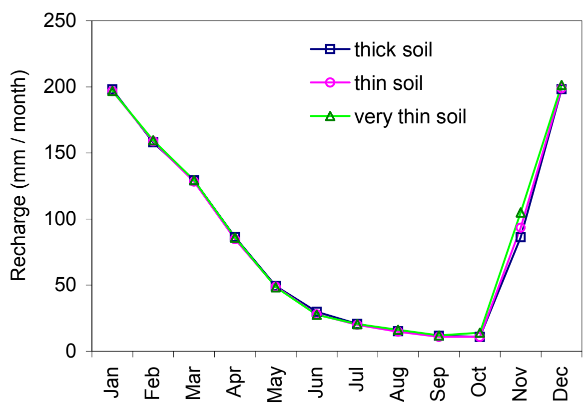

(f) effect of POROSITY of percolation layer on recharge (d = 3 m, med K sat, med soil perm.)

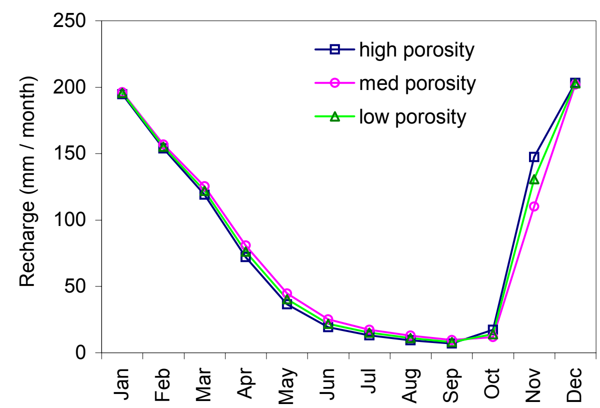

In terms of recharge as a percentage of monthly precipitation (Figure 42), the Abbotsford aquifer receives between approximately 10% and 100% of recharge from precipitation, according to HELP output. Through the winter (Nov to Feb), almost all of the precipitation recharges the aquifer. In spring time (Mar to Jun), the percentage of recharge drops gradually from 100% to approximately 40%. During the summer months (Jul and Aug) there is an increase in the percentage of precipitation contributing to recharge (during this time the model is sensitive to various parameters and so a range is observed). In the fall (Sep and Oct), recharge percent is low (roughly 10%) for all sensitivity simulations.

Figure 42 Sensitivity of HELP modeled recharge estimates, as percentage of monthly precipitation to (a) soil permeability, grouped by different K sat of vadose zone, (b) K sat of vadose zone, grouped by different soil permeability.

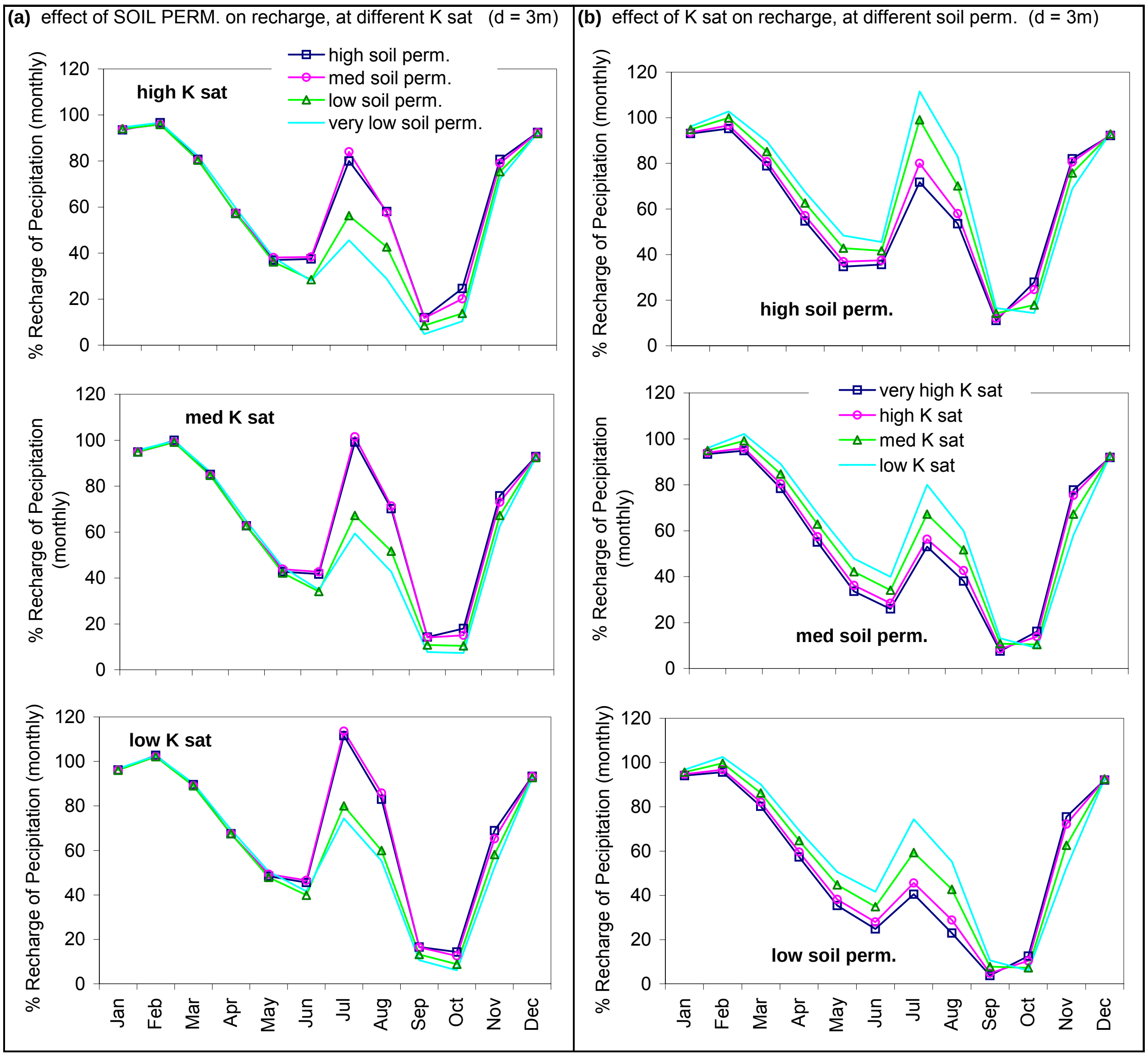

6. RECHARGE RESULTS

Recharge values were modeled for present climate and 3 future climate scenarios (2010-2039, 2040-2069, 2070-2099). These values first mapped for each climate scenario, and then the future recharge scenarios were compared to the historical recharge values.

6.1. HISTORICAL CLIMATE

Map 21 shows the spatially distributed mean annual recharge to the Abbotsford aquifer (mm/year). Values range from near 0 to 120 mm/year. The western and the northwestern portions of the aquifer receive the lowest recharge, while the highest recharge is received in the more central and eastern portions of the aquifer on river terraces, where as the floodplain areas receive lower recharge. According to HELP model results, in this climatic region there isn't enough precipitation to recharge the aquifer where there are thick sand and gravel terraces – most of the precipitation changes moisture content in these areas of thick gravels above water table, but little of it recharges the groundwater aquifer. This situation would be different if this was a wet climatic zone – most recharge would occur in most permeable areas with less influence on depth of sediment to water table.

The lowest recharge occurs from July to October, the highest recharge occurs from November to March, and other months receive moderate recharge. Recharge follows annual distribution of precipitation, when winter rainstorms supply most intense rainfall and most of recharge to aquifer from rainfall. The predicted changes in mean annual recharge were converted to percentage differences: (future – historical) / historical, and are included in Map 22 parts (a) and (b).

All predicted values were graphed as total monthly recharge for each of the 64 recharge zones (Figure 43). There is a lag effect of recharge, whereby areas with a lower K for the vadose zone produce longer lag times for recharge to percolate down to water table (this also increased by depth to water table).

Mean annual recharge as a percentage of total precipitation for each climate scenario is shown in Figure 44.

Map 21 Spatial distribution of mean annual recharge over the Abbotsford-Sumas aquifer model area: (a) recharge not adjusted for precipitation gradient in Fraser Valley, (b) adjusted recharge showing strong South-North precipitation gradient, superimposed on smaller but more detailed variation of recharge depending on aquifer media and surface properties as computed in HELP model. The entire model area has over 800 recharge zones (precipitation bands are visible superimposed on variation in recharge due to subsurface/surface properties.

(a)

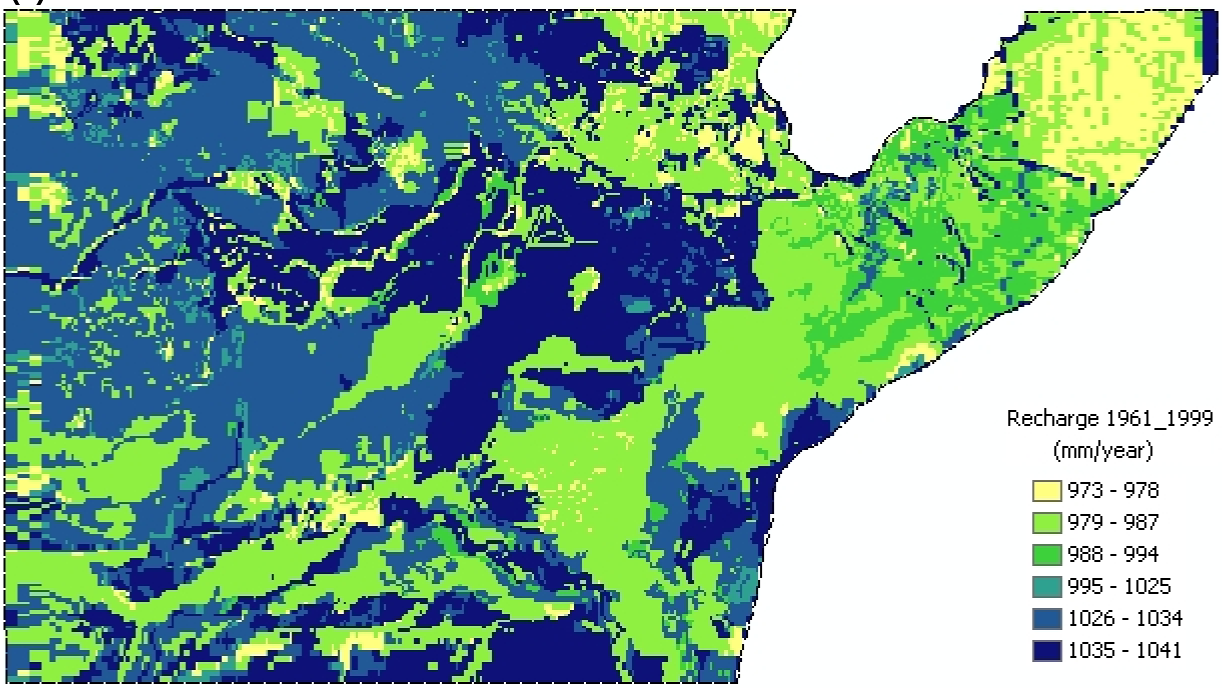

(b)

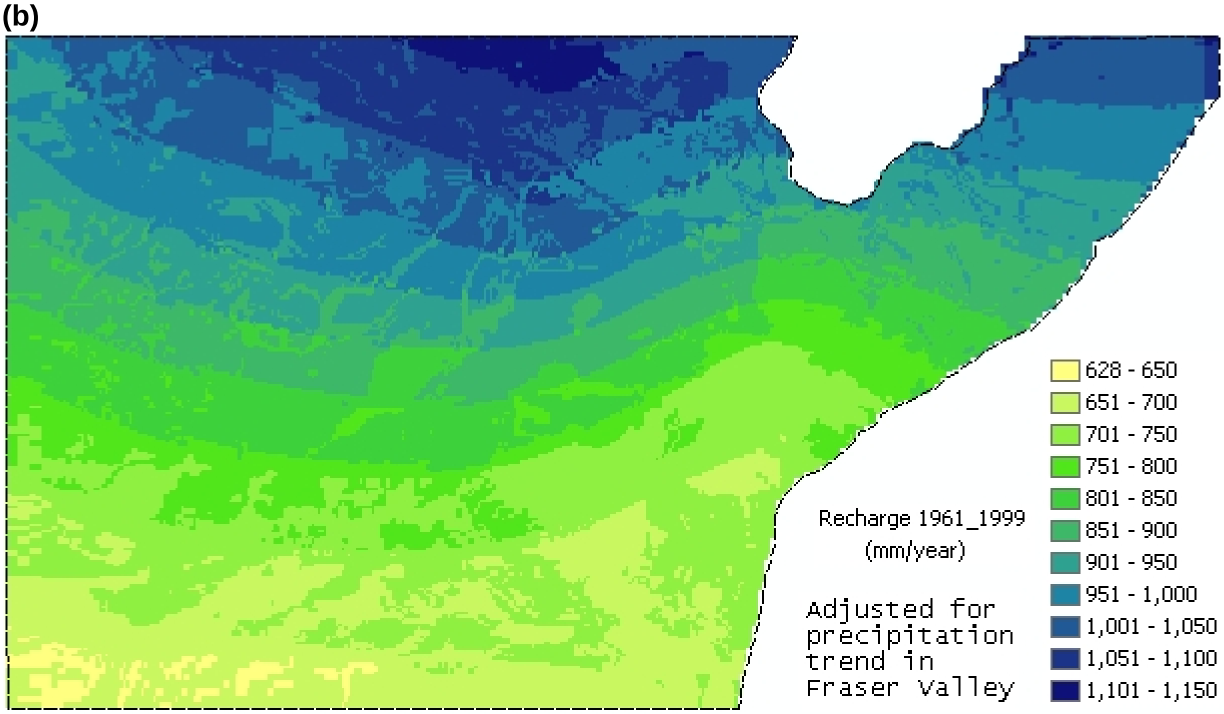

Figure 43 Total monthly recharge for all recharge zones and all months (results from HELP model computations).

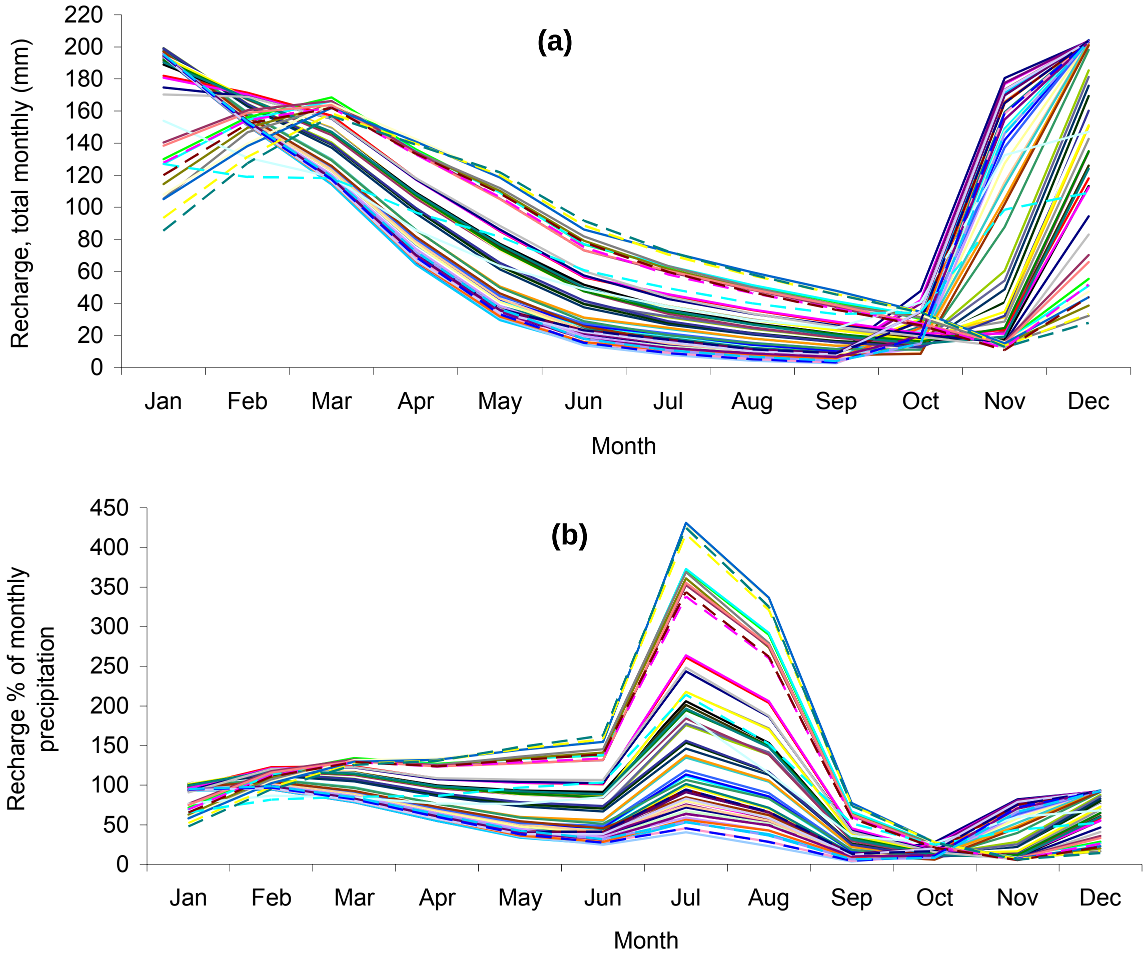

Figure 44 Mean annual recharge as percentage of mean annual precipitation at Abbotsford-Sumas aquifer for present climate and two climate scenarios 2010-2039 and 2040-2069.

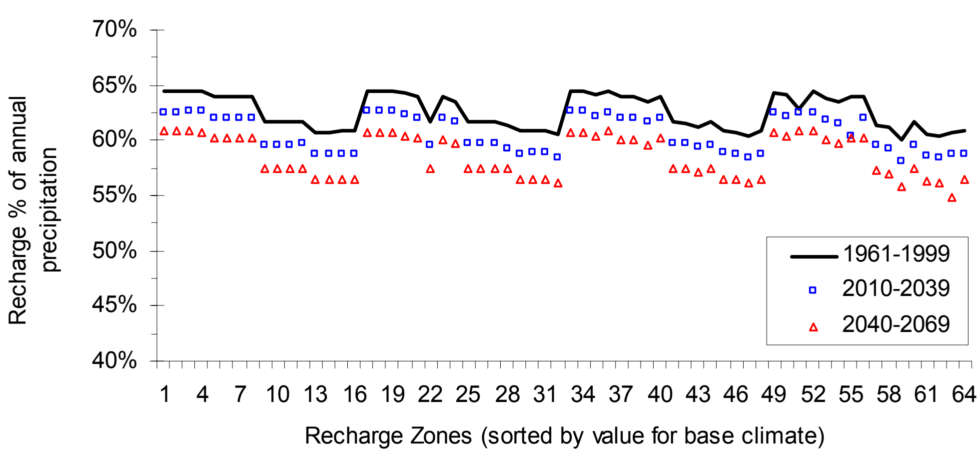

Map 22 Predicted changes in mean annual recharge to Abbotsford-Sumas aquifer compared to the historical climate scenario (1961-1999), modeled in HELP and assigned to recharge zones: (a) percent change between 2010-2039 and historical, (b) percent change between 2040-2069 and historical.

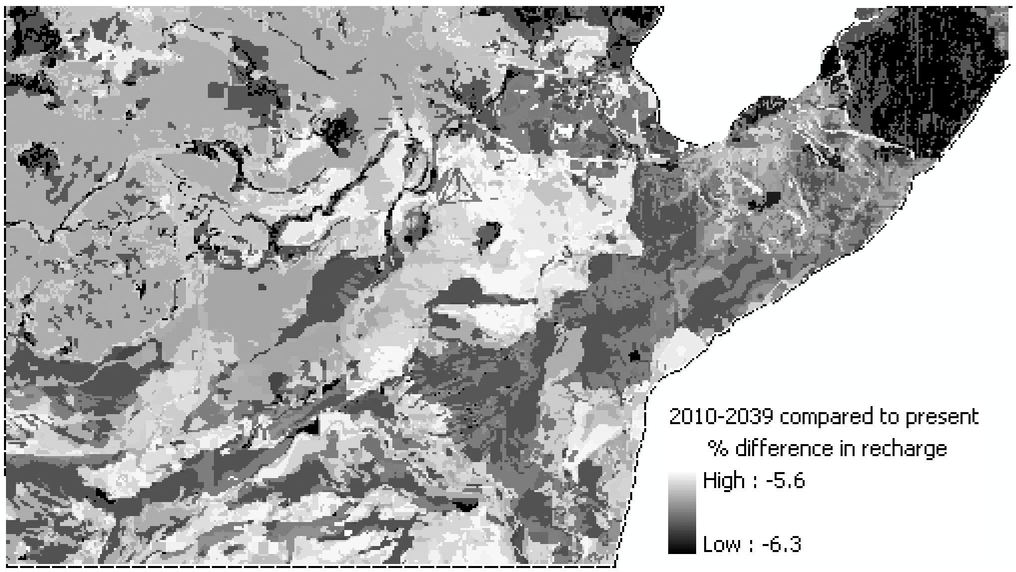

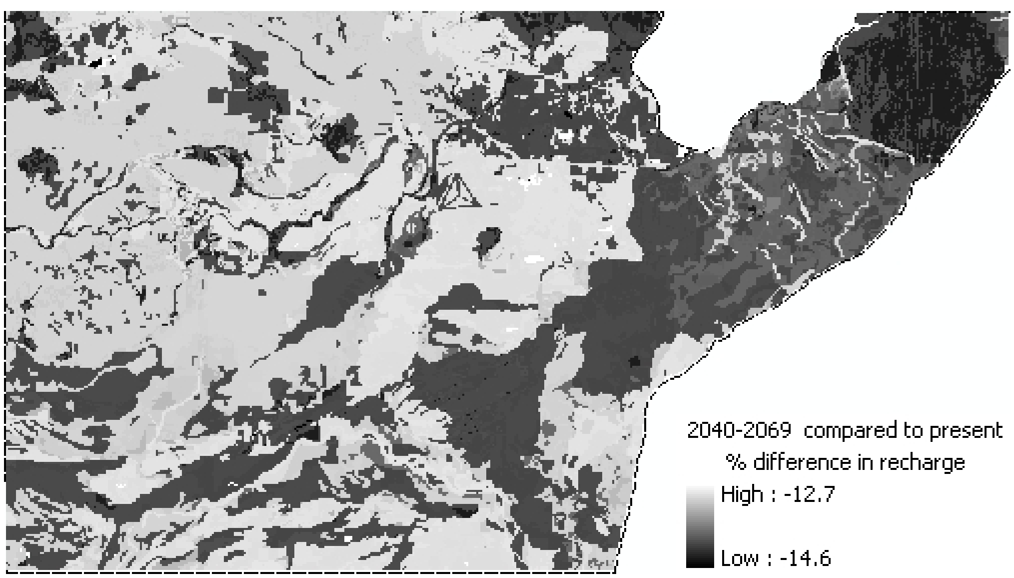

7. IMPACTS OF CLIMATE CHANGE ON GROUNDWATER LEVELS

7.1. METHODOLOGY FOR HEAD DIFFERENCE MAPS

The effects of climate change are difficult to observe on head distribution maps because the highly variable and localized hydraulic gradients in the central Fraser Valley dominate all other trends. The climate-induced changes in water elevations are on the order of less than 0.25 m (25 cm) in most areas, but are up to 2 m in sensitive areas in Abbotsford uplands. The water table elevation in the valley ranges from near 0 to above 80 m asl elevation, so any changes would just shift the water table contours slightly and would be difficult to read. Thus, it was necessary to develop a different strategy for displaying any changes induced by climate, which would exclude the hydraulic gradient of the aquifer, and compare directly changes from present conditions. Accordingly, head difference maps were prepared to show only differences due to climate change between future climate scenario model outputs and present climate scenario model outputs.

Instead of using head values, the water table elevation was used. The model layer surfaces are very irregular near the ground surface, and the use of HUV package in MODFLOW 2000 and 3D raster-grid approach to hydrostratigraphic unit mapping, does not predispose head maps "by model layer" to be used in this case. In layers 1 to 4, there are large areas with dry cells (no head value available), and only in Layer 5 are there mostly wet cells in the model. However, the water table lies in layer 1 to 2 in Abbotsford and Langley uplands, then transitions through layer 3 and 4 to layer 5 in Sumas Valley. Head maps would show some confined and unconfined areas blended together. Water table elevation also includes confining conditions, but it is the best choice in this case.

In Visual MODFLOW, water table elevations were exported at different stress-periods from transient model outputs, at the following Julian Days: 91, 182, 213, 274, and 365. Water levels were saved as ASCII files (default export format in Visual MODFLOW). These contain x,y coordinates for cell and head value. A code was written to assign unique Cell ID value to each exported water level location, which is exported in sequential order along rows and columns of MODFLOW grid (option to export all cells was specified as there are irregular boundaries to active cell area). Previously, the MODFLOW grid had been mapped onto GIS polygon shapefile from exported row & column coordinates, and computed cell corner coordinates. Each cell was assigned unique ID such as RowColumn numbers (integer number of each, joined together into larger unique number). By using code, water level differences were computed on cell by cell basis between the future climate scenarios and the present climate scenario, for each model time step separately. The processed text files were imported to Access database, and converted to D-BASE format for GIS. The polygons of cells, via table join operation of water level difference outputs, were converted to 50 m raster grids for display and further analyses. Contours of head differences were generated from raster maps in ArcGIS – Maps 23 to 27 for separate time steps, and also Map 28 comparing results for climate scenario 2010-2039 to climate scenario 2040-2069.

Examination of the maps showed that most changes were negative, and that there were two populations of larger and smaller changes. To resolve the small changes over most of the area, the raster maps of water level differences were reclassified to show range of 0 to -0.25 m. The areas with larger changes were mapped separately (on the 0 to -0.25 m change maps the larger negative changes are shown as -0.25 and are quite obvious as distinct areas). Most areas experience modeled changes of less than 0.1 m.

The maps were displayed using "classified" by colour, using 0.05 defined interval (equal interval) to classify map colours based on cell values. Identical colour scheme was used for all maps. As the pattern indicates that areas of no change lie along specified head boundary conditions (streams and rivers and lakes); the drainage was included in maps as white lines.

The GIS environment provides better integration with all other spatial data than Visual MODFLOW, and there is much more control of mapping of MODFLOW results. GIS grids, polygons and contour lines in shapefile format are also better for data interchange for other purposes for users that do not have Visual MODFLOW access, and present a ready result format rather than xyz data tables of MODFLOW exports.

Each climate scenario is illustrated with 4 maps for six model time steps, from 91 to 274. The patterns of change are similar between the time steps (between the exported time steps and would not add much to the results).

7.2. CHANGES IN WATER ELEVATIONS DUE TO CLIMATE CHANGE

In the main recharge area of the aquifer, the groundwater levels were predicted to decrease by between -0.05 m to more than -0.25 m due to climate change by the 2010-2039 period. The decrease in groundwater levels was even greater in the next climate scenario 2040-2069, such that in the Abbotsford uplands, groundwater level decreases were between -0.10 and -0.25 m in most areas. In places with suspected perched water tables, which tended to be areas of poor model calibration, the changes were between -0.5 and -3.0 m.

As a consequence of reduced groundwater levels, streams in upland areas, which were treated as drains, are expected to have lower seasonal flows. In lowland areas containing creeks that drain the aquifer, changes in climate and recharge did not produce any significant changes in water table elevation. This result is not surprising, given that both the valley floor and the water table surface are generally flat, and are constrained in the model by constant head boundary conditions. What we expect to see, under a regime of lower recharge, and resulting lower groundwater levels, is a shift in the nature of the groundwater-surface water dynamics for entire streams or stream reaches. Streams at lower elevation could become perched above the water table at certain times of the year, particularly during intense rainfall events, thereby loosing more water along their channels and contributing to indirect groundwater recharge (i.e., becoming effluent streams rather than influent streams). A more likely consequence of reduced groundwater levels across the aquifer would be a lowering of the hydraulic gradients, and a consequent reduction in baseflow, particularly during the summer months as less groundwater is released from storage. To investigate the complex nature of the interactions between groundwater and surface water in this aquifer, a coupled groundwater-surface water model should be used, and consideration should be given to shifts in the hydrologic regime of all streams.

Map 23 Water level differences of the modeled water table at day **91** between future and present climate (a) scenario 2010-2039 and (b) scenario 2040-2069. Values were reclassified to range from 0 to -0.25 m. Values of -0.25 in discrete areas have changes between -0.25 and -3.0 m.

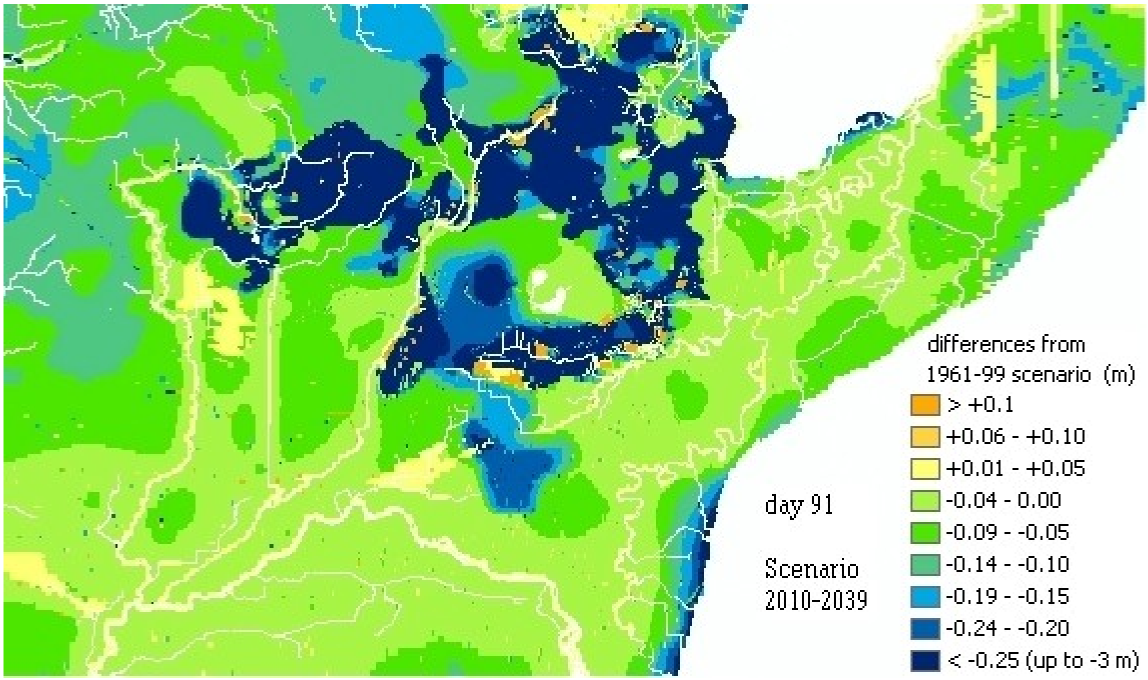

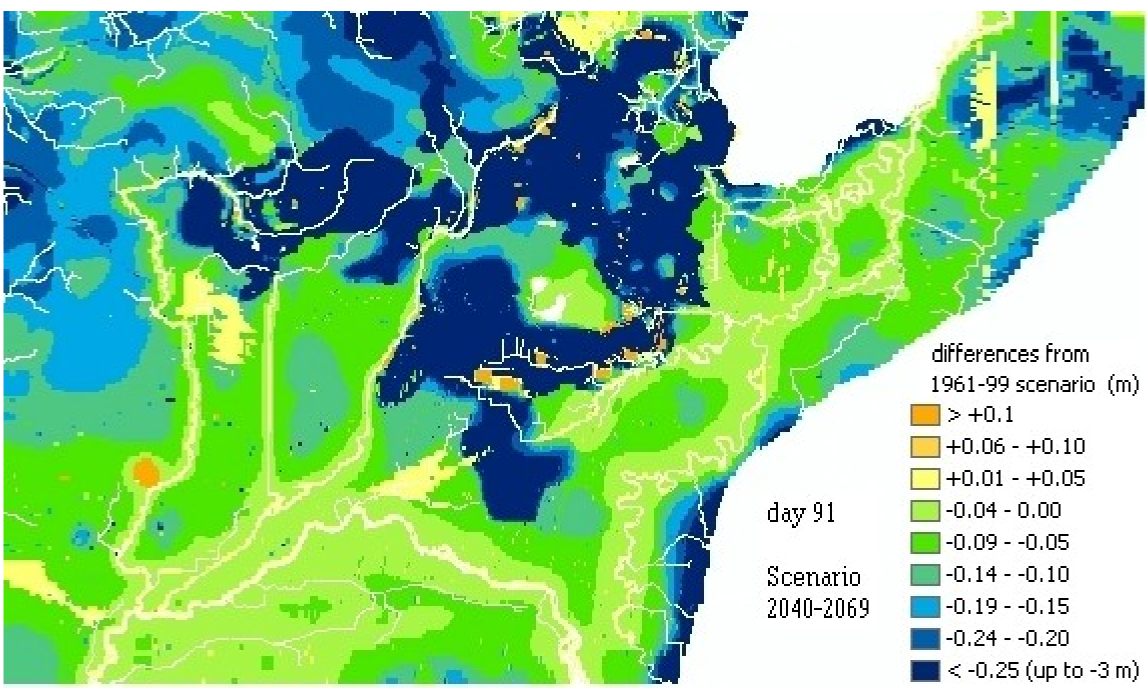

Map 24 Water level differences of the modeled water table at day **182** between future and present climate (a) scenario 2010-2039 and (b) scenario 2040-2069.
Values were reclassified to range from 0 to -0.25 m. Values of -0.25 in discrete areas have changes between -0.25 and -3.0 m.

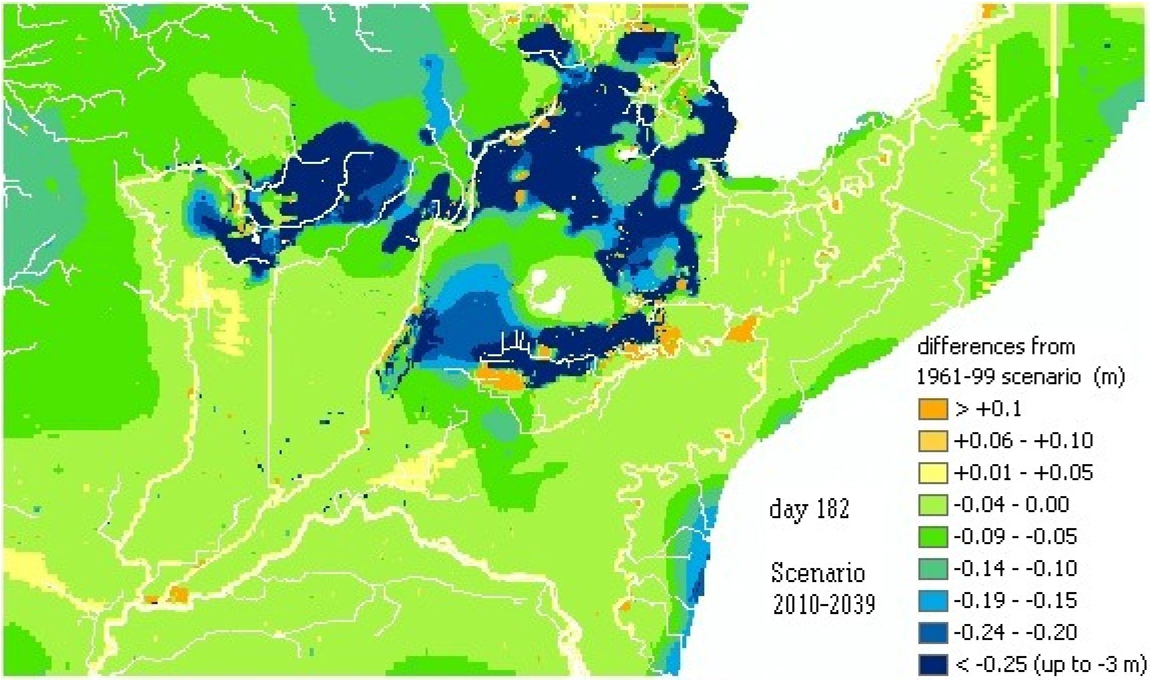

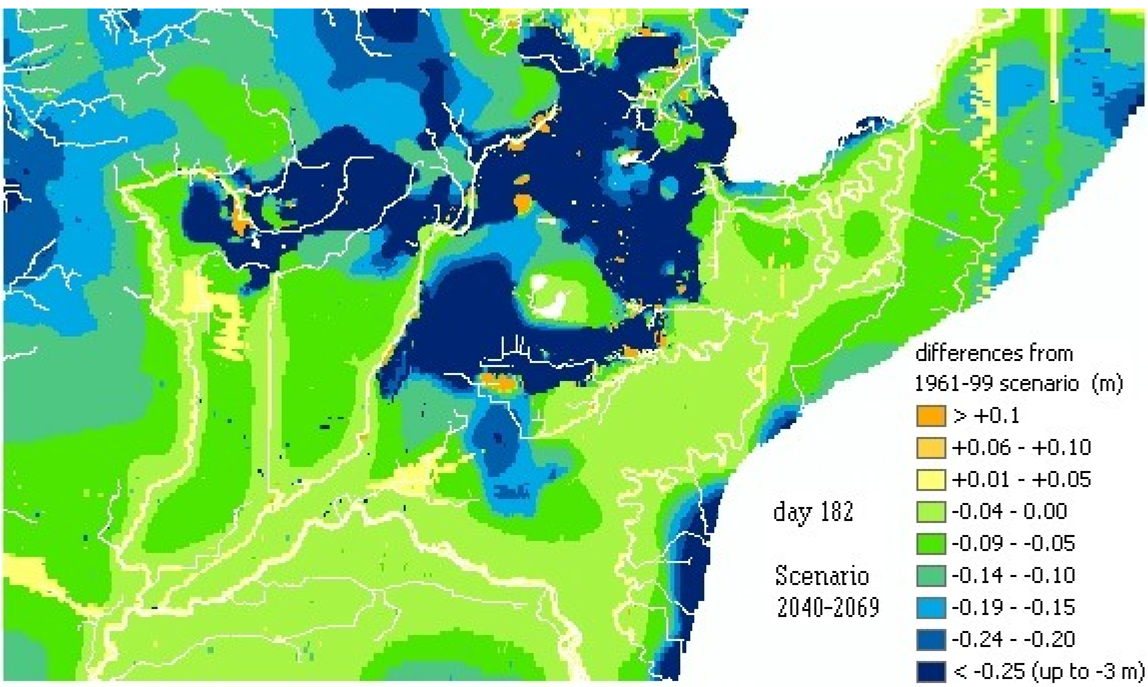

Map 25 Water level differences of the modeled water table at day **213** between future and present climate (a) scenario 2010-2039 and (b) scenario 2040-2069.
Values were reclassified to range from 0 to -0.25 m. Values of -0.25 in discrete areas have changes between -0.25 and -3.0 m.

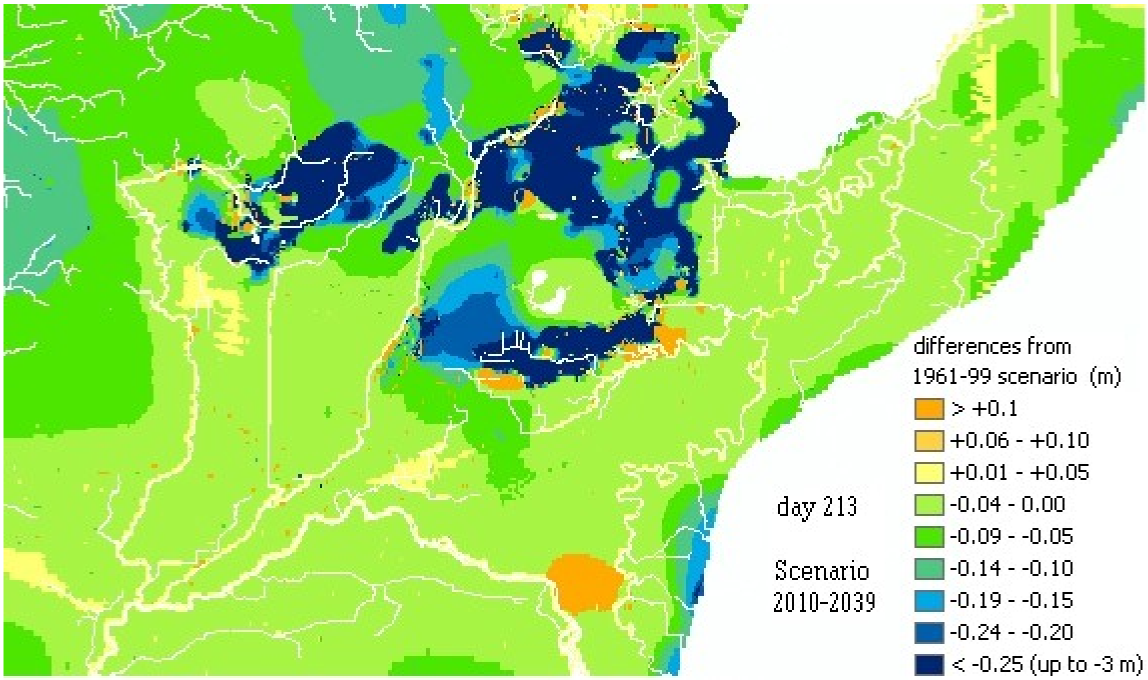

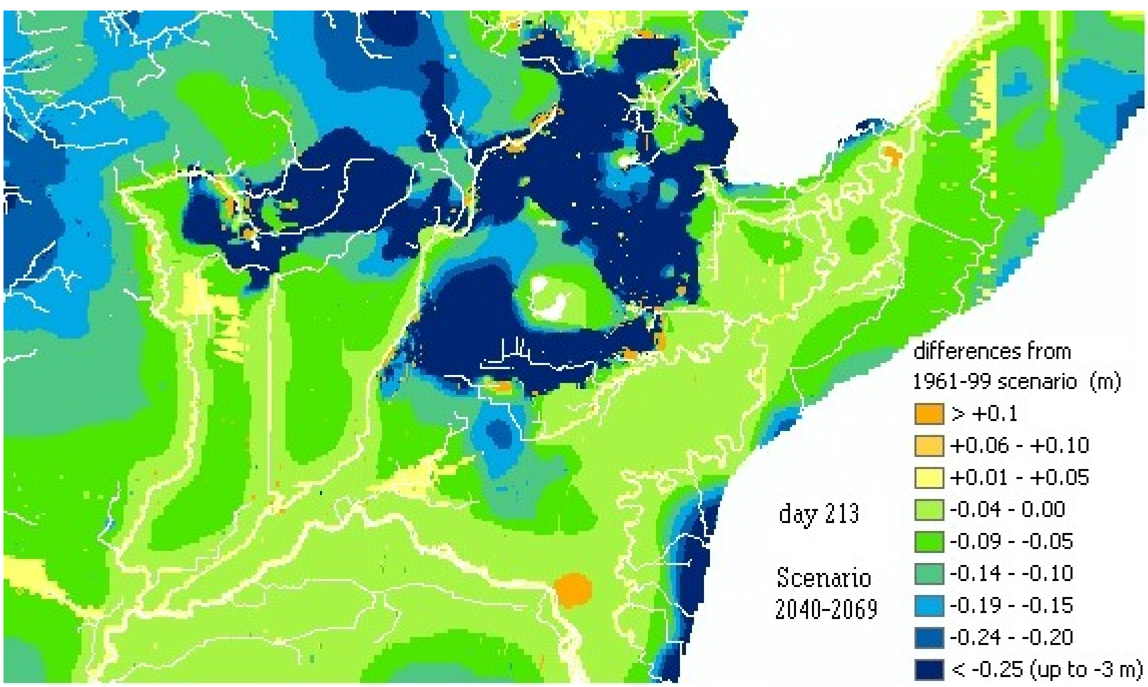

Map 26 Water level differences of the modeled water table at day **274** between future and present climate (a) scenario 2010-2039 and (b) scenario 2040-2069.
Values were reclassified to range from 0 to -0.25 m. Values of -0.25 in discrete areas have changes between -0.25 and -3.0 m.

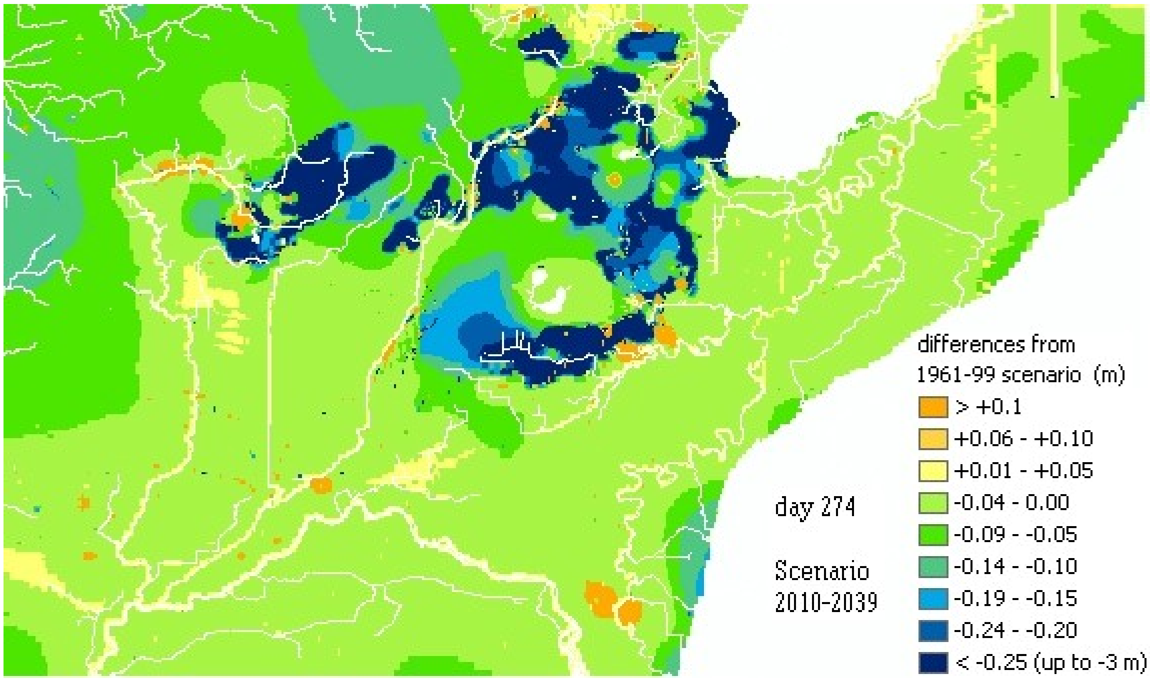

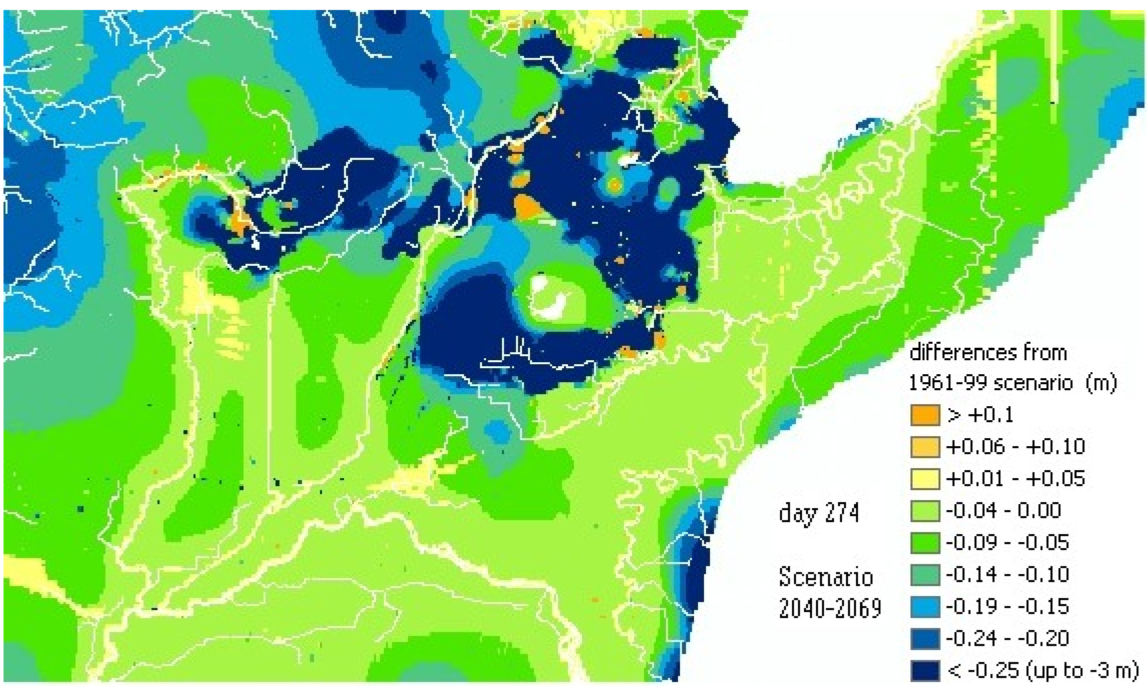

Map 27 Water level differences of the modeled water table at day **365** between future and present climate (a) scenario 2010-2039 and (b) scenario 2040-2069.
Values were reclassified to range from 0 to -0.25 m. Values of -0.25 in discrete areas have changes between -0.25 and -3.0 m.

(2010-2039 is missing because of convergence problem at after day 300 – this can be fixed by watching it run and changing convergence criteria during problems, than changing them back to original when it solves without problems)

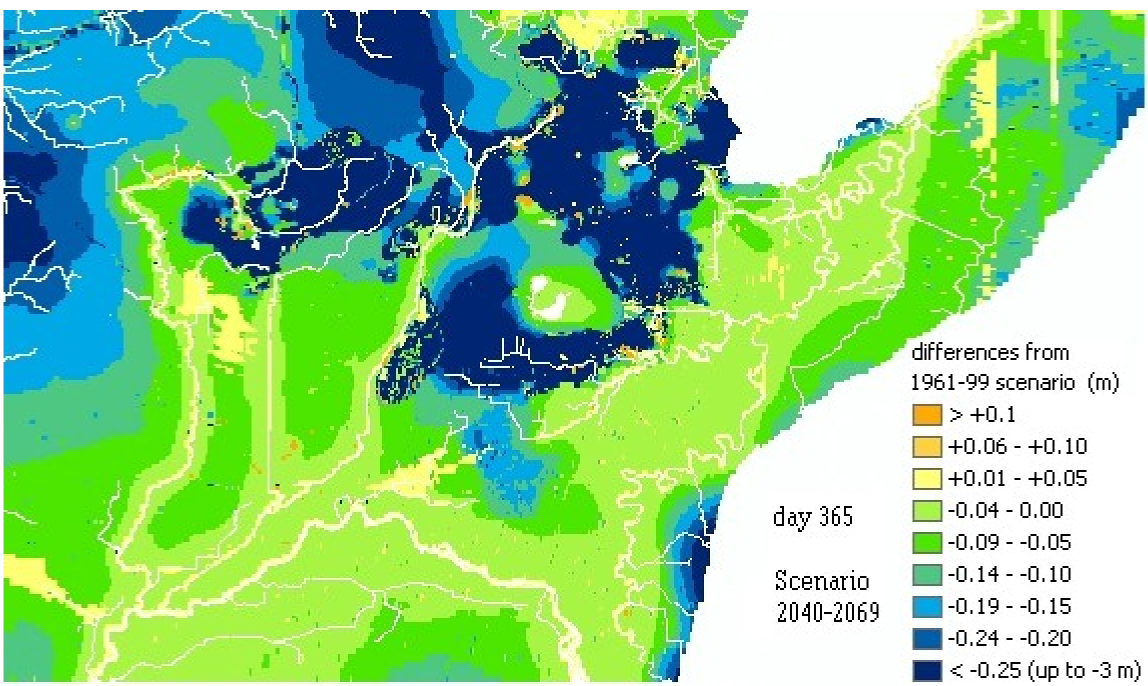

Map 28 Water level differences of the modeled water table at days 91, 182, 213, and 274 between future and present climate (a) scenario 2010-2039 and (b) scenario 2040-2069. Values were reclassified to range from 0 to -0.25 m. Values of -0.25 in discrete areas have changes between -0.25 and -3.0 m.

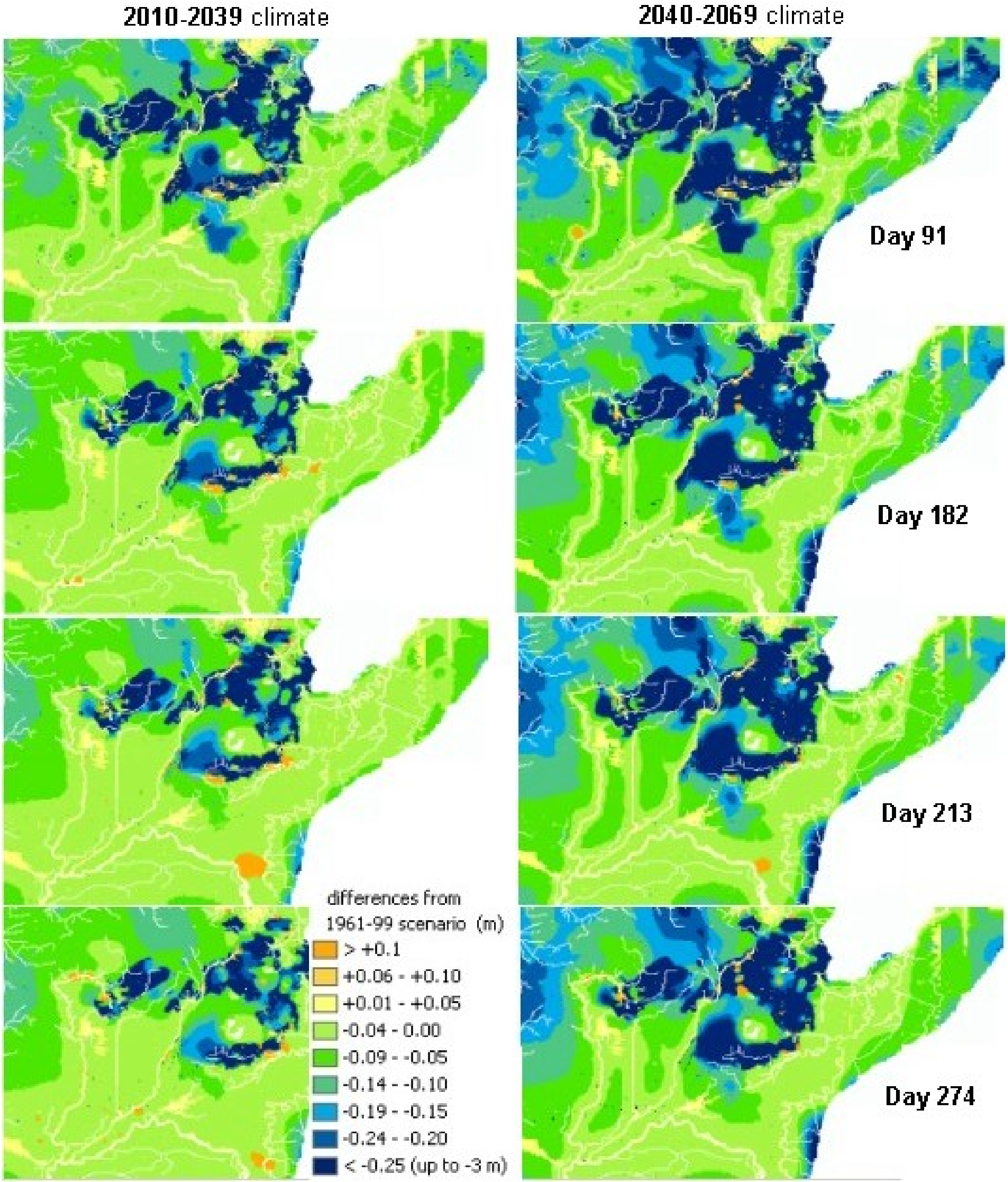

8. CONCLUSIONS

1) The downscaling of CGCM1 results was accomplished using 2 independently calculated methods using: 1) SDSM software, and 2) PCA k-nn (Environment Canada). SDSM overestimated rainfall in November, but it was relatively close to observed in other months. The SDSM model has low calibration bias (about -8%) to the standard NCEP dataset. Thus, for Abbotsford, the CGCM1 model was able to adequately predict current climate in terms of monthly precipitation means. There is some “model bias” between the CGCM1 output and current observed. Summer precipitation is about 30% underestimated, and some autumn rainfall is overestimated by 20%, but in 5 other months the model bias was close to zero, which is very good in light of fundamental limitations of CGCM1. The downscaled temperatures using SDSM were very close to observed in all months. The calibration bias for temperature to NCEP dataset was very small (less than 1%), and the model bias of downscaled CGCM1 to observed was less than 10% for most months, and differed by only 1°C in months where % model bias was greater than 15%. CRCM solar radiation monthly values were used and assumed representative. The changes were relatively small, so the downscaled model is assumed to be not sensitive to errors or scale effects in solar radiation values taken from CRCM.

2) The LARS-WG weather generator allowed for good representation of dry and wet spells and provided a reasonably good fit to observed data. The recharge model in HELP accounted for soil properties, hydraulic conductivity, and depth of unsaturated zone.

3) Overall, the groundwater flow models showed relatively small impacts of changes in climate. In this recharge-dominated aquifer, groundwater levels are predicted to decrease by between 0.05 m to more than 0.25 m due to climate change by the 2010-2039 period. Impacts on water levels are generally restricted to the upland areas, because the lower elevation portions of the model, where the major streams are located, are constrained by specified head boundary conditions; although, reductions in baseflow are anticipated due to the lowering of the groundwater gradient across the aquifer.

4) The ability of a groundwater flow model to predict changes to groundwater levels, as forced by climate change, depends on the locations and types of model boundary conditions, the success of model calibration, and model scale. There are limitations in using codes such as MODFLOW for modeling very complex aquifers, especially where there are perched water tables or where changes in the groundwater regime might be anticipated to cause changes to the surface water regime. This study demonstrated that site-specific linkages exist for climatic impacts on groundwater resources, and that these can be successfully evaluated using standardized and consistent methodologies that allow for comparison of results and quantification of changes to groundwater levels, as well as for accounting for causes to such changes.

9. REFERENCES

Allen D.M., Scibek, J., Whitfield, P. and Wei, M. (2004). Climate Change and Groundwater: Summary Report. Prepared for Natural Resources Canada, Climate Change Action Fund.

Anderson M.P. and W.W. Woessner (1992). Applied Groundwater Modeling: Simulation of Flow and Advective Transport. Academic Press, 381 pp.

Barnett, T. P. and R.W. Preisendorfer (1978). Multifield analog prediction of short-term climate fluctuations using a climate state vector. *Journal of Atmospheric Science*, 35:1771–1787.

Beersma J, M Agnew, D Viner, and M Hulme (Eds.) (2000). Climate Scenarios for Water-related and Coastal Impacts. ECLAT-2 Workshop Report No. 3, Published by Climatic Research Unit, UEA, Norwich, UK.

Boer, G.J., Flato, G.M. and Ramsden, D. (2000b). A transient climate change simulation with historical and projected greenhouse gas and aerosol forcing: projected climate for the 21st century. *Climate Dynamics*,16:427-450.

Boer, G.J., Flato, G.M., Reader, M.C., and Ramsden, D. (2000a). A transient climate change simulation with historical and projected greenhouse gas and aerosol forcing: experimental design and comparison with the instrumental record for the 20th century. *Climate Dynamics*, 16:405-425.

Boer, G.J., N.A. McFarlane, and M. Lazare (1992). Greenhouse Gas-induced Climate Change Simulated with the CCC Second-Generation General Circulation Model. *J. Climate*, 5:1045-1077.

Brodie R.S. (1999). Integrating GIS and RDBMS technologies during construction of a regional groundwater model. *Environmental Modeling & Software*, 14: 119-128.

Cannon A.J. and P.H. Whitfield (2000). Downscaling recent streamflow conditions in British Columbia, Canada using ensemble neural network models. *Journal of Hydrology*, 259:136-151.

Carlson A.B., Kratz D.P., Stackhouse P.W. (2002). Release 3 NASA Surface Meteorology and Solar Energy Data Set For Renewable Energy Industry Use, http://eosweb.larc.nasa.gov/sse/

Caya, D. and Laprise, R. (1999). A semi-implicit semi-Lagrangian regional climate model: the Canadian RCM. *Monthly Weather Review,* 127:341-362.

CCCma (2003) Canadian Climate Centre for Modeling and Analysis, CGCM1 information, website (http://www.cccma.bc.ec.gc.ca/models/cgcm1.shtml).

CEAA, Canadian Environmental Assessment Agency (2003) Stochastic Weather Generators, Appendix E. www.ceaa-acee.gc.ca/0010/0001/0002/0004/appendixE_e.htm.

Changnon S.A., F.A. Huff, C-F Hsu (1988). Relations between precipitation and shallow groundwater in Illinois. *Journal of Climate*, 1:1239-1250.

CICS, Canadian Institute for Climate Studies (2003a). Canadian Climate Change Scenarios, www.cics.uvic.ca/scenarios/

CICS, Canadian Institute for Climate Studies (2003b) Downscaling Tools, SDSM www.cics.uvic.ca/scenarios/sdsm/

Coulson, H. (1997). The impacts of climate change on river and stream flow in British Columbia and Southern Yukon. In: Responding to Global Climate Change in British Columbia and Yukon. Volume I of the Canada Country Study: Climate Impacts and Adaptation, E. Taylor and B. Taylor (Eds.), Environment Canada and BC Ministry of Environment, Lands and Parks.

Danard, M., and J. Galbraith (1997). High resolution analyses of daily precipitation amounts and temperatures in Southwestern British Columbia 31 Oct 1971 to 29 June 1995. Report prepared for BC Hydro by Atmospheric Dynamics Corporation. Victoria, BC.

Fayer M.J., G.W. Gee, M.L. Rockhold, M.D. Freshley, and T.B. Walters (1996). Estimating recharge rates for a groundwater model using a GIS. *Journal of Environmental Quality*, 25 (3):510-518.

Flato, G.M., Boer, G.J., Lee, W.G., McFarlane, N.A., Ramsden, D., Reader, M.C., and Weaver, A.J., (2000). The Canadian Centre for Climate Modeling and Analysis Global Coupled Model and its Climate. *Climate Dynamics*, 16:451-467.

Gleick P.H. (1986). Methods for evaluating the regional hydrologic impacts of global climatic changes. *Journal of Hydrology*, 88:97-116.

Hewitson, BC and RG Crane (1996). Climate downscaling: techniques and application. *Climate Research*, 7:85-96.

Huth, R., J. Kysely, and M. Dubrovsky. (2001). Time structure of observed, GCM-simulated, downscaled, and stochastically generated daily temperature series. *Journal of Climate,* 6:4047-4061.

Jones, P.D. (1994). Hemispheric Surface Air Temperature Variations: A Reanalysis and an Update to 1993. *J. Climate*, 7 :1794-1802.

Jyrkama M.I., J.F. Sykes, and S.D. Normani (2002). Recharge estimation for transient ground water modeling. *Ground Water*, 40 (6): 639-649.

Kalnay, E., M. Kanamitsu, R. Kistler, W. Collins, D. Deaven, L. Gandin, M. Iredell, S. Saha, G. White, J. Woollen, Y. Zhu, M. Chelliah, W. Ebisuzaki, W. Higgins, J. Janowiak, K.C. Mo, C. Ropelewski, J. Wang, A. Leetmaa, R. Reynolds, R. Jenne, and D. Joseph. (1996). The NCEP/NCAR 40-Year Reanalysis Project, *Bulletin of the American Meteorological Society*, 77:437-471.

Kharin, V.V. & F.W. Zwiers (2000). Changes in the extremes in an ensemble of transient climate simulation with a coupled atmosphere-ocean GCM, *Journal of Climate,*13:3760-3788.

Kruger A., U. Ulbrich, and P. Speth (2001). Groundwater recharge in Northrhine-Westfalia predicted by a statistical model for greenhouse gas scenarios. *Physics and Chemistry of the Earth Part B: Hydrology Oceans and Atmosphere*, 26 (11-12): 853-861.

Laprise, R., Caya, D., Giguere, M., Bergeron, G., Cote, H., Blanchet, J.-P., Boer, G.J. and McFarlane, N.A. (1998). Climate and climate change in Western Canada as simulated by the Canadian Regional Climate Model. *Atmosphere-Ocean*, 36:119-167.

Loaiciga H.A., D.R. Maidment, J.B. Valdes (2000). Climate-change impacts in a regional karst aquifer, Texas, USA. Journal of Hydrology, 227:173-194.

Loaiciga H.A., J.B. Valdes, R. Vogel, J. Garvey, H.H. Schwarz (1996). Global warming and the hydrologic cycle. *Journal of Hydrology*, 174(1-2):83-128.

McFarlane, N.A., G.J. Boer, J.-P. Blanchet, and M. Lazare, (1992). The Canadian Climate Centre Second-Generation General Circulation Model and Its Equilibrium Climate. *J. Climate*, 5:1013-1044.

Martin P.J. and E.O. Frind (1998). Modeling a complex multi-aquifer system: The Waterloo Moraine. *Ground Water*, 36(4):679-690.

Richardson C.W. (1981). Stochastic simulation of daily precipitation, temperature, and solar radiation. *Water Resources Research*, 17:182-190.

Richardson C.W. (2000). Data requirements for estimation of weather generation parameters. *Transactions of the American Society of Agricultural Engineers*, 43(4):877-882.

Richardson C.W. and D.A. Wright (1984) WGEN: A model for generating daily weather variables. ARS-8, Washington DC, USDA Agricultural Research Service.

Scibek J. and Allen, D.M. (2005). Numerical Groundwater Flow Model of the Abbotsford-Sumas Aquifer, Central Fraser Lowland of BC, Canada, and Washington State, US. Report prepared for Environment Canada.

Semenov MA, Brooks RJ, Barrow EM & Richardson CW (1998). Comparison of the WGEN and LARS-WG stochastic weather generators for diverse climates. *Climate Research*, 10:95-107.

Semenov M.A., Barrow E.M., 1997. Use of a stochastic weather generator in the development of climate change scenarios. *Climatic Change*, 35:397-414.

Soil Conservation Service (1985). National Engineering Handbook: Section 4-Hydrology. Washington DC, US Department of Agriculture.

Waterloo Hydrogeologic Inc. (2000). WHI UnSat Suite User's Manual: 1-D Unsaturated Zone Groundwater Flow and Contaminant Transport Modeling using VLEACH, PESTAN, VS2DT, and HELP. Waterloo, Canada

Waterloo Hydrogeologic Inc. (2000). Visual MODFLOW v 3.0: User Manual. Waterloo, Canada

Whitfield, P.H., Reynolds, C.J., Cannon, A.J., (2002). Modelling streamflows in present and future climates: examples from Georgia Basin, British Columbia. Canadian Water Resources Journal 27 (4), 427-456.

Whitfield, P.H. and E. Taylor. (1998). Apparent recent changes in hydrology and climate of coastal British Columbia. In: Y. Alila (ed.), *Mountains to Sea: Human Interactions with the Hydrologic Cycle*. Proceedings of the 51st Canadian Water Resources Conference, 22-29.

Wilby, R.L. and Wigley, T.M.L. (1997). Downscaling general circulation model output: a review of methods and limitations. *Progress in Physical Geography*, 21:530-548.

Wilby, R.L., Dawson, C.W., and Barrow, E.M. (2002). SDSM – a decision support tool for the assessment of regional climate change impacts. *Environmental and Modeling Software*, 17:145-157.

Wilks D.S. and Wilby R.L. (1999). The weather generation game: a review of stochastic weather models. *Progress in Physical Geography*, 23:329-357.

Xiao, Q., S.L. Ustin, and W.W. Wallender (1996). A spatial and temporal continuous surface-subsurface hydrologic model.*Journal of Geophysical Research*, 101 (D23):29565-29584.

Xu, C. (1999). From GCMs to river flow: a review of downscaling methods and hydrologic modeling approaches. *Progress in Physical Geography*, 23(2):229-249.

York J.P., M. Person, W.J. Gutowski, T.C. Winter (2002). Putting aquifers into atmospheric simulation models: an example from the Mill Creek Watershed, northeastern Kansas. *Advances in Water Resources*, 25:221-238.

Zektser I.S., H.A. Loaiciga (1993). Groundwater fluxes in the global hydrologic cycle: past, present, and future. *Journal of Hydrology*, 144:405-427.

Zhang L., W.R. Dawes, T.J. Hatton, P.H. Reece, G.T.H. Beale, and I. Packer (1999). Estimation of soil moisture and groundwater recharge using the TOPOG_IRM model. *Water Resources Research*, 35(1):149-161.

Zwiers F. (2001). Climate Change - Case Study: Projected Changes in Extreme 24-hour Precipitation. Canadian Centre for Climate Modeling and Analysis, http://www.math.mcmaster.ca/peter/sora/case_studies_01/climate.html

APPENDIX A

CLIMATE DOWNSCALING AND STOCHASTIC WEATHER GENERATOR

PRECIPITATION SUMMARIES FROM SDSM DOWNSCALING

Table 15 Precipitation (wet days only) at Abbotsford, downscaling results from SDSM and PCA k-nn: (a) mean daily P, (b) mean monthly P.

(a) Precipitation, mean daily (wet days only)

(mm / day)	SDSM				Cal. NCEP	Obs.	PCA k-nn			
Month	1961-2000	2010-2039	2040-2069	2070-2099	1961-2000	1961-2000	1961-2000	2010-2039	2040-2069	2070-2099
Jan	8.4	7.8	8.2	9.2	9.3	11.4	9.9	10.0	9.4	9.6
Feb	6.7	6.7	7.5	8.0	8.1	10.1	9.0	9.0	9.2	8.5
Mar	7.6	6.9	7.2	7.1	7.1	8.2	8.4	7.1	6.8	7.3
Apr	7.0	6.9	7.4	7.3	6.2	7.0	6.7	6.0	6.2	6.3
May	6.1	6.4	6.3	6.5	5.3	4.8	4.4	5.5	5.5	5.7
Jun	3.8	4.0	3.9	4.1	4.6	1.9	3.1	2.5	3.3	4.9
Jul	4.5	4.3	3.9	3.8	4.6	2.8	2.8	2.6	2.5	5.2
Aug	3.4	3.6	3.6	3.7	4.8	3.9	3.1	3.0	3.0	5.3
Sep	6.5	6.5	6.3	6.4	6.8	4.3	4.6	4.5	3.6	7.2
Oct	9.0	9.3	10.1	9.7	8.1	8.6	9.9	10.6	9.4	8.8
Nov	12.6	11.7	11.7	12.0	9.5	11.2	11.3	10.9	11.0	10.1
Dec	8.9	9.0	9.4	9.6	9.3	11.1	11.8	10.5	10.9	9.7
Winter	8.0	7.8	8.4	8.9	8.9	10.9	10.2	9.9	9.8	9.3
Spring	6.9	6.7	6.9	7.0	6.2	6.7	6.5	6.2	6.2	6.4
Summer	3.9	3.9	3.8	3.9	4.7	2.8	3.0	2.7	2.9	5.1
Autumn	9.3	9.1	9.4	9.4	8.1	8.0	8.6	8.7	8.0	8.7
Annual	7.0	6.9	7.1	7.3	7.0	7.1	7.1	6.9	6.7	7.4

(b) Precipitation, mean monthly (wet days only)

(mm / month)	SDSM				Cal. NCEP	Obs.	PCA k-nn			
Month	1961-2000	2010-2039	2040-2069	2070-2099	1961-2000	1961-2000	1961-2000	2010-2039	2040-2069	2070-2099
Jan	261.7	240.8	255.3	284.3	288.8	352.7	307.5	311.5	292.2	298.8
Feb	188.8	188.9	209.1	224.2	227.7	282.3	250.7	252.9	256.7	236.9
Mar	236.1	213.6	222.3	220.5	218.7	254.2	261.6	220.1	211.9	225.6
Apr	208.8	207.6	221.5	220.1	187.3	210.4	199.7	181.4	187.4	188.3
May	189.9	197.9	194.2	200.4	164.4	149.7	137.3	171.0	169.7	177.1
Jun	115.2	120.4	117.8	122.0	137.1	56.8	92.0	75.3	98.6	147.3
Jul	139.4	131.9	119.7	117.3	143.4	85.7	88.2	80.1	77.7	160.3
Aug	106.6	110.6	112.4	114.8	148.0	119.8	97.6	93.9	93.4	163.5
Sep	193.7	194.2	190.4	192.8	203.9	129.4	137.0	136.0	108.7	215.3
Oct	278.3	287.2	312.5	299.6	250.7	265.6	307.2	328.8	292.3	271.8
Nov	377.3	351.1	349.7	360.4	284.5	336.4	338.3	326.8	329.5	304.2
Dec	274.4	277.5	291.6	298.1	288.0	344.9	366.6	325.5	337.4	300.8
Winter	721.1	704.0	753.3	803.8	802.2	977.5	921.0	887.4	884.3	834.1
Spring	634.9	619.3	638.5	641.5	570.5	614.6	598.7	572.3	569.1	591.0
Summer	361.0	363.0	350.0	354.3	428.4	261.3	277.8	249.1	270.0	471.0
Autumn	849.7	832.3	851.8	852.4	739.2	730.8	781.2	789.6	729.1	791.2
Annual	2571.0	2522.6	2598.4	2657.3	2545.3	2592.7	2586.5	2506.2	2459.9	2692.4

Table 16 Precipitation (wet + dry days) at Abbotsford, downscaling results from SDSM and PCA k-nn: (a) mean monthly P, (b) Relative change in Precipitation (future climate / current climate).

(a) Precipitation, mean monthly

(mm / month)	SDSM				Cal. NCEP	Obs.	PCA k-nn			
Month	1961-2000	2010-2039	2040-2069	2070-2099	1961-2000	1961-2000	1961-2000	2010-2039	2040-2069	2070-2099
Jan	190.4	170.1	184.7	209.5	191.8	277.8	245.5	254.3	233.3	205.5
Feb	106.9	112.9	131.8	142.6	145.9	208.7	182.7	181.6	196.0	157.4
Mar	134.7	127.1	135.1	140.9	133.4	179.3	183.6	154.1	153.2	144.3
Apr	138.6	133.3	146.4	143.2	114.1	126.7	129.1	116.7	130.1	117.2
May	84.3	89.1	88.6	91.4	85.0	67.6	63.0	84.7	85.2	93.6
Jun	43.8	42.3	40.4	41.3	63.8	13.0	29.1	25.2	35.7	70.6
Jul	46.1	41.3	36.1	35.2	46.0	15.7	18.8	19.8	23.6	51.2
Aug	36.6	33.2	31.9	28.8	48.0	31.8	23.8	23.4	22.8	52.4
Sep	54.8	58.5	59.3	57.8	78.2	31.6	31.2	34.0	29.8	82.4
Oct	190.6	194.5	202.1	187.3	134.4	127.7	159.6	181.4	154.4	151.9
Nov	300.1	272.7	280.4	283.6	202.9	245.2	240.9	248.0	240.5	223.9
Dec	191.6	200.3	212.2	222.4	203.3	276.7	305.5	259.7	243.8	221.1
Winter	478.8	475.4	522.6	567.8	537.6	758.9	724.6	689.9	673.4	580.2
Spring	355.2	348.3	367.1	373.2	330.2	360.4	360.7	350.8	364.1	352.7
Summer	127.0	116.7	108.3	105.1	158.5	59.0	71.7	69.0	81.8	175.7
Autumn	499.4	487.0	499.8	486.5	402.3	354.2	380.0	410.7	372.4	442.3
Annual	1390.2	1352.4	1406.4	1431.9	1376.4	1343.8	1379.7	1370.7	1362.2	1497.4

(b) Relative change in Precipitation (future climate / current climate)

(mm / mm)	1961-2000	2010-2039	2040-2069	2070-2099	1961-2000	2010-2039	2040-2069	2070-2099
Month	SDSM				k-nn ACS			
Jan	1.00	0.88	0.81	0.91	1.00	1.09	1.05	1.19
Feb	1.00	0.92	0.79	0.75	1.00	0.93	0.93	1.06
Mar	1.00	0.96	0.90	0.96	1.00	1.01	1.20	1.17
Apr	1.00	1.02	0.93	0.97	1.00	0.90	0.99	0.97
May	1.00	0.97	0.98	0.92	1.00	0.99	0.74	0.79
Jun	1.00	0.98	1.03	1.06	1.00	0.71	0.82	0.36
Jul	1.00	1.03	1.17	1.31	1.00	0.84	0.80	0.67
Aug	1.00	1.11	1.15	1.27	1.00	1.03	1.04	1.39
Sep	1.00	1.03	1.01	0.95	1.00	1.14	1.05	1.06
Oct	1.00	1.08	1.04	1.02	1.00	1.17	1.03	0.83
Nov	1.00	0.99	0.96	1.06	1.00	1.03	1.00	1.02
Dec	1.00	0.95	0.90	0.86	1.00	1.07	1.25	1.13
Winter	1.00	0.92	0.84	0.84	1.00	1.02	1.08	1.13
Spring	1.00	0.98	0.93	0.95	1.00	0.96	0.99	0.99
Summer	1.00	1.03	1.11	1.21	1.00	0.84	0.88	0.72
Autumn	1.00	1.03	1.00	1.03	1.00	1.10	1.02	0.95
Annual	1.00	0.98	0.94	0.97	1.00	1.01	1.01	0.99

Table 17 Standard deviation of daily precipitation at Abbotsford, downscaling results from SDSM and PCA k-nn: (a) std dev by month, (b) Relative change in standard deviation of precipitation (future climate / current climate).

(a) Standard deviation in mean daily precipitation

(mm / day)	SDSM				Cal. NCEP	Obs.	PCA k-nn			
Month	1961-2000	2010-2039	2040-2069	2070-2099	1961-2000	1961-2000	1961-2000	2010-2039	2040-2069	2070-2099
Jan	10.4	10.5	10.3	11.2	11.8	9.1	8.8	8.8	8.8	11.3
Feb	9.0	8.3	9.7	9.8	10.4	9.0	8.3	8.6	9.2	10.7
Mar	9.5	8.4	8.9	8.7	8.8	8.1	7.8	6.7	6.7	8.6
Apr	8.8	8.8	9.2	9.3	8.0	6.6	6.9	6.2	5.9	7.6
May	8.5	8.2	8.0	8.3	7.0	5.4	5.4	5.8	5.8	7.5
Jun	5.1	5.3	5.2	5.5	6.1	2.6	4.2	3.4	4.3	7.1
Jul	6.4	6.5	5.8	5.9	6.8	2.4	3.7	3.5	3.5	8.4
Aug	5.3	5.2	5.5	5.7	6.8	2.2	3.3	4.1	4.0	8.0
Sep	7.9	8.2	8.0	7.9	8.8	5.1	6.0	5.5	5.4	9.3
Oct	11.4	11.3	12.5	11.3	9.9	8.2	8.8	8.8	8.7	11.1
Nov	15.5	14.5	14.0	14.4	11.5	8.2	8.2	8.9	8.9	11.9
Dec	11.9	11.4	12.4	12.1	11.6	8.4	9.1	8.9	9.6	11.7
Winter	10.5	10.1	10.9	11.1	11.3	8.8	8.7	8.8	9.2	11.2
Spring	8.9	8.5	8.7	8.8	8.0	6.8	6.8	6.2	6.1	7.9
Summer	5.6	5.7	5.5	5.7	6.6	2.4	3.7	3.7	4.0	7.9
Autumn	12.0	11.6	11.8	11.5	10.1	7.3	7.8	7.9	7.8	10.8
Annual	9.6	9.3	9.5	9.5	9.2	6.8	7.0	6.9	7.1	9.6

(b) Relative change in std. dev. of Precipitation (future climate / current climate)

(mm / mm)	1961-2000	2010-2039	2040-2069	2070-2099	1961-2000	2010-2039	2040-2069	2070-2099
Month	SDSM				k-nn ACS			
Jan	1.00	0.92	0.93	0.92	1.00	1.00	1.00	1.03
Feb	1.00	0.99	0.86	0.92	1.00	0.94	0.90	0.98
Mar	1.00	1.02	0.97	1.08	1.00	1.00	1.17	1.21
Apr	1.00	0.99	0.95	0.95	1.00	1.05	1.16	1.12
May	1.00	0.96	1.00	1.03	1.00	1.01	0.94	0.93
Jun	1.00	0.96	0.97	0.94	1.00	0.78	0.97	0.61
Jul	1.00	0.99	1.12	1.09	1.00	1.00	1.06	0.70
Aug	1.00	0.96	0.92	0.93	1.00	1.02	0.81	0.56
Sep	1.00	1.02	1.05	1.00	1.00	1.01	1.10	0.94
Oct	1.00	1.11	1.00	1.01	1.00	1.01	1.01	0.94
Nov	1.00	0.97	1.01	1.08	1.00	1.00	0.92	0.92
Dec	1.00	1.03	0.94	0.99	1.00	0.92	0.95	0.87
Winter	1.00	0.98	0.92	0.95	1.00	0.95	0.95	0.95
Spring	1.00	0.99	0.97	1.02	1.00	1.02	1.10	1.11
Summer	1.00	0.97	1.01	0.99	1.00	0.93	0.94	0.62
Autumn	1.00	1.03	1.01	1.04	1.00	1.00	0.99	0.93
Annual	1.00	1.00	0.97	1.00	1.00	0.98	0.99	0.96

Table 18 WET days % of month at Abbotsford, downscaling results from SDSM and PCA k-nn: (a) % WET days by month, (b) Relative change in % WET days (future climate / current climate).

(a) Wet days percentage (monthly)

(%)	SDSM				Cal. NCEP	Obs.	PCA k-nn			
Month	1961-2000	2010-2039	2040-2069	2070-2099	1961-2000	1961-2000	1961-2000	2010-2039	2040-2069	2070-2099
Jan	72.8	70.6	72.4	73.7	66.4	78.8	79.9	81.6	79.8	68.8
Feb	56.6	59.8	63.0	63.6	64.1	73.9	72.9	71.8	76.3	66.4
Mar	57.1	59.5	60.8	63.9	61.0	70.5	70.2	70.0	72.3	64.0
Apr	66.4	64.2	66.1	65.0	60.9	60.2	64.7	64.3	69.4	62.3
May	44.4	45.0	45.6	45.6	51.7	45.2	45.9	49.6	50.2	52.9
Jun	38.1	35.2	34.3	33.8	46.5	22.9	31.7	33.4	36.2	47.9
Jul	33.1	31.3	30.2	30.0	32.0	18.3	21.3	24.7	30.3	32.0
Aug	34.4	30.0	28.4	25.1	32.4	26.6	24.4	24.9	24.4	32.0
Sep	28.3	30.1	31.2	30.0	38.3	24.4	22.8	25.0	27.4	38.3
Oct	68.5	67.7	64.7	62.5	53.6	48.1	51.9	55.2	52.8	55.9
Nov	79.6	77.7	80.2	78.7	71.3	72.9	71.2	75.9	73.0	73.6
Dec	69.8	72.2	72.8	74.6	70.6	80.2	83.3	79.8	72.3	73.5
Winter	66.4	67.5	69.4	70.6	67.0	77.6	78.7	77.7	76.1	69.6
Spring	55.9	56.2	57.5	58.2	57.9	58.6	60.3	61.3	64.0	59.7
Summer	35.2	32.2	30.9	29.7	37.0	22.6	25.8	27.7	30.3	37.3
Autumn	58.8	58.5	58.7	57.1	54.4	48.5	48.6	52.0	51.1	55.9
Annual	54.1	53.6	54.1	53.9	54.1	51.8	53.3	54.7	55.4	55.6

(b) Relative change in % Wet days (future climate / current climate)

(% / %)	1961-2000	2010-2039	2040-2069	2070-2099	1961-2000	2010-2039	2040-2069	2070-2099
Month	SDSM				k-nn ACS			
Jan	1.00	0.98	0.96	0.99	1.00	1.02	1.00	0.99
Feb	1.00	0.99	0.94	0.89	1.00	0.94	0.95	0.97
Mar	1.00	0.95	0.93	0.89	1.00	0.97	0.97	0.98
Apr	1.00	1.02	0.99	1.02	1.00	0.93	0.93	0.87
May	1.00	1.00	0.99	0.97	1.00	0.99	0.91	0.90
Jun	1.00	1.01	1.04	1.12	1.00	0.92	0.88	0.63
Jul	1.00	1.01	1.04	1.10	1.00	0.82	0.70	0.60
Aug	1.00	1.13	1.19	1.37	1.00	1.02	1.00	1.09
Sep	1.00	1.04	1.01	0.94	1.00	0.91	0.83	0.89
Oct	1.00	1.03	1.08	1.10	1.00	1.04	0.98	0.91
Nov	1.00	1.02	0.99	1.01	1.00	1.04	0.98	1.00
Dec	1.00	0.98	0.97	0.94	1.00	1.10	1.15	1.11
Winter	1.00	0.98	0.96	0.94	1.00	1.02	1.03	1.02
Spring	1.00	0.99	0.97	0.96	1.00	0.96	0.94	0.92
Summer	1.00	1.04	1.08	1.19	1.00	0.91	0.85	0.74
Autumn	1.00	1.03	1.03	1.03	1.00	1.02	0.95	0.95
Annual	1.00	1.00	0.99	1.00	1.00	0.99	0.96	0.94

Table 19 DRY Spell Length at Abbotsford, downscaling results from SDSM and PCA k-nn: (a) DRY spell length, (b) Relative change in DRY spell length (future climate / current climate).

(a) DRY Spell Length

(days)	SDSM				Cal. NCEP	Obs.	PCA k-nn			
Month	1961-2000	2010-2039	2040-2069	2070-2099	1961-2000	1961-2000	1961-2000	2010-2039	2040-2069	2070-2099
Jan	0.6	0.7	0.6	0.6	1.1	0.6	0.6	0.4	0.8	1.8
Feb	1.1	1.0	0.8	1.0	1.2	1.0	1.1	0.8	0.8	1.7
Mar	1.3	1.2	1.2	1.1	1.2	0.9	0.9	0.9	0.8	1.8
Apr	0.9	0.9	0.9	0.9	1.0	1.1	1.0	1.0	0.9	1.3
May	1.7	1.7	1.7	1.7	1.3	1.9	1.8	1.5	1.3	1.8
Jun	2.4	2.6	2.7	2.8	1.7	3.5	3.2	2.7	2.6	2.5
Jul	2.5	2.7	2.8	2.9	2.6	6.2	5.1	4.1	2.7	3.1
Aug	2.6	3.1	3.4	3.8	3.0	4.5	4.4	4.2	3.8	5.6
Sep	3.5	3.3	3.2	4.0	2.3	4.9	5.0	3.1	4.1	3.2
Oct	1.3	1.1	1.4	1.5	1.6	2.9	3.4	2.9	2.1	2.3
Nov	0.5	0.6	0.5	0.6	0.8	1.1	1.0	0.9	1.0	1.3
Dec	0.7	0.7	0.6	0.7	0.7	0.7	0.7	0.9	0.8	1.4
Winter	0.8	0.8	0.7	0.8	1.0	0.8	0.8	0.7	0.8	1.6
Spring	1.3	1.3	1.3	1.2	1.2	1.3	1.2	1.1	1.0	1.6
Summer	2.5	2.8	3.0	3.1	2.4	4.7	4.3	3.7	3.0	3.7
Autumn	1.7	1.6	1.7	2.0	1.6	3.0	3.2	2.3	2.4	2.3
Annual	1.6	1.6	1.7	1.8	1.5	2.4	2.4	1.9	1.8	2.3

(b) Relative change in DRY spell length (future climate / current climate)

(days / days)	1961-2000	2010-2039	2040-2069	2070-2099	1961-2000	2010-2039	2040-2069	2070-2099
Month	SDSM				k-nn ACS			
Jan	1.00	0.98	1.14	1.03	1.00	0.44	0.76	0.76
Feb	1.00	0.82	1.05	1.12	1.00	0.94	1.33	1.28
Mar	1.00	1.06	1.03	1.17	1.00	1.07	1.08	1.03
Apr	1.00	0.98	1.04	1.04	1.00	1.13	1.12	1.25
May	1.00	0.99	1.00	1.01	1.00	1.20	1.41	1.52
Jun	1.00	0.97	0.92	0.86	1.00	1.04	1.26	1.36
Jul	1.00	0.97	0.95	0.85	1.00	1.52	1.92	2.32
Aug	1.00	0.90	0.83	0.70	1.00	1.10	1.16	1.18
Sep	1.00	0.81	0.82	0.88	1.00	0.76	1.21	1.18
Oct	1.00	0.95	0.75	0.88	1.00	1.40	1.66	1.39
Nov	1.00	0.80	0.92	0.73	1.00	0.96	1.08	1.17
Dec	1.00	0.91	1.02	1.00	1.00	1.12	0.97	0.90
Winter	1.00	0.89	1.07	1.06	1.00	0.82	1.02	0.98
Spring	1.00	1.01	1.02	1.07	1.00	1.14	1.23	1.30
Summer	1.00	0.94	0.89	0.80	1.00	1.21	1.41	1.57
Autumn	1.00	0.84	0.82	0.86	1.00	0.97	1.32	1.24
Annual	1.00	0.92	0.91	0.89	1.00	1.08	1.31	1.36

Table 20 WET Spell Length at Abbotsford, downscaling results from SDSM and k-nn ACS method from Environment Canada: (a) WET spell length in days, (b) Relative change in WET spell length (future climate / current climate).

(a) WET Spell Length

(days)	SDSM				Cal. NCEP	Obs.	PCA k-nn			
Month	1961-2000	2010-2039	2040-2069	2070-2099	1961-2000	1961-2000	1961-2000	2010-2039	2040-2069	2070-2099
Jan	3.5	3.5	3.6	3.7	2.9	6.0	6.7	6.2	5.3	5.2
Feb	2.0	2.2	2.3	2.8	3.0	5.2	4.5	3.8	4.7	4.7
Mar	2.1	2.2	2.5	2.8	2.5	3.6	4.0	3.5	4.1	4.0
Apr	2.6	2.5	2.6	2.6	2.1	2.7	3.0	3.0	3.8	3.1
May	1.6	1.5	1.6	1.7	1.6	1.5	1.7	2.0	1.8	2.4
Jun	1.0	0.9	0.9	0.9	1.4	1.0	1.0	0.9	1.0	2.2
Jul	1.0	0.9	0.9	0.9	0.9	0.6	1.0	1.0	0.7	1.6
Aug	0.8	0.7	0.7	0.6	0.8	0.8	0.8	0.5	0.7	1.4
Sep	0.8	0.8	0.8	0.8	1.0	0.9	0.6	0.7	0.8	1.7
Oct	2.2	2.3	2.1	2.1	1.8	1.4	2.0	1.5	1.6	2.1
Nov	5.0	4.5	4.7	4.5	2.8	4.1	4.0	4.4	3.6	4.8
Dec	3.0	3.3	3.4	4.2	3.5	4.6	5.5	5.6	4.0	6.2
Winter	2.8	3.0	3.1	3.6	3.2	5.3	5.6	5.2	4.7	5.4
Spring	2.1	2.1	2.3	2.3	2.1	2.6	2.9	2.8	3.2	3.2
Summer	0.9	0.8	0.8	0.8	1.0	0.8	1.0	0.8	0.8	1.8
Autumn	2.7	2.5	2.5	2.5	1.9	2.1	2.2	2.2	2.0	2.8
Annual	2.1	2.1	2.2	2.3	2.0	2.7	2.9	2.7	2.7	3.3

(b) Relative change in WET spell length (future climate / current climate)

(days / days)	1961-2000	2010-2039	2040-2069	2070-2099	1961-2000	2010-2039	2040-2069	2070-2099
Month	SDSM				k-nn ACS			
Jan	1.00	0.97	0.94	0.95	1.00	1.16	1.25	1.12
Feb	1.00	0.84	0.78	0.71	1.00	0.80	0.96	1.11
Mar	1.00	0.92	0.82	0.78	1.00	0.84	0.98	0.86
Apr	1.00	1.02	0.98	1.01	1.00	0.79	0.78	0.70
May	1.00	0.96	0.92	0.96	1.00	1.13	0.97	0.87
Jun	1.00	0.99	0.97	1.08	1.00	0.92	1.05	1.02
Jul	1.00	0.97	1.06	1.11	1.00	1.33	1.38	0.82
Aug	1.00	1.12	1.08	1.26	1.00	0.80	1.26	1.26
Sep	1.00	0.94	0.89	0.91	1.00	0.87	0.78	1.09
Oct	1.00	0.99	1.07	1.05	1.00	0.92	1.24	0.90
Nov	1.00	1.05	0.99	1.10	1.00	1.20	1.10	1.12
Dec	1.00	0.81	0.78	0.73	1.00	1.39	1.36	1.15
Winter	1.00	0.87	0.83	0.80	1.00	1.10	1.18	1.12
Spring	1.00	0.96	0.90	0.91	1.00	0.87	0.90	0.80
Summer	1.00	1.02	1.03	1.13	1.00	1.02	1.21	1.02
Autumn	1.00	1.02	1.01	1.07	1.00	1.08	1.09	1.06
Annual	1.00	0.95	0.91	0.93	1.00	1.02	1.08	1.01

TEMPERATURE SUMMARIES FROM SDSM DOWNSCALING

Table 21 Temperature at Abbotsford, downscaling results from SDSM and PCA k-nn: (a) mean monthly temperature, (b) change in temperature (future climate - current climate), in degrees C.

(a) Temperature, mean monthly

(°C)	SDSM				Cal. NCEP	Obs.	PCA k-nn			
Month	1961-2000	2010-2039	2040-2069	2070-2099	1961-2000	1961-2000	1961-2000	2010-2039	2040-2069	2070-2099
Jan	2.5	3.2	4.4	6.0	2.4	2.4	3.7	4.2	5.2	7.7
Feb	4.1	4.7	5.6	6.8	4.8	4.8	2.9	3.4	4.6	6.7
Mar	5.9	6.8	7.4	8.7	6.6	6.6	3.5	4.4	5.4	7.4
Apr	8.2	9.1	10.0	10.7	9.2	9.2	5.4	6.5	8.2	9.9
May	11.7	12.1	12.9	13.9	12.3	12.3	9.1	10.7	12.4	14.4
Jun	15.3	15.9	16.8	18.0	15.1	15.1	14.4	15.7	17.3	18.7
Jul	17.7	18.4	19.0	20.1	17.3	17.3	17.6	18.4	19.1	19.8
Aug	18.0	18.8	19.7	20.6	17.5	17.5	18.6	18.8	19.4	19.7
Sep	14.8	15.9	17.0	17.9	14.8	14.8	16.8	17.4	18.9	19.6
Oct	10.0	11.1	12.0	13.4	10.2	10.2	11.9	13.0	14.5	16.6
Nov	6.4	8.0	8.4	10.0	5.7	5.7	8.0	9.0	10.9	12.7
Dec	3.1	4.4	5.4	6.1	2.8	2.8	4.8	5.5	7.7	9.2
Winter	3.2	4.1	5.1	6.3	3.3	3.3	3.8	4.4	5.9	7.9
Spring	8.6	9.4	10.1	11.1	9.4	9.4	6.0	7.2	8.7	10.6
Summer	17.0	17.7	18.5	19.6	16.7	16.7	16.9	17.6	18.6	19.4
Autumn	10.4	11.7	12.5	13.8	10.2	10.2	12.2	13.1	14.8	16.3
Annual	9.8	10.7	11.5	12.7	9.9	9.9	9.7	10.6	12.0	13.5

(b) Change in Temperature (future climate - current climate)

(°C)	1961-2000	2010-2039	2040-2069	2070-2099	1961-2000	2010-2039	2040-2069	2070-2099
Month	SDSM				k-nn ACS			
Jan	0.00	0.74	1.89	3.54	0.00	0.49	1.54	4.00
Feb	0.00	0.67	1.48	2.76	0.00	0.55	1.78	3.82
Mar	0.00	0.96	1.52	2.84	0.00	0.89	1.88	3.87
Apr	0.00	0.90	1.72	2.49	0.00	1.02	2.74	4.46
May	0.00	0.49	1.22	2.27	0.00	1.59	3.30	5.29
Jun	0.00	0.60	1.43	2.62	0.00	1.28	2.91	4.35
Jul	0.00	0.67	1.25	2.39	0.00	0.80	1.50	2.20
Aug	0.00	0.77	1.68	2.62	0.00	0.16	0.78	1.09
Sep	0.00	1.04	2.19	3.12	0.00	0.63	2.13	2.76
Oct	0.00	1.14	1.99	3.40	0.00	1.05	2.59	4.63
Nov	0.00	1.56	1.99	3.59	0.00	1.00	3.00	4.72
Dec	0.00	1.30	2.26	3.01	0.00	0.74	2.91	4.44
Winter	0.00	0.91	1.88	3.10	0.00	0.59	2.08	4.09
Spring	0.00	0.78	1.48	2.53	0.00	1.17	2.64	4.54
Summer	0.00	0.68	1.45	2.54	0.00	0.75	1.73	2.54
Autumn	0.00	1.25	2.06	3.37	0.00	0.89	2.57	4.04
Annual	0.00	0.90	1.72	2.89	0.00	0.85	2.26	3.80

Table 22 Temperature standard deviation at Abbotsford, downscaling results from SDSM and PCA k-nn: (a) standard deviation of temperature, (b) relative change in standard deviation of temperature (future climate / current climate).

(a) Standard Deviation of daily Temperature

(°C)	SDSM				Cal. NCEP	Obs.	PCA k-nn			
Month	1961-2000	2010-2039	2040-2069	2070-2099	1961-2000	1961-2000	1961-2000	2010-2039	2040-2069	2070-2099
Jan	3.3	3.5	3.6	3.6	4.4	4.4	2.6	2.7	3.0	3.0
Feb	2.7	2.9	3.0	3.0	3.2	3.4	3.0	3.0	3.1	3.2
Mar	2.5	2.5	2.6	2.7	2.6	2.7	2.8	2.7	3.0	3.3
Apr	2.4	2.4	2.4	2.5	2.7	2.7	2.4	2.7	2.9	2.8
May	2.7	2.8	2.7	3.0	2.9	3.0	2.8	3.0	3.2	3.1
Jun	2.4	2.3	2.4	2.5	2.5	2.6	2.8	2.5	2.6	2.6
Jul	2.0	2.0	2.0	2.0	2.4	2.6	2.2	2.1	2.1	1.8
Aug	2.2	2.2	2.2	2.1	2.5	2.5	2.2	2.0	1.9	1.7
Sep	2.7	2.6	2.7	2.7	2.7	2.8	2.8	2.6	2.7	2.4
Oct	2.8	2.8	2.9	3.1	2.9	2.9	3.0	3.0	3.0	3.0
Nov	3.4	3.6	3.6	3.9	3.4	3.5	3.2	3.1	3.2	3.0
Dec	3.5	3.6	3.6	3.8	4.3	4.3	2.9	2.9	2.9	3.1
Winter	3.2	3.4	3.4	3.5	4.0	4.1	2.8	2.8	3.0	3.1
Spring	2.5	2.6	2.6	2.7	2.7	2.8	2.7	2.8	3.1	3.1
Summer	2.2	2.2	2.2	2.2	2.5	2.6	2.4	2.2	2.2	2.0
Autumn	3.0	3.0	3.1	3.3	3.0	3.1	3.0	2.9	3.0	2.8
Annual	2.7	2.8	2.9	3.0	3.1	3.2	2.7	2.7	2.8	2.8

(b) Relative change in std. dev. of temperature (future climate / current climate)

(°C / °C)	1961-2000	2010-2039	2040-2069	2070-2099	1961-2000	2010-2039	2040-2069	2070-2099
Month	SDSM				k-nn ACS			
Jan	1.00	1.16	1.21	1.23	1.00	1.07	1.40	1.37
Feb	1.00	1.21	1.27	1.26	1.00	0.98	1.11	1.18
Mar	1.00	1.02	1.12	1.18	1.00	0.93	1.22	1.47
Apr	1.00	1.04	0.99	1.07	1.00	1.24	1.38	1.35
May	1.00	1.06	1.00	1.24	1.00	1.14	1.31	1.18
Jun	1.00	0.97	1.00	1.09	1.00	0.83	0.88	0.84
Jul	1.00	0.96	0.97	0.98	1.00	0.93	0.91	0.69
Aug	1.00	1.00	0.98	0.95	1.00	0.84	0.73	0.58
Sep	1.00	0.96	1.02	0.98	1.00	0.82	0.92	0.74
Oct	1.00	1.03	1.05	1.25	1.00	1.00	1.01	1.00
Nov	1.00	1.13	1.16	1.34	1.00	0.93	1.01	0.91
Dec	1.00	1.08	1.10	1.18	1.00	0.94	0.96	1.13
Winter	1.00	1.14	1.18	1.22	1.00	0.99	1.14	1.21
Spring	1.00	1.04	1.03	1.17	1.00	1.09	1.29	1.33
Summer	1.00	0.98	0.99	1.01	1.00	0.86	0.85	0.73
Autumn	1.00	1.05	1.09	1.21	1.00	0.92	0.98	0.89
Annual	1.00	1.07	1.09	1.17	1.00	0.97	1.07	1.05

Table 23 Solar radiation at Abbotsford, from CRCM and NASA observed. CRCM not downscaled. Monthly values for climate scenarios and absolute changes relative to current climate.

		NASA	CRCM not downscaled				
CRCM scenarios	years	1990-2000	1975-1984	interpolated	2040-2049	interpolated	2080-2089
	mid year	1995	1980	2020	2045	2055	2085
GCM1 scenarios	years	1990-2000	1961-2000	2010-2039		2040-2069	2070-2099
	mid year	1995	1980	2020		2055	2085
	(W/m2) - units used in CRCM output						
Output from CRCM (not downscaled) and observed from NASA	Jan	45.42	48.97	50.55	51.54	51.20	50.16
	Feb	85.83	80.10	80.49	80.74	80.69	80.53
	Mar	136.67	137.42	139.40	140.64	140.57	140.35
	Apr	182.08	218.69	221.73	223.63	223.37	222.59
	May	222.92	289.75	294.25	297.06	294.33	286.15
	Jun	238.33	332.37	331.42	330.83	330.17	328.19
	Jul	260.83	324.51	326.22	327.30	327.49	328.07
	Aug	212.92	279.48	279.22	279.06	277.54	272.99
	Sep	171.67	196.86	194.03	192.26	191.75	190.20
	Oct	97.50	102.87	104.10	104.86	105.80	108.61
	Nov	47.50	56.99	56.95	56.92	57.51	59.28
	Dec	35.83	42.96	42.63	42.41	42.21	41.58
	(MJ/m2*day) - units used in LARS-WG						
	Jan	3.92	4.23	4.37	4.45	4.42	4.33
	Feb	7.42	6.92	6.95	6.98	6.97	6.96
	Mar	11.81	11.87	12.04	12.15	12.15	12.13
	Apr	15.73	18.89	19.16	19.32	19.30	19.23
	May	19.26	25.03	25.42	25.67	25.43	24.72
	Jun	20.59	28.72	28.63	28.58	28.53	28.36
	Jul	22.54	28.04	28.19	28.28	28.30	28.35
	Aug	18.40	24.15	24.12	24.11	23.98	23.59
	Sep	14.83	17.01	16.76	16.61	16.57	16.43
	Oct	8.42	8.89	8.99	9.06	9.14	9.38
	Nov	4.10	4.92	4.92	4.92	4.97	5.12
	Dec	3.10	3.71	3.68	3.66	3.65	3.59
	Absolute Change (future climate - base climate 1980 mid year)						
Input to LARS-WG for scenario generation	Jan		0.00	0.14	0.22	0.19	0.10
	Feb		0.00	0.03	0.06	0.05	0.04
	Mar		0.00	0.17	0.28	0.27	0.25
	Apr		0.00	0.26	0.43	0.40	0.34
	May		0.00	0.39	0.63	0.40	-0.31
	Jun		0.00	-0.08	-0.13	-0.19	-0.36
	Jul		0.00	0.15	0.24	0.26	0.31
	Aug		0.00	-0.02	-0.04	-0.17	-0.56
	Sep		0.00	-0.24	-0.40	-0.44	-0.58
	Oct		0.00	0.11	0.17	0.25	0.50
	Nov		0.00	0.00	-0.01	0.05	0.20
	Dec		0.00	-0.03	-0.05	-0.07	-0.12

Table 24 Output from LARS-WG for base case scenario: Rainfall and Temperature statistics and tests of time series similarity between observed and modeled.

RAINFALL

(mm)	J	F	M	A	M	J	J	A	S	O	N	D
Obs Mean	207.2	158.7	143.4	117.8	92.2	69.8	50.7	53.2	81.0	148.7	226.2	225.0
Obs stddev	81.1	78.9	51.9	42.4	44.3	42.1	34.1	46.3	49.2	83.4	80.8	78.0
LARS-WG Mean	216.8	163.9	150.8	118.1	94.3	69.5	49.9	55.0	80.6	149.1	236.8	219.9
LARS-WG stddev	69.4	57.5	55.3	41.7	37.4	33.6	31.9	34.5	47.3	61.1	66.0	66.0
t-value	-0.800	-0.510	-0.790	-0.040	-0.320	0.050	0.150	-0.290	0.050	-0.040	-0.920	0.440
p-value	0.426	0.613	0.429	0.966	0.747	0.959	0.884	0.769	0.961	0.971	0.359	0.657
F-value	1.370	1.880	1.130	1.030	1.410	1.570	1.140	1.800	1.080	1.860	1.500	1.400
p-value	0.164	0.004	0.656	0.843	0.128	0.042	0.533	0.008	0.696	0.005	0.072	0.136

Temperature

[MIN MONTHLY]

(oC)	J	F	M	A	M	J	J	A	S	O	N	D
Obs Mean	-0.8	0.9	2.0	4.1	6.9	9.7	11.2	11.3	8.7	5.4	2.3	-0.2
Obs stddev	2.5	1.6	1.4	1.3	1.3	1.1	1.0	1.0	1.1	1.2	1.9	2.0
LARS-WG Mean	-0.4	0.6	2.2	4.1	6.6	9.6	11.3	11.0	8.7	5.4	2.1	-0.2
LARS-WG stddev	1.8	1.4	1.1	1.0	1.0	0.9	0.8	0.9	1.0	1.1	1.4	1.5
t-value	-1.3	1.3	-1.0	0.0	1.7	0.7	-0.7	1.9	0.0	0.0	0.8	0.0
p-value	0.207	0.212	0.301	1.000	0.089	0.513	0.479	0.055	1.000	1.000	0.418	1.000
F-value	2.0	1.4	1.6	1.8	1.8	1.6	1.7	1.3	1.3	1.2	1.9	1.6
p-value	0.002	0.137	0.042	0.006	0.008	0.043	0.023	0.196	0.308	0.517	0.004	0.027

[MIN DAILY]

(oC)	J	F	M	A	M	J	J	A	S	O	N	D
Obs Mean	-0.8	0.9	2.0	4.1	6.9	9.7	11.2	11.3	8.7	5.4	2.3	-0.3
Obs stddev	4.8	3.8	3.2	3.0	3.0	2.5	2.3	2.4	2.9	3.4	4.0	4.6
LARS-WG Mean	-0.4	0.6	2.2	4.1	6.6	9.6	11.3	11.0	8.7	5.4	2.1	-0.2
LARS-WG stddev	4.7	3.9	3.2	2.9	2.9	2.5	2.2	2.5	2.9	3.4	4.0	4.7
t-value	-2.8	2.4	-2.0	0.0	3.4	1.3	-1.5	3.9	0.0	0.0	1.6	-0.7
p-value	0.005	0.015	0.041	1.000	0.001	0.202	0.144	0.000	1.000	1.000	0.104	0.486
F-value	1.1	1.0	1.0	1.0	1.1	1.1	1.1	1.1	1.0	1.0	1.0	1.1
p-value	0.275	0.741	0.658	0.750	0.261	0.209	0.098	0.142	0.990	0.777	0.809	0.282

[MAX MONTHLY]

(oC)	J	F	M	A	M	J	J	A	S	O	N	D
Obs Mean	5.5	8.6	11.1	14.1	17.7	20.4	23.3	23.8	20.8	15.0	9.2	5.9
Obs stddev	2.4	1.9	1.7	1.4	1.7	1.7	1.7	1.9	1.9	1.4	1.9	2.0
LARS-WG Mean	6.1	8.2	11.3	14.1	17.4	20.4	23.3	23.4	20.9	14.9	9.1	6.0
LARS-WG stddev	1.8	1.5	1.4	1.5	1.6	1.6	1.6	1.5	1.6	1.3	1.3	1.6
t-value	-1.9	1.6	-0.8	0.0	1.1	0.0	0.0	1.5	-0.4	0.4	0.4	-0.4
p-value	0.063	0.122	0.402	1.000	0.260	1.000	1.000	0.128	0.721	0.662	0.675	0.717
F-value	1.8	1.7	1.5	1.1	1.1	1.1	1.1	1.6	1.4	1.2	1.9	1.6
p-value	0.010	0.018	0.052	0.782	0.560	0.682	0.597	0.029	0.127	0.504	0.003	0.047

[MAX DAILY]

(oC)	J	F	M	A	M	J	J	A	S	O	N	D
Obs Mean	5.5	8.6	11.1	14.1	17.7	20.4	23.3	23.8	20.8	15.0	9.2	5.9
Obs stddev	4.5	3.8	3.7	4.0	4.5	4.3	4.4	4.3	4.4	3.9	3.8	4.4

Table 25 Output from LARS-WG for base case scenario: Solar Radiation statistics and tests of time series similarity between observed and modeled.

[MEAN MONTHLY]

(MJ/ (m2 day)	J	F	M	A	M	J	J	A	S	O	N	D
Obs Mean	4.9	8.3	13.4	19.0	23.8	25.5	26.3	22.6	17.0	9.3	5.5	4.2
Obs stddev	0.4	0.6	0.9	1.2	1.5	1.8	1.4	1.4	1.0	0.8	0.4	0.3
LARS-WG Mean	4.9	8.3	13.4	18.8	23.7	25.5	26.3	22.8	17.2	10.7	5.9	4.2
LARS-WG stddev	0.4	0.6	0.9	1.2	1.5	1.8	1.4	1.4	1.0	0.8	0.4	0.3

[MEAN DAILY]

(MJ/ (m2 day)	J	F	M	A	M	J	J	A	S	O	N	D
Obs Mean	4.9	8.3	13.4	19.0	23.8	25.5	26.3	22.6	17.0	10.5	5.8	4.2
Obs stddev	1.4	2.4	3.6	4.4	4.9	5.2	4.7	4.4	3.6	3.0	1.7	1.1
LARS-WG Mean	4.9	8.3	13.4	18.8	23.7	25.5	26.3	22.8	17.2	10.7	5.9	4.2
LARS-WG stddev	1.4	2.4	3.5	4.4	4.9	5.2	4.8	4.4	3.6	3.0	1.7	1.1

APPENDIX B

HELP- MODEL FOR RECHARGE ESTIMATES

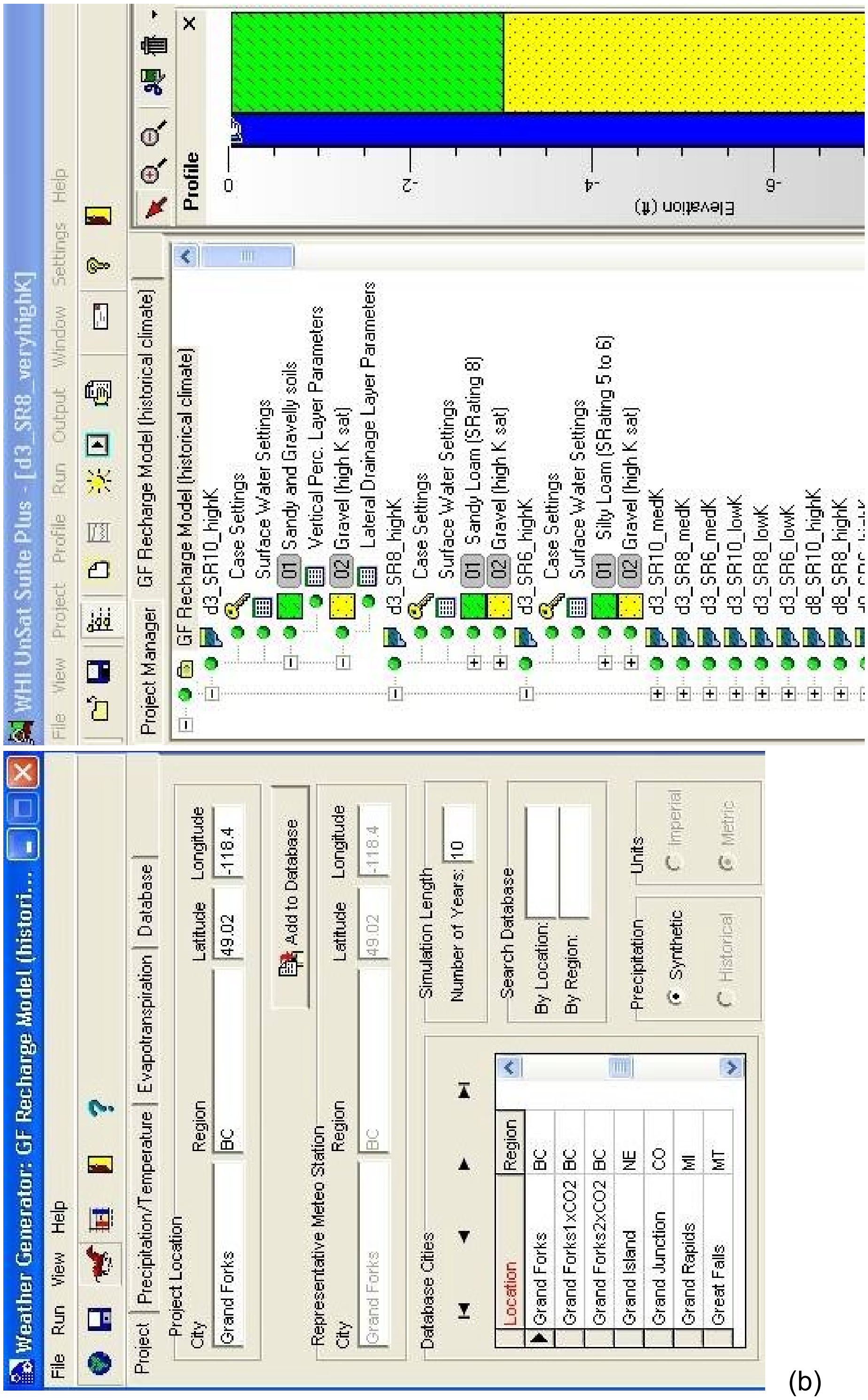

(a)

(b)

Figure 45 UnSat Suite interface: (a) soil columns and scenarios for HELP model; (b) weather generator for climate change scenarios.

Figure 46 Material designer interface in UnSat Suite.

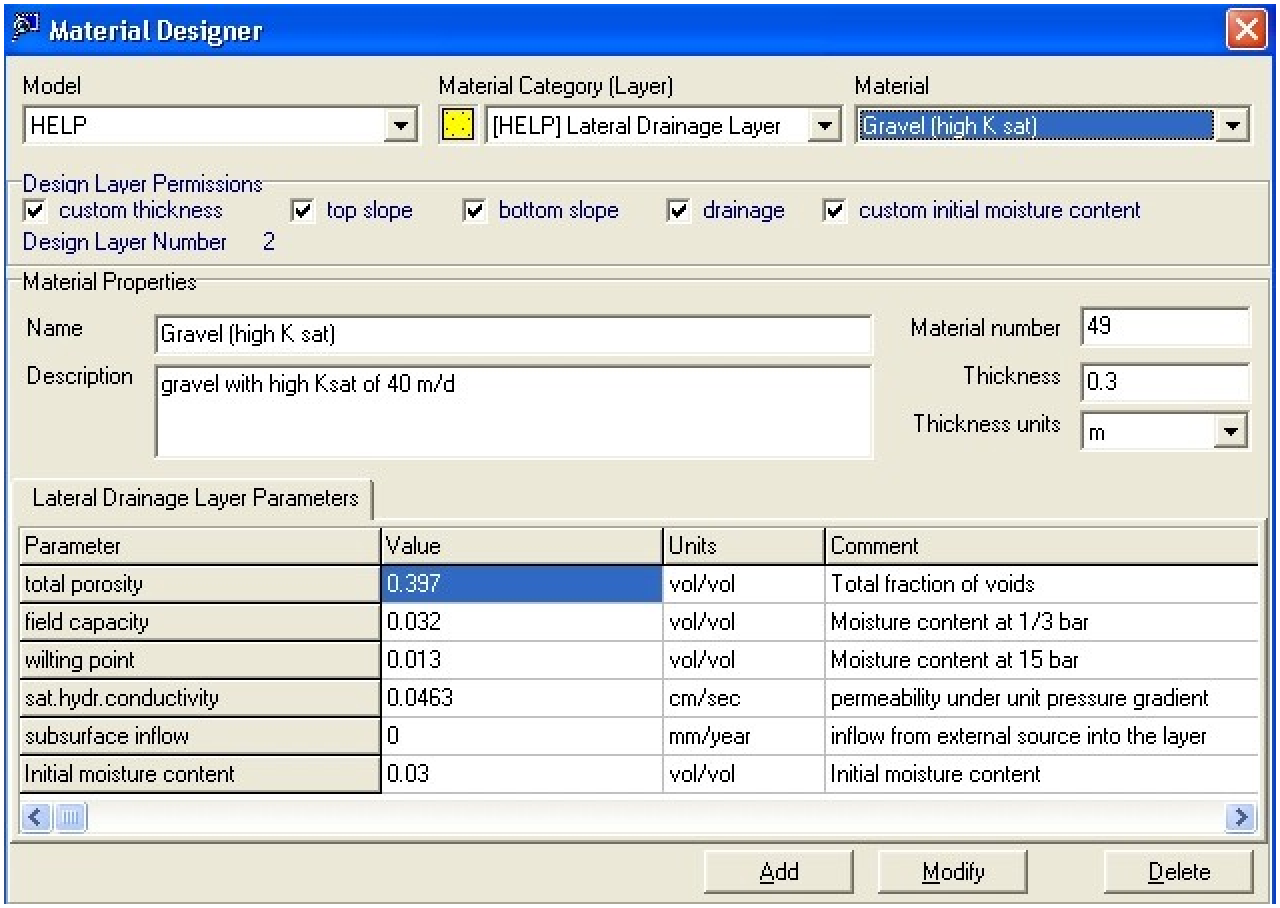

Table 26 HELP weather generator parameters used for modelling aquifer recharge in the Abbotsford aquifer: mean monthly temperature, rainfall, probabilities of rainfall, and gamma distribution parameters.

	Jan	Feb	Mar	Apr	May	Jun	Jul	Aug	Sep	Oct	Nov	Dec
Probability of RAIN on WET day	0.41	0.38	0.50	0.38	0.46	0.30	0.32	0.16	0.16	0.50	0.68	0.50
Probability of RAIN on DRY day	0.27	0.31	0.36	0.34	0.32	0.30	0.19	0.12	0.12	0.26	0.44	0.44
Specified Mean Monthly Rainfall (mm)	173.80	147.60	142.40	119.90	99.10	78.90	50.20	49.30	75.90	145.30	234.30	191.00
Specified Mean Monthly Temperature (oC)	2.60	4.70	6.80	9.50	12.50	15.10	17.50	17.70	15.00	10.20	5.70	2.80
Gamma Distribution Shape Parameter Alpha	0.600	0.600	0.600	0.600	0.600	0.600	0.600	0.600	0.600	0.600	0.600	0.600
Gamma Distribution Scale Parameter Beta	0.500	0.500	0.500	0.500	0.500	0.500	0.500	0.500	0.500	0.500	0.500	0.500

Table 27 HELP weather generator parameters used for modelling aquifer recharge in the Abbotsford aquifer: max and min temperature, solar radiation, growing season, evaporative zone depth, wind speed, humidity.

Mean Tmax (C)		Mean Tmin	Amplitude Tmax	Amplitude Tmin	Coefficient of variance Tmax	Amplitude of Coefficient of variance Tmax	Coefficient of variance Tmin	Amplitude of Coefficient of variance Tmin
Dry	Wet							
14.72	11.94	5.28	-3.61	-9.72	-17.69	-17.82	-17.67	-17.84
Mean Radiation	**Mean Radiation**	**Amplitude Radiation**	**Growing Season Start Day**	**Growing Season End Day**	**Default Max Leaf Area Index**	**Default Evaporative Zone Depth**		
Dry	Wet					Bare Soil	Grass	Excellent Stand of Grass
402	254	311	126	287	4.5	8	20	36
Mean Annual Wind Speed	**Quarterly Mean Relative Humidity**							
9.1	75	69	70	79				

Table 28 UnSat Suite HELP output for scenario (example of larger file):

DAILY OUTPUT FOR YEAR 1

DAY	AIR	SOIL	RAIN MM	RUNOFF MM	ET MM	E. ZONE WATER CM/CM	HEAD #1 CM	DRAIN #1 MM	LEAK #1 MM
1			0.0	0.00	0.67	0.1415	0.0000	.0000E+00	.9630
2			0.0	0.00	0.66	0.1399	0.0000	.0000E+00	.9599
3			0.0	0.00	0.67	0.1383	0.0000	.0000E+00	.9558
4			0.0	0.00	0.61	0.1368	0.0000	.0000E+00	.9350
5			0.0	0.00	0.65	0.1352	0.0000	.0000E+00	.9010
6			0.0	0.00	0.72	0.1335	0.0000	.0000E+00	.8603
7			0.0	0.00	0.68	0.1318	0.0000	.0000E+00	.8186
8			0.0	0.00	0.69	0.1301	0.0000	.0000E+00	.7792
9			0.0	0.00	0.69	0.1285	0.0000	.0000E+00	.7440

MONTHLY TOTALS (MM) FOR YEAR 1

	JAN/JUL	FEB/AUG	MAR/SEP	APR/OCT	MAY/NOV	JUN/DEC
PRECIPITATION	45.4	105.7	117.4	56.4	33.6	90.3
(a)	25.1	24.1	11.7	91.9	192.0	0.0
RUNOFF	0.00	0.00	0.00	0.00	0.00	0.00
	0.00	0.00	0.00	0.00	0.00	0.00
EVAPOTRANSPIRATION	21.33	23.74	48.35	72.71	35.86	93.52
	27.06	31.61	19.50	38.72	23.78	19.66
PERCOLATION/LEAKAGE THROUGH	20.860	11.586	76.150	55.461	20.636	11.081
LAYER 2	7.969	6.555	4.480	3.430	59.508	60.926

ANNUAL TOTALS FOR YEAR 1

	MM	CU. METERS	PERCENT
PRECIPITATION	793.60	3211.585	100.00
RUNOFF	0.000	0.000	0.00
EVAPOTRANSPIRATION	455.843	1844.731	57.44
PERC./LEAKAGE THROUGH LAYER 2	338.642554	1370.438	42.67
CHANGE IN WATER STORAGE	-0.886	-3.584	-0.11
SOIL WATER AT START OF YEAR	317.385	1284.413	
SOIL WATER AT END OF YEAR	316.500	1280.830	

Figure 47 Comparing probability of rain on wet and dry days (monthly averages) for Abbotsford, BC and Seattle, WA – calibrated weather generator in UnSat Suite to observed temperature and precipitation 30 year daily time series 1976–1996.

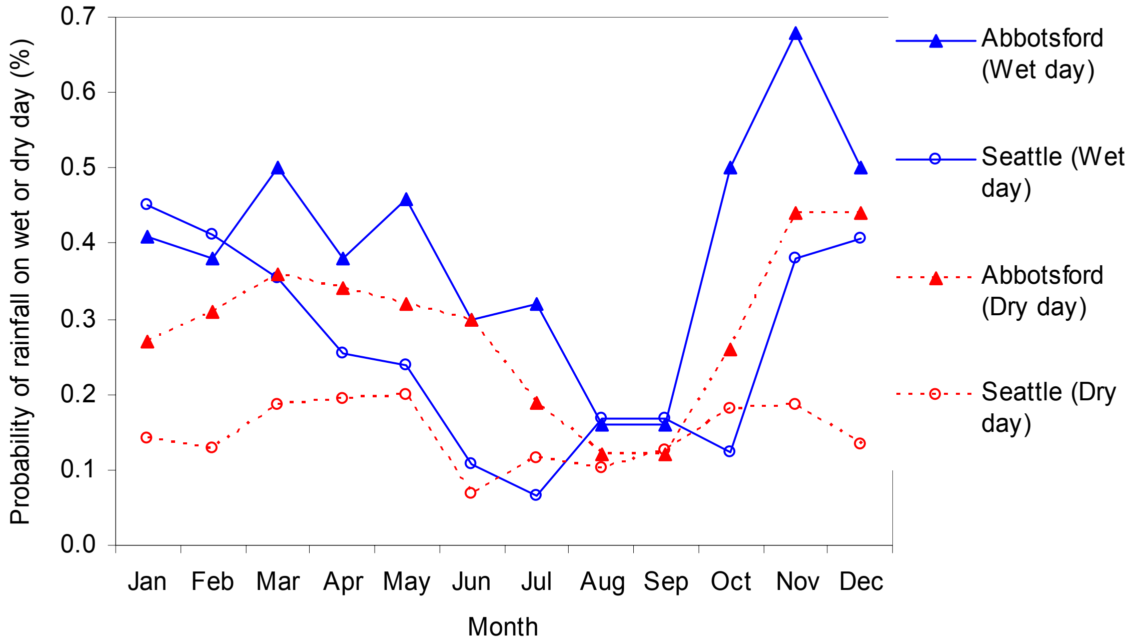

APPENDIX C

RESULTS OF RECHARGE MODELING UNDER DIFFERENT CLIMATE SCENARIOS

Table 29 HELP recharge model zones for soil columns and physical parameters.

Scenario	Scenario	Depth of column	Soil Type	Ksat	Other tests					
(number)	(name)	(depth to water table)	(S rating of soil; permeability)	(of vadose zone)	soil depth	initial soil moisture	porosity	field capacity	wilting point	grass stand
		(m)	(10 to 6)	(m/d)	(m)	(vol/vol)	(vol/vol)	(vol/vol)	(vol/vol)	
1	d3_SR10_veryhighK	3	10	veryhigh	1	0.03	0.397	0.032	0.013	good
2	d3_SR10_highK	3	10	high	1	0.03	0.397	0.032	0.013	good
3	d3_SR10_medK	3	10	med	1	0.03	0.397	0.032	0.013	good
4	d3_SR10_lowK	3	10	low	1	0.03	0.397	0.032	0.013	good
5	d3_SR9_veryhighK	3	9	veryhigh	1	0.03	0.397	0.032	0.013	good
6	d3_SR9_highK	3	9	high	1	0.03	0.397	0.032	0.013	good
7	d3_SR9_medK	3	9	med	1	0.03	0.397	0.032	0.013	good
8	d3_SR9_lowK	3	9	low	1	0.03	0.397	0.032	0.013	good
9	d3_SR8_veryhighK	3	8	veryhigh	1	0.03	0.397	0.032	0.013	good
10	d3_SR8_highK	3	8	high	1	0.03	0.397	0.032	0.013	good
11	d3_SR8_medK	3	8	med	1	0.03	0.397	0.032	0.013	good
12	d3_SR8_lowK	3	8	low	1	0.03	0.397	0.032	0.013	good
13	d3_SR6_veryhighK	3	6	veryhigh	1	0.03	0.397	0.032	0.013	good
14	d3_SR6_highK	3	6	high	1	0.03	0.397	0.032	0.013	good
15	d3_SR6_medK	3	6	med	1	0.03	0.397	0.032	0.013	good
16	d3_SR6_lowK	3	6	low	1	0.03	0.397	0.032	0.013	good
17	d8_SR10_veryhighK	8	10	veryhigh	1	0.03	0.397	0.032	0.013	good
18	d8_SR10_highK	8	10	high	1	0.03	0.397	0.032	0.013	good
19	d8_SR10_medK	8	10	med	1	0.03	0.397	0.032	0.013	good
20	d8_SR10_lowK	8	10	low	1	0.03	0.397	0.032	0.013	good
21	d8_SR9_veryhighK	8	9	veryhigh	1	0.03	0.397	0.032	0.013	good
22	d8_SR9_highK	8	9	high	1	0.03	0.397	0.032	0.013	good
23	d8_SR9_medK	8	9	med	1	0.03	0.397	0.032	0.013	good
24	d8_SR9_lowK	8	9	low	1	0.03	0.397	0.032	0.013	good
25	d8_SR8_veryhighK	8	8	veryhigh	1	0.03	0.397	0.032	0.013	good
26	d8_SR8_highK	8	8	high	1	0.03	0.397	0.032	0.013	good
27	d8_SR8_medK	8	8	med	1	0.03	0.397	0.032	0.013	good
28	d8_SR8_lowK	8	8	low	1	0.03	0.397	0.032	0.013	good
29	d8_SR6_veryhighK	8	6	veryhigh	1	0.03	0.397	0.032	0.013	good
30	d8_SR6_highK	8	6	high	1	0.03	0.397	0.032	0.013	good
31	d8_SR6_medK	8	6	med	1	0.03	0.397	0.032	0.013	good
32	d8_SR6_lowK	8	6	low	1	0.03	0.397	0.032	0.013	good
33	d11_SR10_veryhighK	11	10	veryhigh	1	0.03	0.397	0.032	0.013	good
34	d11_SR10_highK	11	10	high	1	0.03	0.397	0.032	0.013	good
35	d11_SR10_medK	11	10	med	1	0.03	0.397	0.032	0.013	good
36	d11_SR10_lowK	11	10	low	1	0.03	0.397	0.032	0.013	good
37	d11_SR9_veryhighK	11	9	veryhigh	1	0.03	0.397	0.032	0.013	good
38	d11_SR9_highK	11	9	high	1	0.03	0.397	0.032	0.013	good
39	d11_SR9_medK	11	9	med	1	0.03	0.397	0.032	0.013	good
40	d11_SR9_lowK	11	9	low	1	0.03	0.397	0.032	0.013	good
41	d11_SR8_veryhighK	11	8	veryhigh	1	0.03	0.397	0.032	0.013	good
42	d11_SR8_highK	11	8	high	1	0.03	0.397	0.032	0.013	good
43	d11_SR8_medK	11	8	med	1	0.03	0.397	0.032	0.013	good
44	d11_SR8_lowK	11	8	low	1	0.03	0.397	0.032	0.013	good
45	d11_SR6_veryhighK	11	6	veryhigh	1	0.03	0.397	0.032	0.013	good
46	d11_SR6_highK	11	6	high	1	0.03	0.397	0.032	0.013	good
47	d11_SR6_medK	11	6	med	1	0.03	0.397	0.032	0.013	good
48	d11_SR6_lowK	11	6	low	1	0.03	0.397	0.032	0.013	good
49	d25_SR10_veryhighK	25	10	veryhigh	1	0.03	0.397	0.032	0.013	good
50	d25_SR10_highK	25	10	high	1	0.03	0.397	0.032	0.013	good
51	d25_SR10_medK	25	10	med	1	0.03	0.397	0.032	0.013	good
52	d25_SR10_lowK	25	10	low	1	0.03	0.397	0.032	0.013	good
53	d25_SR9_veryhighK	25	9	veryhigh	1	0.03	0.397	0.032	0.013	good
54	d25_SR9_highK	25	9	high	1	0.03	0.397	0.032	0.013	good
55	d25_SR9_medK	25	9	med	1	0.03	0.397	0.032	0.013	good
56	d25_SR9_lowK	25	9	low	1	0.03	0.397	0.032	0.013	good
57	d25_SR8_veryhighK	25	8	veryhigh	1	0.03	0.397	0.032	0.013	good
58	d25_SR8_highK	25	8	high	1	0.03	0.397	0.032	0.013	good
59	d25_SR8_medK	25	8	med	1	0.03	0.397	0.032	0.013	good
60	d25_SR8_lowK	25	8	low	1	0.03	0.397	0.032	0.013	good
61	d25_SR6_veryhighK	25	6	veryhigh	1	0.03	0.397	0.032	0.013	good
62	d25_SR6_highK	25	6	high	1	0.03	0.397	0.032	0.013	good
63	d25_SR6_medK	25	6	med	1	0.03	0.397	0.032	0.013	good
64	d25_SR6_lowK	25	6	low	1	0.03	0.397	0.032	0.013	good

Table 30 HELP recharge model zones for soil columns and physical parameters: sensitivity analysis to secondary soil properties.

Scenario	Scenario	Depth of column	Soil Type	Ksat	Other tests					
(number)	(name)	(depth to water table)	(S rating of soil; permeability)	(of vadose zone)	soil depth	initial soil moisture	porosity	field capacity	wilting point	grass stand
		(m)	(10 to 6)	(m/d)	(m)	(vol/vol)	(vol/vol)	(vol/vol)	(vol/vol)	
65	d3_thicksoil	3	8	med	1.5	0.03	0.397	0.032	0.013	good
66	d3_thinsoil	3	8	med	0.5	0.03	0.397	0.032	0.013	good
67	d3_verythinsoil	3	8	med	0.2	0.03	0.397	0.032	0.013	good
68	d3_highmoist	3	8	med	1	0.12	0.397	0.032	0.013	good
69	d3_modmoist	3	8	med	1	0.1	0.397	0.032	0.013	good
70	d3_lowmoist	3	8	med	1	0.08	0.397	0.032	0.013	good
71	d3_medporosity	3	8	med	1	0.03	0.32	0.032	0.013	good
72	d3_lowporosity	3	8	med	1	0.03	0.25	0.032	0.013	good
73	d3_highFC	3	8	med	1	0.03	0.397	0.038	0.013	good
74	d3_lowFC	3	8	med	1	0.03	0.397	0.028	0.013	good
75	d3_highWP	3	8	med	1	0.03	0.397	0.032	0.015	good
76	d3_lowWP	3	8	med	1	0.03	0.397	0.032	0.01	good
77	d3_poorstandgrass	3	8	med	1	0.03	0.397	0.032	0.013	bare
78	d3_excelstandgrass	3	8	med	1	0.03	0.397	0.032	0.013	excellent
79	d3_highmoist_highKsat	3	8	high	1	0.12	0.397	0.032	0.013	good
80	d3_modmoist_highKsat	3	8	high	1	0.1	0.397	0.032	0.013	good
81	d3_lowmoist_highKsat	3	8	high	1	0.08	0.397	0.032	0.013	good
82	d3_thicksoil_highKsat	3	8	high	1.5	0.03	0.397	0.032	0.013	good
83	d3_thinsoil_highKsat	3	8	high	0.5	0.03	0.397	0.032	0.013	good
84	d3_verythinsoil_highKsat	3	8	high	0.2	0.03	0.397	0.032	0.013	good
85	d3_thicksoil_highKsat_SR10	3	10	high	1.5	0.03	0.397	0.032	0.013	good
86	d3_thinsoil_highKsat_SR10	3	10	high	0.5	0.03	0.397	0.032	0.013	good
87	d3_verythinsoil_highKsat_SR10	3	10	high	0.2	0.03	0.397	0.032	0.013	good

Table 31 HELP model recharge monthly output for base case climate (1961-1999), listed by HELP recharge zone.

				Average Recharge (mm / month)								
Recharge Zone	Jan	Feb	Mar	Apr	May	Jun	Jul	Aug	Sep	Oct	Nov	Dec
1	193.0	151.7	114.9	64.5	31.3	21.0	14.4	9.4	8.2	47.7	180.6	203.6
2	193.2	152.6	116.2	66.8	33.0	21.8	15.3	10.3	8.5	42.1	176.8	203.8
3	194.5	154.5	119.4	72.1	37.5	23.7	17.8	12.2	9.4	30.4	164.8	204.1
4	195.6	156.0	123.1	76.9	41.8	25.8	20.1	14.0	10.6	23.2	149.1	204.4
5	193.4	151.1	114.8	64.7	32.2	21.3	14.9	9.4	7.8	40.0	177.7	203.6
6	193.8	151.9	116.1	66.9	33.9	22.1	16.0	10.2	8.1	35.0	173.3	203.6
7	194.5	153.9	119.3	72.1	38.3	24.2	18.4	12.2	9.3	25.5	159.3	203.9
8	195.5	155.6	122.8	76.9	42.5	26.3	20.6	14.2	10.4	20.0	141.9	204.2
9	193.5	151.2	114.3	64.3	29.6	14.7	10.1	6.7	5.5	29.2	171.2	203.2
10	194.2	151.7	115.8	66.6	31.7	16.0	10.9	7.5	5.8	24.7	165.6	203.0
11	194.7	153.9	119.0	72.2	36.6	19.2	13.2	9.5	7.0	17.5	147.4	203.3
12	195.5	155.6	122.7	76.9	41.0	22.5	15.6	11.3	8.4	13.5	127.4	203.2
13	194.4	151.3	115.8	66.4	31.0	13.8	8.0	4.2	2.6	23.4	165.9	203.4
14	194.9	151.9	117.2	68.6	33.2	15.6	9.2	5.2	3.1	19.3	158.5	203.3
15	195.8	153.9	120.3	74.0	38.5	19.6	12.2	7.8	5.0	12.3	137.5	203.4
16	196.6	155.6	123.6	78.7	43.1	23.5	15.0	10.1	6.8	9.1	115.6	202.7
17	195.8	157.3	125.3	80.1	44.5	27.5	21.4	15.5	11.5	20.2	137.3	204.2
18	197.1	159.2	129.8	86.0	49.9	30.8	24.2	18.0	13.4	16.2	113.2	202.7
19	199.3	164.4	140.3	98.6	63.1	39.5	31.3	24.1	18.6	15.5	60.4	185.3
20	195.1	168.4	149.5	108.5	74.9	48.2	38.3	29.9	23.5	19.5	31.3	150.4
21	197.0	158.7	129.3	85.7	50.6	31.2	24.9	18.1	13.7	14.8	105.2	201.6
22	194.2	151.7	115.8	66.6	31.7	16.0	10.9	7.5	5.8	24.7	165.6	203.0
23	199.2	163.7	139.4	98.2	63.7	40.0	31.9	24.4	18.8	16.0	54.4	181.2
24	193.4	167.3	149.2	107.6	75.2	48.6	38.3	30.1	23.6	20.0	28.8	142.6
25	198.0	163.0	137.1	96.2	61.2	37.5	26.8	20.6	15.8	12.8	48.8	175.9
26	197.2	158.7	129.1	85.8	49.8	29.0	20.2	15.2	11.6	11.2	87.7	198.1
27	198.8	163.7	139.1	98.4	63.3	39.5	28.1	21.4	16.6	14.4	40.7	169.5
28	191.5	167.5	147.9	108.4	75.3	49.3	35.8	27.4	21.4	18.6	21.6	126.0
29	197.2	156.5	125.7	81.7	46.2	25.7	16.7	11.4	7.8	8.4	102.0	201.0
30	194.2	167.1	144.9	105.6	73.1	47.4	33.6	25.1	18.6	14.3	22.1	134.5
31	198.9	164.3	139.5	99.5	65.4	41.6	28.9	21.2	15.8	12.7	32.4	160.2
32	188.9	168.4	147.9	109.1	77.2	51.6	37.1	27.7	21.1	17.3	17.6	113.3
33	194.7	168.9	148.1	107.9	73.2	47.2	37.4	29.5	22.5	16.2	38.9	156.1
34	182.1	171.4	157.2	118.1	85.1	56.3	45.0	35.9	27.8	20.0	23.3	118.1
35	130.0	156.2	168.6	136.1	109.3	76.8	62.9	51.2	40.8	30.5	16.2	55.3
36	194.0	154.0	118.2	70.0	35.8	22.9	16.8	11.4	9.0	34.6	169.9	203.8
37	194.1	167.9	146.7	107.1	73.6	47.6	38.2	29.7	23.2	17.1	34.8	151.1
38	180.7	170.2	155.6	117.2	85.3	56.6	45.8	36.1	28.5	21.2	21.0	112.3
39	127.0	154.5	166.3	135.0	109.1	76.9	63.3	51.5	41.3	32.2	15.8	51.2
40	194.3	153.3	118.1	70.2	36.6	23.3	17.5	11.4	8.9	28.8	165.0	203.7
41	192.1	167.5	146.5	107.3	74.1	47.6	34.8	27.1	21.0	16.2	24.7	135.1
42	174.7	169.0	155.2	117.4	86.1	57.5	42.8	33.6	26.3	20.6	15.6	94.4
43	114.4	149.5	164.0	134.6	110.2	79.1	61.5	49.2	39.2	31.7	14.8	38.7
44	194.6	153.1	117.7	70.1	34.7	17.9	12.3	8.8	6.6	19.8	154.7	203.1
45	190.4	167.9	147.1	108.3	76.5	49.9	35.6	26.8	19.9	14.7	19.4	124.0
46	170.4	168.9	155.5	118.1	88.3	60.1	44.1	33.7	25.5	19.3	12.9	83.0
47	105.3	146.7	163.0	134.5	111.9	81.8	63.4	50.0	39.2	31.1	14.4	32.2
48	195.4	153.3	119.1	72.1	36.5	17.9	10.9	6.7	4.1	14.8	146.0	203.5
49	140.3	160.6	166.3	134.6	105.1	73.0	59.7	48.5	37.8	25.6	16.2	70.3
50	107.9	139.8	164.7	142.4	119.0	86.0	71.7	59.2	47.0	32.6	15.7	47.3
51	153.9	130.9	118.9	85.7	63.3	48.8	38.1	29.7	24.7	40.6	132.5	147.1
52	194.1	153.9	118.2	70.1	35.8	22.9	16.9	11.4	9.1	34.6	169.7	204.0
53	138.3	159.0	163.7	133.1	105.0	73.2	60.4	48.7	38.8	27.3	15.0	65.8
54	105.0	138.1	162.0	140.8	118.6	86.0	72.2	59.4	47.9	34.7	15.1	43.8
55	193.8	152.0	116.1	67.1	34.0	22.1	15.9	10.2	8.1	35.0	173.2	203.5
56	194.3	153.3	118.0	70.2	36.6	23.3	17.5	11.4	8.9	28.7	164.9	203.8
57	127.7	154.4	162.1	132.8	106.3	75.0	58.0	46.5	36.7	27.4	12.1	51.7
58	93.4	131.2	158.6	139.6	119.9	88.5	70.4	57.3	45.9	35.0	13.4	33.3
59	127.0	118.9	118.2	96.6	81.5	60.7	49.5	40.2	33.3	34.4	98.5	109.0
60	194.6	153.2	117.7	70.1	34.7	17.9	12.3	8.8	6.6	19.7	154.7	203.1
61	120.0	152.1	162.0	133.2	108.6	78.0	59.6	46.9	36.1	26.4	10.8	43.8
62	85.4	127.5	156.9	139.2	121.7	91.5	72.4	58.1	45.6	34.5	12.7	27.8
63	195.1	151.9	117.3	68.8	33.3	15.4	9.1	5.2	3.1	19.4	158.4	203.3
64	195.4	153.2	119.1	72.2	36.5	17.9	10.9	6.7	4.1	14.8	146.1	203.4
65	198.1	158.0	129.1	86.4	49.3	29.8	20.7	15.1	11.7	10.8	86.2	198.3
66	196.8	158.7	128.2	84.6	48.8	28.0	19.9	14.6	10.8	10.8	93.5	198.8
67	197.0	159.6	129.5	85.9	48.3	27.5	20.4	16.2	12.0	13.9	104.9	201.5
68	195.9	157.9	129.0	85.7	49.4	28.9	20.1	15.0	11.4	11.3	88.2	198.8
69	195.9	157.9	128.6	85.7	49.4	28.9	20.1	15.0	11.4	11.3	88.2	198.8
70	195.9	157.8	128.3	85.7	49.4	28.9	20.1	15.0	11.4	11.3	88.2	198.8
71	196.3	156.9	125.5	80.8	44.7	25.2	17.4	12.9	9.7	11.9	110.2	202.0
72	195.6	155.3	122.0	76.1	40.4	22.0	15.1	11.1	8.2	14.1	130.8	203.0
73	197.4	158.5	129.1	85.7	49.3	28.7	19.9	14.8	11.2	11.2	88.8	199.0
74	197.4	158.4	128.9	85.5	49.2	28.8	20.0	14.9	11.4	11.3	88.8	198.9
75	197.3	158.3	128.7	85.3	49.1	28.8	20.0	14.9	11.4	11.4	89.4	199.1
76	197.5	158.6	129.3	85.9	49.3	28.8	19.9	14.8	11.2	11.1	88.4	198.9
77	197.4	158.5	129.0	85.6	49.3	28.8	20.0	14.9	11.3	11.3	88.7	198.9
78	197.4	158.5	129.0	85.6	49.3	28.8	20.0	14.9	11.3	11.3	88.7	198.9
79	195.0	155.1	122.0	76.2	40.4	22.0	15.1	11.1	8.3	14.1	130.7	203.0
80	194.6	155.1	122.0	76.2	40.4	22.0	15.1	11.1	8.3	14.1	130.7	203.0
81	194.3	154.9	122.0	76.2	40.4	22.0	15.1	11.1	8.3	14.1	130.7	203.0
82	196.2	156.0	124.3	79.4	43.3	24.5	17.0	12.5	9.4	12.0	116.3	202.7
83	195.3	154.3	119.9	73.4	37.7	19.9	14.1	9.7	7.0	16.6	142.8	203.0
84	194.9	154.7	119.5	72.3	35.7	19.9	15.7	11.0	8.4	28.6	160.1	203.7
85	195.8	156.3	124.0	77.9	42.9	26.3	20.8	14.5	10.9	21.9	144.9	204.4
86	194.9	155.8	121.2	74.7	39.5	24.8	18.5	13.4	9.8	27.1	156.5	204.4
87	194.8	155.5	120.5	73.8	38.5	24.4	18.2	12.8	9.6	32.4	161.8	204.2

Table 32 HELP model recharge monthly output for future climate (2010-2039), listed by HELP recharge zone.

				Average Recharge (mm / month)								
Recharge Zone	Jan	Feb	Mar	Apr	May	Jun	Jul	Aug	Sep	Oct	Nov	Dec
1	165.1	136.7	98.7	61.1	35.3	17.8	13.4	9.2	9.0	59.9	172.2	201.8
2	165.6	137.2	100.6	62.8	36.8	19.4	14.0	10.0	8.9	54.0	168.8	202.4
3	167.4	137.8	105.2	67.0	40.6	22.9	15.8	12.0	9.1	40.5	159.4	203.0
4	169.4	138.8	109.6	70.8	44.4	26.0	17.7	13.8	10.3	29.6	147.4	203.2
5	165.3	136.1	98.7	61.5	35.9	18.6	13.7	9.5	7.8	51.4	170.6	201.6
6	165.5	136.6	100.6	63.1	37.3	20.1	14.4	10.2	7.9	45.7	166.8	202.3
7	167.3	137.5	105.1	67.3	41.1	23.5	16.2	12.2	9.1	32.9	155.8	203.0
8	169.1	138.4	109.4	71.1	44.9	26.5	18.2	14.0	10.5	24.1	141.5	203.5
9	165.5	136.1	98.5	60.0	32.5	15.3	8.8	6.7	5.4	38.8	165.5	200.9
10	165.8	136.6	100.4	61.7	34.4	16.9	9.7	7.4	5.9	33.1	160.5	201.8
11	167.1	137.8	105.0	66.0	38.9	20.5	12.6	8.9	7.1	22.2	145.7	202.4
12	168.9	138.8	109.4	70.0	42.8	24.0	15.5	10.5	8.4	16.6	127.2	202.6
13	166.0	135.8	100.4	62.0	33.8	15.1	6.5	4.1	2.9	31.5	160.6	201.7
14	166.5	136.2	102.5	63.7	35.7	17.2	8.0	4.9	3.5	25.8	154.4	202.2
15	167.9	137.8	106.8	68.0	40.2	21.6	11.8	7.0	5.0	16.5	136.3	202.0
16	169.4	139.2	111.0	71.8	44.1	25.4	15.3	9.0	6.7	12.0	115.6	201.6
17	170.6	139.9	112.2	72.9	46.7	28.3	18.9	15.2	10.9	25.4	136.6	203.5
18	173.0	141.9	117.4	77.4	51.3	32.3	21.9	17.5	12.8	19.1	114.3	202.5
19	178.0	146.7	128.9	87.9	62.1	41.9	29.7	23.2	18.0	15.4	61.8	188.4
20	176.8	149.8	137.5	97.1	71.8	50.6	37.4	28.8	23.0	18.3	33.2	153.8
21	172.5	141.5	117.0	77.6	51.9	32.7	22.6	17.6	13.5	16.7	105.8	202.3
22	165.8	136.6	100.4	61.7	34.4	16.9	9.7	7.4	5.9	33.1	160.5	201.8
23	177.3	146.1	128.3	88.0	62.6	42.2	30.4	23.4	18.7	15.4	54.5	185.3
24	175.5	149.2	136.3	96.1	71.5	50.7	38.0	29.0	23.6	19.1	29.4	147.6
25	175.3	145.3	126.1	86.1	59.8	39.1	27.1	20.0	15.8	12.1	48.5	180.3
26	172.1	141.7	117.0	77.1	50.2	30.7	20.4	14.5	11.6	12.2	87.8	200.0
27	176.0	146.4	128.2	88.0	61.3	40.9	29.1	20.6	16.6	14.0	40.5	173.9
28	172.2	149.2	136.2	96.5	70.3	49.8	37.0	26.7	21.4	18.2	21.7	129.6
29	170.5	140.2	113.3	74.2	46.8	28.1	16.6	10.7	7.7	10.5	101.8	200.9
30	174.0	148.5	134.3	95.3	69.3	49.0	34.6	24.5	18.5	13.8	23.0	137.2
31	175.5	147.2	128.6	89.5	62.6	43.1	30.3	20.5	15.6	12.7	32.7	163.5
32	170.1	149.9	136.3	97.6	71.6	52.0	38.8	27.3	20.9	17.3	18.1	115.7
33	178.8	149.1	136.9	96.3	70.8	49.6	35.5	28.7	21.6	15.7	40.5	158.6
34	171.7	150.6	145.5	105.9	80.8	58.5	43.3	34.9	26.8	18.7	24.7	120.1
35	128.8	139.0	153.8	123.5	101.2	77.9	61.2	49.8	39.6	28.2	16.0	56.0
36	167.0	137.6	103.4	65.4	39.1	21.6	14.9	11.3	8.9	45.8	162.9	202.7
37	177.1	148.5	135.9	96.1	71.2	50.0	36.3	28.9	22.6	15.9	35.5	154.4
38	169.0	149.9	144.4	105.6	81.0	58.8	44.0	35.1	27.9	19.5	21.7	114.7
39	124.5	137.3	152.4	123.0	101.2	77.9	61.9	50.0	40.7	29.6	15.3	51.7
40	166.6	137.3	103.5	65.6	39.7	22.3	15.3	11.5	8.5	37.6	160.3	202.7
41	173.7	148.4	135.8	96.5	70.7	48.8	35.2	26.5	21.0	14.9	25.1	139.1
42	162.2	148.8	144.0	106.2	81.0	58.1	43.4	32.9	26.3	19.1	15.7	97.5
43	111.8	132.1	150.1	123.4	101.9	78.1	62.0	48.2	39.1	29.9	13.8	39.4
44	166.8	137.3	103.5	64.3	37.1	19.0	11.3	8.5	6.7	25.8	151.8	202.0
45	172.1	148.7	136.5	97.9	72.2	51.6	36.4	26.3	19.7	14.0	20.4	126.3
46	157.3	148.7	144.3	107.4	82.4	60.9	45.1	33.2	25.4	18.4	13.2	85.1
47	103.0	128.9	148.5	123.6	102.8	80.6	64.4	49.3	38.9	29.9	13.4	32.8
48	167.5	137.3	105.2	66.4	38.5	19.9	9.8	6.2	4.3	19.7	143.9	202.1
49	137.9	142.0	153.5	121.0	98.3	74.6	57.3	47.2	36.5	23.7	16.5	70.8
50	108.2	125.7	151.1	128.6	109.9	86.7	69.1	57.5	45.4	30.1	15.5	47.2
51	165.6	137.3	100.7	62.9	36.8	19.3	13.9	10.1	8.9	54.0	168.3	202.7
52	166.8	137.6	103.6	65.3	39.2	21.6	14.9	11.3	8.9	45.7	162.9	202.8
53	134.2	140.5	151.8	120.2	98.2	74.8	58.1	47.5	37.9	24.8	14.8	66.7
54	104.3	123.6	149.2	127.7	109.6	86.6	69.8	57.7	46.8	31.5	14.5	43.8
55	95.2	94.6	115.2	108.3	97.2	78.5	65.7	55.5	46.7	46.3	65.5	77.6
56	166.6	137.3	103.5	65.6	39.7	22.3	15.3	11.5	8.5	37.5	160.4	202.7
57	123.1	136.2	150.1	120.9	98.7	74.5	58.0	45.6	36.5	24.9	11.7	52.9
58	92.2	117.0	145.5	127.7	110.1	86.7	70.0	56.0	45.5	32.0	12.7	33.5
59	144.7	124.3	101.8	69.3	46.9	30.0	22.3	18.0	15.0	33.1	134.4	170.1
60	166.7	137.4	103.4	64.4	37.1	19.1	11.3	8.5	6.7	25.8	151.8	202.1
61	115.5	133.6	149.4	121.6	100.1	77.7	60.0	46.1	35.8	24.6	10.5	44.4
62	84.2	113.0	143.2	127.6	111.0	89.6	72.4	56.9	45.1	32.1	12.1	27.9
63	166.8	136.4	102.7	63.8	35.7	17.0	7.7	4.9	3.4	26.1	154.3	202.0
64	167.7	137.2	105.3	66.4	38.5	19.9	9.8	6.2	4.3	19.6	144.1	201.9
65	171.9	142.4	117.0	77.6	49.6	31.1	21.1	14.9	11.3	11.9	85.7	200.8
66	172.3	142.0	115.9	76.1	49.5	29.7	19.4	14.3	10.6	12.2	93.5	199.9
67	173.5	142.1	117.4	76.8	49.0	29.2	19.5	16.1	11.6	16.8	105.0	201.9
68	169.5	141.2	116.8	77.0	49.8	30.5	20.5	14.1	11.4	12.4	87.9	200.8
69	169.4	141.2	116.5	77.0	49.8	30.5	20.5	14.1	11.4	12.4	87.9	200.8
70	169.4	141.1	116.2	76.9	49.8	30.5	20.5	14.1	11.4	12.4	87.9	200.8
71	170.2	140.0	112.7	73.0	45.9	26.9	17.5	12.1	9.8	14.1	110.4	202.4
72	168.5	138.7	108.6	69.2	42.2	23.5	14.7	10.5	8.3	17.4	130.3	202.6
73	172.0	141.9	117.0	77.0	49.7	30.3	20.3	13.9	11.2	12.4	88.6	200.9
74	171.9	141.7	116.8	76.9	49.7	30.4	20.5	14.1	11.4	12.5	88.6	200.9
75	171.7	141.6	116.5	76.7	49.6	30.3	20.5	14.1	11.4	12.6	89.2	201.0
76	172.1	142.0	117.2	77.1	49.8	30.4	20.3	13.9	11.2	12.3	88.1	200.9
77	171.9	141.8	116.9	76.9	49.7	30.4	20.5	14.0	11.3	12.4	88.5	200.9
78	171.9	141.8	116.9	76.9	49.7	30.4	20.5	14.0	11.3	12.4	88.5	200.9
79	167.4	138.5	108.6	69.2	42.2	23.5	14.7	10.5	8.3	17.4	130.3	202.6
80	167.0	138.4	108.6	69.2	42.2	23.5	14.7	10.5	8.3	17.4	130.3	202.6
81	166.7	138.3	108.6	69.2	42.2	23.5	14.7	10.5	8.3	17.4	130.3	202.6
82	169.6	139.5	111.5	72.0	44.6	26.0	17.1	11.8	9.2	14.6	116.6	202.3
83	168.0	138.4	106.0	67.0	39.8	21.3	12.8	9.6	6.9	21.4	141.3	202.1
84	168.0	138.3	105.7	65.9	38.2	20.6	14.5	10.9	8.8	38.3	154.6	203.1
85	169.6	139.3	110.5	71.6	45.3	26.9	18.3	14.3	10.7	27.4	144.0	203.2
86	168.7	138.9	107.2	68.7	42.5	24.4	16.4	13.2	9.3	36.1	152.1	203.5
87	168.4	138.7	106.8	67.8	41.8	23.2	16.7	12.5	10.0	42.6	155.7	203.5

Table 33 HELP model recharge monthly output for future climate (2040-2069), listed by HELP recharge zone.

			Average Recharge (mm / month)									
Recharge Zone	Jan	Feb	Mar	Apr	May	Jun	Jul	Aug	Sep	Oct	Nov	Dec
1	160.0	116.3	90.3	49.6	30.2	18.3	12.5	9.2	8.5	52.6	161.7	197.1
2	160.7	117.1	92.0	51.1	31.7	19.3	13.3	9.8	8.6	47.2	158.1	197.4
3	162.6	119.3	95.6	55.1	35.3	21.9	15.6	11.4	9.1	35.1	147.4	197.9
4	164.0	121.6	98.8	59.4	38.4	24.3	18.0	12.9	10.2	26.3	134.0	198.2
5	159.5	116.0	90.4	50.3	30.8	18.6	12.7	9.1	7.5	45.1	159.4	197.6
6	160.3	116.8	92.1	51.7	32.3	19.7	13.5	9.7	7.8	39.9	155.1	198.0
7	162.6	118.9	95.8	55.4	35.9	22.4	15.9	11.4	8.7	29.4	142.5	198.0
8	163.9	121.3	99.1	59.4	39.0	24.9	18.4	13.0	10.0	22.1	128.2	197.4
9	159.7	115.9	90.5	49.0	25.8	13.4	8.8	6.0	4.5	33.4	152.1	197.2
10	160.3	117.0	91.9	50.7	27.6	14.6	9.8	6.8	5.0	28.6	146.3	197.6
11	162.3	119.5	95.2	55.3	31.5	18.0	12.3	8.6	6.5	20.0	129.8	197.2
12	163.8	121.8	98.7	59.6	34.9	21.2	14.7	10.4	7.9	14.3	113.0	195.7
13	160.3	116.7	92.1	50.9	26.3	12.5	6.5	3.6	2.1	26.3	147.9	197.7
14	161.0	117.6	93.5	52.8	28.2	14.2	7.9	4.5	2.8	21.7	140.6	197.9
15	163.1	119.9	97.1	57.2	32.3	18.3	11.3	6.8	4.6	13.8	121.5	196.8
16	164.4	122.2	100.4	61.5	36.0	21.9	14.2	9.0	6.2	9.4	102.8	194.7
17	165.4	122.8	101.6	61.8	40.5	26.1	19.2	14.3	11.2	22.4	123.5	197.5
18	167.7	125.8	105.5	67.1	44.4	29.4	22.2	16.4	13.1	17.0	102.8	194.5
19	173.3	132.4	114.4	79.3	54.2	37.6	29.5	22.0	17.8	14.7	55.3	175.4
20	172.8	136.5	121.4	88.2	62.5	45.0	36.2	27.5	22.2	18.2	29.1	140.6
21	167.4	125.4	105.5	67.2	44.9	30.0	22.7	16.5	13.1	15.1	95.9	192.8
22	160.3	117.0	91.9	50.7	27.6	14.6	9.8	6.8	5.0	28.6	146.3	197.6
23	172.2	132.3	114.2	79.4	54.6	38.2	30.0	22.3	17.9	14.8	49.2	171.4
24	170.5	135.1	121.9	89.1	62.9	45.7	36.1	27.3	22.1	18.8	28.5	132.6
25	170.0	130.8	112.7	77.7	52.1	34.4	25.4	19.3	15.0	11.5	41.4	165.4
26	167.3	125.7	105.0	67.7	42.4	26.9	19.2	14.2	11.0	10.6	77.7	188.2
27	170.9	132.6	113.9	80.0	53.5	36.3	26.5	20.2	15.8	13.3	34.0	158.9
28	166.9	137.4	121.7	90.1	63.6	44.7	33.5	25.9	20.5	17.5	18.7	115.3
29	165.9	123.3	102.5	64.3	38.9	23.8	15.7	10.3	7.2	8.6	89.9	192.1
30	166.9	135.3	120.2	87.5	62.1	43.0	31.6	23.3	17.5	13.3	17.8	123.8
31	170.5	132.9	115.1	81.4	55.2	37.7	27.4	19.7	14.8	12.0	25.3	150.2
32	163.4	136.0	123.1	90.7	64.8	45.4	34.6	25.4	19.4	16.2	16.4	101.3
33	171.9	136.6	122.4	87.4	62.9	44.4	34.7	27.2	21.6	14.8	35.7	146.5
34	163.4	139.4	129.8	97.2	72.5	52.5	41.9	33.1	26.6	18.1	22.1	109.1
35	120.3	128.5	137.4	114.1	92.1	70.5	58.4	47.2	38.6	27.8	15.6	50.1
36	161.9	118.5	94.6	53.4	33.9	20.8	14.5	10.8	8.9	39.6	151.6	197.8
37	170.0	136.0	121.7	87.4	63.2	44.9	35.4	27.5	22.0	15.6	31.2	141.5
38	160.3	138.5	129.1	97.1	72.7	53.0	42.5	33.5	27.0	19.2	19.7	103.5
39	115.6	126.7	135.8	113.3	91.4	70.5	58.7	47.5	38.9	29.2	15.5	45.8
40	161.8	118.1	94.5	54.0	34.4	21.3	14.8	10.8	8.3	33.3	147.4	198.0
41	166.0	135.5	121.2	88.5	63.1	43.3	32.7	25.4	20.0	14.6	21.2	124.4
42	152.2	137.0	128.2	98.1	73.4	52.0	40.1	31.5	25.0	18.7	14.3	84.9
43	101.6	120.6	133.0	113.6	93.6	70.8	56.9	45.9	37.2	29.2	14.4	33.7
44	161.6	118.5	94.1	53.5	30.0	16.6	11.3	8.0	5.9	22.9	136.2	197.5
45	164.0	135.8	122.3	90.0	65.1	45.3	33.4	24.8	18.7	13.6	15.9	113.4
46	147.6	136.2	129.0	99.5	75.4	54.2	41.3	31.4	24.1	17.9	11.8	73.6
47	93.9	116.8	132.1	113.9	95.4	73.0	58.8	46.5	36.8	28.9	13.7	27.4
48	162.7	118.9	95.9	55.5	30.8	16.5	9.7	5.8	3.8	16.8	129.3	197.2
49	129.8	131.7	137.9	111.2	89.1	67.1	54.9	44.7	35.9	22.8	15.3	63.5
50	101.5	116.7	135.4	118.0	99.7	78.0	65.7	54.2	44.2	29.2	14.7	42.1
51	160.9	117.2	92.3	51.0	31.6	19.3	13.2	9.9	8.6	47.2	157.6	197.5
52	162.0	118.5	94.5	53.4	33.9	20.8	14.5	10.8	8.8	39.6	151.5	197.9
53	125.7	130.0	136.1	110.7	89.1	67.5	55.6	45.1	36.6	24.6	14.3	58.9
54	97.0	114.5	133.4	117.1	99.5	78.4	66.2	54.6	44.9	31.2	14.4	38.6
55	160.5	116.9	92.2	51.8	32.2	19.7	13.4	9.8	7.7	39.9	154.9	197.8
56	161.9	118.1	94.5	54.1	34.4	21.3	14.8	10.8	8.3	33.3	147.4	198.0
57	112.9	124.6	133.4	111.4	90.6	67.2	53.8	43.4	34.8	24.6	11.9	45.1
58	83.6	107.0	128.6	116.6	101.0	78.4	64.6	53.0	43.2	31.6	13.1	28.8
59	62.7	78.4	101.4	102.1	100.0	82.9	71.9	61.3	51.4	41.9	35.1	42.3
60	161.7	118.5	94.1	53.5	30.0	16.6	11.4	8.0	5.9	22.9	136.3	197.4
61	105.8	121.7	133.0	112.3	92.8	69.8	55.2	43.4	34.0	24.1	10.5	37.4
62	76.5	102.5	126.9	116.8	102.8	80.9	66.4	53.4	42.7	31.4	12.4	23.4
63	61.4	74.5	99.5	99.1	98.3	82.2	71.4	60.2	49.7	41.3	36.9	43.5
64	162.9	118.9	95.8	55.5	30.9	16.5	9.7	5.8	3.8	16.8	129.2	197.1

Table 34 HELP model recharge monthly output for future climate (2070-2099), listed by HELP recharge zone.

				Average Recharge (mm / month)								
Recharge Zone	Jan	Feb	Mar	Apr	May	Jun	Jul	Aug	Sep	Oct	Nov	Dec
1	165.4	116.1	100.9	54.1	28.9	18.5	14.1	10.2	9.3	44.3	188.1	186.2
2	165.7	117.4	101.8	56.6	30.2	19.5	14.7	10.7	9.7	39.0	183.2	187.7
3	166.2	120.6	103.7	62.5	33.6	22.1	16.2	12.2	10.5	28.8	167.8	191.8
4	166.4	124.0	105.4	67.4	37.4	24.4	18.3	13.8	11.2	21.9	150.7	195.1
5	165.2	115.9	101.3	54.8	29.2	18.8	14.0	10.0	8.5	37.2	186.4	185.8
6	165.6	117.1	102.3	57.0	30.6	19.9	14.7	10.5	9.0	32.7	180.9	186.8
7	166.3	120.1	104.3	62.6	34.3	22.3	16.6	11.9	9.9	24.1	163.7	190.7
8	166.5	123.4	105.8	67.6	38.2	24.6	18.8	13.4	10.9	18.8	144.9	194.1
9	165.2	115.7	101.1	53.9	25.8	13.7	9.4	6.6	5.3	24.3	177.2	185.9
10	165.5	116.7	102.2	56.2	27.6	15.1	10.1	7.4	5.8	20.7	169.5	187.2
11	166.5	119.7	104.4	61.6	32.2	18.3	12.3	9.2	6.9	14.6	147.9	190.5
12	167.0	122.9	105.9	66.7	36.5	21.3	14.7	10.9	8.2	11.1	125.8	193.1
13	164.9	117.2	102.4	56.0	26.5	12.5	6.7	4.3	2.9	19.5	170.9	186.9
14	165.1	118.5	103.2	58.3	28.7	14.3	7.9	5.1	3.4	16.0	161.8	188.4
15	166.0	121.4	105.2	63.6	33.7	18.3	11.1	7.2	5.0	10.2	137.6	191.3
16	166.4	124.6	106.5	68.8	38.0	21.9	14.1	9.2	6.6	7.5	113.7	193.4
17	166.7	125.9	106.8	70.5	39.9	26.1	19.5	14.9	12.1	18.8	137.9	196.9
18	167.1	130.0	109.0	76.5	44.8	29.4	22.3	17.0	13.7	15.0	112.2	199.0
19	168.8	138.9	114.9	88.7	57.0	37.9	29.2	22.5	18.1	15.1	57.1	187.9
20	167.8	144.2	120.4	97.2	67.1	45.6	35.7	27.9	22.4	18.9	29.4	153.7
21	167.1	129.4	109.3	76.5	45.6	29.6	22.9	16.8	13.6	13.9	105.2	197.1
22	165.5	116.7	102.2	56.2	27.6	15.1	10.1	7.4	5.8	20.7	169.5	187.2
23	168.6	138.0	115.2	88.7	57.6	38.1	29.9	22.5	18.0	15.4	51.4	183.6
24	167.0	143.4	120.4	97.1	67.6	45.8	36.2	28.1	22.4	19.4	26.4	147.3
25	167.3	136.4	114.3	86.5	55.0	35.3	25.4	19.6	15.1	12.0	42.3	174.7
26	167.2	129.2	109.3	76.0	44.5	27.3	19.2	14.5	11.1	10.0	82.8	192.9
27	167.8	138.1	114.9	88.5	57.2	37.1	26.9	20.4	16.0	13.6	33.9	169.5
28	164.2	144.6	120.8	98.1	68.5	45.9	34.2	26.2	20.7	17.9	18.3	124.1
29	166.5	126.5	107.6	72.0	41.1	23.9	15.3	10.6	7.6	7.2	98.9	193.3
30	164.1	142.1	119.8	95.9	66.3	44.2	31.5	23.6	17.9	13.7	18.2	133.1
31	167.4	139.0	115.4	90.1	59.2	38.7	27.3	19.9	15.1	12.1	26.8	159.5
32	161.8	145.0	121.4	99.4	70.4	47.9	35.2	26.1	20.2	16.7	15.3	110.7
33	167.6	144.0	121.7	96.8	66.0	44.9	34.8	27.6	21.8	15.8	35.4	159.4
34	159.8	147.2	128.7	105.9	76.6	53.4	41.9	33.5	26.7	19.6	21.0	120.8
35	118.6	136.3	137.1	121.3	97.8	72.2	58.5	47.7	38.6	29.8	14.6	56.6
36	166.1	119.5	103.0	60.2	32.2	21.0	15.6	11.7	10.1	32.4	173.9	190.3
37	166.6	142.6	121.5	96.6	66.6	45.2	35.5	27.6	22.2	16.5	31.6	154.2
38	157.5	145.9	128.4	105.6	77.1	53.7	42.6	33.6	27.1	20.7	18.6	115.0
39	114.9	134.4	136.1	120.6	98.1	72.4	59.3	47.9	39.0	31.3	14.4	51.8
40	165.8	119.3	103.6	60.4	32.9	21.3	15.8	11.4	9.6	27.2	170.3	189.4
41	162.8	142.7	121.2	96.9	66.8	44.6	33.0	25.8	20.1	15.5	20.2	134.0
42	149.7	144.8	127.6	105.9	77.8	53.7	40.7	32.0	25.2	19.9	13.0	92.4
43	99.5	128.6	132.8	120.2	99.2	73.2	58.1	46.6	37.4	31.1	14.1	36.7
44	165.8	118.9	103.6	59.6	30.3	17.0	11.4	8.6	6.5	16.5	156.0	189.7
45	161.2	143.0	121.7	98.3	69.3	46.5	33.3	25.2	19.0	14.2	16.0	122.4
46	145.4	144.2	128.0	107.1	80.3	55.9	41.4	31.8	24.4	18.8	11.2	80.8
47	91.7	124.7	131.8	120.3	101.2	75.6	59.7	47.1	37.3	30.2	14.3	30.1
48	165.6	120.6	104.4	61.7	31.8	16.5	9.5	6.4	4.3	12.4	147.2	190.4
49	127.3	139.4	136.8	119.4	94.0	68.5	55.3	45.2	35.9	25.1	14.2	71.6
50	99.2	123.9	135.2	125.7	105.5	80.0	66.1	54.8	44.2	31.9	13.8	47.9
51	165.6	117.7	101.7	56.6	30.2	19.5	14.7	10.8	9.6	39.0	182.7	187.9
52	166.0	119.6	103.0	60.2	32.3	21.0	15.6	11.6	10.1	32.3	174.0	190.2
53	124.1	137.4	135.6	118.7	94.3	68.8	56.0	45.4	36.7	26.6	12.8	66.9
54	95.5	121.7	133.8	124.7	105.6	80.2	66.8	55.0	45.0	33.7	13.2	43.9
55	165.5	117.4	102.3	57.0	30.7	19.8	14.6	10.6	9.0	32.6	180.3	187.3
56	166.0	119.3	103.5	60.4	32.9	21.3	15.8	11.4	9.6	27.1	170.4	189.3
57	110.2	132.7	133.1	118.7	95.5	69.6	54.7	44.1	35.0	26.8	10.7	49.6
58	80.8	113.9	128.9	123.6	106.6	81.2	65.8	53.9	43.5	34.3	12.4	31.4
59	165.5	117.0	102.3	56.3	27.6	15.0	10.1	7.4	5.8	20.7	168.9	187.5
60	165.9	118.9	103.5	59.7	30.3	16.9	11.4	8.6	6.5	16.6	156.0	189.5
61	103.5	129.7	132.6	119.3	98.2	72.0	55.8	44.0	34.3	26.0	10.1	41.6
62	74.0	109.4	127.1	123.2	108.9	83.7	67.4	54.2	43.1	33.8	12.3	25.8
63	162.1	116.7	101.2	57.2	28.1	13.8	7.4	4.9	3.3	15.8	157.7	183.8
64	165.6	120.5	104.4	61.6	31.8	16.5	9.5	6.4	4.3	12.4	147.1	190.5

Table 35 HELP model recharge monthly output converted to % of monthly precipitation for historical climate (1961-1999), listed by HELP recharge zone.

	Recharge (% precipitation), average monthly											
Recharge Zone	Jan	Feb	Mar	Apr	May	Jun	Jul	Aug	Sep	Oct	Nov	Dec
1	93.1	95.2	78.8	54.8	34.7	35.7	71.8	53.5	11.1	27.9	82.0	92.2
2	93.5	96.7	80.7	57.1	36.9	37.5	80.0	58.0	11.9	24.6	80.7	92.5
3	94.8	99.9	85.1	62.7	42.8	41.6	99.1	70.2	14.2	18.0	75.8	92.9
4	96.2	102.8	89.6	67.4	48.4	45.5	111.6	83.0	16.5	14.3	68.9	93.3
5	93.2	94.6	78.6	55.1	35.9	36.5	75.8	53.2	10.9	22.8	80.7	92.1
6	93.8	95.9	80.4	57.4	38.1	38.3	84.0	57.6	11.7	20.1	79.0	92.3
7	94.8	99.2	84.7	62.7	43.8	42.7	101.5	71.3	14.1	15.1	73.0	92.7
8	96.0	102.2	89.1	67.5	49.3	46.5	113.6	85.8	16.4	12.6	65.2	93.2
9	93.3	94.8	78.4	55.1	33.6	26.0	53.0	38.0	7.5	16.1	77.7	91.9
10	94.0	95.9	80.4	57.4	36.2	28.4	56.3	42.6	8.5	13.8	75.4	92.0
11	95.0	99.2	84.7	62.9	42.2	34.1	67.2	51.7	10.8	10.5	67.3	92.4
12	96.0	102.2	89.1	67.5	47.8	39.9	80.0	59.9	13.2	8.9	58.1	92.7
13	94.1	95.6	80.2	57.3	35.3	24.7	40.5	23.0	3.7	12.5	75.4	92.1
14	94.7	96.7	82.1	59.5	38.1	27.9	45.6	28.9	4.8	10.4	72.2	92.3
15	95.6	99.7	86.2	64.7	44.7	34.9	59.3	42.7	7.7	7.3	62.6	92.6
16	96.7	102.6	90.2	69.3	50.5	41.6	74.4	55.3	10.6	6.1	52.5	92.6
17	96.8	104.7	92.0	70.7	51.9	49.0	118.6	90.1	18.1	13.0	63.5	93.6
18	98.5	107.8	97.1	76.5	58.9	54.9	134.8	104.3	21.4	11.3	52.5	93.6
19	102.4	114.7	107.9	89.0	75.7	70.4	175.9	138.5	29.6	12.1	28.4	87.7
20	101.4	119.3	116.8	99.0	90.5	85.7	216.2	170.5	37.5	15.3	15.3	73.1
21	98.4	107.1	96.4	76.3	59.8	55.8	137.6	106.0	21.8	10.7	48.5	93.0
22	94.0	95.9	80.4	57.4	36.2	28.4	56.3	42.6	8.5	13.8	75.4	92.0
23	102.1	113.7	107.2	88.7	76.4	71.2	177.7	141.3	30.0	12.5	25.4	85.7
24	101.4	118.1	116.4	98.3	90.8	86.2	217.0	171.5	37.6	15.6	13.9	69.2
25	100.9	112.4	104.9	86.7	73.3	66.7	146.1	113.0	25.2	10.2	22.4	82.7
26	98.5	107.1	96.4	76.3	59.0	51.5	106.7	82.7	18.3	8.5	39.9	91.4
27	101.8	113.7	107.1	88.8	76.0	70.3	153.7	116.3	26.4	11.2	18.8	80.2
28	99.1	118.3	115.7	98.8	90.8	87.7	201.2	149.5	34.2	14.4	10.4	61.2
29	97.6	104.2	92.6	72.4	54.6	45.6	84.7	62.2	12.2	6.0	46.2	92.2
30	100.9	117.3	112.8	96.1	88.1	84.0	184.2	138.3	29.6	11.2	10.4	64.6
31	102.0	114.3	107.6	90.0	78.7	73.6	156.0	116.8	24.9	9.9	14.9	76.0
32	98.1	119.0	115.9	99.6	93.2	91.4	206.1	153.2	33.5	13.4	8.5	55.1
33	101.9	119.5	115.6	98.3	88.1	84.9	214.9	168.3	36.3	13.0	18.9	75.3
34	97.2	122.9	123.9	108.5	102.9	101.2	261.2	204.0	44.9	16.0	11.7	58.3
35	71.6	114.8	134.2	127.1	133.4	137.5	371.5	289.7	66.0	24.3	8.2	28.6
36	94.4	98.9	83.4	60.5	40.5	40.0	91.0	65.7	13.3	20.3	77.9	92.7
37	101.2	118.1	114.2	97.6	88.6	85.5	218.0	169.9	37.1	13.7	16.6	72.7
38	96.0	121.4	122.5	107.7	103.1	101.7	263.9	205.9	45.7	17.0	10.4	55.3
39	69.5	113.2	132.4	126.0	133.1	137.7	373.0	291.9	66.6	25.7	7.9	26.4
40	94.5	97.9	83.1	60.8	41.5	40.9	94.4	66.1	13.3	16.8	75.5	92.5
41	100.1	117.7	114.1	97.7	89.1	84.7	194.6	149.6	33.6	13.0	11.7	65.0
42	92.8	120.6	122.3	107.7	103.9	102.5	243.7	186.3	42.2	16.4	7.7	46.6
43	62.8	109.5	130.9	125.6	134.0	140.9	360.8	273.9	63.3	25.0	7.3	19.9
44	94.6	98.0	83.1	60.9	39.9	31.6	63.7	49.1	10.0	11.4	70.6	92.3
45	99.5	118.2	114.9	98.8	92.2	88.6	196.8	147.9	31.6	11.7	9.1	59.9
46	90.7	120.6	122.7	108.6	106.8	106.7	248.2	187.2	40.8	15.3	6.3	41.0
47	58.1	107.5	129.9	125.7	136.2	145.2	369.1	279.3	62.9	24.4	7.0	16.5
48	95.3	98.8	84.8	63.0	42.2	31.8	53.8	36.6	6.4	8.4	66.5	92.5
49	76.4	117.7	132.4	125.0	127.7	131.7	352.5	275.4	61.6	20.8	8.4	35.9
50	60.1	104.4	131.8	133.6	145.4	154.6	428.9	335.0	76.6	26.5	8.1	24.7
51	76.4	86.9	84.4	76.7	76.5	84.7	188.5	115.4	35.8	27.0	60.1	68.2
52	94.4	98.8	83.3	60.5	40.5	40.0	91.0	65.4	13.4	20.4	77.8	92.7
53	74.9	115.8	130.3	123.7	127.5	132.0	355.3	277.0	62.7	22.2	7.7	33.4
54	58.2	102.7	129.7	132.0	144.8	154.6	431.1	336.6	77.7	28.1	7.7	22.8
55	93.9	96.1	80.5	57.6	38.1	38.3	82.7	58.6	11.8	20.1	79.0	92.2
56	94.5	98.0	83.0	60.8	41.6	41.0	94.3	66.2	13.3	16.7	75.4	92.6
57	69.2	112.4	129.2	123.3	128.8	134.0	338.0	260.2	59.4	22.0	6.0	26.3
58	51.9	97.6	127.2	130.9	145.9	157.7	416.6	320.8	74.4	28.1	6.7	17.4
59	65.3	81.7	85.4	86.4	96.8	103.3	213.7	151.6	51.7	24.8	43.8	52.6
60	94.7	98.1	83.1	60.9	39.9	31.7	63.7	49.4	10.0	11.4	70.5	92.3
61	65.3	110.9	129.1	123.8	131.7	138.9	343.9	262.1	58.1	21.2	5.3	22.4
62	47.7	94.8	125.7	130.7	148.3	162.6	424.8	325.1	73.7	27.5	6.3	14.5
63	94.7	96.8	82.3	59.8	38.2	27.4	45.4	28.3	4.7	10.5	72.2	92.3
64	95.3	98.7	84.8	63.0	42.2	31.8	53.6	36.6	6.4	8.4	66.5	92.5
65	98.8	106.8	96.6	76.8	58.8	53.1	113.5	80.0	18.3	8.2	39.2	91.4
66	98.1	106.6	95.2	75.2	57.9	49.8	106.0	80.6	17.0	7.9	42.6	91.8
67	98.6	108.0	96.7	76.4	57.2	48.9	112.1	90.3	19.0	9.7	48.5	93.1
68	96.8	106.5	96.3	76.2	58.6	51.3	105.8	80.2	18.0	8.5	40.1	91.6
69	96.7	106.4	96.1	76.2	58.6	51.3	105.8	80.2	18.0	8.5	40.1	91.6
70	96.7	106.4	95.9	76.2	58.6	51.3	105.8	80.2	18.0	8.5	40.1	91.6
71	97.1	104.4	92.2	71.3	52.6	44.8	90.5	69.6	15.3	8.4	50.2	92.6
72	95.9	101.6	88.2	66.8	47.0	38.9	77.7	60.4	13.0	9.1	59.6	92.6
73	98.5	107.0	96.5	76.2	58.4	51.0	104.7	79.3	17.8	8.4	40.4	91.7
74	98.4	106.8	96.2	76.0	58.4	51.2	105.6	80.1	18.0	8.6	40.4	91.7
75	98.3	106.7	96.0	75.8	58.2	51.1	105.5	80.1	18.0	8.6	40.7	91.7
76	98.6	107.1	96.6	76.3	58.5	51.1	104.6	79.3	17.7	8.4	40.2	91.7
77	98.5	106.9	96.3	76.1	58.4	51.2	105.4	79.9	17.9	8.5	40.3	91.7
78	98.5	106.9	96.3	76.1	58.4	51.2	105.4	79.9	17.9	8.5	40.3	91.7
79	95.3	101.5	88.2	66.8	47.1	39.0	77.8	60.5	13.0	9.1	59.6	92.6
80	94.8	101.4	88.2	66.8	47.1	39.0	77.8	60.5	13.0	9.1	59.6	92.6
81	94.5	101.3	88.2	66.8	47.1	39.0	77.8	60.5	13.0	9.1	59.6	92.6
82	96.7	103.2	91.0	69.9	50.8	43.6	89.7	66.3	14.7	8.2	52.9	92.7
83	95.5	99.9	85.6	64.2	43.8	35.6	74.2	53.9	10.8	9.9	65.1	92.5
84	95.2	100.3	85.1	63.1	41.2	35.4	84.9	60.5	12.2	17.2	73.5	92.8
85	96.5	103.3	90.5	68.5	49.8	46.5	115.4	86.9	17.1	13.7	66.9	93.4
86	95.4	101.7	87.0	65.3	45.4	44.2	100.4	77.9	14.8	16.4	72.1	93.3
87	95.3	101.3	86.1	64.3	44.2	43.3	97.0	74.0	13.9	19.6	74.4	93.1